A Study of Striatal Markers as Disease Modifiers in Huntington's Disease

Laetitia Francelle

UNIVERSITÉ PARIS-SUD

ÉCOLE DOCTORALE 419 :
BIOSIGNE

Laboratoire :

THÈSE DE DOCTORAT SUR TRAVAUX

ASPECTS MOLÉCULAIRES ET CELLULAIRES DE LA BIOLOGIE

par

Laetitia FRANCELLE

A study of striatal markers as disease modifiers in Huntington's Disease

Date de soutenance : 26/11/2014

Composition du jury :

Directeur de thèse :	Dr Emmanuel BROUILLET	Laboratoire des maladies neurodégénératives, URA CEA-CNRS 2210, Service MlRCen, lnstitut d'lmagerie Biomédicale, CEA, Fontenay aux Roses, France.
Président du jury:	Pr Dr Hervé DANIEL	Pharmacologie et Biochimie de la Synapse, lnstitut de Biochimie et de Biophysique Moléculaire et Cellulaire, UMR 8619, Centre Universitaire d'Orsay, Orsay, France.
Rapporteurs :	Dr Jocelyne CABOCHE	SIgnalisation Neuronale et Régulation Génique, Unité Neurosciences Paris Scène, INSERM/UMR-S1130; CNRS/UMR8246, Paris France.
	Dr Karine MERIENNE	Interactive Dynamics of Memory Systems, Laboratoire de Neurosciences Cognitives et Adaptatives (LNCA), UMR7364/ Université de Strasbourg/CNRS, Strasbourg, France.
Examinateurs :	Pr Dr Tiago FLEMING OUTEIRO	Department of NeuroDegeneration and Restorative Research Center for Nanoscale Microscopy and Molecular Physiology of the Brain, University Medical Center Göttingen, Göttingen, Germany.
	Dr Jean-Vianney BARNIER	Centre de Neurosciences Paris-Sud (CNPS), UMR 8195 CNRS-UPS, Bât 444, Centre Universitaire d'Orsay, Orsay, France.

“Ever tried. Ever failed. No matter. Try Again. Fail again. Fail better.”

Samuel Barclay Beckett

(April 13, 1906 - December 22, 1989)

Irish avant-garde novelist, playwright, theatre director, and poet.

1969 Nobel Prize in Literature.

REMERCIEMENTS

Je remercie mes rapportrices, **Jocelyne Caboche** et **Karine Merienne**, pour avoir accepté de faire la lecture critique de mon manuscrit. Je tiens également à remercier **Jean-Vianney Barnier** et **Hervé Daniel** pour avoir accepté d'être membres de mon jury de thèse. I thank **Tiago Fleming Outeiro** to have accepted to be part of my thesis committee, I am grateful for your time and consideration.

Je remercie **Philippe Hantraye** d'avoir accepté que je puisse réaliser ma thèse au sein de MIRCen.

Je ne remercierai jamais assez mon directeur de thèse **Emmanuel Brouillet**, pour m'avoir fait confiance en me prenant en thèse, pour avoir fait son maximum, malgré un emploi du temps surchargé, pour me former et me faire progresser et pour m'avoir permis de parcourir le globe pour ma formation. J'ai adoré ces années à travailler avec vous.

Merci à **Sandrine Humbert, Fréderic Saudou, Diana Zala** et leurs équipes à l'Institut Curie d'Orsay pour avoir toujours accepté de partager leur savoir-faire et leurs compétences scientifiques avec moi.

Merci à **Anselme Perrier** pour m'avoir fourni en neurones quelques temps, mais surtout pour les nombreux échanges que nous avons pu avoir sur le projet DCLK3.

Je remercie **Gilles Bonvento** et **Carole Escartin** pour leurs précieux conseils.

Merci à **Martine** et **Diane** pour m'avoir formée à l'expérimentation animale, mais aussi à leur bonne (et mauvaise) humeur partagée en A2/A3.

Je remercie **Noëlle** pour m'avoir très gentiment fourni toutes ces années en cellules HEK, ainsi qu'avec l'aide de Charlène et Alexis, pour la production de tous les virus qui m'ont servi à faire de mon travail ce qu'il est. Du même bureau, merci à **Aurélie** pour sa bonne humeur, sa gentillesse et son interprétation des chansons en histo qui donnait plus de vie au montage des coupes….

Merci à **Carole, Fanny** et **Caroline** pour m'avoir formée et assistée dans mes diverses expériences de biochimie ou histologie. Merci à **Gwenn** et **Pauline** pour m'avoir faire profiter de leurs multi-compétences.

Merci à **Karine** pour son aide et ses précieux conseils en comportement animal, mais également pour sa bonne humeur.

Merci à **Marie Claude** pour m'avoir formée et aidée en B.M., et surtout pour m'avoir encouragée tout au long de ma thèse. Les marqueurs striataux ont commencé dans tes mains, et le resteront encore un peu j'espère avec DCLK3…

Je tiens à remercier les autres étudiants en thèse à MIRCen, notamment **Lucile** pour avoir supporté mon mutisme intempestif, et avec **Noémie** pour avoir partagé notre bureau, de nombreuses discussions scientifiques passionnantes, et plus encore … Merci à **Chloé** et **Marie-Anne** pour leur gentillesse et leur capacité à être très rassurante et encourageante par moment. Merci à **Juliette, Micka, Romain, Marie, Charlotte** et **Brice** pour leur bonne humeur et leur entrain à sortir et faire mil et une activités en-dehors de MIRCen. Gardez ce cap et bon courage pour la suite !

Merci à **Sandro** pour ses nombreux conseils.

Bon courage aux post-doc **Jérôme**, **Benoit** et **Pierrick** dans cet univers impitoyable qu'est la Recherche.

Merci aux ex-MIRCenniens, notamment **Fabien** et **Maria-Angeles** avec qui j'ai partagé mon bureau pendant quelques temps, pour leur bonne humeur et amitié. Merci à **Emilie** et **Matthias V.** pour tous nos moments de décompression autour de quelques bières…

Je remercie **Marc, Nicolas, Léo** et **Lina** pour m'avoir encouragée à reprendre mes études, ainsi que **Pierre, Rémi C.** et **Natacha** pour leur amitié depuis le Master.

Merci à **Kento**, **Olivier, Marco** et **Matthias T.** pour m'avoir fait découvrir tout un univers musical électro qui me fait toujours autant vibrer, ainsi que **Laurence, Sylvie, Clotilde, Franck, Gérard, Valérie** et **Florence** pour avoir mis un peu de son des années 70' dans mes oreilles, cordes vocales et doigts.

Merci à **Rémi N.** pour sa patience, sa motivation et sa bonne humeur durant nos sessions d'escalade, on finira par faire notre via ferrata un jour !

Je remercie **ma famille** pour avoir toujours cru en moi, et en particulier ma grand-mère qui m'a toujours poussée et encouragée à aller toujours plus loin, mon grand-père pour sa générosité, ma mère et mes frères pour être toujours présents dans les bons moments, comme les moments difficiles, qui ont faits de ces 3 ans et demi une période riche en émotions et moins difficile que ça aurait pu être. Merci à Gisèle, Laurent et Annie pour leur bienveillance et générosité. Merci à Sarah et Caro pour leur gentillesse.

Je tiens à remercier **Sina** pour n'avoir cessé de m'encourager, de me soutenir et de m'aimer quand je m'essoufflais et en devenais impossible à vivre ! Je n'y serais pas arrivée sans toi, ton optimisme à toute épreuve, ton humour fracassant et ton amour sans faille !

Good reading.

TABLE OF CONTENTS

LIST OF FIGURES

LIST OF TABLES

ABBREVIATIONS

3-NP: 3-nitropropionic acid
AAV: adeno-associated virus
AIF: apoptosis inducing factor
Akt: murine thymoma viral oncogene homolog 1
AMPA: alpha-amino-5-méthyl-3-hydroxy-4-isoxazolepropionoate
ASOs: single-stranded DNA-based antisense oligonucleotides
BDNF: Brain derived neurotrophic factor
cAMP: cyclic adenosine monophosphate
CBP: cAMP response element-binding protein-binding protein
CDK5: cyclin-dependent kinase 5
CNS: central nervous system
COX: cytochrome c oxydase
CRYM: mu-crystallin
CtBP: C-terminal binding protein
DARPP32: dopamine and cyclic AMP-regulated phosphoprotein 32 kDa
DCLK3: doublecortin-like kinase 3
DNA: deoxyribonucleic acid
DTI: Diffusion Tensor Imaging
ENTH: epsin NH2-terminal homology
ENK: enkephalin
GABA: gamma-aminobutyric acid
GAD: glutamic acid decarboxylase
GFAP: glial fibrillary acidic protein
GLUT: glutamate
GPe: external segment of the globus pallidus
GPi: internal segment of the globus pallidus
GTP: Guanosine triphosphate
HAP-1: Huntingtin-associated protein-1,
HEAT: Huntingtin-Elongation-A subunit-TOR
HIP-1: huntingtin-interacting protein 1
HIP-14: huntingtin-interacting protein 14
Hippi: huntingtin-interacting protein 1 interactor
HSP: Heat shock protein
IEG: Immediate Early Gene
InsP3R1: inositol 1,4,5-triphosphate receptor 1
iPSC: induced pluripotent stem cell
kDa: kiloDalton
KI: Knock-In
KO: Knock-Out
miRNA: microRNA
MPTP: 1-Methyl-4-phenyl-1,2,3,6-tetrahydropyridine
MRI: Magnetic Resonance Imaging
mRNA: messenger RNA
MSN: medium spiny neuron
NADP: nicotinamide adenine dinucleotide phosphate
NADPH: reduced nicotinamide adenine dinucleotide phosphate
N-CoR: nuclear receptor corepressor
NMDA: N-méthyl-D-aspartate

NOS: synthase de l'oxyde nitrique
NRSE: neuron restrictive silencer element
PACSIN-1: Protein Kinase C and casein kinase Substrate In Neurons 1,
PCR: polymerase chain reation
PINK-1: PTEN–induced kinase 1
PKA: protein kinase A
PNS: peripheral nervous system
PSD-95/ postsynaptic density protein 95 kDa
RE1/NRSE: repressor element 1 / neuron-restrictive silencer element
REST/NRSF: repressor element-1 transcription factor / neuron restrictive silencer factor
RNA: ribonucleic acid
RNAi: RNA interference
RT-PCR: Reverse transcriptase polymerase chain reaction
RXR: retinoid-x-receptor
SAGE: Serial Analysis of Gene Expression
siRNA: short interfering RNA
SNc: substantia nigra pars compacta
SNr: substantia nigra pars reticulata
SOD: superoxyde dismutase
STN: subthalamic nucleus
T3: triiodothyronine or 3,5,3'-triiodo-L-thyronine
T4: thyroxine or 3,5,3',5'-tetraiodo-L-thyronine
TAFII 130: RNA polymerase II TATA-binding protein TBP-associated factor de 130kDa
TBP: TATA-binding protein
TR: thyroid hormone nuclear receptor
ZFP : Zinc finger protein

PART1 INTRODUCTION

1.1 Neurodegenerative disorders

Neurodegeneration is a term used to describe progressive deterioration of structure and/or function of neurons that affects different parts of the central nervous system and peripheral systems, and leads to eventual death.

Important advances have been made in our understanding of the pathways that lead to cell dysfunction and death in the majority of neurodegenerative disorders, in particular on Alzheimer's disease, Parkinson's disease, Huntington's disease and Amyotrophic Lateral Sclerosis. These advances have been informed by both direct analysis of the post-mortem brain and by study of the biological consequences of the causes of these diseases. Some of the pathways that have been implicated so far include mitochondrial dysfunction, oxidative stress, kinase pathways, calcium dysregulation, inflammation and protein handling processes. Intriguingly, these pathways seem to be important in the pathogenesis of all the diseases and have led to the identification of molecular targets for candidate interventions designed to slow or reverse their course.

1.2 Huntington's disease

1.2.1 First descriptions of Huntington's disease

Thanks to the precise description by the American physician George Huntington (1850-1916) in 1872 (**Figure 1**) of an "hereditary chorea" affecting humans that was widespread in extreme East of Long Island "limited by few families transmitted as an heritage, appearing in the adult age and getting worse with time", it has become possible to give a name to the illness with jerky dancelike movements that was passing as evil possession at that time in some parts of the world (Bates 2005).
George Huntington noted that in these patients the movement disorder is accompanied by personality changes and a cognitive decline. He also noticed that families that suffer from this disease were characterized by an increased incidence of suicide.

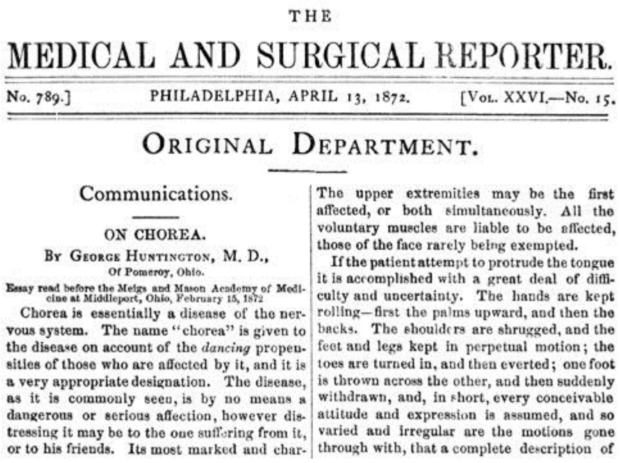

THE

MEDICAL AND SURGICAL REPORTER.

No. 789.] PHILADELPHIA, APRIL 13, 1872. [VOL. XXVI.—No. 15.

ORIGINAL DEPARTMENT.

Communications.

ON CHOREA.

BY GEORGE HUNTINGTON, M. D.,
Of Pomeroy, Ohio.

Essay read before the Meigs and Mason Academy of Medicine at Middleport, Ohio, February 15, 1872

Chorea is essentially a disease of the nervous system. The name "chorea" is given to the disease on account of the *dancing* propensities of those who are affected by it, and it is a very appropriate designation. The disease, as it is commonly seen, is by no means a dangerous or serious affection, however distressing it may be to the one suffering from it, or to his friends. Its most marked and char- The upper extremities may be the first affected, or both simultaneously. All the voluntary muscles are liable to be affected, those of the face rarely being exempted.

If the patient attempt to protrude the tongue it is accomplished with a great deal of difficulty and uncertainty. The hands are kept rolling—first the palms upward, and then the backs. The shoulders are shrugged, and the feet and legs kept in perpetual motion; the toes are turned in, and then everted; one foot is thrown across the other, and then suddenly withdrawn, and, in short, every conceivable attitude and expression is assumed, and so varied and irregular are the motions gone through with, that a complete description of

Figure 1 First page of George Huntington paper "On Chorea", 1872 (Bates 2005).

This description permits Vessie at that time to identify among the first Americans affected by Huntington's disease (HD) three men originated from the East of England that ran away from witchcraft persecution law to Salem (now called Danvers, New-England, USA). Unfortunately, the law was voted in this region of USA, which seen executions, including descendents of the three expatriates, during the famous "Salem witch trials". The example of Bures family, one of the three descendant families, helped to better understand the hereditary hallmark of HD (Bates 2005).

1.2.2. Actual description of HD

HD is an autosomal dominant neurodegenerative disease, characterized by a triad of symptoms: motor dysfunction, cognitive decline, and psychiatric disturbance. It appears in early adulthood, and progresses to significant functional disability and, ultimately, death within 15 years after the appearance of the first symptoms.

1.2.2.1.Motor dysfunction

It used to be called Huntington's chorea because of involuntary jerky dancelike movements as motor symptoms. These symptoms progressively appear around 35 to 40 years old and are more and more accentuated and incapacitating with time, even if patients show reduced awareness of their involuntary movements (Sitek et al 2014, Snowden et al 1998).
Before the symptomatic phase, patients are healthy and have no detectable clinical abnormalities, but in the presymptomatic phase they present subtle changes of motor functions, as decreased speed of movement and reaction times, and slowed saccadic eye movements (Lasker & Zee 1997, Siemers et al 1996).
Distinct chorea leads to a clinical diagnosis (HDSG 1996). Chorea are manifesting in the same time as incoordination, difficulty to swallow, motor impersistence, difficulty controlling the speed, decline in fine motor function, gait disturbances, dysarthria, and rigidity (Gusella & MacDonald 1995, Shoulson & Chase 1975). At late stage, patients present severe dystonia affecting the entire body while chorea disappears. Affected reflexes and oro-lingual muscles functions lead to "wrong-way" swallowing, broncho-pulmonary complications, pneumonia and eventually death.

1.2.2.2.Cognitive decline

In the presymptomatic phase, HD patients present also subtle cognitive changes, as impairment in motor sequence learning (Feigin et al 2006), or emotion recognition (Johnson et al 2007).
Cognitive dysfunction in HD, often spares long-term memory, but impairs executive functions, such as organizing, planning, checking, or adapting alternatives, and affects the acquisition of new motor skills and recall/recognition memory (Ho et al 2003, Montoya et al 2006a, Montoya et al 2006b). These features worsen over time; speech deteriorates faster than comprehension (Walker 2007).

1.2.2.3.Psychiatric disturbance

HD is associated with a wide range of psychiatric disturbances, including affective disorders, irritability, apathy, and psychosis (Caine & Shoulson 1983, Craufurd et al 2001). Some of these disorders can be measured in asymptomatic patients, as irritability (Berrios et al 2002). Manic and psychotic symptoms can develop (Cummings 1995). Depression has been observed to occur up to 20 years before the onset of motor symptoms (Folstein et al 1983) and increases as a function of proximity to clinical onset (Julien et al 2007).
Despite the denial of symptoms appearance (Sitek et al 2014), depression is typical and suicide is estimated to be about five to ten times that of the general population. Suicidal ideation is a frequent finding in patients with HD, even if the first cause of death in HD patients is pneumonia (see as review (Roos 2010)).

1.2.3. Prevalence

The prevalence of HD varies greatly geographically as a result of ethnicity, local migration and past immigration patterns. The Caucasian populations of North America and Western Europe having 5-10 subjects affected by HD per 100,000 people (Agostinho et al 2013). The rate of occurrence is highest in peoples of Western European descent, averaging around 7 per 100,000 people, and is lower in the rest of the world, e.g. one per million people of Asian and African descent. One of the highest prevalence is in the isolated populations of the Lake Maracaibo region of Venezuela, where HD affects up to 700 per 100,000 persons (Walker 2007). Other areas of high localization have been found in some regions of Scotland, Wales, Sweden and Tasmania (Harper 2002).

1.2.4. Neuropathology

As many neurodegenerative disorders, HD induces preferential early vulnerability of a particular region in the brain, which is the striatum, composed in human by the caudate nucleus and putamen (**Figure 2**). The striatum play a key role in a group of nuclei called the basal ganglia.

Basal ganglia consist of four nuclei (**Figure 2**), portions of which play a major role in normal voluntary movements. Motor functions of basal ganglia are in large part mediated by motor areas of frontal cortex (Wichmann & Delong 2007).

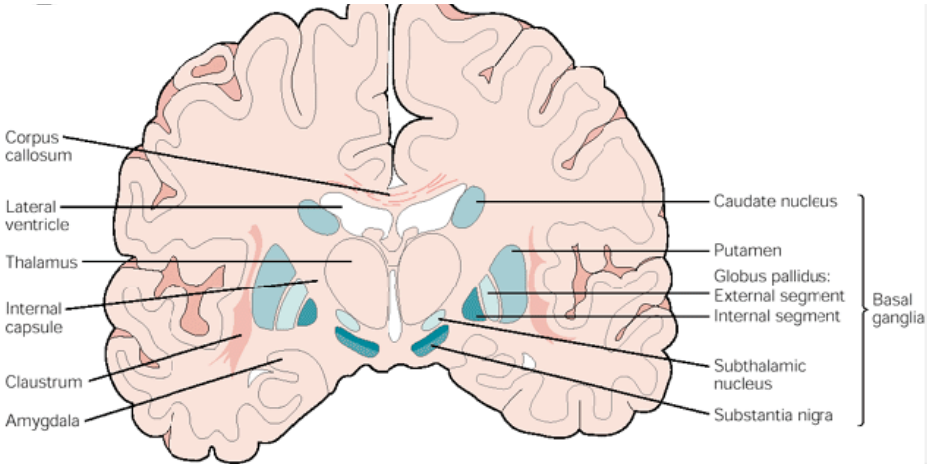

Figure 2 Representation of human brain coronal section showing basal ganglia (in blue) in relation to surrounding structures (adapted from Nieuwenhuys et al 1981) (Wichmann & Delong 2007).

The striatum is the primary site of HD pathology (Albin et al 1992, de la Monte et al 1988), accompanied by dilatation of the anterior horns of the lateral ventricles, which are obvious on MRI in advanced cases. Indeed, Hobbs and colleagues measured at onset of HD patient caudate volume was 2.58 mL smaller than in controls; ventricular volume was 9.27 mL larger. They showed that differences in caudate and ventricular volumes between patients with HD and controls were respectively evident 14 years and 5 years, before motor onset (Hobbs et al 2010, Tabrizi et al 2009) (Track-HD) (**Figure 3A**).

The output structures of the striatum, substantia nigra reticulata and globus pallidus (externa and internal segments) are also altered in symptomatic patients. The nucleus accumbens is relatively preserved.

Cortical atrophy is also present in advanced cases and detectable thanks to generation of magnitude map (Rosas et al 2011, Tabrizi et al 2009) (**Figure 3B**).

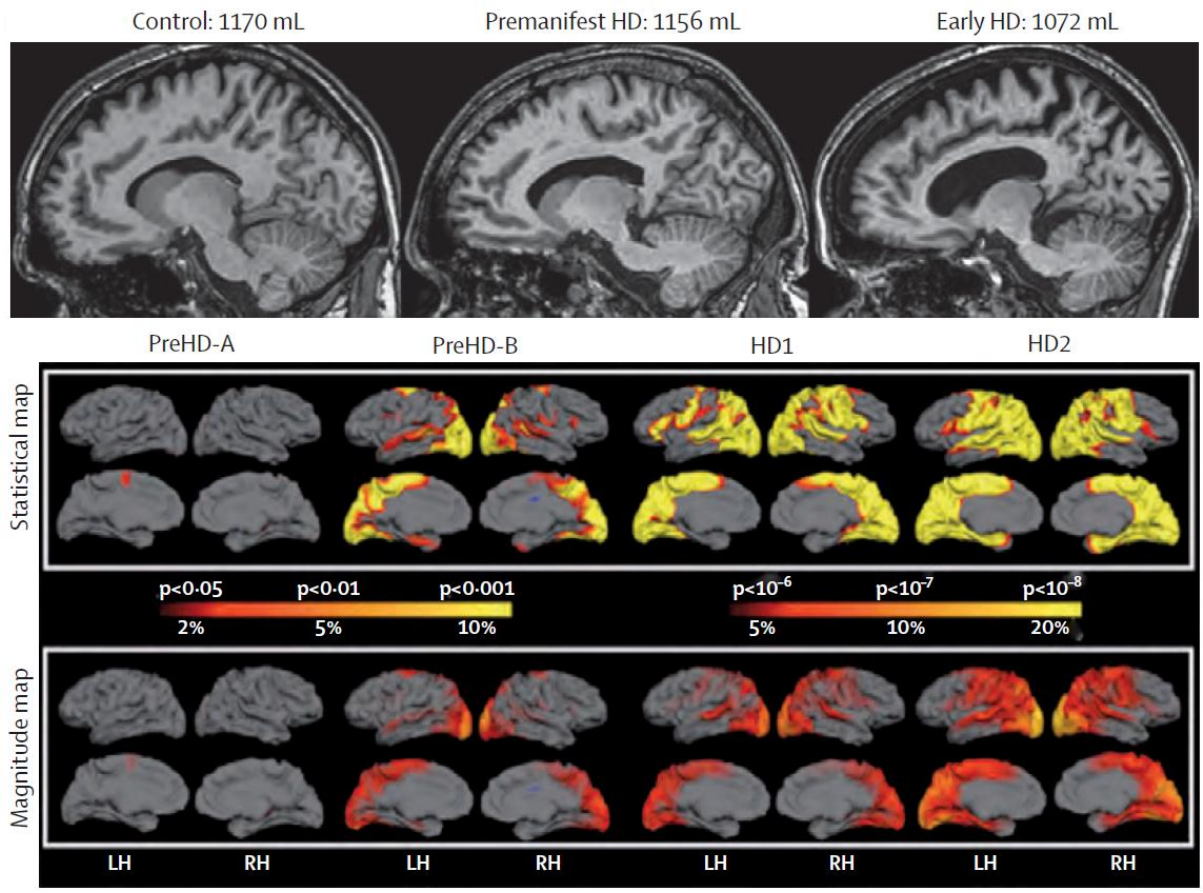

Figure 3 Whole brain and regional atrophy in the controls, premanifest, and early Huntington's disease patients (Tabrizi et al 2009).

Figure 3**A,** 3T volumetric MRI scan in a 50-year-old control, a 55-year-old individual with preHD, and a 49-year-old with early Huntington's disease. Brain volumes are corrected for intracranial volume. **B,** Cortical thinning in the Huntington's disease groups compared with controls. The top panel shows statistical maps corrected with the false discovery rate; magnitude maps are shown below. All results are adjusted for age and sex. ICV=intracranial volume. LH=left hemisphere. RH=right hemisphere.

Interestingly, within the striatal neuronal population, different degrees of degeneration can be observed (Ferrante et al 1997, Ferrante et al 1985). GABAergic medium-sized spiny neurons (MSN) are found to preferentially degenerate in HD, occurring first in the caudate and then the putamen (Rosas et al 2001, Vonsattel & DiFiglia 1998). Because these neurons represent 95% of the neurons in the striatum, their loss are likely responsible for the atrophy of the structure.

In contrast, medium-sized aspiny interneurons containing somatostatin, neuropeptide Y, or NADPH diaphorase, as well as the large cholinergic interneurons which both represent approximately 5% of striatal neurons are relatively spared. However, the extreme striatal atrophy and the loss of neurons observed in grade 4 indicate that both spiny and aspiny neurons are vulnerable at the end stage of the disease (Reiner et al 1988).

Early neuropathological studies showed that in advanced cases of HD, the cerebral cortex (particularly layers III, V, and VI), globus pallidus, thalamus, subthalamic nucleus, substantia nigra, white matter, and the cerebellum could be markedly affected (Vonsattel & DiFiglia 1998). Neuropathological characterization of HD brains also showed that the hypothalamus is probably damaged at very early stages in HD patients (Kremer et al 1990). It has been confirmed using PET scan and MRI imaging [for example (Douaud et al 2006, Politis et al 2008)].
In addition, diffusion tensor imaging (DTI) has demonstrated pathology of the white matter in pre- and early symptomatic patients (Rosas et al 2006).

1.2.5. Striatal neurotransmission

Medium-sized spiny neurons constitute 95% of all striatal neurons and utilize gamma-aminobutyric acid (GABA) as their principal neurotransmitters (Schaefer et al 2012). The dorsal striatum receives parallel sets of diffuse glutamatergic inputs from almost all neocortical areas and several thalamic nuclei (Tepper et al 2008). These inputs primarily synapse onto spines of MSN (Leavitt et al 2006). The striatum also contains a number of modulatory components including dopamine (DA) projections from the substantia nigra pars compacta (SNc) (Raymond et al 2011) and cholinergic or GABAergic inputs from striatal interneurons (Tepper et al 2008). These elements constitute the basic striatal microcircuit (see as review (Raymond et al 2011)).
Striatal output is largely segregated into two populations of MSN with distinct projections, as well as DA receptor and neuropeptide expression, constituting the direct and indirect pathways (Calabresi et al 2014, Gerfen et al 1990, Hallett 1993, Kawaguchi et al 1995) (**Figure 4**).
In the physiological condition, the direct pathway (**red lines, Figure 4**) consists of MSN that predominantly express D1 DA receptors, substance P and dynorphin, and project to the substantia nigra (SN) and the internal segment of the globus pallidus (GPi).
The indirect pathway (**blue lines, Figure 4**) is comprised of MSN that express predominantly D2 DA receptors, enkephalin or neurotensin, and project to the external segment of the globus pallidus (Gpe).

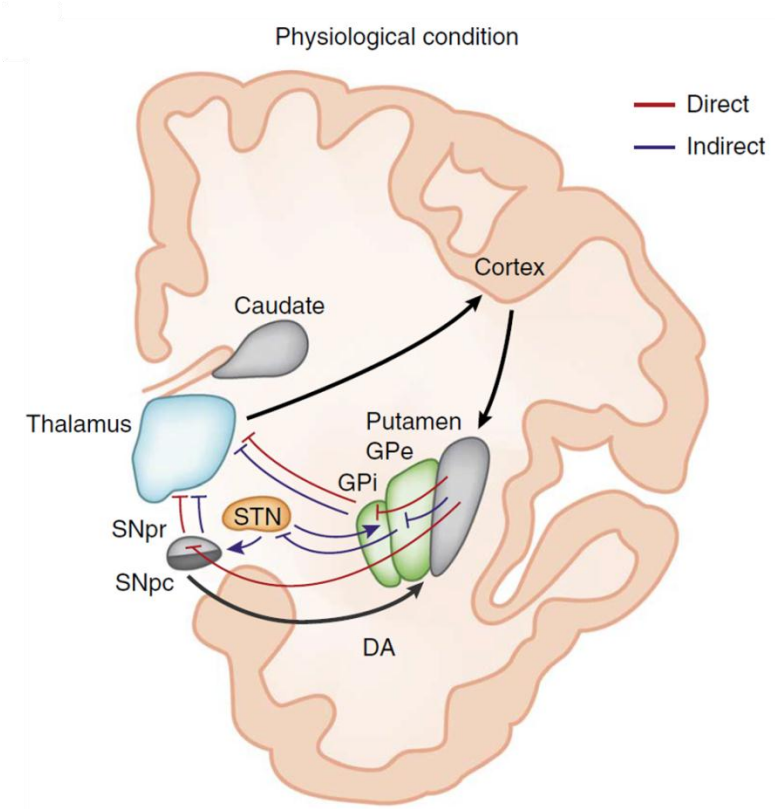

Figure 4 Schematic representation of the direct (red lines) and indirect (blue lines) pathway classical model in the physiological condition (Calabresi et al 2014).
Abbreviations: DA, dopamine; STN, subthalamic nucleus; SNpc, substantia nigra pars compacta; SNpr, substantia nigra pars reticulata; GPi, globus pallidus pars interna; GPe, globus pallidus pars externa.

DA arising from the SNpc is thought to activate D1-expressing striatal MSN of the direct pathway and to inhibit D2-expressing striatal neurons of the indirect pathway. The output nuclei GPi and SNpr project to the thalamus, which in turn send efferents that complete the cortico-basal ganglia-thalamo-cortical loop.

Two of the most important disorders affecting the basal ganglia are Parkinson's disease (PD) and HD. Several studies compared the ravages of this brain structure on the two diseases, giving an overview on the basal ganglia circuitry and its main pathologies (Albin et al 1989, Alexi et al 2000, Fernandez-Ruiz 2009, Fernandez-Ruiz et al 2011).
PD is also a progressive neurodegenerative disorder whose origin has been associated with environmental insults, genetic susceptibility or interactions between both causes (Schapira et al 2014). The major clinical symptoms in PD are tremor, bradykinesia, postural instability and rigidity, symptoms that mainly result from the severe dopaminergic denervation of the striatum caused by the progressive death of dopaminergic neurons of the SNc (Clabough & Zeitlin 2006, Obeso et al 2014).

HD pathology is associated with abnormal neurotransmitter regulation and synaptic communication, as well as glutamate-mediated excitotoxicity (Chen et al 1999, Sepers & Raymond 2014, Taylor-Robinson et al 1994).

It has been suggested that one early event in HD is the preferential degeneration of the GABA (met-enkephalin) neurons of the indirect pathway (producing the arrest of inhibition of the pallidum), so that an imbalance between the indirect and directly pathways would lead to an abnormal activation of thalamic motor neurons, in turn abnormally activating cortical motor neurons, which could explain the hyperkinetic symptoms in HD, in contrast to PD where the repression of thalamic nuclei leads to loss of activation of cortical neurons and the hypo/akinetic movements. However, this basal ganglia neurophysiology model of motor symptoms in HD first suggested by Albin (Albin et al 1989) has been debated and did not help to design efficacious therapy.

Another important part of the imbalanced neurotransmission in HD is the compensatory mechanism occurring over time that attempts to stabilize this system, well described by Levine and colleagues (Andre et al 2010, Raymond et al 2011) (**Figure 5**).

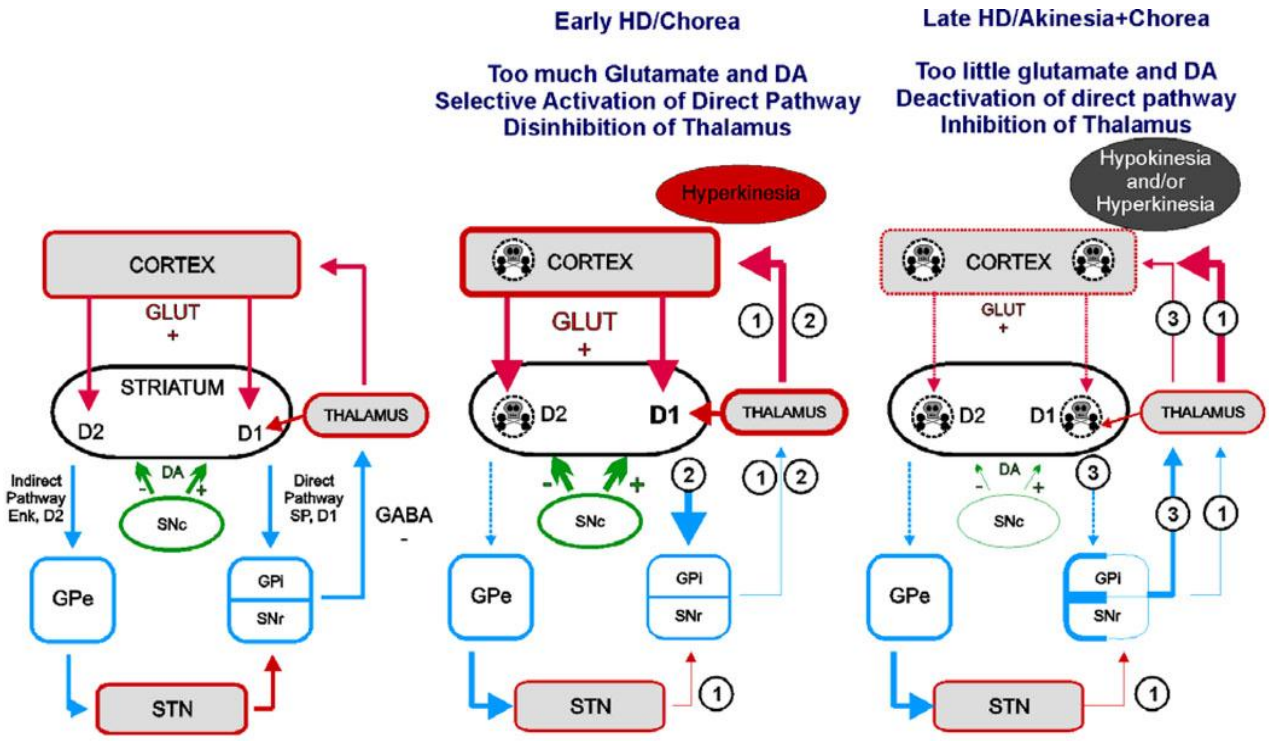

Figure 5 Glutamate and DA in basal ganglia function in intact brain and during HD (André et al 2010).
Left is a simplified schematic showing normal basal ganglia circuitry.
Red: glutamate inputs; blue: GABA; green: DA.
Abbreviations: Enk: enkephalin; GLUT: glutamate; GPe: external segment of the globus pallidus; GPi: internal segment of the globus pallidus; SNc: substantia nigra pars compacta; SNr: substantia nigra pars reticulata; STN: subthalamic nucleus.

Under **normal conditions** (Left panel Figure 5), the thalamus is inhibited by GPi and SNr GABA projections.

In **early HD** (Middle panel Figure 5), cortical dysfunction induces excessive glutamate release in the striatum. Abnormally elevated striatal glutamate and DA levels trigger selective dysfunction of enkephalin-containing MSN.
Imbalance between the direct and indirect pathways induces hyperkinesia via two pathways:

1) Selective dysfunction/degeneration (dashed lines Figure 5) of enkephalin-containing MSN leads to decreased release of GABA in the GPe and to its disinhibition. In turn, overactivation of GABA neurons of the GPe leads to increased release of GABA and to inhibition of STN which decreases glutamate release and decreases activity of the GPi and SNr.

2) Overactivation of the direct pathway MSN (by abnormal DA modulation and/or excessive glutamate) leads to increased release of GABA and to inhibition of GPi and SNr. Together, alterations in direct and indirect pathways in early HD induce inhibition of GPi and SNr GABA neurons and to a decreased release of GABA in their output structure, the thalamus. Disinhibition of the thalamus is responsible for abnormal movements.

In **late HD** (Right panel Figure 5), corticostriatal and nigrostriatal inputs progressively degenerate, leading to decreased striatal glutamate and DA release. Low striatal glutamate and DA levels trigger dysfunction of both direct and indirect pathway MSN.
Imbalance between the direct and indirect pathways induces hyperkinesia and hypokinesia via two pathways:

1) Alterations in the indirect pathway are similar to early HD and lead to hyperkinetic movements.

3) Dysfunction/degeneration of direct pathway MSN induces decreased release of GABA and disinhibition of GPi and SNr. Increased activity in GPi and SNr leads to inhibition of the thalamus and hypokinesia.

Depending on the stage of dysfunction of direct and indirect pathway MSN, activity in the basal ganglia could result in hypokinesia or hyperkinesia and would explain why some symptomatic patients display both chorea and akinesia.

Levine group review evidences that the evolution of neurotransmission alteration in the striatum and cortex are bi-phasic, with changes in excitation and inhibition in early and late HD for cortex and striatum compared to healthy situation (**Figure 5**). In other words, HD is associated with complex dysfunctions within the cortex and basal ganglia that involve glutamate and dopamine neurotransmissions. Normally these two systems interact such that dopamine modulates glutamate-mediated transmission. In HD, this modulation is altered in complex ways by the initial overactivation of glutamate function which induces concomitant dysregulation of dopaminergic function. Thus, the normal balance between these systems is upset.

1.2.6. Cause of the disease

The highest concentration of HD sufferers was found in a tiny and isolated community around Venezuela's Lake Maracaibo. Starting from 1979, a group of geneticists and physicians kept medical records, took blood and skin samples, and charted the transmission of the disease within families of this community. This allowed to narrow the genetic defect responsible for HD on the chromosome 4 (Gusella et al 1983). Scientists from all over the world joined together into a team that was collectively named the Huntington Disease Collaborative Research Group that, after 14 years reported the discovery of the IT15 gene responsible for HD and of its associated mutation (HDCRG 1993). The first exon of the IT15 gene contains a repetitive DNA element consisting of three nucleotides: C (cytosine), A (adenine), and G (guanine). When researchers examined this region of IT15 in non-HD controls, they found that the number of CAG repeats varied from 6 to 35. Analysis of the same region in the IT15 gene in individuals with HD showed that they always had 40 or more CAG repeats (HDCRG 1993).
The length of the CAG repeat accounts for 50 to 70% of the variability in age at clinical onset, whereby individuals with longer repeat lengths commonly have an earlier onset than those with shorter repeat lengths. When considering hundreds of HD patients, the number of CAG repeats negatively correlates with the onset of symptoms. Long expansion can lead to juvenile forms of HD, while short expansion can lead to relatively late onset disease. However, at the individual level, the number of CAG repeats cannot predict the age of onset.

It was concluded that the CAG repeat expansion in the IT15 gene was responsible for HD. The IT15 gene is now renamed the huntingtin (HTT) gene because of the name assigned to the protein. HTT gene is composed by 67 exons and codes for 3144 amino acids (~350kDa). It is found in metazoans, with the highest degree of conservation among vertebrates (Clabough 2013).

Normal Htt has been found to play a major key role in most if not all cells, especially neurons. In HD, the mutation results in an elongated stretch of glutamine near the NH2 terminus of the protein (Andrew et al 1993, Hannan 1996, Ratovitski et al 2007, Trottier et al 1994) (**Figure 6**).

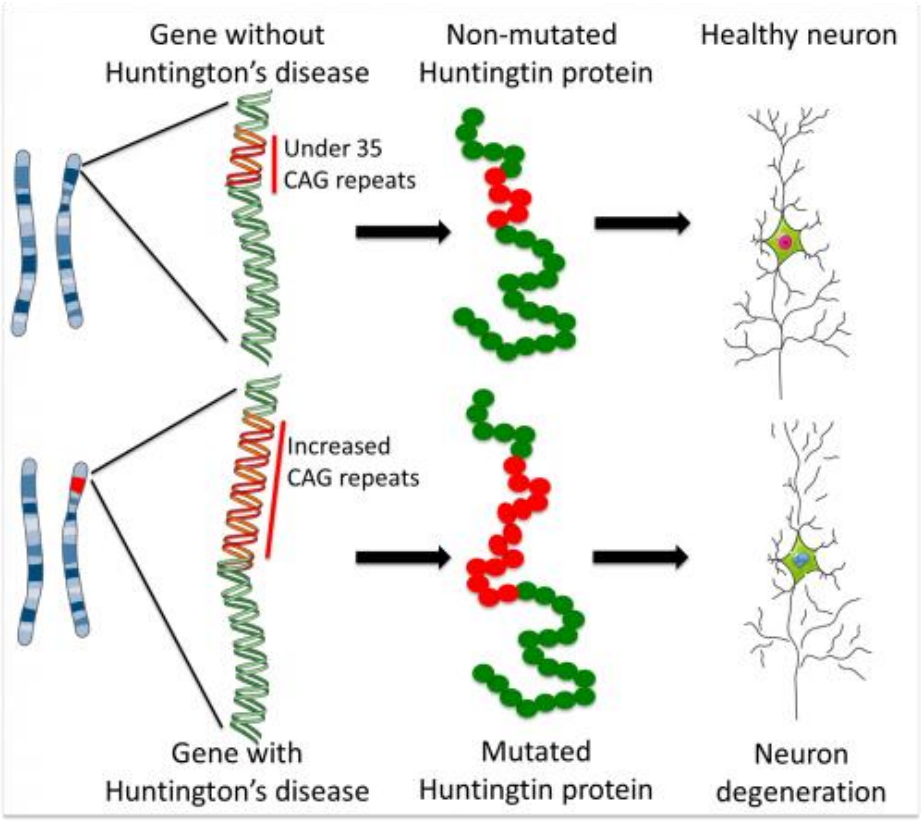

Figure 6 Consequences of the number of CAG repeats in htt gene and elongated stretch of glutamine in Htt protein on neuron survival.

This mutation in Htt protein is thought to confer to the protein a gain of function that is toxic to neurons (**Figure 6**). In addition, the disease is likely associated to a loss of function of normal Htt that would be detrimental to neurons.

1.2.6.1.Normal functions of wt-Htt protein

Htt protein is ubiquitously expressed with a highest expression level in the brain compared to peripheral nervous system (Moffitt et al 2009, Vonsattel & DiFiglia 1998).
It is present in neurons, but also in glia cells (Ross & Tabrizi 2011, Zuccato & Cattaneo 2007) and immune cells (Li & DiFiglia 2012).
It exists evidences that cell–cell interaction plays an important role in HD pathogenesis (Ross & Tabrizi 2011, Zuccato & Cattaneo 2007). In the brain, glia-neuron interactions are important for maintaining the normal function of neurons, but in this chapter I will focus on neurons dysfunction in HD pathology.

At the cellular level, Htt is widely expressed, predominantly in the cytoplasm, but can also be found in the nucleus (**Figure 7**), playing roles in transcriptional regulation (Kegel et al 2002, Xia et al 2003), which has been studied in depth by Luthi-Carter and their colleagues over these past 15 years (more details in paragraph 1.2.6.3.E Transcriptional deregulation).
The subcellular localization of Htt is complex and dynamic, and may change conformation depending on its compartmental localization.

Htt normally localizes along microtubules and participates in the transport of a variety of cargo, including mRNAs, proteins, vesicles, and organelles, such as mitochondria (DiFiglia et al 1995, Kegel et al 2000, Kegel et al 2009, Schulte & Littleton 2011) (**Figure 7**).
Notably, Htt is present in excitatory synapses where it associates with synaptic vesicles in the presynaptic terminal and facilitates neurotransmitter release (DiFiglia et al 1995, Jeong et al 2009). In the postsynaptic density, Htt is associated with the postsynaptic scaffolding protein PSD95 (**Figure 7**) (Sun et al 2001).

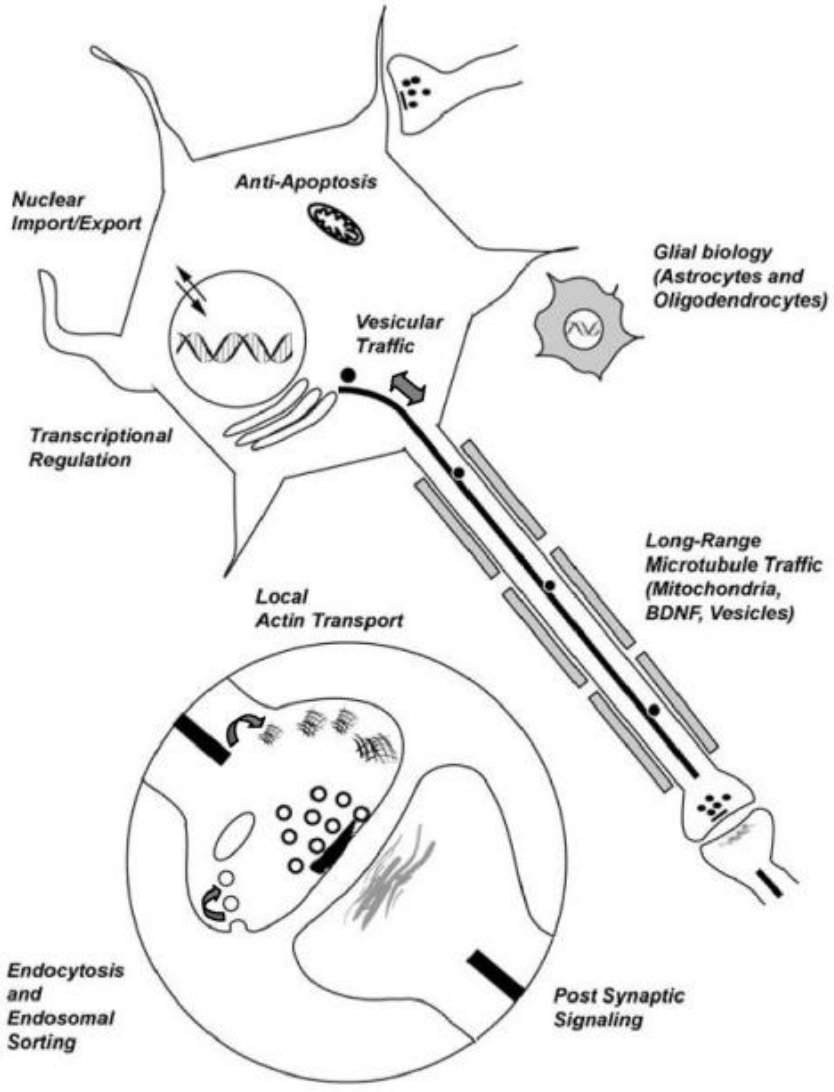

Figure 7 Schematic illustrating the biological functions of wt-Htt (Schulte & Littleton 2011).

The **Figure 7** shows a generic neuron with an unsheathed axon (grey boxes represent oligodendrocyte wrapping) and an astrocyte (grey stellate shape). Enlarged circle is a magnified view of a synapse. The Htt protein has been suggested to regulate both neuronal and glial function. Within neurons, Htt has been implicated in nuclear import and transcriptional regulation. In addition, Htt regulates apoptotic signaling and axonal transport. At the synapse, Htt has been suggested to have both pre- and post-synaptic roles.

Wt-Htt has multiple effects in development and neuronal physiology, including regulation of transcription (Nucifora et al 2001), membrane dynamics (Kegel et al 2009), mitochondrial efficiency (Aoyama et al 2006), brain-derived neurotrophic factor (BDNF) transcription (Zuccato et al 2001), autophagy (Cortes & La Spada 2014, Jeong et al 2009, Kegel et al 2000, Qin et al 2003), and endosomal recycling (Li & DiFiglia 2012) (**Figure 7**).
Several studies reported multiple physiological functions that are particularly important for the brain neurons affected in HD.
Htt is required for normal excitatory synapse development in cortical and striatal circuits (Margulis & Finkbeiner 2014). More globally, it has been shown to be essential for embryonic development, as the knockout of the gene in mice causes embryonic death at the pre-gastrulation stage (Muhlau et al 2012), and in conditional knockout mice (Cre Lox KO under the CamKII promoter) late disruption of the gene in adult leads to progressive neurodegeneration (Dragatsis et al 2000). The antiapoptotic role of Htt was also supported by Michael Hayden's group. They found that primary striatal neurons from YAC18 transgenic mice (for details on animal models of HD, see paragraph 1.2.7. Animal models of HD) overexpressing full-length wild-type human huntingtin were protected from apoptosis compared with cultured striatal neurons from nontransgenic littermates and YAC72 mice expressing mutant human huntingtin (Leavitt et al 2006).
It is known that increased wt-Htt expression improves brain cell survival by modulating caspase-3 and 9 apoptosis signaling. Another way huntingtin produces antiapoptotic effects is through regulation of the neurotrophic factor BDNF. Indeed, wt-Htt regulates BDNF gene transcription, downregulated in HD (Rigamonti et al 2000, Rigamonti et al 2001, Zuccato et al 2001, Zuccato et al 2003). More particularly, Htt levels modulate the sensitivity of neurons to apoptotic death elicited by N-methyl-D-aspartate (NMDA) receptor-mediated excitotoxicity (Leavitt et al 2006), where wt-Htt can decrease cellular toxicity of mHtt in vivo.
On the contrary, cells depleted of wt-Htt were more sensitive to apoptotic cell death and showed increased level of caspase-3 activity, with respect to control cells (Zhang et al 2008).

Wild-type Htt has beneficial activities in the development and mature brain. It is therefore possible that its loss in human HD reduces the ability of neurons to survive and to counteract the toxic effects of the mutant protein.

1.2.6.2.Loss of function of wt-Htt and toxic gain of function of mHtt

Indeed, this single mutation in Htt is the triggering event that endows the protein with new toxic functions that are deleterious for brain cells. At the same time, it also impairs the ability of normal Htt protein to exert molecular activities that are fundamental for the survival and functioning of the neurons that predominantly degenerate in the disease (Bjorkqvist et al 2005, Schulte & Littleton 2011).

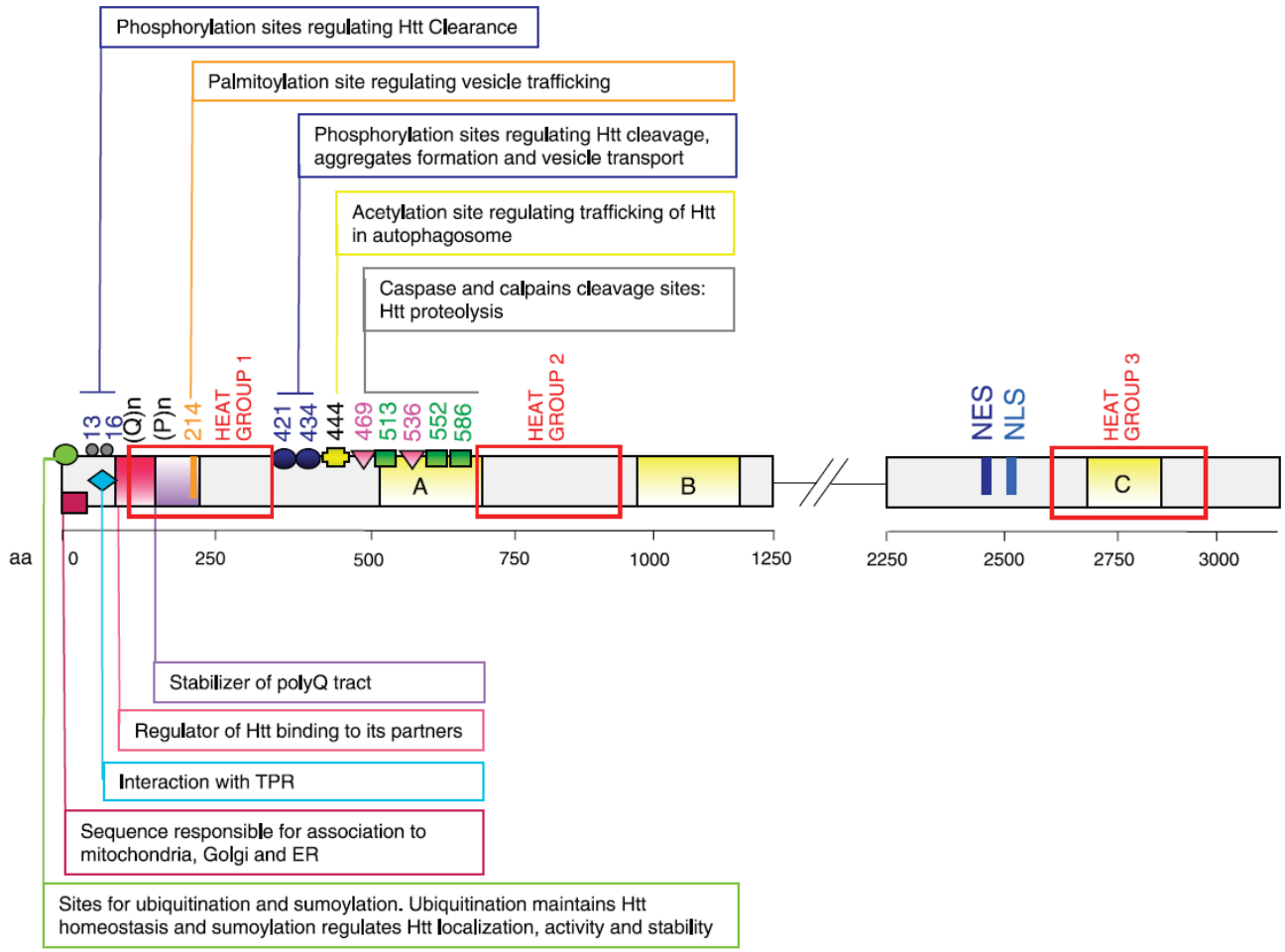

Figure 8 Schematic diagram of the huntingtin amino acid sequence (Zuccato et al 2010).
Details:(Q)n is polyglutamine tract, followed by the polyproline sequence (P)n; red emptied rectangles indicate the three main groups of HEAT repeats (HEAT group 1, 2, 3). The small green rectangles indicate the caspase cleavage sites and their amino acid position (513, 552, 586), while the small pink triangles indicate the calpain cleavage sites and their amino acid positions (469, 536). Boxes in yellow: B, regions cleaved preferentially in the cerebral cortex; C, regions of the protein cleaved mainly in the striatum; A, regions cleaved in both. Post-translational modifications: ubiquitination (UBI) and/or sumoylation (SUMO) sites (green); palmitoylation site (orange); phosphorylation at serines 13, 16, 421, and 434 (blue); acetylation at lysine 444 (yellow). NES is the nuclear export signal while NLS is the nuclear localization signal. The nuclear pore protein translocated promoter region (TPR, azure) is necessary for nuclear export. Htt, huntingtin; ER, endoplasmic reticulum.

Thanks to its polar zipper structure (Perutz 1995) and its diverse configurations, i.e. alpha helix, random coil, and extended loop (Ratovitski et al 2007), this polyQ domain may be important for modulation of wt-Htt function, longevity and energy status of cells (Clabough & Zeitlin 2006), and for stabilization of protein interactions (Schaefer et al 2012), but wouldn't be essential for normal function of Htt.
Htt is also enriched in consensus sequences called huntingtin elongation factor 3, protein phosphatase 2A, and TOR 1 (HEAT) repeats that are organized into protein domains important for protein-protein interactions (**Figure 8**). Htt protein also goes through post-translational modifications and presents consensus sites for proteolytic enzymes (**Figure 8**) (Ratovitski et al 2007).

Functionally active nuclear export signal (NES) sequence and a less active nuclear localization signal (NLS) are present in Htt (**Figure 8)**, which indicate that the protein is involved in transporting molecules from the nucleus to the cytoplasm (Xia et al 2003).
The first 17 N-terminal amino acids of huntingtin revealed that the sequence forms an amphipathic-helical membrane-binding domain that is required and is sufficient for Htt association to mitochondria and for its colocalization with Golgi and endoplasmic reticulum (ER) (**Figure 8**) (Atwal et al 2007, Rockabrand et al 2007). This sequence also enhances the formation of visible aggregates.

Post- translational modifications of Htt protein are various: acetylation, phosphorylation, SUMOylation, ubiquitination, palmitoylation and proteolysis (**Figure 8**). These processes are important for modulation of its interactor affinity, subcellular localization, proteolysis or degradation (Ehrnhoefer et al 2011).
These characteristics make Htt indispensable for the proper functioning of cells.

Thus, it appears that Htt has crucial roles in cells, potentially via different domains, and that loss of the antiapoptotic functions of Htt may contribute to HD (**Figures 7, 8 & 9**).

Processing of mHtt generates an amino-terminal fragment that translocates into the nucleus and a C-terminal portion that remains in the cytoplasm. Some of the full-length protein might also move into the nucleus. The generation of amino-terminal fragments coincides with increased toxic activity in cells. At the same time, extension of the CAG would cause a loss of function in the mutant protein (**Figure 9a**) and/or the mutant protein could act negatively on the functions of the normal one (**Figure 9b**). Finally, loss of Htt function might result as a consequence of decreased protein levels and stability.

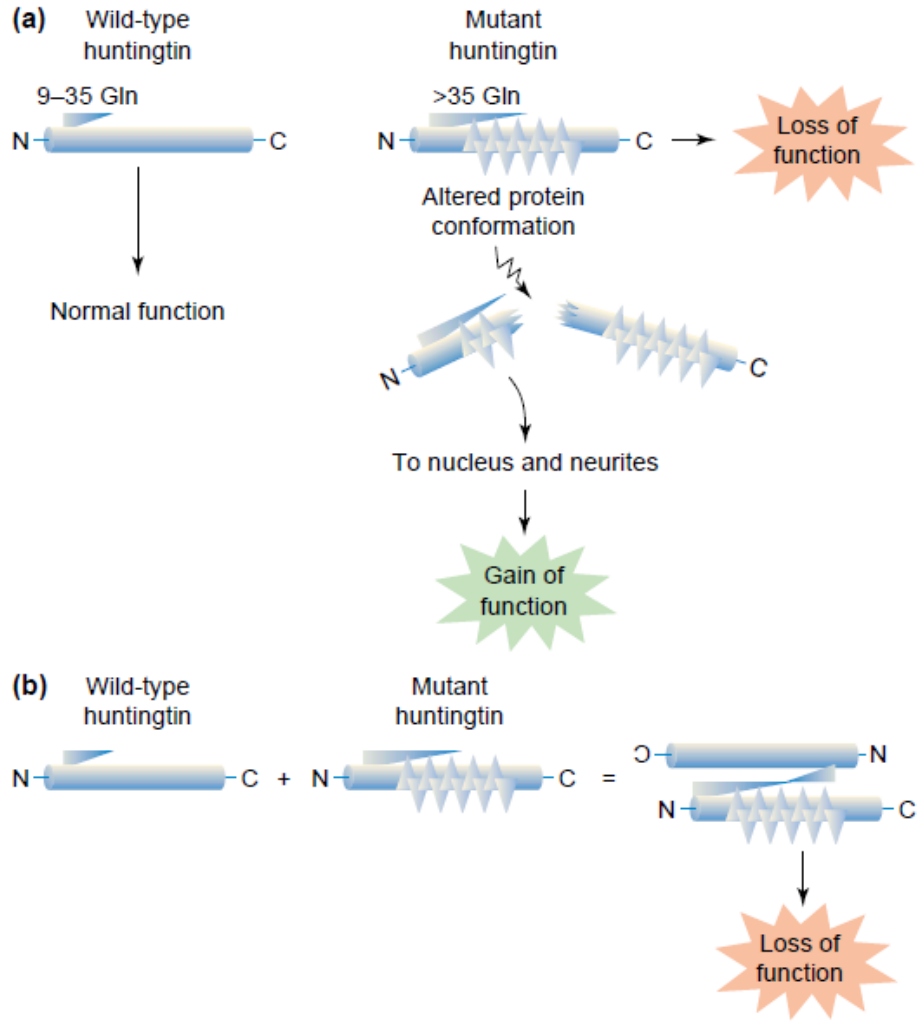

Figure 9 Potential mechanism of cell death in HD (Cattaneo et al 2001).

As such HD may be viewed as a double disease (**Figure 9**), that is caused by both a new toxic property of mHtt and by a loss of the neuroprotective activity of wt-Htt (see as review (Cattaneo et al 2001)).
Overall, these combined effects alter several cellular processes, such as protein degradation, mitochondrial respiration and transcription among many others, leading to neuronal dysfunction and cell loss.

1.2.6.3.Molecular Mechanisms in HD

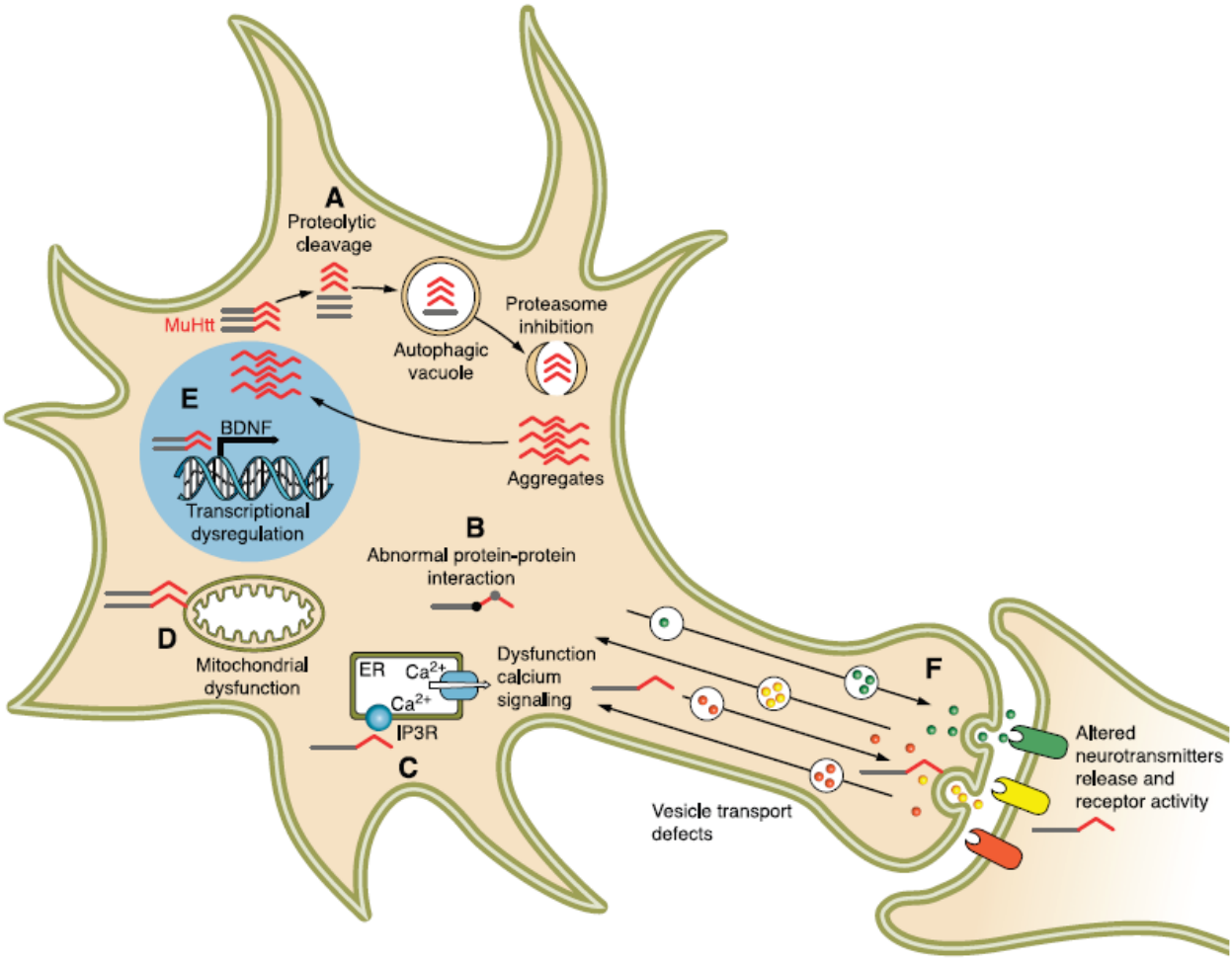

Figure 10 Key cellular pathogenic mechanisms in Huntington's disease HD (Zuccato et al 2010).

Multiple cellular pathways have been implicated in the pathogenesis of HD. These mechanisms could be exclusive or, more likely, have a high degree of cross-talk. The mutation in Htt causes a conformational change of the protein that leads to partial unfolding or abnormal folding of the protein. Full-length mHtt is cleaved by proteases in the cytoplasm. In an attempt to eliminate the toxic Htt, fragments are ubiquitinated and targeted to the proteasome for degradation. However, the proteasome becomes less efficient in HD. Induction of the proteasome activity as well as of autophagy protects against the toxic insults of mHtt proteins by enhancing its clearance (**Figure 10.A**). NH2-terminal fragments containing the poly-glutamine stretch accumulate in the cell cytoplasm and interact with several proteins (**Figure 10.B**) causing impairment of calcium signaling and homeostasis (**Figure 10.C**) and mitochondrial dysfunction (**Figure 10.D**). NH2-terminal mHtt fragments translocate to the nucleus where they impair gene transcription or form intranuclear inclusions (**Figure 10.E**). mHtt alters vesicular transport and recycling (**Figure 10.F**).

From this rapid description, I will go further on details, following the order of the previous description of pathogenic mechanisms in HD, from A to F of Figure 10.

A. Huntingtin cleavages, aggregation and elimination **(Figure 10.A)**

Htt contains well-characterized consensus cleavage sites for proteolytic enzymes that cleave the protein and generate a wide range of fragments (Goldberg et al 1996). Caspases, calpain, and aspartyl proteases are all involved in this process (**Figure 8**). In addition, Htt fragments produced by caspase-independent cleavage accumulate in the cytoplasm and nucleus (Lunkes et al 2002, Ratovitski et al 2007). Proteolytic processing is likely an important initial step in pathogenesis, since expressing the smaller Htt truncation product results in greater cell toxicity than expressing the entire mutant Htt protein (Graham et al 2006, Martindale et al 1998, Qin & Gu 2004) and inhibition of cleavage can lessen neurotoxicity in animal models (Gafni et al 2004, Pattison et al 2006).

PolyQ tracts in proteins might stabilize protein interactions. This happens most likely through structural changes whereby the polyQ sequence extends a neighboring coiled-coil region to facilitate its interaction with a coiled-coil region in another protein. Alteration of this important biological function due to polyQ expansion results in gain of abnormal interactions, leading to pathological effects like protein aggregation (Schaefer et al 2012).

N-terminal fragments of mHtt form aggregates (Davies et al 1997, DiFiglia et al 1997, Scherzinger et al 1997). In HD mouse models and human patients, the appearance of visible mHtt aggregates called inclusion bodies (IBs) correlates with the onset of behavioral deficits.

IBs formation indicates a mismatch between the production and clearance of aggregation-prone protein (Margulis & Finkbeiner 2014). Cell biology studies (Arrasate et al 2004) however indicate that the presence of neuronal intranuclear inclusions may represent a self-defense mechanism to store and neutralize more soluble toxic species. Oligomers of mHtt may represent the toxic species which can interact with many proteins and trigger deleterious events, possibly more than visible "macroscopic" inclusions. mHtt aggregates constitute a neuropathological hallmark of HD. Huntingtin-containing inclusions and aggregates have been previously characterized by immunohistochemistry using the EM48 antibody or other anti-ubiquitin antibodies (Gutekunst et al 1999).

Whether mHtt aggregates are neuroprotective, neurotoxic, or both remains unclear, disordered protein folding and aggregation are a potentially tractable hallmark of HD.

It is tempting to think that aggregation is an event that occurs in response to toxicity of soluble mHtt. It has been shown that soluble mHtt, inducing mitochondrial defects, can be toxic for cultured hippocampal neurons (Tian et al 2014). This is consistent for early stage of the disease, because with progression of the disease, UPS and autophagy are dysfunctionning and overactivated by mHtt aggregates, resulting in a toxic effect of mHtt aggregation in late stage. This is supporting by the group of Lotz (Marcellin et al 2012) putting in evidence that soluble mHtt decrease with aging of Q150 mice whereas mHtt aggregates increase. Different studies have shown when testing therapeutic agents in HD animal models, a recovery of the symptoms arise and a lower number of mHtt aggregates is observed.

For example, Yamamoto et al have shown that in a conditional model of HD by using the tet-regulatable system, blockade of expression in symptomatic mice leads to a disappearance of mHtt inclusions and an amelioration of the behavioral phenotype (Yamamoto et al 2000),

which suggests that aggregation would participate to neuronal dysfunction at late stage in HD models presenting inclusions.
But there are differences between HD animal models and HD patients concerning mHtt aggregates. Indeed, patients have low number of aggregates in the striatum, and mainly in nucleus and somatodendritic cellular compartments (Gutekunst et al 1999).

PolyQ inclusions are also found in post-mitotic non-CNS cells of HD transgenic mice (R6/2 and Q150) (Bjorkqvist et al 2005, Moffitt et al 2009), suggesting that either aggregates are not as deleterious in non-CNS tissues, or that in brain and more particularly in the striatum, additional components come into play to trigger neuronal cell death.

What regulates accumulation of aggregates and inclusions is not totally understood.
The probable misfolding of mHtt due to the polyQ stretch may engender cell stress. Protein misfolding is naturally regulated by chaperone proteins in cells. The fact that several chaperone proteins can reduce mHtt toxicity indicates that indeed, protein misfolding in HD contributes to neurodegeneration.
For example, overexpression of a chaperone HSJ1 in R6/2 mice was shown to reduce the formation of large nuclear aggregates detergent-insoluble mHtt species beginning to aggregate. This approach lightly delayed disease progression (Labbadia et al 2012). Another similar example concerns the chaperone TCP1-ring complex (TRiC) which suppresses mHtt aggregation (Tam et al 2006). It has been shown that an Nterminal fragment of Htt (Htt 171-82Q) induces the up-regulation of endogenous Heat-Shock protein (HSP) 70, found to be colocalized with Htt inclusions. The overexpression of HSP104 and HSP27 modifies the subcellular localization of HSP70 that becomes cytoplasmic, which rescues striatal dysfunction in primary neuronal cultures and HD rat models (Perrin et al 2007)(**Figure 14**).

A possible important mechanism involved in the accumulation of aggregation and more generally mHtt fate, is a defect of systems important for the clearance of misfold and aggregated proteins. Indeed, several important systems for clearance of mHtt are deregulated in HD animal models and humans, as the ubiquitin-dependent proteasome.
The presence of ubiquitinated Htt suggests a failure of the ubiquitin–proteasome system (UPS) (Atkin & Paulson 2014). As mHtt aberrantly accumulates in perinuclear regions and in numerous punctate cytoplasmic structures that resembled endosomal–lysosomal organelles (Sapp et al 1997), it has been proposed that the proteasome may be unable to process expanded polyQ stretches, resulting instead in the accumulation of peptide fragments containing polyQ (Venkatraman et al 2004).

In addition SUMOylation is also another key regulator of protein degradation. The SUMOylation of mHtt may increase its toxic species in the cytoplasm, enhancing neuronal death.

Another important mechanism of mHtt protein degradation and possibly elimination of aggregates is autophagy, which is a process whereby cells remove cytosolic proteins and organelles and in certain circumstances degrade themselves from within.

Autophagy can be induced by apoptotic stimuli in the presence of caspase inhibitors (Merienne et al 2003), and may contribute to cell death through the regulation of lysosomal proteases cathepsin B and D (Goula et al 2012)(Ohsawa et al., 1998). Mutant Htt can be cleared by macro-autophagy but impairs its own clearance through impaired cargo recognition (Martinez-Vicente et al 2010). Enhancement of autophagy can be obtained by inhibition of mammalian target of rapamycin (mTOR) by Rapamycin. It produces on the HD mouse model R6/2 an improvement of survival curve (Ravikumar et al 2004), which is a good trail to follow to develop new therapeutic tools (see **Figure 14)**.

B. Abnormal protein-protein interaction **(Figure 10.B)**

Mutant Htt is toxic to striatal neurons, but this toxicity is probably related to one or a few of the more than hundred proteins that interact with Htt. Indeed, being a large protein, Htt has numerous binding partners [see as review (Clabough 2013, Harjes & Wanker 2003)] (**Figure 8**), including transcription co-activators, co-repressors, and apoptosis-related kinases, protein involved in signaling, cell transport, energy metabolism (**Figure 7**). The presence of the expanded polyQ stretch, can lead to changes (increase or decrease) in the interaction of mHtt with binding partners **(Table 1**) (see as review (Clabough 2013)). It also exists evidences of post-translational differences between healthy and HD conditions, for example mHtt would impact on Tau phosphorylation leading to a toxic hyperphosphorylation of Tau [(Blum et al 2014); see **Annexe 6.2.**].

Alterations in numerous signal transduction pathways and aberrant activity of specific kinases have been identified in multiple cell and mouse models of Huntington's disease (HD), as well as in human HD brain. The balance and integration of a network of kinase signaling pathways is paramount for the regulation of a wide range of cellular and physiological processes, such as proliferation, differentiation, inflammation, neuronal plasticity and apoptosis. mHtt has wide ranging effects on multiple pro- and anti-apoptotic kinases, resulting in the dysregulation of numerous complex interactions within a dynamic network (see as review (Bowles & Jones 2014)).

For example, activation of the C-terminus part of c-Jun (jnk) pathway would be the consequence of the weaker interaction between Htt and the mixed-lineage kinase 2 (MLK2), which is important for jnk activation (Liu et al 2000). It has been seen an higher activation of this pathway in striatal culture cells expressing mHtt in presence of DA (Charvin et al 2005). Jnk activation is followed by nuclear translocation and a higher phosphorylation of c-Jun, inducing apoptosis (Herdegen & Waetzig 2001).

Akt, a serine-threonine kinase, also known as protein kinase B (PKB), is a potent pro-survival kinase that exerts its survival effect in neurons by phosphorylating several substrates (Franke et al 2003). These substrates include components of the cell death machinery (e.g. BAD), glycogen synthase kinase-3β (GSK3β) and transcription factors of the forkhead (FOXOs) family. In HD, Akt phosphorylates mHtt and this phosphorylation abrogates its toxicity (Humbert et al 2002). Saudou and Humbert's group showed that during late stages of the disease, Akt is cleaved into an inactive form by caspase-3, which ensures the irreversible deactivation of Akt and abolishes the ability of Akt to promote survival in cells expressing polyQ-huntingtin (Colin et al 2005).

HD mutation leads to aggregate sequestration of various proteins, including transcription factors. Indeed, proteolytically cleaved N-terminal fragments of mHtt can translocate into the nucleus to form neuronal intranuclear inclusions, which recruit transcription factors such as CBP, TBP, CA150 and Sin3A (**Table 1**) and therefore disrupt gene transcription, leading to neurodegeneration.

Name	Protein function	Htt binding region	Influence of mu HTT
Transcription			
CA150	Transcription activator	Unknown	None
CBP	Transcription activator	Amino acids 1-588	Enhances
CtBP	Transcription repressor	Unknown	Decreases
HYP-A, B	RNA splicing factors	Polyproline	Enhances
HYP-C	Transcription factor	Polyproline	Enhances
NCOR	Transcription repressor	Amino acids 1-171	Enhances
NF-κB	Transcription factor	HEAT repeats	Unknown
SP1	Transcription activator	Amino acids 1-171	Enhances
TAFII130	Transcription activator	Amino acids 1-480	None
TBP	Basal transcription factor	Unknown	Unknown
P53	Transcription factor	Polyproline	None
REST-NRSE	Trascription suppressor	Amino acids 1-548	Decreases
Trafficking and endocytosis			
HAP1	Trafficking, endocytosis	Amino acids 1-230	Enhances
HIP1	Endocytosis, pro-apoptotic	Amino acids 1-540	Decreases
HIP14	Trafficking, endocytosis	Amino acids 1-550	Decreases
PACSIN1	Endocytosis	Polyproline	Enhances
Phosphatidylethanolamine PI(3,4,5)P3	Phospholipids	Amino acids 171-287	Enhances
PSD-905	Synaptic scaffolding	Unknown	Decreases
Signaling			
Calmodulin	Calcium-binding regulatory protein	Unknown	Enhances
CIP-4	Cdc42-related signaling	Amino acids 1-152	Enhances
FIP2 (HYP-L)	GTPase Rab8 interactor	Amino acids 1-550	Unknown
GRb2	Growth factor signaling	Polyproline	Unknown
IP31	Calcium release channel	Amino acids 1-158	Enhances
SH3GL3	Endocytosis and vesicle recycling	Polyproline	Enhances
RasGAP	Ras GTPase-activating protein	Polyproline	Unknown
Metabolism			
Cystathionine b-synthase	Generation of cysteine	Amino acids 1-171	None
GAPDH	Glycolitic enzyme	Polyproline	Enhances
gp78	ER membrane-anchored ubiquitin ligase	HEAT repeats 2/3	Enhances
HIP2	Ubiquitin-conjugated enzyme	Amino acids 1-540	None
Protein Synthesis			
Gnb211	Translation (indirect,) ribosomal protein	Unknown	Decreases
Myo5a	RNA transport to spines	Unknown	Decreases
Rps6	Translation (direct), Ribosomal protein	Unknown	Decreases
Prkra	Translation (indirect), PKR regulation	Unknown	Decreases

Table 1 Huntingtin interacting proteins and impact of mHtt on interactors protein expression (Clabough 2013).

Abbreviations: CA150, co-activator 150; CBP, (cAMP-response element binding protein) binding protein; CiP-4, cdc42-interacting protein 4; Co-iP, co-immunoprecipitation; CtBP, C-terminal-binding protein; FiP2, for 14.7K interacting protein; GAPDH, glyceraldehyde 3-phosphate dehydrogenase; Gnb2l1, guanine nucleotide-

binding protein (G protein) polypeptide 2-like 1; gp78, glycoprotein 78; GRB2, growth factor receptor-binding protein 2; GST, glutathione S-transferase; HAP1, htt-associated protein 1; HiP, htt-interacting protein; HyP, htt-yeast partner; iP31, inositol (1,4,5)-trisphosphate receptor type 1; Myo5a, myosin V;A NCOR, nuclear receptor co-repressor; NF-kB, nuclear factor-kB transcription factor; PACSiN1, protein kinase C and casein kinase substrate in neurons 1; [Pi(3,4,5)P3] phosphoinositol, (Pi) 3,4-bisphosphate, Pi 3,5-bisphosphate, and Pi 3,4,5-triphosphate; PKR, doublestranded RNA-activated protein kinase; Prkra, interferon inducible double-stranded RNA-dependent protein kinase activator A; PSD- 95, postsynaptic density 95; RasGAP, Ras GTPase-activating protein; REST–NRSE, the repressor element-1 transcription factor–the neuron restrictive silencer element; Rps6, ribosomal protein S6; SH3GL3, SH3-containing GRB2-like protein 3; SP1, specificity protein-1; TAFii130, TBP-associated factor; TBP, TATA box binding protein.

C. Dysfunction calcium signaling **(Figure 10.C)**

Mutant Htt causes cytosolic and mitochondrial calcium (Ca^{2+}) overload and apoptosis of HD MSN. Mutant Htt perturbs Ca^{2+} signaling by enhancing NMDA receptor function, possibly through decreased interaction with the PSD95-NR1A/NR2B complex (Song et al 2003, Zeron et al 2001). Moreover, mHtt binds the COOH terminus of the inositol 1,4,5-triphosphate receptor 1 (InsP3R1) on the endoplasmic reticulum and renders the receptors more sensitive to IP3, which causes Ca^{2+} release through the InsP3 R1 (Tang et al 2003). DA released from midbrain dopaminergic neurons stimulates D1 and D2 receptors (D1R, D2R). D1R are coupled to activation of adenyl cyclase, increase in cAMP levels, and activation of protein kinase A (PKA), which potentiates glutamate-induced Ca2+ signals by facilitating the activity of NMDAR and InsP3 R1. D2R are coupled directly to InsP3 production and activation of InsP3 R1. Ca^{2+} signals activate calpain, which cleave Htt and other substrates. Excessive cytosolic Ca^{2+} signals result also in mitochondrial Ca^{2+} uptake, which eventually triggers apoptosis (Choo et al 2004).
The mitochondrial Ca^{2+} handling is further destabilized by direct association of mHtt with mitochondria (Panov et al 2002). All this Ca2+ deregulation may lead to enhanced vulnerability to excitotoxicity at glutamatergic synapses. In line with this some HD mouse models show, at early ages, increased susceptibility to intrastriatal injection of the NMDA-R agonist quinolinate. However, older mice become resistant to excitotoxicity.

D. Energy defects **(Figure 10.D)**

The hypothesis that energy impairment could play a key role in HD was proposed by Beal (Beal 1992) and Albin (Albin et al 1992), who suggested that chronic defects in energy metabolism could indirect excitotoxicity.

First evidence of a mitochondrial defect in HD came from very early studies indicating biochemical abnormalities in mitochondria isolated from HD cortical autoptic tissue (Gardian & Vecsei 2004, Goebel et al 1978).
Biochemical studies of brain and peripheral tissues from HD patients, as well as studies on HD cells and animal models, revealed decreased activity of several enzymes involved in oxidative phosphorylation such as complex I, II, III, and IV (Arenas et al 1998, Brouillet et al 1995, Damiano et al 2010, Gu et al 1996, Mochel & Haller 2011, Tabrizi et al 1999).

More generally, PET scan studies showed very early defects in brain energy metabolism, in particular in the striatum (for a review Brouillet et al., 1999). NMR spectroscopy indicated increased lactate concentrations in HD patients, suggesting defects in oxidative energy metabolism (Jenkins et al. 1993 ; 1998), possibly at the level of mitochondria.
Supporting the hypothesis that chronic energy impairment could play a role in HD, it has been shown that chronic intoxication with the mitochondrial toxin 3-nitropropionic acid , an inhibitor of mitochondrial complex II (C-II) leads to preferential degeneration in rats (Beal et al JN 1993) and non-human primates (Brouillet et al., 1995); these pioneering studies led several groups to more closely look at the possible effects of mHtt on mitochondria. mHtt binds directly to mitochondria, thereby altering their metabolic activity, Ca2+ handling capacity, motility within the cells and shape through abnormal interaction with the DRP-1 protein trigerring increased mitochondrial fission (Damiano et al 2010, Trushina et al 2004).
Mutant Htt also produces an increased production of reactive oxygen species (ROS), possibly through perturbation of oxidative phosphorylation in mitochondria. Although data on post mortem tissues show contrasting results on the presence of oxidative stress products (Browne et al 1997), different approaches in vitro and in vivo indicated that mHtt produces preferential loss of C-II subunits (Benchoua 2006; Damiano 2013) in animal models of HD and HD patients. In HD models, reduced expression of C-II, associated with loss of mitochondrial membrane potential and cell death. Overexpression of these subunits using lentiviral strategy in neuroprotective against mHtt, indicating that this event is causal in HD.
There are a number of transcription factors known to regulate genes responsible for mitochondrial function and oxidative stress (Cha 2007). The group of Dimitri Krainc and colleagues showed that mHtt also represses transcription of PGC-1α, a gene encoding for a transcriptional co-activator that regulates expression of genes involved in mitochondrial biogenesis and respiration. The expression of these genes is severely impaired in the disease. Moreover, PGC-1α knock-out mice exhibit mitochondrial defects accompanied by hyperkinetic movement disorder and striatal degeneration (Cui et al 2006). Another group has shown that PGC-1α promoted Htt turnover and the elimination of protein aggregates by activating transcription factor EB (TFEB), a master regulator of the autophagy-lysosome pathway (Tsunemi et al 2012).

The majority of the cellular events compromised during disease progression are highly energy dependent processes. Hence, impairments of these functions could stem from or be amplified by mHtt-induced mitochondrial and energetic defects.

E. Transcriptional deregulation **(Figure 10.E)**

Initial reports during the 1980s and 1990s demonstrated selective altered expression of highly identifiable neuronal genes, such as neurotransmitter receptors and neuropeptides, first in patients brain and later in animal models (Augood et al 1997, Cha et al 1998, Emson et al 1980).
It was hypothesized that mHtt reduces the expression of a distinct set of genes involved in signaling pathways known to be critical to striatal neuron function (Luthi-Carter et al 2000).

The importance of transcriptional dysregulation in the pathology of HD was demonstrated by nuclear-restricted variants of mHtt transgenes that reproduced part of the HD symptoms (Benn et al 2005, Schilling et al 2004).

Some of the major conclusions derived from HD transcriptomics are that 1) transcriptional dysregulation is an early and progressive event, 2) transcriptional dysregulation affects relevant genes for brain function, 3) HD transcriptional signatures are a complex mixture of common and specific changes, 4) HD is not fully explained by mitochondrial dysfunction.

Transcriptional dysregulation has been proposed to comprise one of the earliest and most central mechanisms of HD pathogenesis, and a large body of experimental evidence supports this hypothesis. Transcriptional profiling of HD human brain and *in vivo* and *in vitro* disease models demonstrates large changes in the expression of coding and non-coding RNAs (Desplats et al 2006, Hodges et al 2006, Lee et al 2011, Luthi-Carter et al 2002, Luthi-Carter et al 2000, Marti et al 2010, Runne et al 2008). A variety of mechanisms have been proposed to explain how mHtt causes transcriptional dysregulation (reviewed in (Beal & Ferrante 2004, Cha 2007, Helmlinger et al 2006). These include inhibition of positive regulators of transcription by both sequestration and soluble interaction mechanisms, as well as loss of inhibition of negative regulators of transcription (**Figure 11**).

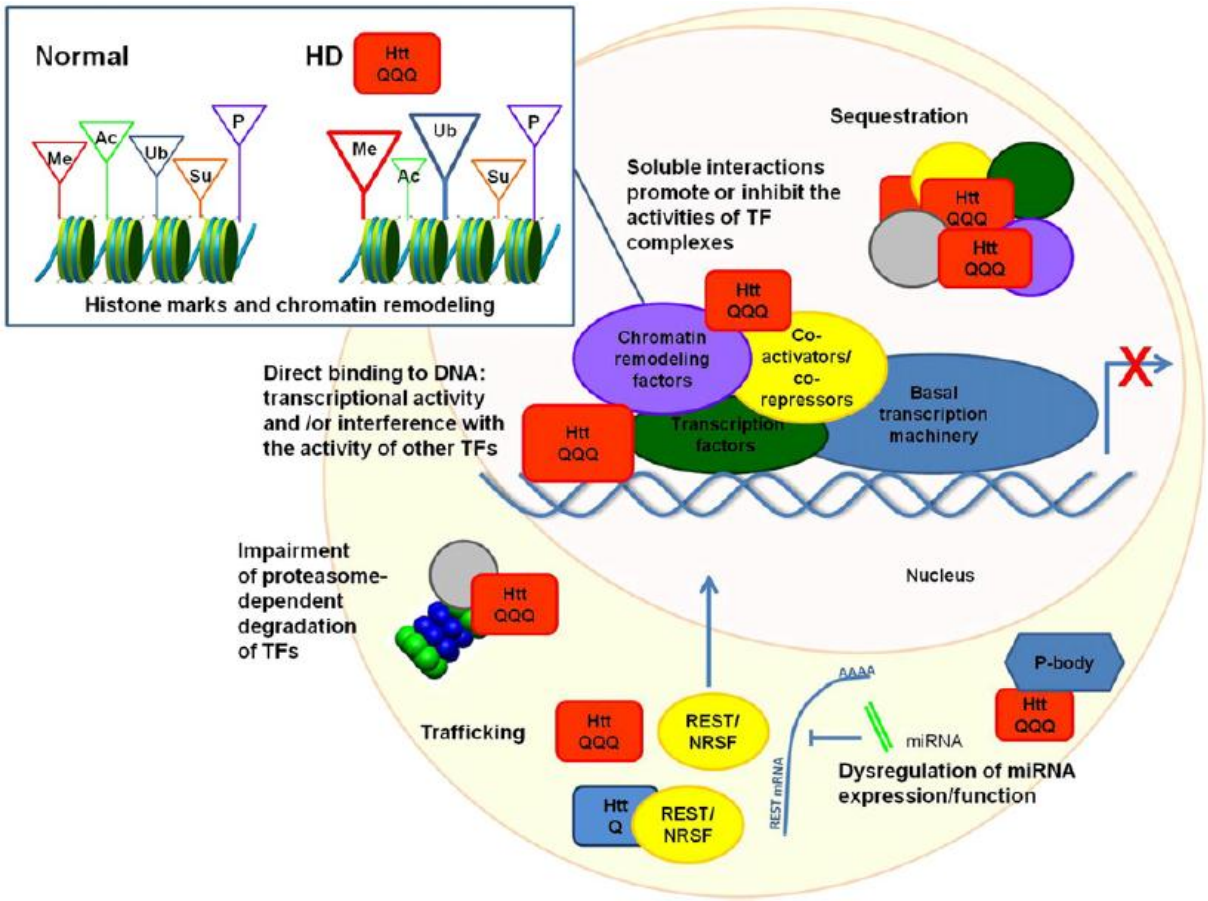

Figure 11 Mechanisms of dysregulation of gene expression in Huntington's disease (Seredenina & Luthi-Carter 2012).

Mutant Htt interferes with the transcriptional machinery at different levels (**Figure 11**).

Mutant Htt sequesters transcription factors and co-factors into insoluble aggregates (Andrew et al 1993, Kazantsev et al 1999, Nucifora et al 2001, Steffan et al 2000). Soluble interactions of mHtt with transcriptional regulators inhibit or promote the activity of transcription factor complexes (Dunah et al 2002, Hannan 1996, Li et al 2002). The RE-1 silencing transcription factor (REST) is a repressor that is proposed to silence transcription of numerous neuron-specific genes. Htt regulates nuclear-cytoplasmatic trafficking of REST/NRSF and mHtt fails to retain REST/NRSF in the cytoplasm, thereby allowing it to enter the nucleus and repress the expression of neuronal genes (Zuccato & Cattaneo 2007, Zuccato et al 2003). Htt might bind to DNA and regulate DNA structure and/or the binding of other transcriptional regulatory proteins. Mutant Htt changes chromatin status by increasing histone methylation and ubiquitination and by decreasing histone acetylation (Ferrante et al 2003, Steffan et al 2001). Mutant Htt changes the activity of transcription factors by impairing their clearance by the proteasome. Mutant Htt alters the transcription or processing of miRNAs, resulting in an altered stability of their target mRNAs (Chen et al 1999, Dunah et al 2002).

Investigations based on DNA microarray technology showed a large number of gene expression changes in cellular and mouse models of HD. They indicate also that gene dysregulation occurs before the onset of symptoms, suggesting that transcriptional dysregulation is an important causative factor in the disease (Cha 2007). A large set of data also indicates the absence of a single transcriptional regulator having a primary role in HD and rather demonstrates the involvement of different transcription factors and DNA target sequences and some critical pathways in HD, such as the GC-box/Sp1-mediated, the CRE/CREB regulation systems, and the REST/NRSF regulon (Cha 2007, Johnson & Buckley 2009) (**Figure 12**).

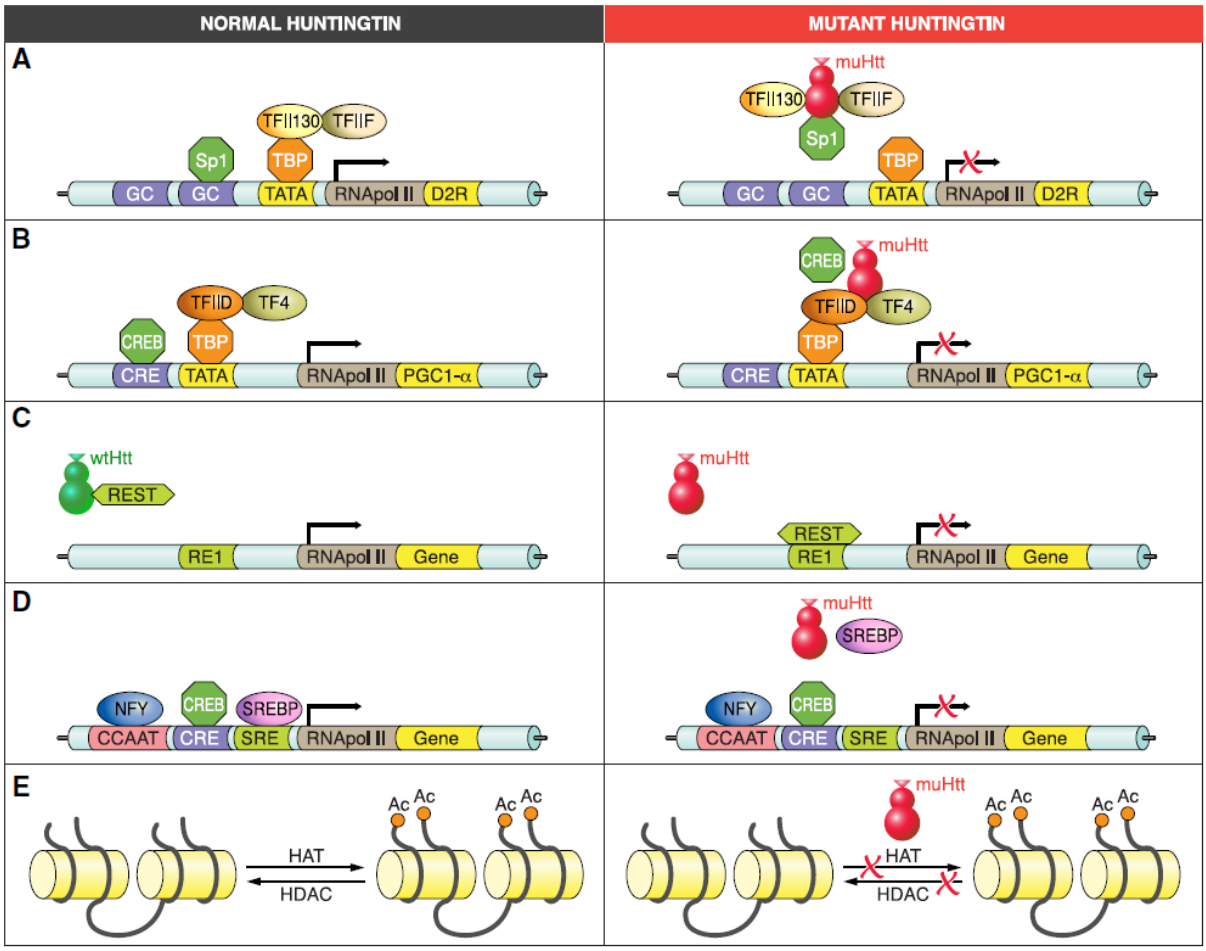

Figure 12 Transcription factors, DNA target sequences, and chromatin structure in HD (Zuccato 2010).

Expanded polyQ in huntingtin represses transcription of Sp1-dependent promoters (i.e., D2R gene) by abnormally interacting with specific transcription cofactors such as Sp1 itself, TFIIF, and TFII130 (**Figure 12, A**).

The transcription factor cAMP-responsive element (CRE)-binding protein (CREB) binds to DNA elements that contain a CRE sequence, as in the promoter of the PGC1-α gene, a master regulator of genes involved in mitochondrial function and energy metabolism. Mutant Htt interferes with CREB and TFIID, leading to reduced activation of PGC1-α gene, reduced PGC1-α protein levels, and consequently, downregulation of its mitochondrial target genes (**Figure 12, B**).

The transcription factor REST/NRSF binds to RE1/NRSE elements in neuronal gene promoters such as in the BDNF gene. Wild-type Htt sustains the production of BDNF by interacting with REST/NRSF in the cytoplasm, thereby reducing its availability in the nucleus to bind to RE1/NRSE sites. Under these conditions, transcription of BDNF and of other RE1/NRSE regulated neuronal genes is promoted. Mutant Htt fails to interact with REST/NRSF in the cytoplasm, which leads to increased levels of REST/NRSF in the nucleus. Under these conditions, REST/NRSF binds avidly to the RE1/NRSE sites, suppressing the transcription of BDNF and of other RE1/NRSE regulated neuronal genes (**Figure 12, C**).

SREBP binds to SRE to regulate the transcription of genes involved in the cholesterol biosynthesis pathway.

Under physiological conditions, SREBP is transported from the endoplasmic reticulum to the Golgi region, where it is cleaved to obtain a fragment that enters the nucleus and activates cholesterogenic genes. In the presence of mutant huntingtin, this mechanism is impaired, which leads to the reduced expression of SREBP-dependent genes and decreases the biological effects of cholesterol biosynthesis (**Figure 12, D**).
E, levels of histone acetylation at specific lysine residues are determined by concurrent reactions of acetylation (Ac) and deacetylation, which are mediated by histone acetylases (HATs) and histone deacetylases (HDACs). Histone acetylation is vital for establishing the conformational structure of DNA-chromatin complexes suitable for transcriptional gene expression. Mutant huntingtin leads to disruptions in HAT and HDAC balance, leading to general transcriptional repression (**Figure 12, E**).

F. Abnormal axonal transport **(Figure 10.F)**

Striatal neurons depend on BDNF to maintain their health, delivered from cortex to striatum (Zuccato & Cattaneo 2007). Thus early loss of BDNF release in the striatum would favor striatal vulnerability in HD.
The expression of the N-terminal fragments of mHtt is enough to cause neuronal degeneration, but is not sufficient to maintain Htt axonal transport functions (Gauthier et al 2004). Interestingly, the proteins involved in other neurodegenerative diseases do not affect BDNF transport.
It has been shown that wt-Htt specifically enhances anterograde and retrograde BDNF vesicle transport in cell system. The group of Frederic Saudou proposed that reduced BDNF levels in the HD striatum may depend also on reduced transport of BDNF vesicles along the cortico-striatal afferents (Gauthier et al 2004). They explained it by the inhibition of Htt, HAP1, and motor proteins' association to microtubules caused by polyQ expansion.
Several studies support the hypothesis that a deficit in BDNF is a major contributor to HD pathogenesis, suggesting the possibility that delivering BDNF or increasing endogenous BDNF production may stop or delay the progression of the human disease. In addition they showed that the release of BDNF may be reduced in HD, possibly through the involvement of the chaperone HSJ1B (Borrell-Pages et al 2006).

Consequences of gain of toxic function of mHtt detailed in this current chapter can be linked. For example, it has been shown that phosphorylation of mutant huntingtin at S421 restores anterograde and retrograde transport in neurons (Zala et al 2008), thanks to restoration of the interaction between Htt and a subunit of dynactin, and their association with microtubules in vitro. This phosphorylation at S421 can be induced by the insulin growth factor type I (IGF-1)/Akt pathway. Because of alteration of interaction protein-protein with mHtt, some roles of wt-Htt are impaired, which is leading to opposite effects of Htt protein.

1.2.7. Animal models of HD

There is no known naturally occurring animal model of HD. For that reason, numerous genetic animal models of HD have been generated since the discovery and cloning of the HTT gene in patients in the past twenty years, by the introduction of the mutant gene into non-human primate, mouse, fly, fish, and worm has generated disease models.

1.2.7.1.Non genetic models

Before the discovery of the main cause of HD, i.e. mutation in the HTT gene, non-genetic models were used, and are still used in some studies. They typically induce cell death either by direct triggering of excitotoxicity (DiFiglia 1990) or by primary blockade of energy metabolism.
Quinolinic acid (QA) and kainic acid (KA) have been the two most commonly used excitotoxic agents in both rodent (Beal et al 1986, Vecsei & Beal 1991) and non-human primate models of HD (Hantraye et al 1990). These amino acids (QA and KA) induce cell death by binding to their cognate receptors, N-methyl-D-aspartic acid (NMDA) and non-NMDA, respectively, on striatal neurons.
The mitochondrial toxins 3-nitropropionic acid (3-NP) and malonic acid (MA) have also been used in both rodents (Beal et al 1993, Ludolph et al 1991) and non-human primates (Brouillet et al 1995) to produce cell death in striatal neurons via inhibition of the Complex II (succinate dehydrogenase) of the tricarboxylic acid cycle and the electron transport chain in mitochondria, effectively reducing production of adenosine triphosphate (ATP) (see as review (Brouillet 2014)).
The excitotoxic lesion models of HD are useful to highlight potential pathways and processes that are implicated in the pathogenesis of HD, including aberrant glutamate signaling, and mitochondrial dysfunction and associated energetic defects.
Nevertheless, these models have a number of limitations, including the nature of the lesions, the acute appearance of striatal lesions within a few hours to few days that contrasts with decades in HD patients, the restricted pathology in striatal neurons that doesn't take into account the other brain regions and peripheral incidence of the expression of mHtt in all cells of the body, and the lack of Htt cytoplasmic inclusions that are a pathological hallmark of the disease.

1.2.7.2.Genetic models

In 1996, the first transgenic mouse model was generated by introducing a fragment of a juvenile HD patient's HTT gene into the mouse genome (Mangiarini et al 1996). The mouse models generated in this pioneering study, called R6/2 mice and R6/1 mice (Mangiarini et al 1996) have been widely used since and are often studied at present. Since, many other models have been developed in mice, rats, zebrafish, Drosophilia Melanogaster, C.elegans, song birds, mini-pigs, sheep and non-human primates (Pouladi et al 2013). All these models have in common that they express part or the entire mutant HTT but they have major differences in terms of symptomatology, neuropathology, onset of disease and life span.

What differentiates one model to another can be summarized according to the following considerations (**Figure 13**):

a) use of full-length or only a fragment of mutated HTT;
b) length of the CAG repeat incorporated into the genetic construct;
   use of a coding region containing only CAG repeats or one containing repeats that are interrupted with one or more CAA codons (which also code for glutamine, but stabilize the number of repeat from generation to generation avoiding the anticipation phenomenon);
c) expression of the HD mutation from a transgene or knock-in of the mutation into the endogenous Hdh locus;
   use of human HTT gene or the endogenous HTT gene of the animal;
d) use of complementary DNA (cDNA) or genomic DNA containing all the introns and regulatory sequences in YAC or BAC vectors;
e) use of the HTT promoter or another promoter to drive expression of the mutant protein, which leads to major differences in the level of expression, and the spatial/cellular pattern of expression.

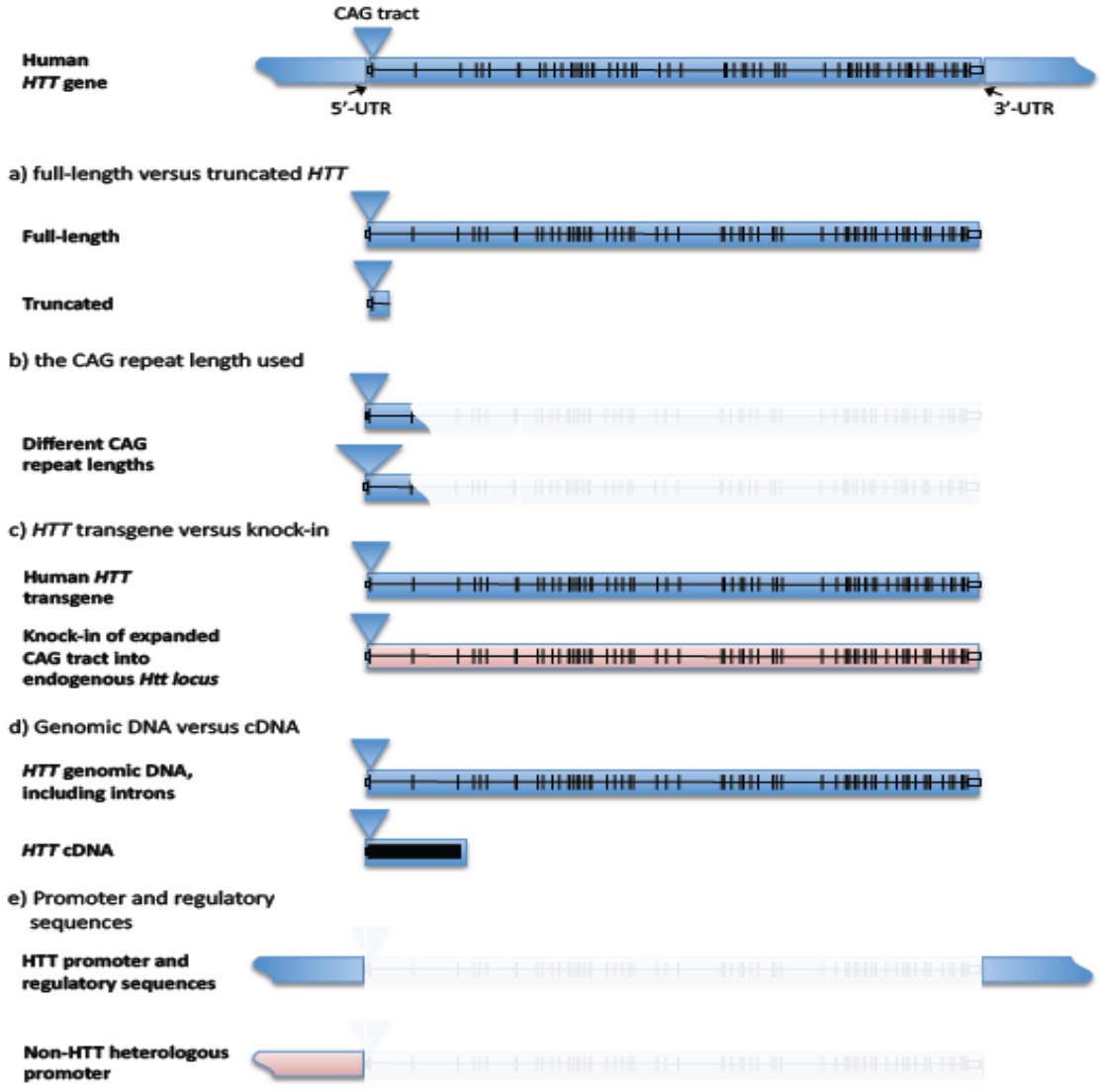

Figure 13 Genetic attributes of animal models of HD (Pouladi et al 2013).

Because of the number of diverse models, I shall only mention here the models used for my PhD study.

1.2.7.3.Transgenic models

Transgenic models result from the random insertion of a portion of the human htt gene, containing the polyglutamine repeat, in the mouse genome, the expression of which can be driven by different promoters.
Borchelt and colleagues created the N171-82Q transgenic mouse model by inserting the first 171 amino acids from the N-terminal of the human htt gene into the mouse genome (Schilling et al 1999). Expression of the N-terminal fragment of htt in this model is driven by the mouse prion promoter and, as such, mutant htt is expressed throughout the mouse brain. But its expression is restricted to neurons and is not found in glia. These transgenic mice contain two normal (wild-type) copies of the HTT genes along with one mutated copy of the truncated human htt gene. This model has fewer 82 polyglutamine repeats, which leads to displaying resting tremor, hypokinesia, hindlimb and forelimb clasping, and abnormal gait beginning at week 11, and showing a progressive decline in performance on the rotarod test as well as the onset of clasping. They have a reduced life span, dying around 120-150 days. This model has been often used to study genetic modifiers and experimental therapeutic interventions (Beal & Ferrante 2004).

1.2.7.4.Knock-in models

"Knocking in" a portion of the human HTT gene in the HTT gene locus results in the creation of knock-in models (Ki). The exogenous htt promoter drives expression of the mutant htt protein in these animals and so production of the mutant protein is both spatially and temporally accurate.
It exist Ki mice with different length of the CAG repeats sequence: from 50Q to 175Q. The main characteristics of these models are the slowly progressive appearance of the symptoms, reflecting human HD pathology (Lin et al 2001, Menalled et al 2012, Menalled et al 2003, Rising et al 2011, Wheeler et al 2000). The first model that has been generated is the Hdh(Q111) knock-in mice by Marcy MacDonald's group (Wheeler et al 2002).
Zeitlin's group created a slowly progressing mouse model of HD, the knock-in mice expressing chimeric mouse/human exon 1 containing 140 CAG repeats inserted in the murine HTT gene (Ki140CAG) (Menalled et al 2003). Mice were N3 (B6) on a 129 Sv×C57BL/6 J background. Ki140CAG mice are described in the literature with minor hypoactivity at 1 month of age, as seen using an open-field test, but at 12 months motor dysfunction is more apparent, seen by overt gait abnormalities and decrease in stride length. These mice show increased rearing behavior using forelimbs compared to wild-type mice at 1 month of age, but a significantly decline of rearing at 4 months is reported. These mice show significant rotarod deficits at 9 months old compared to wild-type littermate controls. Inclusion bodies appear in CAG140 knock-in mouse brains—in the striatum, cortex, hippocampus, and cerebellum—starting at 2 months, and progressively increase in both size and number. These aggregates form in both the nucleus and neuropil as seen in HD patients.

1.2.7.5.Viral-mediated HTT gene transfer models

In parallel of the use of transgenic and Ki models, various viral vectors have been developed and utilized for transferring genes in the brain (Deglon & Hantraye 2005, Kirik & Bjorklund 2003). The recombinant viral vectors utilized for CNS gene transfer studies have been derived from adeno-associated virus (AAV), lentivirus (LV), adenovirus (Ad), and herpes-simplex virus (HSV).
In our study, we used the *in vivo* HD LV model , described to be a highly flexible approach for the targeted overexpression of mHtt, with rapid and progressive degeneration of striatal neurons in rat and mice (Ruiz & Deglon 2012). A similar approach in non-human primates showed that intrastriatal injection of LV coding the first 171 amino acids of mHtt with 82Q (LV-Htt171-82Q) leads to progressive appearance of dyskinesia and choreiform movements (Palfi et al 2007). The LV-Htt171-82Q model in rodent has often been used to study mechanisms underlying mHtt toxicity and provides the proof of principle of testing new experimental therapeutics targeting different cellular component such as protein chaperones, mitochondrial enzymes, kinases (JNK and MSK1) transcription factors (CA150) and mHtt itself (Damiano et al 2013, Drouet et al 2009, Galvan et al 2012, Perrin et al 2009, Perrin et al 2007) (review Ruiz et al, 2012). The expression level of mHtt produced by the LV-Htt171-82Q vector (which uses the pan-neuronal promoter PGK) is approximately 25-fold higher than the level of endogenous Htt (Drouet et al 2009). Striatal degeneration occurs within 8-12 weeks in rats and 4-6 weeks in mice.

Infection of a limited number of cells, or a subtype of cells, is particularly suited for dissecting the contribution of specific circuitry and pathways in these pathogenic processes.
HD models have been also developed using similar strategy with adeno-associated virus (AAV) model. The first in vivo study in adult rats was performed using an AAV vector for expressing a GFP fusion protein containing a long polyQ tract (Senut et al 2000). Intrastriatal injection of this vector caused rapidly intracytoplasmic and ubiquitinated intranuclear aggregates in neurons. This study demonstrated that expression of an Htt polyQ tract throughout life does not necessarily induce cell death, but rather that acute overexpression of a polyQ tract in adult neurons is sufficient to induce pathology.

1.2.7.6.HD models diversity

From cells to non-human primates, a large spectrum of organisms has been used to model HD, but a particular effort has been made on rodent models, more complex than culture cells but less expensive than non-human primates (see as review (Perrin 2014, Pouladi et al 2013, Ramaswamy et al 2007)).

1.2.8. Past and future HD therapies

Current therapies for HD provide control of some of the major troublesome symptoms (chorea, psychosis, depression). However, these treatments are only "symptomatic", meaning that they ameliorate the clinical features of the illness, but the benefits are only temporary and disappear when the treatment is stopped. Unfortunately, no current therapy has shown to interfere with the underlying natural history of the disease, slowing or halting its progression.

1.2.8.1.Symptomatic treatments

Some symptoms can be managed with medication (Im & Kim 2014, Ross & Tabrizi 2011) (**Table 2**).

Treatment of chorea		
Antidopaminergic agents	Tetrabenazine	Jankovic & Beach 1997; Ondo et al., 2002
Antipsychotic agents	Haloperidol, Pimozide, Clozapine, Olanzapine, Ziprasidone, Aripiprazole, Risperidone, Quetiapine	Koller & Trimble, 1985; Girotti et al., 1984; van Vugt et al., 1997; Bogelman et al., 2001; Bonelli et al., 2003; Brusa et al., 2009; Parsa et al., 1997; Bonelli & Niederwieser, 2002
N-methyl-D-aspartic acid receptor antagornists	Amantadine, Memantine	Verhagen et al, 2002; Ondo et al., 2007
Omega-3 fatty acids	Ethyl-eicosapentaenoic acid	Puri et al., 2005
Treatment of cognitive dysfuction associated with HD		
Cognition	Rivastigmine, Donepezil	de Tommaso et al., 2007; Fernandez et al., 2000
Treatment of behavioral disturbances associated with HD		
Depression	Fluoxetine, Venlafaxine, Mirtazapine, Clozapine	Como et al., 1997; Holl et al., 2010; Bonelli, 2003; Sajatovic et al., 1991
Psychosis	Risperidone	Erdemoglu et al., 2002
Irritability, agitation	Olanzapine, Quetiapine, Sertraline, Buspirone, Valproate, Propranolol	Squitieri et al., 2001; Alpay & Koroshetz, 2006; Ranen et al., 1996; Bhandary & Masand, 1997; Grove et al., 2000; Stewart, 1987

Table 2 Pharmacological drugs on symptoms of HD (adapted from Im & Kim 2014).

Tetrabenazine is the most commonly used drug for chorea. It reduces the amount of the chemical dopamine reaching some of the nerve cells in the brain.
Antipsychotic agents, including Haloperidol, Pimozide, and Clozapine, are used to treat patients with psychiatric/behavioral comorbidities, particularly to control delusions, hallucinations and violent outbursts. But they may have severe side effects, such as stiffness and rigidity, sedation, tremor, slowness of movement. Because of these side effects, the lowest possible dose of antipsychotics will be prescribed.
Rivastigmine and Donepezil are the preferred treatments for improving cognitive function.
Antidepressants improve mood swings and treat depression. Mood stabilizers, particularly carbamazepine, is considered as a treatment for irritability (Im & Kim 2014).
The European Huntington's Disease Network (EHDN) has a major program of research into these symptomatic treatments.

It aims to establish which treatments and combinations are most effective, in order to develop guidelines to help guide treatment choices in patients with symptoms of HD.

1.2.8.2.Preventive or curative treatments

More than 30 clinical trials have been conducted these past years for HD, but none of them has shown conclusive results. Currently promising clinical trials are conducted (see **Annexe 6.3. Clinical trials status report Table3**).

As HD is a progressive neurodegenerative disorder, therapies aimed at treating patients at different stages of the disease are being pursued. Early- and mid-stage HD patients already see a marked loss of MSN within the caudate nucleus and putamen as well as dramatic decrease in BDNF, while late-stage HD patients have lost an overwhelming number of neurons within the basal ganglia and cerebral cortex. Early interventions with MSCs engineered to overexpress the trophic factor BDNF or RNAi show the ability to protect against neurodegeneration, while later interventions with iPSCs are aimed at cell-replacement.

In the past few years, our increased understanding of how the HD gene causes disease has led to laboratory studies of HD animal models, in which experimental treatments have been shown to slow down the damage caused by HD. Many possible treatments for HD are being developed. They are at different stages of development — some are very early in laboratory models of HD, while others have already been tested in HD patients. The following lines explain some of the latest and most promising approaches to the development of treatments for HD [see as review (Ross et al 2014, Wild & Tabrizi 2014); (**Figure 14**)].

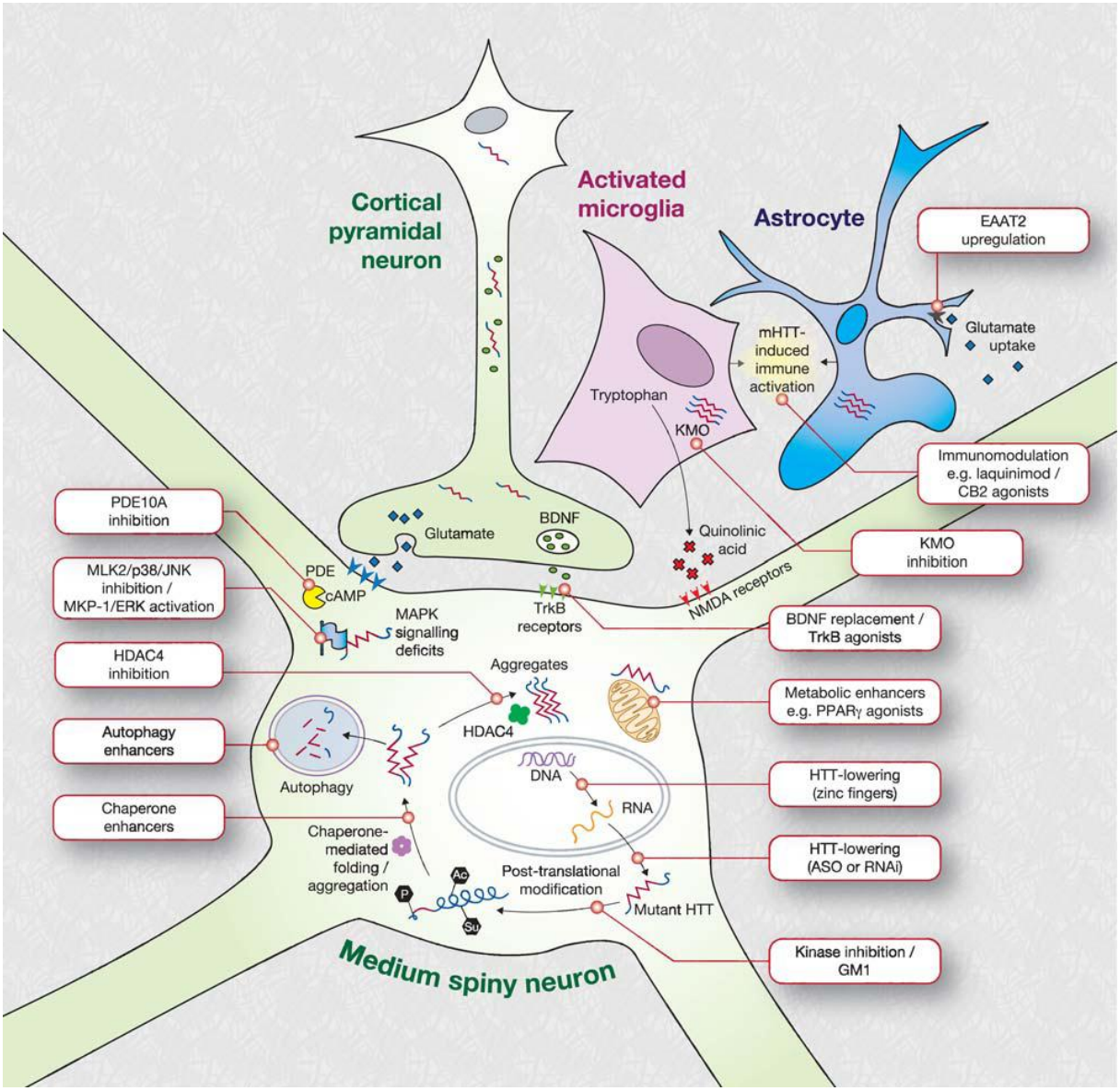

Figure 14 Schematic depicting current priority preclinical therapeutic targets under investigation for HD (Adapted from Ross et al 2014)(Wild & Tabrizi 2014).
Abbreviations: HTT, huntingtin; KMO, kynurenine monooxygenase; NMDA, N-methyl-D-aspartate; PDE, phosphodiesterase; BDNF, brain-derived neurotrophic factor; HDAC, histone deacetylase deacetylase; Trk, tropomyosin-related kinase.

a) Gene silencing therapy

Several strategies have been designed to reduce Htt mRNA expression or protein amounts in experimental models. The first of these strategies is to ablate mHtt expression.
Lowering expression of mHtt at the level of DNA on transcription or RNA on translation ought to reduce all of the downstream deleterious effects of the protein that lead to the manifestations of HD if it is delivered to the key affected cells.. Such strategies are sometimes known as "gene silencing"—somewhat misleadingly, because no approach is expected to stop mHtt expression altogether—or "huntingtin lowering" or "huntingtin suppression".

These approaches aimed at reducing HTT expression are considered among the most promising emerging therapeutics to slow or prevent HD (Garriga-Canut et al 2012, Magen & Hornstein 2014).
The blockade of mHtt expression in a tet-regulated conditional mouse model of Huntington's disease resulted in a behavioral improvement and a reduction of inclusion bodies (Yamamoto et al 2000). Thus, some of the effects produced by mHtt are reversible.
Gene silencing therapy is already used in human patients in other diseases. One major problem with gene silencing is getting the molecules where they are needed. RNA and DNA molecules don't enter the brain easily, and getting them to spread through the whole brain is difficult. New methods of designing the molecules have improved the efficiency of spread through the brain, and there are now devices that can deliver drugs directly into the fluid surrounding the brain.

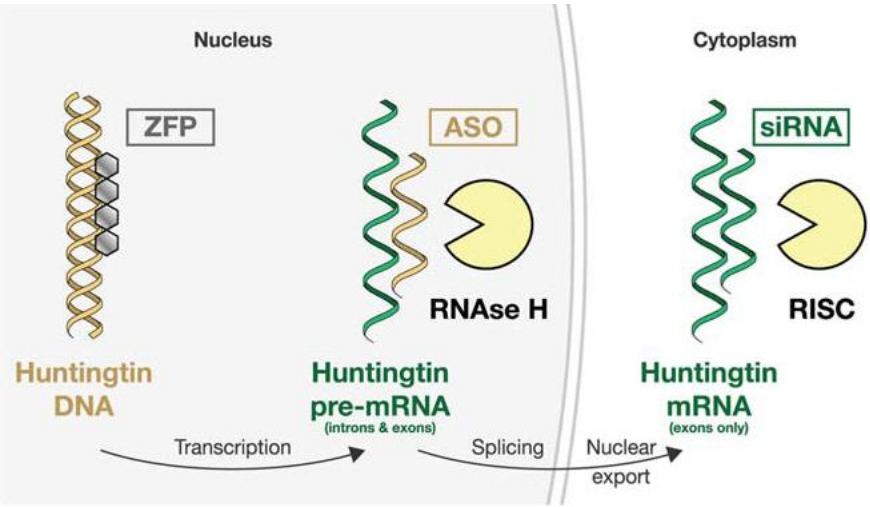

Figure 15 Schematic illustration of the three main approaches to lowering HTT (Wild & Tabrizi 2014).

Zinc finger protein (ZFP) therapeutics aim to reduce transcription of the huntingtin gene. Translational repression can be attempted at the pre-mRNA level using DNA-based antisense oligonucleotides (ASOs) or on mature mRNA using short interfering RNA (siRNA) compounds.

Three broad approaches are under investigation to reduce mHtt expression: RNA interference (RNAi) using short interfering RNA (siRNA); translational repression using single-stranded DNA-based antisense oligonucleotides (ASOs); and transcriptional repression using zinc finger proteins (ZFPs) (**Figures 14 & 15**).
RNAi and ASO repression use synthetic modified nucleotide agents designed to bind to a chosen sequence in the Htt messenger RNA (mRNA), using Watson-Crick complementarity. Once bound, different cellular mRNA disposal mechanisms remove the Htt mRNA, resulting in reduced translation and lowered protein expression (Bennett & Swayze 2010).
In RNAi, the drug molecule can be either an siRNA or a microRNA (miRNA) molecule. Degradation of siRNA-bound mRNA is performed by the RNA-induced silencing complex (RISC), which incorporates the RNAse enzyme argonaute (**Figure 15**).

The ASOs are modified single-stranded DNA molecules, and ASO-bound mRNA is degraded by RNAse H (Martinez et al 2013). ASO have also been developed for the CAG repeat region to decrease specifically the mutant huntingtin load without affecting the wild type (Hu et al 2009).
Plans for phase 1 trials in Huntington's disease are underway with ASO using intrathecal delivery.
Several clinically relevant methods include intracerebroventricular infusion to viral vector-mediated delivery (Hu et al 2009, Kordasiewicz et al 2012, Ramachandran et al 2013, San Sebastian et al 2013).
Transient infusion into the cerebrospinal fluid of symptomatic HD mouse models of ASO that catalyze RNase H-mediated degradation of Htt mRNA not only delays disease progression but also mediates a sustained reversal of disease phenotype that persists longer than the huntingtin knockdown (Kordasiewicz et al 2012).

As with ASO, the RNAi are designed to target either the mutant HTT (allele-specific) or both mutant and wild-type forms (nonallele-specific) (**Figure 14**). Non-allele-specific safety studies in non-human primates achieved a significant reduction in striatal huntingtin load without any safety concerns (Grondin et al 2012, McBride et al 2011). Other strategies include targeting of the single-nucleotide polymorphisms occurring in some, but not all, mutant alleles of HTT (Carroll et al 2011).
Another technique is the trans-splicing technique, and consists in HD in replacing exon 1 of HTT gene with a corrected, non-pathogenic exon 1 sequence using spliceosome-mediated pre-mRNA trans-splicing (Rindt et al 2012). It is part of the allele-specific strategies which preserve expression from the wild-type allele and reduce the levels of mutant protein. It is a promising technique to correct HTT gene in HD patients, but is at an early stage of development for the moment.

Using these techniques, researchers have recently been able to slow down the progression of HD in mouse models. Gene silencing is very promising in HD because, unlike in many other diseases, the exact genetic cause of HD is known.
Before it can be tried in humans, gene silencing therapy needs to be tested in HD model animals that have brains as large as a human brain, to test whether the combination of new molecules and new delivery techniques can get the treatment to where it is needed. It will probably also need refining to minimize any side effects of switching off the HTT gene.

b) Cystamine and cysteamine

These drugs where initially found to decrease the activity of transglutaminases. These ubiquitous enzymes catalyze post-translational modifications of proteins and their activity is increased in HD.
The neuroprotective capacity of cystamine was established in studies in which cystamine treatment was initiated before the HD symptomatic phase. Tested in the transgenic R6/2 HD mouse model, various doses and modes of cystamine administration showed beneficial effects on survival and motor performances (Dedeoglu et al 2002).

Cystamine, as well as its reduced form cysteamine, have also been found to be neuroprotective in the R6/1 mouse model, potentially via the increase brain levels of BDNF and indirect upregulation of the heat shock DnaJ-containing protein 1b (HSJ1b) (Borrell-Pages et al 2006, Saudou & Humbert 2006). Karpuj et al. were the first to unveil the beneficial effects of post-symptomatic cystamine treatment on survival and motor performance of R6/2 mice (Karpuj et al 2002). (See as review (Gibrat & Cicchetti 2011)).
Given the significant benefits observed in HD models, cysteamine has recently leaped to clinical trial. Raptor Pharmaceutical amended collaboration agreement with the University Hospital Center (CHU) of Angers, in France, to conduct the Phase 2/3 clinical trial of RP103, delayed-release cysteamine, between 2010 and 2014. While the results did not reach statistical significance, an overall positive trend was observed. The full results of the trial and the open-label extension study are awaited, as the third-part statistical analysis of clinical trial data.

Another way to play on BDNF levels is to stimulate the corresponding receptor on which BDNF is bound: the tyrosine receptor kinase B (TrkB) receptor. One approach to overcome the limitations of a protein-based therapeutic has been to develop small-molecule TrkB agonists. Simmons and colleagues demonstrated benefits from a TrkB agonist, LM22A-4, in the R6/2 and BACHD models, and additionally showed reduced intranuclear aggregation of mHtt in striatum and cortex (Simmons et al 2013). Monoclonal antibodies were shown to agonize TrkB in a manner akin to BDNF and protected striatal neurons from mHtt-induced toxicity (Todd et al 2014). Though challenging, the use of monoclonal antibodies as BDNF mimics warrants further study.

c) Autophagy enhancers

Strategies that enhance clearance of unwanted proteins are explored in several neurodegenerative disorders.
Looking for drugs that make autophagy happen more efficiently might help cells get rid of huntingtin and live longer. Rapamycin belongs to a group of drugs called mTOR inhibitors, which activate autophagy, and it has been shown to slow down HD in a mouse model. However, rapamycin causes lots of side-effects in humans and when tested in patients, it was not shown to be effective. HD researchers looking for more efficient, less toxic activators of autophagy have identified several drugs that might be better than rapamycin, and these now need testing in animal models of HD.
Native or modified polyQ binding peptide 1 inhibits misfolding and aggregation of huntingtin in vitro (Okamoto et al 2009), inhibits neurodegeneration in drosophila models (Nagai et al 2003), and is beneficial in a mouse model of Huntington's disease (Bauer et al 2010). Other small peptides and molecules are being developed.

d) Synaptic plasticity

Altered synaptic plasticity is one potentially reversible cause of dysfunction in HD. Phosphodiesterase (PDE) 10A is almost exclusively expressed in the striatum, and its activity is intimately linked to the synaptic biology of MSN.

In the R6/2 mouse, PDE10A inhibition with TP-10 ameliorated motor deficits, reduced striatal atrophy and increased brain-derived neurotrophic factor (BDNF) levels (Giampa et al 2010). Clinical trials of PDE10A inhibition in HD patients are already underway, with motor and functional MRI endpoints (Pfizer study). Other phosphodiesterases implicated in HD are also under investigation. PDE4 inhibition with rolipram, meanwhile, improved survival and ameliorated neuropathology and motor phenotypes in the R6/2 mouse (DeMarch et al 2008).

e) Modulation of inflammation

It has been shown that the immune system is overactive in HD, and evidence is mounting that microglia are overactive, too. Kynurenine 3-monooxygenase (KMO), an enzyme found in microglia, can affect how fast HD progresses (Thevandavakkam et al 2010). Researchers are now working on drugs that will switch off KMO, reducing the damage microglia do to brain cells, and preliminary results have shown that KMO inhibitors may be effective at slowing down the damage done by HD in mice.

CB2 cannabinoid receptors are expressed in microglia and peripheral immune cells; their activation is anti-inflammatory, and their levels are increased in postmortem HD brain. Genetic deletion of CB2 receptors was found to accelerate the phenotype in BACHD mice, whereas treatment with the CB2 agonist GW405833 ameliorated it and prolonged survival. This effect was reversed by co-administration of a peripherally acting CB2 antagonist, suggesting again that peripheral immuno-modulation may be capable of altering the CNS phenotype of HD (Bouchard et al 2012).

f) HDAC inhibitors

As mentioned previously, it has been shown that mHtt directly interacts with HAT and HDAC proteins, leading to altered histone acetylation and deacetylation (Jiang et al 2006, Steffan et al 2000). Numerous studies revealed that treatment with HDAC inhibitors arrested the ongoing progressive neuronal degeneration in both fly and mouse models of HD (see as review (Gray 2010)). Some recent examples using selective HDAC inhibitors showed their neuroprotective effects in different neurodegenerative disorders (see (Coppede 2014), and in particular in HD (Chopra et al 2012, Jia et al 2012). For example, HDAC inhibitors such as the nonselective HDAC inhibitor suberoylanilide hydroxamic acid (SAHA) have been shown to be effective in slowing down the cellular damage and to ameliorate the motor phenotype in R6/2 mice (Hockly et al 2003). This effect would pass by reduction of HDAC4 activity through increased its degradation, accompanied by restoration of BDNF cortical transcript levels (Mielcarek et al 2011).

However, HDAC inhibitors, which are often used to treat cancer (see as review (Bose et al 2014, Falkenberg & Johnstone 2014)), are toxic drugs with serious side effects. More effective HDAC inhibitors with less severe side effects are prospected.

g) Caspase inhibitors

Minocycline is a drug that acts as a caspase inhibitor. Initially there was some optimism that minocycline might help in HD but so far no double-blind, controlled trial (the most reliable kind of clinical trial) has shown evidence that minocycline is helpful in HD, but these clinical trials are underway.
There are 11 types of caspase, and caspase 6 is thought to be the one that generates the most toxic huntingtin fragment. Work is underway to develop and test inhibitors of caspase 6 that might be more powerful than minocycline, but with fewer side effects.

h) Apoptosis

Recent evidence suggests the value of targeting of pro-apoptotic pathways in HD. In striatal neurons from both patients with HD and animal models, markers for apoptotic cell death are activated. Indeed, in the brains of HD patients, caspases 1, 3, 8, and 9, are activated and cytochrome c is released from the mitochondria into the cytosol (Kiechle et al 2002).
More in details, p53 is a cell protein with many functions, but it's known to be involved in energy production, the response to stress and controlling when cells divide. Recently, it has been shown that p53 accumulates in the brain cells most affected by HD, and that the Htt protein and p53 interact (Bae et al 2005). Mutant Htt binds more efficiently to p53 than does wild-type Htt (Steffan et al 2000), which causes an upregulation in nuclear p53, and consequently significantly higher amounts of downstream targets of p53, such as Bax and Puma, which are key effectors in the apoptotic cascade of events. Work is underway to identify targets in the p53 pathway that drugs might be able to alter, so that the negative effects of Htt on cells can be minimized.

i) Cell therapy strategies

Stem cells have been investigated for use in neurodegenerative disorders to develop cell therapy strategies (Crane et al 2014, Im & Kim 2014). The ultimate goal of cell therapy is the replacement or neuroprotection of dead or dying cells.
Cell therapy strategies can be classified into two broad categories based on the use of either fetal tissues/cells or stem cells. Studies using fetal brain tissue were performed using animal models of HD prior to 1990 (Hantraye et al 1992, Palfi et al 1998). Several clinical trials on HD patients have been performed with fetal tissues or cells. However, effective recovery has not been reported in any clinical trials, although some studies showed that fetal tissue transplantation provided cellular improvement around lesions (Nakao et al 1996, Slow et al 2003). Moreover, fetal tissue transplantation led to localized effects only and did not persist long-term (Cicchetti et al 2009, Slow et al 2003).
Several types of stem cells, such as embryonic stem cells (ESCs), bone marrow mesenchymal stem cells (BM-MSCs), neural stem cells (NSCs), adipose stem cells (ASCs), and induced pluripotent stem cells (iPSCs), are used to develop cell therapy strategies.
Embryonic stem cells are pluripotent, and mouse ESCs can differentiate into neurons, astrocytes, and oligodendrocytes (Li et al 1998).

It has been reported that human ESCs (hESCs) can differentiate into neurons in the lesions of HD animal models, attenuating progressive symptoms (Song et al 2007). Despite these benefits of hESCs, complications arising from their use include immune rejection, ethical concerns, and tumor formation. On the other hand, somatic stem cells such as BMMSCs, NSCs, ASCs, and iPSs are ideal sources for clinical trials because these stem cells do not present the above mentioned immune rejection and ethical problems.
Other studies reported that transplanted NSCs differentiated into neurons, oligodendrocytes, and predominantly, astrocytes, in *in vivo* HD models, resulting in partial functional recovery (Johann et al 2007, McBride et al 2004, Visnyei et al 2006). Bone marrow mesenchymal stem cells and ASCs are easily obtained multipotent somatic stem cells that can be differentiated into neuronal cells. Moreover, these stem cells have the ability to secrete neuroprotective factors, such as growth factors, chemokines, and cytokines. Recent studies have shown that intrastriatal transplantation of BM-MSCs reduced striatal atrophy, although transplanted cells only survived for up to 7 days in transgenic HD mice. BMMSCs can be genetically modified to provide sustained and long-term delivery of neuroprotective factors (Choong et al 2007, Erba et al 2010, Zavan et al 2010).
iPSCs provide a potential solution because they have the ability to differentiate into various cell types and can be induced from the fibroblasts of an HD patient. iPSCs from an HD patient with 72 CAG repeats have been efficiently induced to form GABAergiq neurons and were functional following transplantation into a rat model of HD (Jeon et al 2012, Takahashi & Yamanaka 2006).

A current observational clinical study aims at establish a clinical baseline and measure changes over time in movement, thinking, behavior, brain imaging, blood and spinal fluid markers in subjects with early stage HD. Participants enrolled in this study may be eligible to participate in a future planned study of stem cell therapy for HD (PRE-CELL project).

j) Dietary supplements

CREATINE
Creatine is a guanidine compound, which plays a key role in energy buffering within the cell, which is thought to be particularly important in tissues with high and fluctuating energy requirements such as brain and muscle (Burklen et al 2006). Among the ways that mHtt damages brain cells is by interfering with cellular energy production, leading to a depletion of ATP. Known to help restore ATP and maintain cellular energy, creatine is being investigated to treat a number of neurological conditions – including Parkinson disease, amyotrophic lateral sclerosis and spinal cord injury. Studies in mouse models of HD showed that creatine raises brain ATP levels and protects against neurodegeneration (Andreassen et al 2001, Dedeoglu et al 2003, Ferrante et al 2000). Creatine has been shown to reduce brain shrinkage and to extend survival of HD transgenic mice, and to reduce oxidative stress markers in blood and brain. The Huntington Study Group (HSG), in a partnership between Massachusetts General Hospital , Boston, USA (MGH) and the University of Rochester, is conducting a global, multi-center, randomized, double-blind, placebo-controlled clinical trial in individuals 18 years of age and older with HD.

CREST-E project is designed to assess the potential of high-dose pharmaceutical grade creatine to slow the progressive functional decline that occurs in HD, to examine the long-term safety and tolerability of creatine, and to assess potential changes in the body and brain due to creatine. The phase II PRECREST trial enrolled 64 adult participants. Followup MRI scans at six months showed a slower rate of atrophy in participants taking creatine compared to those on placebo.
At the end of the second phase, the rate of brain atrophy had also slowed in presymptomatic participants that started taking creatine after 6 months on placebo. Hersch S. and Rosas D. (Massachusetts General Hospital), with Schifitto G. (University of Rochester,) are currently leading a world-wide Phase III trial (CREST-E) of high-dose creatine in individuals with early symptomatic HD.

COENZYME Q10 (CoQ10)

CoQ_{10} is an essential cofactor of the electron transport chain where it accepts electrons from complex I and complex II (Ernster & Dallner 1995). It is soluble and mobile in the hydrophobic core of the phospholipid bilayer of the inner membrane of mitochondria, where it transfers electrons one at a time, to complex III of the electron transport chain. CoQ_{10} also serves as an important antioxidant in both mitochondria and in lipid membranes (Forsmark-Andree et al 1997, Noack et al 1994). CoQ_{10} is also an obligatory cofactor of mitochondrial uncoupling proteins, which regulate ATP production and reduce free radical generation (Echtay et al 2002). CoQ_{10} exerts neuroprotective effects both in vitro and in vivo in animal models of neurodegenerative diseases (Beal & Shults 2003). Due to initial promising results, CoQ_{10} has entered trials for the treatment of HD. Recent PREQUEL study of coenzyme Q10 in presymptomatic gene carriers showed the feasibility of carrying out clinical trials to slow or halt onset of HD. PREQUEL is a phase II randomized, double-blind, multicenter trial of 600 mg, 1200 mg, and 2400 mg per day of CoQ. The 90 study participants were adults who had previously tested positive for the HD CAGn expansion (> 36 repeats) and who were deemed pre-manifest by having a diagnostic confidence score of inferior or egal 3 on the Unified HD Rating Scale (UHDRS). Tolerability was defined as the ability to complete the 20-week study on the originally randomized treatment assignment. A CoQ dosage was deemed tolerable if the observed tolerability was higher than a pre-specified threshold of 75 %. CoQ was well tolerated at dosages up to 2400 mg/day for 20 weeks in patients with pre-manifest HD, with rates of study completion on the assigned dosage surpassing the pre-defined tolerability threshold in all treatment groups. The study shows the feasibility of conducting clinical trials in this population.

SYNERGY BETWEEN CREATINE AND CoQ10

As it has been shown by Beal's team in 2010 that a combination of CoQ_{10} with creatine can exert additive neuroprotective effects in a 3-NP rat model of HD and the R6/2 transgenic mouse model of HD (Yang et al 2009). If both CoQ_{10} and creatine show efficacy in HD clinical trials, then future studies of the two compounds in combination may be warranted. A combination of the two compounds would also be a promising approach for treating presymptomatic individuals, since both compounds are natural products and are well tolerated with few side effects.

CURCUMIN

Multiple beneficial effects of curcumin, which could be linked to its ability to act as a strong anti-oxidant and anti-inflammatory, have been reported during the last ten years against a wide variety of diseases (Monroy et al 2013).

A recent study has shown that Ki140CAG mice fed a curcumin-containing diet since conception showed decreased htt aggregates and increased striatal DARPP-32 and D1 receptor mRNAs, as well as an amelioration of rearing deficits (Hickey et al 2012). An Indian team has used curcumin encapsulated solid lipid nanoparticles (C-SLNs) to ameliorate 3-nitropropionic acid (3-NP)-induced HD in rats (Sandhir et al 2014). C-SLN-treated animals showed significant increase in the activity of mitochondrial complexes and cytochrome levels. C-SLNs also restored the glutathione levels and superoxide dismutase activity, as significant reduction in mitochondrial swelling, lipid peroxidation, protein carbonyls and reactive oxygen species. C-SLN-treated rats showed significant improvement in neuromotor coordination when compared with non-treated rats.

As our understanding of the consequences of the HD mutation increases, the possibility of tractable targets for therapeutic development is amplified, but few are well-validated, and many single studies of purported success have yet to be replicated.

PART2 THESIS OBJECTIVES

2.1.Working hypothesis to study striatal vulnerability

As previously detailed on the introduction of this manuscript, since the discovery of the cause of HD, a lot of work has been done to elucidate the molecular mechanisms explaining consequences of the mHtt toxicity within the CNS and the peripheral nervous system (PNS).
One obvious observation is that Htt is ubiquitously expressed. Mutant Htt is also ubiquitously expressed in HD mouse models and patients, but it has dramatic consequences, primarily on the striatum. Thus it is likely that complex molecular mechanisms render striatal cells more vulnerable to mHtt as compared to the cells of the other part of the brain.

The hypothesis of our laboratory and other teams is that gene products selectively expressed in the striatum may be involved in its high vulnerability to mHtt.

From this hypothesis, numerous studies have recently emerged to study "markers of the striatum" that are genes product enriched in the striatum whose expression are up- or down-regulated in HD compared to healthy condition (Brochier et al 2008, de Chaldee et al 2003, Desplats et al 2006, Hodges et al 2006, Mazarei et al 2009, Sepers & Raymond 2014) .
Experiment results in different models indicate that some of these striatal markers have neuroprotective role (e.g. MSK1, A2A and CB1 receptors) whereas others enhance the vulnerability of striatal neurons to mHtt (e.g. Rhes, RGS2, D2 receptors).

The recent review we wrote (Francelle et al 2014) provides a comprehensive view of the possible involvement of these striatal markers in HD pathogenesis. We classified the different striatal gene products that have been experimentally studied for their capacity to change mHtt toxicity as "protoxic" if they amplify this toxicity, "neuroprotective" if they slow toxicity, and "neutral" if changing their level of expression doesn't modify mHtt toxicity.
Mutant Htt is expressed since birth in HD gene carriers, but symptoms appear during adulthood. However, subtle changes on motor and cognitive functions are observed in presymptomatic patients, and thanks to imaging techniques, it has been described that neuropathology is beginning before the appearance of symptoms (Feigin et al 2006). Indeed, enhanced activation of thalamocortical pathways during motor learning can compensate for caudate degeneration in presymptomatic HD patients, but this mechanism may not be sufficient to sustain a normal level of task performance. These observations reflect a progressive settle of compensatory mechanisms affecting the whole brain since early in the development of the organism to counteract mHtt toxicity. From this point, the second part of the review hypothesizes the existence of compensatory mechanisms in HD at the molecular level, in particular in the striatum, considering the down-regulation of the "protoxic" striatal markers as a potential self-defense mechanism to slow degeneration.
In view of the few striatal markers that have been reviewed in this publication, many others, not yet studied in these conditions, may also act as modifiers of mHtt, which let place to better define the molecular and functional complexity of the striatum and further develop new therapeutic targets of HD.

The review on the vulnerability of the striatum and the possible involvement of some striatal markers has been published in the Frontiers in Cellular Neuroscience journal.

Review article

Possible involvement of self-defense mechanisms in the preferential vulnerability of the striatum in Huntington's disease.

Possible involvement of self-defense mechanisms in the preferential vulnerability of the striatum in Huntington's disease

Laetitia Francelle [a,b] , Laurie Galvan [a,b,c], Emmanuel Brouillet [a,b,*]

[a] Neurodegenerative Disease Laboratory, *Commissariat à l'energie Atomique (CEA), Direction des Sciences du Vivant (DSV), Institut d'Imagerie BioMédicale (I²BM), Molecular Imaging Research Center (MIRCen), F-92265 Fontenay-aux-Roses, France*

[b] *Centre National de la Recherche Scientifique (CNRS)- CEA Unité de Recherche Associée 2210, F-92265 Fontenay-aux-Roses, France*

[c] *Intellectual and Developmental Disabilities Research Center, Semel Institute for Neuroscience and Human Behavior, Brain Research Institute, David Geffen School of Medicine, University of California Los Angeles, Los Angeles, California, USA*

* Corresponding author at: Neurodegenerative Disease Laboratory, URA CEA-CNRS 2210, MIRCen, I²BM, CEA, 18 route du Panorama, BP 6, 92265 Fontenay-aux-Roses, France. Tel.: 0033-1-46549622; fax: 0033-1-46549116.
E-mail address: emmanuel.brouillet@cea.fr

Abstract

HD is caused by a mutation in the huntingtin gene that consists in a CAG repeat expansion translated into an abnormal poly-glutamine (polyQ) tract in the huntingtin (Htt) protein. The most striking neuropathological finding in HD is the atrophy of the striatum. The regional expression of mutant Htt (mHtt) is ubiquitous in the brain and cannot explain by itself the preferential vulnerability of the striatum in HD. mHtt has been shown to produce an early defect in transcription, through direct alteration of the function of key regulators of transcription and in addition, more indirectly, as a result of compensatory responses to cellular stress. In this review, we focus on gene products that are preferentially expressed in the striatum and have down- or up-regulated expression in HD and, as such, may play a crucial role in the susceptibility of the striatum to mHtt. Many of these striatal gene products are for a vast majority down-regulated and more rarely increased in HD. Recent research shows that some of these striatal markers have a pro-survival/neuroprotective role in neurons (e.g. MSK1, A2A and CB1 receptors) whereas others enhance the susceptibility of striatal neurons to mHtt (e.g. Rhes, RGS2, D2 receptors). The down-regulation of these latter proteins may be considered as a potential self-defense mechanism to slow degeneration. For a majority of the striatal gene products that have been identified so far, their function in the striatum is unknown and their modifying effects on mHtt toxicity remain to be experimentally addressed. Focusing on these striatal markers may contribute to a better understanding of HD pathogenesis, and possibly the identification of novel therapeutic targets.

Running title

Compensatory mechanisms in the striatum in Huntington's disease

Key words

Striatum, Huntington, Markers, Cell death, Excitotoxicity, Signaling , gene products

Introduction

A summary of what is HD

HD is a dominantly inherited disorder generally affecting young adults. Symptoms include involuntary abnormal movements (chorea, dyskinesia, dystonia), frontal cognitive deficits (e.g. perseveration) and psychiatric disturbances (Harper, 1991; Walker, 2007). The disease is fatal approximately 15 years after the onset of symptoms. There is no treatment available to slow the progression of this devastating disorder.

HD is caused by a mutation in the *HTT* gene encoding the protein huntingtin (Htt) that consists in a CAG triplet repeat expansion translated into an abnormal poly-glutamine (polyQ) tract within the N-terminal region of the protein (The-Huntington's-Disease-Collaborative-Research-Group, 1993). When considering cohorts of HD gene carriers, genetic studies showed that the longer is the CAG repeat expansion the earlier the disease onsets. However, there is a huge inter-individual variability in age of onset (and nature) of symptoms for gene carriers with similar CAG repeat numbers. Thus, apart from HD gene mutation, many genetic, epigenetic and environmental factors may affect the course of the disease (Sturrock and Leavitt, 2010). Deciphering these factors and the underlying mechanisms affecting the onset of this disease could constitute a real hope to find an efficacious treatment to slow the disease.

The mutant protein is cleaved by many proteases leading to the production of N-terminal fragments that form toxic oligomers (Roze et al., 2008b). Eventually mutant Htt (mHtt) forms intranuclear inclusions and somatodendritic aggregates that also contain ubiquitin and represent a histopathological hallmark of HD (Li and Li, 2004a).

Mechanisms of HD pathogenesis have been extensively studied in the past twenty years, since the gene has been identified and cloned. Thanks to many different genetic models (in cells, mice, rat and even monkeys) a large spectrum of cellular defects has been identified and could contribute to neurodegeneration. For this reason the pathogenesis of HD is often considered multi-factorial. The polyQ expansion in mutated Htt (mHtt) produces a gain-of-function that is toxic to neurons through several mechanisms. One major early event in HD is the alteration of transcription (Cha, 2007; Seredenina and Luthi-Carter, 2012). Importantly, reduced transcription of Brain Derived Neurotrophic Factor (BDNF), a major neurotrophic factor for striatal cells has been found (Zuccato and Cattaneo, 2007). Axonal transport alterations (Li and Li, 2004b; Roze et al., 2008b) leading to several cellular disturbance, including defects in BDNF secretion and transport (Gauthier et al., 2004) also contribute to neurodegeneration. Other alterations include intracellular signaling defects (Borrell-Pages et al., 2006), deregulated of the proteasome pathway (Finkbeiner and Mitra, 2008) and autophagy (Ravikumar and Rubinsztein, 2006), perturbation of calcium homeostasis leading to excitotoxicity (Cowan and Raymond, 2006; Raymond et al., 2011), mitochondrial defects and oxidative stress (Damiano et al., 2010).

In addition, the mutation in one allele is thought to produce a loss of function of wild type Htt (Cattaneo et al., 2005). Indeed, htt is involved in a large variety of physiological cellular processes.

It regulates vesicle transport through regulation of molecular motors of the cytoskeleton, transcription of important pro-survival factors (such a BDNF) by interacting with key transcription factors and co-activators of transcription, cell division, intracellular signaling and ATP production (Zuccato and Cattaneo, 2014).

While wild type and mHtt protein are ubiquitously expressed in the brain, degeneration primarily affects the striatum. The contribution of striatal degeneration in motor and cognitive symptoms is not totally understood but neuropathological studies showed that striatal atrophy correlates with severity of symptoms (Myers et al., 1988). Recently, follow up of HD gene carriers cohort using Magnetic Resonance Imaging (MRI) and Positron Emission Tomography (PET) showed that even at presymptomatic stages, the atrophy of the striatum is detectable and may start even 10 years before onset of symptoms (Tabrizi et al., 2013). Other brain regions may also be damaged at early stages, such as the hypothalamus, and at later stages the cerebral cortex and other regions also degenerate [for a review, (Brouillet et al., 1999; Petersen and Bjorkqvist, 2006)]. Thus HD is not a selective striatal disease. Many innovative studies discovered extra-striatal and peripheral anomalies in HD animal models and for particular studies in HD patients (Martin et al., 2008; Obeso et al., 2014). However, the preferential striatal degeneration is an intriguing characteristic of this illness, and the underlying mechanisms may represent an important aspect of HD pathogenesis.

Existence of possible compensatory mechanisms in HD

The existence of compensatory mechanisms in HD (as for other neurodegenerative diseases) is probable. Possibly, the best circumstantial evidence for this is that although mHtt is expressed in the brain of HD gene carriers since birth, degeneration and symptoms appear during adulthood (with the exception of long CAG repeat expansion carriers who develop the disease during childhood) (Harper, 1991; Walker, 2007). Similarly in genetic animal models, degeneration and symptoms occur in adult or aged animals (Menalled, 2005; Menalled and Chesselet, 2002). It has been shown that when mHtt is expressed in striatal neurons at similar levels for the same duration, its neurotoxic effects are significantly higher in aged animals, as compared to young animals (Diguet et al., 2009). The reason for this age-dependent phenomenon is unknown but it indicates that neurons possess the ability to partially counteract cellular stress induced by mHtt, a plasticity mechanism that may be progressively lost with aging. The aim of this review is not to cover all the possible compensatory mechanisms that may occur in the HD brain, but to focus on those that can be found in the striatum. However, a few examples of potential compensatory mechanisms that could be encountered in all cell types can be given.

There likely exist compensatory mechanisms at whole human brain level, to overcome cell dysfunction and/or neurodegeneration in the striatum of HD patients. For example, PET studies showed that effective learning performance on motor sequence learning tasks, normally associated with activation of the dorsolateral prefrontal cortex and the caudate nucleus, was not requiring the same brain regions in presymptomatic HD (pre-HD) patients and healthy volunteers (Feigin et al., 2006).

In presymptomatic HD gene carriers, ventral prefrontal and orbitofrontal regions were used possibly via thalamic projections.

At cellular level, transient/reversible transcriptional and post-transcriptional mechanisms may intervene to compensate for cell suffering and degeneration pathways. For example, the loss of expression of the kinase PKCδ (Rue et al., 2014) is likely a compensatory mechanism. Indeed, the overexpression of PKCδ enhances mHtt toxicity *in vitro*. On the contrary, the knock down of PKCδ (using siRNA strategy or expression of a dominant negative form) significantly reduces mHtt effects. Interestingly the loss of PKCδ seems to occur through an increased degradation of the protein by neurons expressing mHtt (Rue et al., 2014).

Examples of potential compensatory mechanisms in HD can be found in studies related to defects energy metabolism that are thought to occur early in HD. Unexpectedly, recent experiments show that an early increase in the levels of high energy phosphate metabolites (ATP, phosphocreatine) can be found in the brain of HD mouse models (Mochel et al., 2012a; Tkac et al., 2012). Consistent with these observation in genetic models of HD, dynamic measurements of brain phosphocreatine levels during synaptic activation in HD patients using ^{31}P NMR spectroscopy also demonstrate abnormalities in the use of high energy phosphate metabolites (Mochel et al., 2012b). In R6/2 and Knock-in 111Q mouse models, early biochemical changes indicate that neurons tend to compensate by activating energy promoting cellular pathways (Mochel et al., 2012a). In particular, possible compensatory changes occur at the post-translational levels, leading to an increase in AMPK phosphorylation in HD mice, which could activate pathways leading to a more efficient metabolism.

Large scale analyses trying to broadly identify mRNA and/or protein expression changes provide a huge amount of information from which potential compensatory mechanisms in HD may be discovered. A well-controlled proteomic analysis of brain of R6/2 HD mice at different ages underlined that a number of proteins display transient /biphasic expression changes rather than an age-dependent progressive decline (Zabel et al., 2009). For instance, the absolute expression of the mitochondrial complex II subunit Ip (iron-sulfur), a key regulator of oxidative energy metabolism which is neuroprotective against mHtt (Benchoua et al., 2006; Damiano et al., 2013), is early reduced in 2 week-old R6/2 mice, but is found to be increased in 8 weeks old of these mice and brings back at basal levels at 12 weeks old (Zabel et al., 2009).

Changes in the expression levels (decreases and more rarely increases) of mRNA in HD have been extensively explored in the last decade (Seredenina and Luthi-Carter, 2012). These changes may indicate two types of phenomena. On one hand, it indicates primary defects of transcription inherent to the presence of mHtt. In many cases, the direct interaction of mHtt with proteins that are part of macromolecular complexes involved in transcription regulation leads to a reduction of transcription and reduced levels of a large spectrum of gene products (Seredenina and Luthi-Carter, 2012). On the other hand, changes in mRNA levels (or protein) may not be directly linked to a primary effect of mHtt but could rather result from a physiological response engendered by the cellular stress induced by toxic gain of function of mHtt. Many expression changes identified in large scale analyses have been studied with the hypothesis that they were causal in HD pathogenesis. It is not always the case. Expression changes can represent self-defense mechanisms.

To differentiate between the two above mentioned mechanisms, knock-down/knock-out or overexpression/neuro-rescue experiments in HD models are needed. It is beyond the scope of the present review to provide a detailed description of the gene products that have been experimentally tested. Here we will limit our review to gene products that have deregulated expression and that are preferentially expressed in the striatum. The review of the studies focused on "striatal gene products" illustrates that in some cases, expression changes may represent compensation or self-defense mechanisms while in others they directly contribute to degeneration of striatal neurons.

Studying the preferential vulnerability of the striatum to identify potential modifiers

Working hypothesis

The particular vulnerability of the striatum in HD likely resides in its molecular complexity. Whether its particular vulnerability depends on only one or a subset of gene products, acting together, is unknown. Recent publications indicate that the experimental knock-down or overexpression of only one striatal gene product can significantly change the toxicity of muHtt in cell models and mouse models. In one instance, a single nucleotide polymorphism in a striatal gene, *ADORA2A* (adenosine receptor 2a) has been found to be associated with earlier onset of symptoms in large cohorts of HD patients (Dhaenens et al., 2009). Thus, striatal gene products can have a significant impact of HD. From a therapeutic point of view, this indicates that acting on one single target may be sufficient to alter the course of the disease. Therefore, trying to decipher the complex mechanisms underlying neurodegeneration in the striatum may help to more broadly highlight important factors of neuronal dysfunction and death, and to point potential therapeutic interventions for HD (Brochier et al., 2008; Brouillet et al., 2005; Mazarei et al., 2010; Thomas, 2006).

The study of these causal or compensatory changes in the striatum in HD may also help to better understand other neurological diseases where the striatum is functionally affected (e.g. Wilson, Parkinson, metabolic diseases, addiction, depression etc.).

The notion of striatal markers

The hypothesis that gene products preferentially expressed in the striatum (or more generally particularities of this brain region) could play an important role in the susceptibility of the MSN to mHtt toxicity has been studied for many years. Hypotheses related to particular properties of the MSN related to energy metabolism/oxidative stress, or glutamate –related excitotoxicity, and other types of neurotransmitter systems that could explain striatal atrophy in HD where proposed in the 80's and 90's (for a review [(Brouillet et al., 1999)]). The most recent developments of transcriptomic analysis led to a broader "without ***a priori"*** approach of the working hypothesis that striatum vulnerability to mHtt could reside in the expression of one or a subset of striatal enriched gene products.

The notion of striatal marker stems on the contrast of expression between the striatum and other brain regions. Relatively old studies identified striatal markers based on studies using *in situ* hybridization, immunohistochemistry, and biochemistry [see references in (Desplats et al., 2006) for a number of validated striatal markers].

The identification of approximately fifty validated markers took approximately two decades. In-depth transcriptomic analyses using serial analysis of gene expression (SAGE) further characterized the molecular complexity of the striatum as compared with other brain regions in mice allowed for the identification of a large list of “striatal markers” in wild type mice (Brochier et al., 2008; de Chaldee et al., 2003; Mazarei et al., 2010). This approach, based on the collection of polyA-containing RNA, provided a ranking of the number of copies of the different RNA species in different regions in the mouse brain. Comparison between brain regions led to the identification of gene products whose expression shows high enrichment in the striatum. Known striatal markers were found, but many annotated gene products whose function in the striatum is unknown were also identified. Approximately, 100-150 striatal markers can be listed, many of which have been cross-validated in different studies (Brochier et al., 2008; de Chaldee et al., 2003; Desplats et al., 2006; Mazarei et al., 2010). Transcriptomic studies using oligonucleotide array or RT-PCR showed that the magnitude of transcriptional changes in the striatum of HD mouse models for these genes preferentially expressed in the striatum was higher than that of ubiquitously expressed genes (Desplats et al., 2006). In the SAGE studies by Brochier and collaborators (Brochier et al., 2008), a number of gene products of unknown neurobiological function showed reduced expression in the striatum of R6/2 HD mice. Transcriptomic DNA array data in HD models and HD brain show that amongst the RNAs whose expression is deregulated, those coding for striatal markers are proportionally more frequently altered (Hodges et al., 2006; Kuhn et al., 2007). Another study validated a number of these striatal markers and identified potentially new ones that were found to be deregulated in YAC128 HD mice (Mazarei et al., 2010). Supplemental Table 1 indicates the striatal markers that have been well validated based on the studies quoted above.

Thus, the notion of striatal marker has evolved with the progression of the analytical methods. The criteria to decide whether a gene product is “preferentially” expressed in the striatum remains debatable. In most cases, the currently available public databases (Allen Brain Atlas) providing gene products expression in the brain in mice and humans generally confirm that the “striatal markers” identified in the studies described above have preferential striatal expression. In general, the contrast of “striatal specificity” in comparison to the somatosensory and motor cerebral cortex is in the range of 3 to 10-fold enrichment. If we were to consider a lower contrast (a two-fold difference between cortex and striatum for example), the list of striatal markers would be much longer. In addition, it must be mentioned that some striatal gene products, although referenced as “striatal markers” can have stronger expression in other anatomically restricted brain regions such as the hippocampus or some thalamic nuclei.

This review aims at providing a concise overview of the striatal markers that have been experimentally assessed for their capacity to modify mHtt toxicity. These markers have a large spectrum of biological functions and the alteration of the expression levels in HD is not *a priori* indicative of their role in striatal vulnerability. The different striatal gene products that have been experimentally studied for their capacity to change mHtt toxicity can be classified as “protoxic”, “neuroprotective”, and “neutral”.

In some instances, the expression changes (up or down) suggest the existence of a compensatory "self-defense" mechanism. We will also point to the large list of the other striatal markers that remain to be fully investigated to determine their potential role in HD.

Potential protoxic striatal gene products

D2-R (Dopamine type 2 receptor)

The hypothesis that dopamine, which is at high concentrations in the striatum compared to other brain areas, might play an important role in the preferential vulnerability of the striatum in HD has been suggested long time ago (Jakel and Maragos, 2000; Reynolds et al., 1998).

Anatomically, MSNs expressing D2-R (D2 MSN) receive preferentially inputs from the Pyramidal Track type (PT-type) cortical neurons whose projects ipsilaterally to the striatum. This preferential innervation is believed to release more glutamate which could contribute to make D2 MSNs more vulnerable to excitotoxicity (Ballion et al., 2008; Reiner et al., 2003). Many electrophysiological evidences suggest that D2 MSNs are more excitable than D1 MSNs (Cepeda et al., 2007; Kreitzer and Malenka, 2007) partly because they display fewer primary dendrites (Gertler et al., 2008). Electrophysiological recordings of D2 MSNs show a higher frequency of spontaneous excitatory postsynaptic currents (sEPSCs) than direct pathway. Moreover, D2 MSNs display large membrane depolarizations rarely seen in direct pathway MSNs (Cepeda et al., 2008) after the addition of $GABA_A$ receptor blockers inducing epileptic form activity in CPN (Galvan, 2012). Taken together, these evidences support the idea that D2-MSN is a fertile ground to develop abnormal responses.

Studies performed in YAC128 HD mouse model conducted at a presymptomatic age (1.5 months) and at symptomatic age (12 months) revealed interesting findings concerning the indirect pathways. At presymptomatic age, no differences were observed in excitatory and inhibitory synaptic transmission compared to WT. When the animals are symptomatic and become resistant to excitotoxicity, the inhibitory transmission in YAC128 D2 MSNs is greatly increased (Andre et al., 2011). This may indicate that the indirect pathway is subject to compensatory mechanism in HD, resulting in turn to the slowdown of excitatory glutamatergic synapses in the striatum.

Whether these changes in D2 MSN are only related to D2-R signaling is not known. Direct support for a causal role for DA and D2-R in HD comes from the recent demonstration that the toxicity of the N-terminal fragments of mHtt is potentiated by dopamine in cells expressing mHtt exon 1 and transgenic HD mouse models (Benchoua et al., 2008; Charvin et al., 2005; Cyr et al., 2006; Stack et al., 2007). Dopamine modifies the formation of Htt-containing aggregates in primary striatal neurons transfected with exon 1 of Htt gene and exacerbates mHtt-induced cell death (Charvin et al., 2005). Of interest, this effect involves D2-R signaling, since dopamine effect is blocked by D2 antagonists (Benchoua et al., 2006; Charvin et al., 2005). Dopamine loses its detrimental effect when neurons are prepared from D2 receptor null mice (Charvin et al., 2005). Chronic blockade of the D2-R with a selective antagonist significantly reduces death of MSN in a lentiviral model of mHtt expression in rats (Charvin et al., 2008). Possibly, this "protoxic" effect of dopamine through D2-R stimulation may involve a reduction of the mitochondrial complex II, a key regulator of energy metabolism in neurons (Benchoua et al., 2008).

D2-R stimulation increases mHtt toxicity in mouse striatal neurons via, among others, the activation of JNK pathway and activation of the Rho/ROCK-II pathway (Charvin et al., 2005; Deyts et al., 2009).

Thus the presence of D2-R on MSN may render these neurons more susceptible to HD. However, expression of these receptors is down regulated early in HD as seen using biochemical experiments and PET scans in patients (Antonini et al., 1998; Glass et al., 2000). Whether this decrease is entirely caused by a direct regulation of D2-R transcription by mHtt is unknown. It is conceivable that this decrease is, at least in part, an attempt of MSN to reduce cellular stress generated by mHtt.

D1-R (Dopamine type 1 receptor)

In line with a role of D2-R, D1-R may also be involved in the vulnerability of the striatum. Stimulation of D1-R promotes the aggregation of N-terminal fragments of mHtt and cell death in cell line in culture (Robinson et al., 2008). The mechanisms are unknown but a protoxic role for D1-R has been suggested to be mediated by regulation of glutamatergic synapse and facilitation of excitotoxicity (Tang et al., 2007). Supporting this view, experiments in cells immortalized from knock-in HD mice (111Q) showed that activation of D1-R exacerbates mHtt–induced cell death (Paoletti et al., 2008). D1-R activation facilitates glutamate receptor-mediated activation of the Ca^{2+}-dependent protease calpain that in turn cleaves Cyclin dependent kinase 5 (Cdk5). Cleavage of Cdk5 activator p35 into p25 would be neurotoxic to striatal neurons (Paoletti et al., 2008). As for D2-R, D1-R expression being reduced in HD patients and HD models, this may also be seen as a self-defense mechanism to reduce mHtt toxicity.

CalDAG-GEFI (a.k.a. RASGRP2*, Calcium And DAG-Regulated Guanine Nucleotide Exchange Factor I)*

CalDAG-GEF I is a guanine-nucleotide exchange factors (GEFs) activated by diacylglycerol (DAG) and Ca2+. CalDAG-GEFI has substrate specificity for Rap1A, and was found to be enriched in the basal ganglia (Kawasaki et al., 1998). This striatal gene product has been rarely studied, and its neurobiological function is not totally understood.

A pioneering study showed that expression of this gene product may render striatal cells more vulnerable to mHtt (Crittenden et al., 2010). Interesting, it was shown that striatal neurons of R6/2 mice with the highest level of mHtt-containing aggregates had the lowest levels of CalDAG-GEF. Since macroscopic aggregates are thought to be neuroprotective since they sequester mHtt toxic soluble oligomeric species, these results indicated that the presence of high levels of CalDAG-GEF may lead to increased levels of toxic species of mHtt in transgenic mice. Supporting this view, knock-down of CalDAG-GEF in a brain slice model of HD is neuroprotective against mHtt-induced neurodegeneration. The mechanisms underlying its “pro-toxic” properties are not determined. One possibility is that it may inhibit Ras-dependent activation of the Erk/MAP kinase cascade in striatal neurons. Thus, its diminished expression in HD may allow “re-activation” of the pro-survival Erk/MAP kinase pathway to block mHtt toxicity (Crittenden et al., 2010).

RGS2 (Regulator of G-protein signaling 2)

The RGS2 protein is a member of the RGS family of proteins that binds G subunits of heterotrimeric G proteins. RGS2 interfere with Gq and Gi to reduce their rate of hydrolysis of GTP to GDP and thus inhibits the signal transduction from GPCRs. RGS2 play a key role in synaptic plasticity (Kehrl and Sinnarajah, 2002). RGS2 directly interacts with adenylyl cyclases to inhibit the production of cAMP. RGS2 may also regulate GPCR-mediated Akt signaling (Anger et al., 2007). RGS2 expression is reduced in the HD brain and HD mouse models. Seredinina and collaborators studied whether the loss of RGS2 could exacerbate or reduce neurodegeneration induced by overexpression of mHtt in striatal neurons using lentiviral vectors (Seredenina et al., 2011). Results showed that increased expression of RGS2 further aggravates mHtt-induced neurodegeneration. Underlying mechanisms of RGS2 protoxic effects are not fully deciphered but the authors provided preliminary data indicating that they may implicate regulation of Erk/MAP kinase signaling.

RHES (a.k.a. RASD2*, Ras homolog enriched in striatum)*

Rhes is a small G-protein that displays striking enrichment in the striatum and can regulate signaling through G-protein coupled receptors (Falk et al., 1999; Mealer and Snyder, 2012; Vargiu et al., 2004). It has been described as a mediator of mHtt cytotoxicity (Subramaniam et al., 2009), acting as a regulator of SUMOylation. The presence of Rhes in MSN would favor the accumulation of toxic oligomeric species of mHtt in the cytoplasm. More recently, the deletion of Rhes has been found neuroprotective in HD R6/1 mice (Baiamonte et al., 2013).

Rhes binds Beclin-1 and activates autophagy, a lysosomal degradation pathway critical in aging and neurodegeneration (Mealer et al., 2014). Activation of autophagy has been shown to be neuroprotective in HD models (Ravikumar and Rubinsztein, 2006). Rhes-induced autophagy is inhibited by mHtt. The restricted expression of Rhes and its effect on autophagy may explain the selective striatal pathology and delayed onset of HD.

DGK (Diacylglycerol kinase)

The expression of DGK is increased in the striatum of R6/2 HD mice. Zhang and collaborators deciphered the potential role that this increase may have in striatal degeneration/dysfunction after having identified this kinase as a potential therapeutic target based on a screening of kinase inhibitors in a cellular models expressing mHtt (Zhang et al., 2012). The inhibitor of DGK (R59949) blocked induction of cell death pathways triggered by serum withdrawal in knock-in (111Q/111Q) HD striatal cells. Knockdown of all isoforms of DGK using siRNA strategy demonstrated that selective inhibition of DGK was responsible for the neuroprotective effect of the inhibitor. Zhang and collaborators found that knocking down DGK gene in a fly model of HD was neuroprotective. Altogether these data indicate that increased DGK in the striatum could contribute to striatal degeneration. DGK increase could be considered as a protoxic event in HD pathogenesis.

Calcineurin (or protein phosphatase 3, formerly known as protein phosphatase 2B)

Since 1986, calcineurin has been identified by Goto as a marker of neuronal degeneration in the striatum of HD patients (Goto et al., 1986). Calcineurin has preferential expression in the striatum and is downregulated in HD patients and mouse models of HD (Xifro et al., 2009). Calcineurin dephosphorylates Htt at serine 421, inhibition of calcineurin restores axonal transport and transport of BDNF vesicles (Pineda et al., 2009). It is known that Htt phosphorylation is an important protective mechanism in striatal neurons (Humbert et al., 2002). Phosphorylation of mHtt at serine 421 promotes neuroprotection in HD, by restoring Htt function and the transport of BDNF. Supporting the view that reduced calcineurin may be neuroprotective in HD, increased Htt phosphorylation can be produced by pharmacological inhibition of calcineurin with the immunosuppressor FK506 (also known as tacrolimus and fujimycine) (Pardo et al., 2006), or by overexpression of the regulators of calcineurin RCAN1-1L (Ermak et al., 2009) leading to neuroprotective effects.

Thus, the reduction of calcineurin expression and function would lead to a diminution of its activity, increasing phosphorylated state of key proteins, especially mHtt at S421, that activate survival pathways. These mechanisms may be regarded as a compensatory phenomenon that could retard the progression of striatal degeneration.

PDE1B and PDE10A (Phosphodiesterase 1B and 10A)

Studies on phosphodiesterase (PDE) in HD models have shown preferential reduction of the isoforms PDE1B and PDE10A in HD models, while expression of other PDEs seems relatively maintained (Hebb et al., 2004). The loss is detected before onset of symptoms in R6/2 and R6/1 models. Because, PDE regulates levels of cAMP, which plays a key role in modulation of gene expression which is altered in HD, the effects of a treatment with a PDE10 inhibitor has been studied in the R6/2 mouse model of HD. Results showed that chronic pharmacological blockade of PDE10 is neuroprotective and reverses a number of transcriptomic anomalies in HD mice (Giampa et al., 2010). In line with this, the characterization of the effects of a pharmacological inhibition of PDE indirectly suggests that the reduction of PDE activity in HD could lead to multiple effects: it up-regulates cAMP-responsive element –dependent transcription, it down-regulates HDAC4 (histone deacetylase 4) mRNA, and could activate Mitogen- and stress-activated kinase-1 (MSK1). These latter effects should contribute to striatal neurons against mHtt toxicity. Thus, the presence of PDE in striatal cells may be considered protoxic, and its decrease in HD could be seen as a compensatory mechanism to counteract the effect of mHtt. Interestingly, further inhibition of the enzyme may allow the triggering of neuroprotective pathway and as such may constitute an interesting pharmacological therapy.

Potential Neuroprotective striatal gene products

BCL11 (*B-cell leukemia/lymphoma 11B)*

B-cell leukemia/lymphoma 11B (Bcl11b) (a.k.a. CTIP2) is a transcription factor that has been described to be a key gene for differentiation of medium sized spiny neurons in the striatum.

Since MSN represent ~95% of the neurons in the striatum, Bcl11b likely possesses a central role that determines the architecture and organization of the striatum, and as such its function is likely crucial in HD (Arlotta et al., 2008). Bcl11b mRNA levels are reduced in the HD striatum. The overexpression of Bcl11b has been found neuroprotective in cell models of HD in vitro (Desplats et al., 2008). The direct interaction of Bcl11b with mHtt and its possible sequestration in inclusions may further abolish its capacity to regulate the expression of many striatal genes that are crucial for the survival of MSN. In particular, there exists a functional interaction between Bcl11b and BDNF. Chromatin-immunoprecipitation experiment and sequencing (ChIP-seq) indicated that Bcl11b is a regulator of the BDNF signaling pathway (Tang et al., 2011). Thus, the loss of Bcl11b in the striatum may lead to a striatal-selective cascade of events that could explain the preferential vulnerability of MSNs against mHtt.

FOXP1 (Forkhead box protein P1)

FOXP1 is thought to be an important transcription factor regulating cell-cell interaction signaling. FOXP1 shows highly expression in the striatum (Desplats et al., 2006; Desplats et al., 2008). Its expression is regulated by Bcl11b. There exist overlaps between the genes that are regulated by FOXP1 in normal neurons and the genes that are deregulated in HD (Tang et al., 2012). No rescue or knock-down experiments have been performed, but FOXP1 seems to interact with mHtt and to be trapped in mHtt-containing aggregates (Tang 2012). Therefore, its reduced expression likely contributes to the preferential vulnerability of the striatum in HD.

MSK-1 (Mitogen- and stress-activated kinase-1)

In healthy conditions, the mitogen- and stress-activated kinase-1 (MSK-1), a striatum-enriched nuclear protein kinase downstream Extracellular Regulated Kinase (ERK), promotes activation of the transcriptional factor kappa-light-chain-enhancer of activated B cells (NF-kappaB) signaling, inducing c-Fos transcriptional activation important for immune and inflammatory responses (Vermeulen et al., 2003). MSK-1 is downregulated in R6/2 HD model mice and in caudate from HD patients (Roze et al., 2008a). Overexpression of MSK-1 in primary culture of striatal neurons expressing a short fragment of mHtt is neuroprotective, whereas knockdown of MSK-1 is protoxic. Interestingly Roze and collaborators found evidence of ERK, Elk-1 and CREB nuclear activation in the striatum of R6/2 mice. This suggested the existence of a possible self-defense response in striatal neurons. However this response appeared to be blunted, since neither phosphorylation of histone H3 phosphorylation nor c-Fos activation were detected. Indeed, loss of MSK-1 in the striatum in HD mice impeaches activated ERK to produce its downstream effects on transcription. In the normal brain, MSK-1 phosphorylates histone H3, CREB and up-regulates peroxisome proliferator-activated receptor co-activator-1α (PGC-1α), playing role in bioenergetic stability in MSNs. The MSK-1 downregulation likely produces mitochondrial dysfunction rendering MSNs more susceptible to mHtt. Consistent with this hypothesis, MSK-1 overexpression in striatal neurons using lentiviral vectors was neuroprotective against mHtt in mouse models of HD (Martin et al., 2011). Therefore, because MSK-1 shows enrichment in the striatum, its loss would contribute to render the striatum more fragile in HD.

ADORA2 (Adenosine receptor type 2A)

A2A receptors (A2A-R), coded by the *ADORA2A* gene have a highly enriched expression in the striatum. The expression of A2A receptor is down regulated in the striatum of HD patients (Glass et al., 2000) and in several HD mouse models (R6/2,N171-82Q) (Chou et al., 2005; Menalled et al., 2000) These receptors are located at the terminal of cortico-striatal pathway (presynaptic receptors) and in the D2-MSNs (postsynaptic receptors). The mRNA level of A2A-R in the striatum is higher in the striatum than in the cerebral cortex. These two types (pre- and post-synaptic) seem to differ in their contribution to neurodegenerative process. Evidences in HD area suggest that activation of presynaptic A2A-R is pro-toxic for MSNs by modulation of glutamate release whereas activation of postsynaptic A2A-R are protective (Popoli et al., 2007). Both agonists and antagonists were proposed to treat HD symptoms. Interestingly, the A2A-R agonist, CGS21680, produces an opposite effect in WT and symptomatic R6/2 in slices. Field potentials (FP) were recorded with and without NMDA and CGS21680. The NMDA toxicity is observed by the only partial recovery after the FP stimulation. The addition of CGS21680 increases NMDA-mediated toxicity in WT MSNs whereas it decreases it in symptomatic R6/2 mice (Martire et al., 2007). Thus, it seems that complex regulatory mechanisms, possibly compensatory, involve A2A-R in HD mice.

The chronic effect of the presence of A2A-R, especially expressed at high level in MSN is not totally understood. Genetic deletion of the *ADORA2A* gene precipitates motor symptoms and death in HD mice expressing a short N-terminal fragment of mHtt (Mievis et al., 2011a). In support of the hypothesis that A2A-R may have an impact on the disease progression, a single genetic polymorphism in the *ADORA2A* gene in HD patient can modify the age of onset (Dhaenens et al., 2009). Thus, the loss of A2A-R may be detrimental. These receptors are likely neuroprotective. However, it must be underscored that the exact contribution of presynaptic receptors of the cortico-striatal pathway versus the post-synaptic receptors expressed by MSN in these experiments remains to be fully elucidated.

CNR1 (Cannabinoid type 1 receptor)

The profound and early loss of striatal type 1 cannabinoid receptors (CB1-R) in the striatum and projection area (substantia nigra reticulate and globus pallidus externus) in HD has been demonstrated by autoradiography studies on post mortem brain samples from patients at early stages as for the A2A-R (Glass et al., 2000). Loss of CB1 binding sites have been confirmed in vivo by PET studies in HD patients (Van Laere et al., 2010). Elegant studies demonstrated that genetic deletion/knockout of CB1 receptors exacerbates the motor phenotype in HD mice (Blazquez et al., 2011; Mievis et al., 2011b). The loss of CB1-R might be due to direct transcriptional deregulation produced by mHtt (via mHtt-induced deregulation of REST) (Blazquez et al., 2011) but also may result from more complex mechanisms. Indeed, exposure of immortalized striatal cells with endogenous cannabinoids produced an increase in CB1-R expression (Laprairie et al., 2013). Treatment of HD striatal cells (Q111/Q111) with cannabinoid markedly increases CB1-R expression.

Available results from *in vitro* experiments indicate that the loss of CB1-R in HD would lead to reduced levels of BDNF, which in turn should render striatal cells more vulnerable to mHtt toxicity, possibly through decreases in PGC-1α levels (Laprairie et al., 2013). However a convincing work recently performed in R6/2 HD mice showed that only the presynaptic CB1-R at the cortico-striatal terminals actually underlie the neuroprotective effects of the CB1-R agonists *in vivo* (Chiarlone et al., 2014). Thus CB1-R can be considered as neuroprotective. However, the impact of the reduced striatal expression of CB1-R in HD is uncertain.

SCN4B (Sodium channel beta 4b subunit)

SCN4b mRNA expression is down regulated in HD models and HD patients (Brochier et al., 2008; Kuhn et al., 2007; Oyama et al., 2006). Its reduced expression is more severe than that of other sodium channel subunits (Oyama et al., 2006). The function of this sodium channel subunit is unknown. The good correlation between loss of its expression and progression of the disease in R6/2 mice suggested a potential role in striatal vulnerability. In line with this, SCN4b levels seem to be more reduced in regions of the central nervous system that are the most affected by mHtt expression. Interestingly, overexpression of SCN4b in neurons in primary culture produces trophic effects characterized by increased dendritic genesis (Oyama et al., 2006). Thus SCN4b may be a "neuroprotective" striatal marker whose reduced expression in HD may contribute to the preferential degeneration of the striatal in HD. However, its putative neuroprotective effect needs to be directly assessed against mHtt toxicity.

*STEP61 (*PTPN5 *gene, Striatal-enriched protein tyrosine phosphatase 61)*

Reduced expression of STEP61 mRNA has been found in HD transgenic models and HD brain (Desplats et al., 2006). In different mouse models (YAC1128, TET-HDH94, R6/1 and KI111) the protein is reduced and its level of phosphorylation is increased, which should further contribute to a reduction of its phosphatase activity (Gladding et al., 2014; Saavedra et al., 2011). Convincing results indicate that the loss of STEP61 is globally detrimental to MSN, although it may also partially represent a compensatory mechanism trying to block excitotoxicity in striatal cells. In R6/1 mice, whereas STEP protein levels are reduced in young (excitotoxicity sensitive) mice, its levels of phosphorylation is much increased, leading to its further inactivation (Saavedra et al., 2011). In line with this, intrastriatal injection of a permeable and active form of SETP61 (TAT-STEP), could increase the excitotoxic lesions produced by the NMDA receptor agonist quinolinate. In addition, an increased cleavage of STEP61 has been observed, resulting from increased calpain activation due to entry of Ca^{2+} through NMDA receptors. An accumulation of the breakdown product STEP33 (inactive and unable to dephosphorylate MAPK/p38) is associated with elevated p38 phosphorylation (Saavedra et al., 2011), which his detrimental for cell survival. STEP dephosphorylates ERK , reducing its activation and pro-survival signals. There is an increased activation of pro-survival MAPK/ERK1/2 signaling in older mice resistant to excitotoxicity. In young YAC128CAG HD mice that are sensitive to excitotoxicity, STEP61 levels have also been found reduced, as STEP33 (Gladding et al., 2014).

At later stage, when YAC128 mice become resistant to excitotoxicity, the loss of STEP61 may be associated with the induction of ERK1 (blocking excitotoxicity) while maintaining activation of MAPK/p38 that favors cell death pathways. These very interesting studies clearly show the existence of complex “striatum-specific” compensatory mechanisms in HD mice, and their evolution over time, possibly to block sequentially mHtt toxicity.

Thus the role of STEP61 in striatal vulnerability is ambivalent. Its loss in HD may reduce excitotoxicity, consistent with a neuroprotective compensatory mechanism. In this case STEP61 could be considered as a protoxic actor in MSN. However its loss also contributes to activate MAPK/p38 pathway. In this latter case, STEP61 may be seen as a neuroprotective agent for MSNs.

ELK-1 (ETS-Like Gene 1)

In basal condition, Elk-1 is ubiquitously expressed in the brain, but in HD mice models R6/1 and R6/2, and in immortalized HD mouse (Q111/Q111) cells, Elk-1 has a higher protein expression level and phosphorylation , and is found in the nucleus of the MSNs of 30 weeks old R6/1 mice and 12 weeks old R6/2 mice. Elk-1 does not co-localize with mHtt, which suggests a higher transcriptional activity compared to WT mice (Anglada-Huguet et al., 2012; Roze et al., 2008a). The authors suggested that the change in Elk-1 expression may be a compensatory mechanism to protect MSN in response to mHtt-induced stress.

Elk-1 is a member of a subfamily of proteins called ternary complex factors (TCF). Elk-1 is a transcriptional activator, as it interacts with serum response factor to bind jointly to serum response elements in the promoters of several immediate-early genes (IEGs), such as c-fos and egr-1. In the CNS, Elk-1 is activated by ERKs in response to neurotrophins and neurotransmitters.

Anglada-Huguet and collaborators have shown that down-regulation of Elk-1 by siRNAs produces caspase 3 cleavage and cell death in immortalized HD mouse (Q111/Q111) cells, but not in wild-type cells (Anglada-Huguet et al., 2012). Thus the induction of Elk-1 expression in HD may be considered to be a neuroprotective compensatory mechanism. However, transcriptional activity at the *c-fos* promoter was impaired in the striatum of R6/2 transgenic mice, despite activation/phosphorylation of Elk-1 (Roze et al., 2008a). As mentioned above, the reduction of MSK1 in R6/2 mice may partially impair the impact of Elk-1 activation. Elk-1 can be considered as an “inducible” striatal marker in HD, likely producing a neuroprotective self-defense mechanism. Further studies are awaited to better understand how the increase in Elk-1 plays a role in striatal degeneration at late stage in animal models of HD.

Neutral striatal markers

Capucin (a.k.a. Tmem90a*)*

Capucin, a gene of unknown function is preferentially expressed in the striatum (de Chaldee et al., 2003). Notably, lower capucin mRNA levels have been detected in the R6/1 transgenic mouse model of HD (Desplats et al., 2006), R6/2 and in primary cultures of rat striatal neurons expressing a mutant fragment of human Htt than in the corresponding controls (de Chaldee et al., 2006).

However, in vivo experiments showed that capucin overexpression is not able to counterbalance mHtt-induced toxicity in the striatum in a lentiviral mouse model of HD (Galvan et al., 2012). Mice that were knockout for capucin gene had similar susceptibility to mHtt-induced toxicity as wild type age-matched littermates. Size and number of ubiquitin-containing inclusion produced by overexpression of mHtt is these mice were similar to those detected in wild type mice (Galvan et al., 2012). Capucin downregulation in HD mouse models could be a direct consequence of the transcriptional dysfunction occurring in HD without major consequence on MSN survival. Thus capucin may be considered as a "neutral" striatal gene.

Hippocalcin

Hippocalcin, a neuronal calcium sensor protein, is also known as p23k. Although the physiological role of hippocalcin is not completely understood, it is implicated in the regulation of neuronal viability and plasticity. Evidences showed that hippocalcin is important for the homeostasis of intracellular calcium levels (Amici et al., 2009). Hippocalcin can protect hippocampal neurons against excitotoxicity induced damage by enhancing Ca^{2+} extrusion and maintaining ideal intracellular Ca^{2+} levels (Masuo et al., 2007).

The decreased expression of hippocalcin in different mouse models of HD suggested a role of this protein in striatal vulnerability. Rudinskiy and collaborators studied this hypothesis in primary culture of striatal neurons (Rudinskiy et al., 2009). Hippocalcin was overexpressed using lentiviral vectors in neurons that expressed mHtt (N-terminal fragments with 82 glutamine repeat). Analysis of different outcomes related to degeneration indicated that hippocalcin was not neuroprotective. In addition, overexpression of hippocalcin did not protect neurons subjected to mitochondrial dysfunction caused by 3-nitropropionic acid or glutamate-induced excitotoxicity, two conditions inducing increase in cytoplasmic Ca^{2+} concentrations (Rudinskiy et al., 2009). Thus, hippocalcin may have deregulated expression, in absence of major consequences in neuronal survival. In this case, as capucin, hippocalcin may be seen as "neutral" striatal marker. However, it cannot be excluded that hippocalcin could have an effect in different HD models, including animal models that express full length mHtt.

Other possible pathways to be investigated

Nowadays, the number of studies trying to decipher the functions of this small number of striatal genes is limited. However, these pioneering studies which tried to understand their roles with regard to mHtt toxicity provided key results indicating that possibly, they are regulators of cell survival, upstream master gene/protein networks of neuronal survival (Fig.1). In particular, deregulation of membrane receptors (D1-R, D2-R, CB1-R, A2A-R, SCN4B) involved in neurotransmission in HD could directly modulate cell survival processes through different routes (e.g. MAP Kinase pathway, regulation of PGC1- etc.). How these different receptors act to positively or negatively regulate striatal cell survival remains to be uncovered. It is likely that, for the GPCR, their effects are related to the activation of heterotrimeric G proteins leading to increased or decreased cAMP levels but could also be mediated through other pathways such as the endocytosis/-arrestin-mediated pathway and/or interaction of heterotrimeric subunits with transmembrane ion channels (Ritter and Hall, 2009).

Increased cAMP levels may be considered neuroprotective while reduction of cAMP should be "protoxic". It is likely that mechanisms converging on cAMP level regulation are important for opposing mHtt toxicity. Indeed PDE which reduce cAMP levels is considered to increase striatal cell vulnerability to mHtt (see below). However, it is probable that the effects of striatal membrane receptors on mHtt toxicity cannot be only explained according to their inherent capability to change cAMP levels. For example, D2-R and D1-R are thought to be coupled to different subunits (□i/o and □s/olf, leading, when stimulated separately, to a reduction and decrease in cAMP levels respectively) (Beaulieu and Gainetdinov, 2011), but both receptors seem to increase mHtt toxicity. Downstream cAMP changes (and possible through independent mechanisms) the protoxic effects of D2-R may involve inhibition of the pro-survival kinase Akt (Marion et al., 2014) while D1-R effects may involve CDK5 (Paoletti et al., 2008). In line with these complex mechanisms, CB1-R which decrease cAMP levels when stimulated alone, are rather neuroprotective against mHtt through a mechanism that remains to be elucidated. One possibility is that co-activation of D2-R and CB1-R which increase cAMP so that the loss of CB1-R in HD may result in reduced cAMP levels and a protoxic effect which would depend on the presence of D2-R (Glass and Felder, 1997). There also exist a number of very complex cross talks between membrane receptors signaling in striatal neurons that could participate to more complex/integrated biological effects when their stimulation occurs simultaneously. In particular, receptors can heteromerize, which changes their intracellular signaling impact. For example, D1-R/D2-R heteromers act preferentially through G□q changing signaling as compared to each receptos separately. Another interesting example is related to A2A-R/D2-R heteromers. The activation of A2A-R in these heteromers reduced the binding of dopamine on the D2-R (Ferre et al., 2008). Reciprocally, stimulation of D2-R represses the activation of adenylyl cyclase by A2-R. Other pathways may also be involved. For example, the activation of □-arrestin signaling by A2A-R/D2-R heteromers is stronger and more transient as compared to D2-R alone (Borroto-Escuela et al., 2011). In summary, the mechanisms through which those different membrane receptors act all together on mHtt toxicity (as causal factors or as key actors of compensatory/self-defense mechanisms) are largely unknown but likely involve extremely complex /integrated signaling.

Similarly cytoplasmic signaling proteins (PDE, MSK1, STEP61, DGK) can also act upstream or downstream master regulators of cell survival (CREB, MAPK/Erk1). Other striatal markers seem to be involved in molecular steps between membrane receptor signaling and downstream cytoplasmic effectors. This is the case for RGS2 and CalDAG-GEF1. Other striatal markers may not act directly on signaling processes regulating transcription or survival. Indeed, it is likely that some markers, such as Rhes, may involve key cellular "housekeeping" mechanisms such as SUMOylation of proteins and autophagy. Finally, Bcl11b and FOXP1 are good examples of striatal marker that can be directly implicated in the regulation of transcription, and the inherent state of differentiation of MSN.

The study of the role of striatal markers in striatal vulnerability in HD suggests that these gene products, likely associated with highly specific neurobiological functions (and as such they are markers of highly differentiated non-dividing cells), may be, on the one hand, the most vulnerable targets of mHtt-induced transcription deregulations and, on the other hand, key "switches" of striatal adaptive changes, that may be considered as self-defense mechanisms.

How these different striatal markers functionally interact each other remains to be precisely assessed. It is quite obvious that currently the puzzle is not complete and that many more actors are involved in the vulnerability of the striatum. Indeed, beyond the few striatal markers that have been reviewed above, many others may also act as modifiers of mHtt. When considering striatal markers with relatively stringent criteria (see paragraph above), it clearly appears that only a small proportion of striatal markers has been experimentally studied. It is beyond the scope of this review to provide extensive speculations on every striatal marker that have never been studied in the context of HD research. However, it is worth mentioning that many of them, which abnormal expression in the striatum of HD patients have been observed long ago, have never been studied for their capacity to modify mHtt toxicity. For example, neurotensin, whose expression is high in the striatum as compared to other brain regions, has been found abnormally increased in the HD striatum (Nemeroff et al., 1983). Many newly identified striatal markers have been found deregulated in HD mouse models (Brochier et al., 2008; Mazarei et al., 2010). For example, the upregulation of IDO-1 (indoleamine 2,3-dioxygenase) in YAC128 HD mice may be seen as a risk factor for striatal cells, since deletion of IDO-1 protects the striatum against excitotoxicity (Mazarei et al., 2013b). Since kynurenine pathway likely plays a role in HD pathogenesis (Thevandavakkam et al., 2010), it is possible that IDO-1 is a modifier of mHtt toxicity (Mazarei et al., 2013a). This remains to be further assessed.

Conclusion

It is very difficult to know whether a change in expression of a given striatal marker in HD represents a compensatory mechanism, and/or a phenomenon that will contribute to striatal degeneration. This question needs to be experimentally addressed. However, all the gene products that have not yet been explored represent a pool of potential candidate modifiers of mHtt, relevant to striatal vulnerability. Our group and others are currently testing the effects of many newly identified striatal markers of unknown biological functions. Preliminary observations indicate that a majority of them are neuroprotective or protoxic modifiers of mHtt in cell and mouse models. As such, they could represent innovative therapeutic targets. Promoting the activity of the neuroprotective markers or blocking the activity of the protoxic gene products could help to slow the progression of symptoms and degeneration in HD. In addition, since a majority of these striatal markers have ill-defined neurobiological functions, research focused on these striatal gene products could be a unique opportunity to better define the molecular and functional complexity of the striatum, a brain region which is central stage in a broad spectrum of motor and cognitive functions and is likely implicated in different neurological and psychiatric illnesses.

Figure Legend:

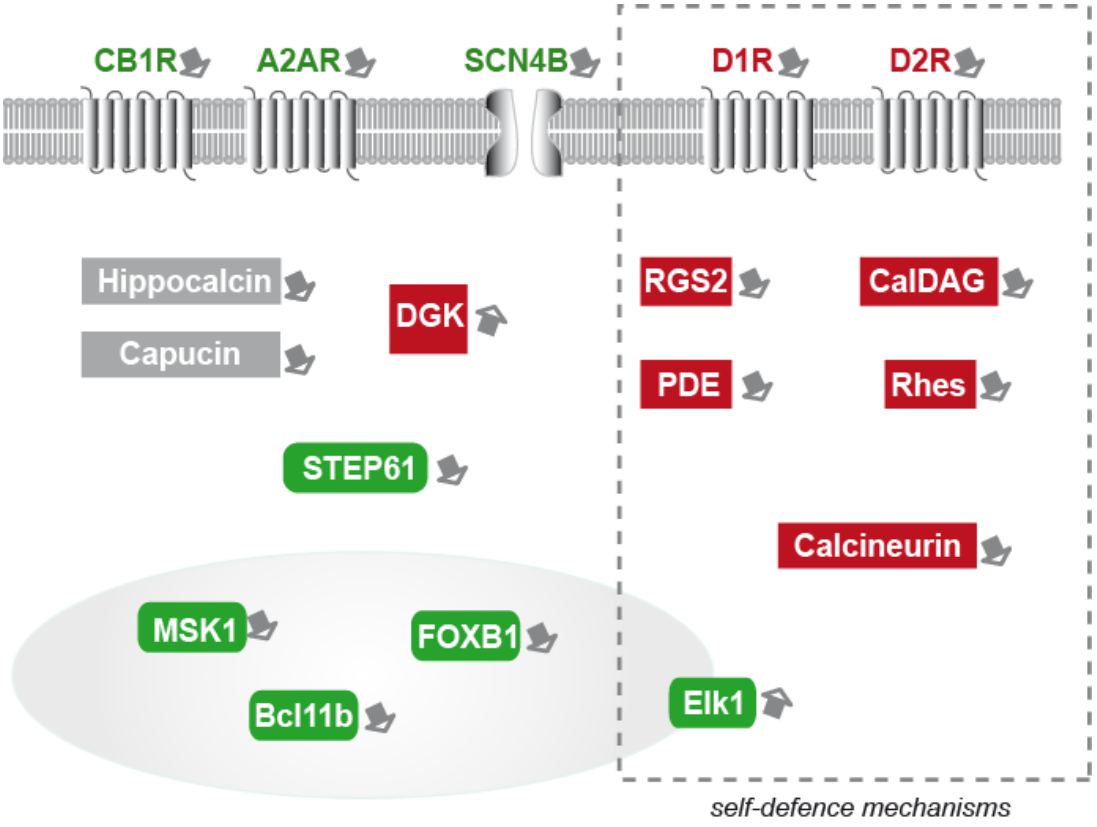

Figure 1: Schematic representation of the striatal markers that have been experimentally studied as potential modifiers of mutant huntingtin toxicity in HD. Green boxes symbolize markers that are "neuroprotective". Red boxes symbolize markers that are "protoxic". Expression changes in markers included in the dotted-line rectangle may represent, at least in part, self-defense-mechanisms. Markers in grey boxes would have altered expression without major consequences on mHtt. Note that striatal gene modifiers have broad biological functions and cellular localization, including neurotransmitters binding, intracellular signaling (kinases and phosphatases), and transcription activators. The nucleus is symbolized by the grey colored round form. MSK1 and Elk1 can be found in the cytoplasm and upon activation translocate in the nucleus.

(A) Enriched striatal markers with characterized disease modifier effects						
Human Gene Symbol	**Human Gene Name**	**regulated expression in HD**	**Overexpression effect against mHtt : compensatory ?**	**HD disease modifier studies**	**Models**	**mHtt used**
ADORA2A	Adenosine A_{2A} receptor	down	neuroprotective	Blum, J Neurosc, 2003; Mievis, Neurobiol Dis, 2011	3-nitropropionic acid injection to both wild-type and $A_{2A}^{-/-}$ mice; N171-82Q mice; HD A2A+/+ and HD A2A−/−	N171-82Q mice = first 171 aa of human HTT (exons 1, 2, part of 3) with 82 CAG repeats (Htt171-82Q) under Prnp promoter
BCL11B	B-cell leukemia/lymphoma 11B	down	neuroprotective	Desplats et al., 2008	STHdhQ111 cells	Htt 111 CAG repeats
CalDAG GEFI / RASGRP2	Calcium And DAG-Regulated Guanine Nucleotide Exchange Factor I / RAS, Guanyl Releasing Protein 2	down	protoxic	Crittenden et al., 2010; Graybiel et al., 2010	brain-slice explant model of HD + knock-down of CalDAG-GEFI expression	polyglutamine-expanded Htt exon 1
CNR1	Cannabinoid Receptor 1 (brain)	down	neuroprotective	Blázquez et al., 2011	R6/2 mice (Mangiarini)	Exon 1 of human HTT gene with around 150 CAG repeats under 1kb of human HTT promoter
DGK	Diacylglycerol kinase	up	protoxic	Zhang et al., 2012	STHdhQ111 cells; Drosophila HD model	Htt 111 CAG repeats / N-terminal Htt with 128 CAG repeats using the neuronal elav-GAL4 driver in Drosophila
DRD1	Dopamine D1 receptor	down	protoxic	Robinson P, Lebel M, Cyr M., 2008	SK-N-MC human neuroblastoma cell transfected with Htt	exon-1 of human htt with 25 or 103 CAG repeats
DRD2	Dopamine D2 receptor	down	protoxic	Charvin 2005; Cyr 2006; Stack 2007; Tang 2007; Benchoua 2008	lentivirus mediated Htt171-82Q infected striatal neurons; R6/2 mice ; YAC128 mice (Slow et al., 2003); 3NP model injection	First 171 aa of human HTT with 18 CAG repeats or mutant HTT with 82 CAG ; Exon 1 of human HTT gene with around 150 CAG repeats under 1kb of human HTT promoter; Human Htt protein containing a 128 CAG repeat expansion
ELK-1	ETS-Like Gene 1 / ETS Domain-Containing Protein / Tyrosine Kinase (ELK1) Oncogene	up	neuroprotective	Anglada-Huguet et al. J Neurochem, 2012	R6/1 mice and R6/2 mice; STHdh(Q111/Q111) cells	Exon 1 of human HTT gene with 116 CAG repeats under 1kb of human HTT promoter or with around 150 CAG repeats
FOXP1	Forkhead box protein P1	down	neuroprotective	Tang et al., 2012	STHdhQ111 cells; R6/1 mice	Htt 111 CAG repeats / Exon 1 of human HTT gene with around 114 CAG repeats under 1kb of human HTT promoter; Htt 111 CAG repeats
HPCA	Hippocalcin	down	neutral	Rudinskiy et al., J Neurochem, 2009	Striatal neuron (ganglionic eminence) cultures infected with lentiviral-mediated over-expression of first 171 aa of human HTT with 18 CAG repeats or mutant HTT with 82 CAG repeats under the control of TRE promoter / 3-NP and glutamate-induced excitotoxicity	First 171 aa of human HTT with 18 CAG repeats or mutant HTT with 82 CAG
IDO-1	indoleamine 2,3-dioxygenase	up	protoxic	Mazarei et al., 2013	YAC128 mice; Ido1 null mice (Ido−/−)	Human Htt protein containing a 128 CAG repeat expansion
MSK-1	mitogen- and stress-activated kinase-1	down	neuroprotective	Martin et al., 2011	rat model of HD based on striatal lentiviral expression of mHtt	First 171 aa of human HTT with 18 CAG repeats or mutant HTT with 82 CAG
PDE1B	phosphodiesterase 1B, calmodulin-dependent	down	protoxic	Hebb et al., 2004	R6/1 mice; R6/2 mice; HD human caudate	Exon 1 of human HTT gene with 116 CAG repeats under 1kb of human HTT promoter or with around 150 CAG repeats
PDE10A	phosphodiesterase 10A, calmodulin-dependent	down	protoxic	Hebb et al., 2004; Giampà et al., 2010	R6/1 mice; R6/2 mice; HD human caudate; R6/2 mice treated with PDE10A inhibitor TP-10	Exon 1 of human HTT gene with 116 CAG repeats under 1kb of human HTT promoter or with around 150 CAG repeats
PPP3CC	calcineurin / protein phosphatase 3 / protein phosphatase 2B	down	protoxic	Pardo et al., J Neurosc, 2006; Ermak et al., JBiolChem, 2009	rat model of HD based on striatal lentiviral expression of mHtt; ST14A cells expressing normal Htt (15 CAG repeat, no negative effect on cells) or mHtt (120 CAG repeat, toxic when cells are induced to differentiate)	First 480 aa of huntingtin containing 17 (wild-type, 480-17Q) or 68 glutamine residues (mutant, 480-68Q) with either an intact S421, an S421 to alanine (S421A) or an S421 to aspartic acid (S421D) mutation. ; Htt with 15 CAG repeat or with 120 CAG repeat
PTPN5	Striatal-enriched protein tyrosine phosphatase 61 (STEP61) / protein tyrosine phosphatase, non-receptor type 5 (striatum-enriched)	down	neuroprotective and protoxic in some cases	Saavedra et al., 2011 / Gladding et al., 2014	HdhQ7/Q111 knock-in mice; R6/1 mice and R6/2 mice; YAC128 mice	Htt 111 CAG repeats; Exon 1 of human HTT gene with 116 CAG repeats or around 150 CAG repeats under 1kb of human HTT promoter; Human Htt protein containing a 128 CAG repeat expansion
RASD2	Ras homolog enriched in striatum Rhes	down	protoxic	Subramaniam et al., 2009; Baiamonte et al., Plos One 2013; Mealer et al., J Neurosc 2013;	STHdhQ111 cells; R6/1 mice crossed with Rhes knockout mice; striatal-specific model of HD elicited by 3-nitropropionic acid	Htt 111 CAG repeats; Exon 1 of human HTT gene with around 116 CAG repeats under 1kb of human HTT promoter
RGS2	Regulator of G-protein signaling 2	down	protoxic	Seredenina et al., Plos One 2011	cultured rat primary striatal neurons	First 171 aa of human HTT (exons 1, 2, part of 3) with 82 CAG repeats (Htt171-82Q) / 3NP
SCN4B	sodium channel. voltage-gated. type IV. beta	down	neuroprotective	Oyama et al., 2006	HD190QG mice (Kotliarova); R6/2 mice	First 67 amino acids with 155 and 190 CAG repeats; Exon 1 of human HTT gene with around 150 CAG repeats under 1kb of human HTT promoter
TMEM90A / CAPUCIN	transmembrane protein 90A / Synapse Differentiation Inducing 1-Like	down	neutral	Galvan et al., 2012	LV-mediated mHtt mice	First 171 aa of human HTT (exons 1, 2, part of 3) with 82 CAG repeats (Htt171-82Q)

(B) Enriched striatal markers with disease modifier effect not studied		
Human Gene Symbol	**Human Gene Name**	**regulated expression in HD**
ACTN2	Actinin. alpha 2	down
ADCY5	Adenylate cyclase type V	down
AP1S1	Adaptor-related protein complex 1, sigma 1 subunit	down
ARPP-16/19	16/19-kDa cyclic AMP-regulated phosphoprotein	down
ARPP-21	21-kDa cyclic AMP-regulated phosphoprotein	down
B3GNT1	β-1,3-N-acetylglucosaminyltransferase 1	down
BAIAP2	Insulin rec. substrate p53	down
BC092620	echinoderm microtubule associated protein like 5 (Eml5)	down
CARHSP1	calcium-regulated heat stable protein 1. 24 kDa	not changed
CD4	CD4 antigen (membrane glycoprotein of T lymphocytes)	up in caudate HD patient / down in YAC128
CHCHD3	coiled-coil-helix-coiled-coil-helix domain containing 3	not changed
CPNE5	Copine V	down
CRYM	crystallin, mu	down
DARPP-32 / PPP1R1B	Dopamine- and cAMP-regulated phosphoprotein, 32 kDa / protein phosphatase 1, regulatory (inhibitor) subunit 1B	down
DCLK3	doublecortin-like kinase 3	down
DRD3	Dopamine D3 receptor	down
DRRF / KLF16	dopamine receptor regulating factor	down
EPHA4	Eph family receptor interacting proteins / ephrin ligands	up
FLJ46347	hypothetical LOC389064	no data
FOXP2	Forkhead box protein P2	down
GALNAC4S6ST	B-cell RAG ass'd protein / carbohydrate (N-acetylgalactosamine 4-sulfate 6-O) sulfotransferase 15	down
Gm705	Gene model 705 (NCBI)	down
GNG7	G protein. c7 subunit	down
GNAL	G protein. aolf	down
GPR88	G protein-coupled receptor 88	down
GPR155	G protein-coupled receptor 155	down
hCG2040376	hCG2040376	no data
HS6ST2	heparan sulfate 6-O-sulfotransferase 2	not changed
HTR4	5-HT4 receptor	no data
HTR6	5-HT6 receptor	up
ISL-1	Insulin gene enhancer protein	down
KLF9 / BTE binding protein	Kruppel-like factor 9	down
KCNIP2	K_v channel-interacting protein 2	down
LINC00035	Long Intergenic Non-Protein Coding RNA 35	down
LOC390205	similar to Serdin1	no data

Human Gene Symbol	Human Gene Name	regulated expression in HD
MBA51		down
MBA52		down
MBA55		no data
Mbd2	Methyl-CpG Binding Domain Protein 2	not changed
MCTP1	multiple C2 domains. transmembrane 1	not changed
MGAT5B	mannosyl (alpha-1,6-)-glycoprotein beta-1,6-N-acetyl-glucosaminyltransferase, isozyme B	not changed
MYT1L	Myelin transcription factor 1-like	not changed
NEXN	nexilin (F actin binding protein)	not changed
NGEF	neuronal guanine nucleotide exchange factor	down
Nolz-1 / ZNF503	zinc-finger 503 (developmentally regulated striatum-enriched)	no data
NTS	Neurotensin	up
OPRD1	Delta opioid receptor	down
OPRK1	Kappa opioid receptor	down
OPRM1	Mu-opioid receptor	no data
OSBPL8	oxysterol binding protein-like 8	down
PENK	Preproenkephalin 1	down
PPP1R16B	Protein phosphatase 1, regulatory (inhibitor) subunit 16B	down
PPP3CA	Protein phosphatase 3, catalytic subunit, alpha isozyme	down
RARB	Retinoic acid receptor beta receptor 1	down
RGS9	Regulator of G-protein signalling 9	down
RNF13	Ring finger protein 13	up
RXRG / NR2B3	Retinoic acid receptor gamma / nuclear receptor subfamily 2, group B, member 3	down
SH2D5	Src Homology 2 domain containing 5	down
SLC41A1	Solute Carrier Family 41 (Magnesium Transporter), Member 1	down
SP9	Sp9 transcription factor	not changed
SPOCK3	Sparc/osteonectin, cwcv and kazal-like domains proteoglycan (testican) 3	down
ST8SIA3	ST8 alpha-N-acetyl-neuraminide alpha-2,8-sialyltransferase 3	down
STRN	Striatin	down
SYNPR	Synaptoporin	down
TAC1	Substance P	down
TBL1X	Transducin (beta)-like 1X-linked	not changed (but tendancy up)
TMEM158	Transmembrane Protein 158	not changed in YAC128 mouse model of HD
TESC	Tescalcin	down
WFS1	Wolfram syndrome 1 (wolframin)	not changed

Supplementary Table 1. List of striatal-enriched gene products and their expression changes in HD transgenic mice and HD patients studies. The non-exhaustive list of striatal markers has been selected on the basis of the list of striatal-enriched markers in Desplats's study (2006) and completed by other transcriptomic and SAGE studies (Desplats et al., 2006; Brochier et al., 2008; Hodges et al., 2006; Kuhn et al., 2007; Mazarei et al., 2010). **A**, the upper part of the table shows the short list of striatal markers which have been experimentally studied for their properties to change mutant Htt toxicity in cell or animal models. Markers with suspected involvement in self-defense mechanisms are indicated in blue. For these markers, the right columns indicate the potential qualification as "neuroprotective, protoxic, or neutral", the corresponding references, the models used and the molecular forms of mutant Htt that have been used in the experiments. **B**, the lower part of the table presents a list of striatal markers whose effects on mHtt toxicity have never been experimentally studied (list non exhaustive).

References

Amici, M., Doherty, A., Jo, J., Jane, D., Cho, K., Collingridge, G., and Dargan, S. (2009). Neuronal calcium sensors and synaptic plasticity. Biochemical Society transactions *37*, 1359-1363.

Andre, V.M., Cepeda, C., Fisher, Y.E., Huynh, M., Bardakjian, N., Singh, S., Yang, X.W., and Levine, M.S. (2011). Differential electrophysiological changes in striatal output neurons in Huntington's disease. J Neurosci *31*, 1170-1182.

Anger, T., Klintworth, N., Stumpf, C., Daniel, W.G., Mende, U., and Garlichs, C.D. (2007). RGS protein specificity towards Gq- and Gi/o-mediated ERK 1/2 and Akt activation, in vitro. Journal of biochemistry and molecular biology *40*, 899-910.

Anglada-Huguet, M., Giralt, A., Perez-Navarro, E., Alberch, J., and Xifro, X. (2012). Activation of Elk-1 participates as a neuroprotective compensatory mechanism in models of Huntington's disease. J Neurochem *121*, 639-648.

Antonini, A., Leenders, K.L., and Eidelberg, D. (1998). [11C]raclopride-PET studies of the Huntington's disease rate of progression: relevance of the trinucleotide repeat length. Annals of neurology *43*, 253-255.

Arlotta, P., Molyneaux, B.J., Jabaudon, D., Yoshida, Y., and Macklis, J.D. (2008). Ctip2 controls the differentiation of medium spiny neurons and the establishment of the cellular architecture of the striatum. J Neurosci *28*, 622-632.

Baiamonte, B.A., Lee, F.A., Brewer, S.T., Spano, D., and LaHoste, G.J. (2013). Attenuation of Rhes activity significantly delays the appearance of behavioral symptoms in a mouse model of Huntington's disease. PLoS One *8*, e53606.

Ballion, B., Mallet, N., Bezard, E., Lanciego, J.L., and Gonon, F. (2008). Intratelencephalic corticostriatal neurons equally excite striatonigral and striatopallidal neurons and their discharge activity is selectively reduced in experimental parkinsonism. Eur J Neurosci *27*, 2313-2321.

Beaulieu, J.M., and Gainetdinov, R.R. (2011). The physiology, signaling, and pharmacology of dopamine receptors. Pharmacological reviews *63*, 182-217.

Benchoua, A., Trioulier, Y., Diguet, E., Malgorn, C., Gaillard, M.C., Dufour, N., Elalouf, J.M., Krajewski, S., Hantraye, P., Deglon, N.*, et al.* (2008). Dopamine determines the vulnerability of striatal neurons to the N-terminal fragment of mutant huntingtin through the regulation of mitochondrial complex II. Hum Mol Genet *17*, 1446-1456.

Benchoua, A., Trioulier, Y., Zala, D., Gaillard, M.C., Lefort, N., Dufour, N., Saudou, F., Elalouf, J.M., Hirsch, E., Hantraye, P.*, et al.* (2006). Involvement of mitochondrial complex II defects in neuronal death produced by N-terminus fragment of mutated huntingtin. Mol Biol Cell *17*, 1652-1663.

Blazquez, C., Chiarlone, A., Sagredo, O., Aguado, T., Pazos, M.R., Resel, E., Palazuelos, J., Julien, B., Salazar, M., Borner, C.*, et al.* (2011). Loss of striatal type 1 cannabinoid receptors is a key pathogenic factor in Huntington's disease. Brain : a journal of neurology *134*, 119-136.

Borrell-Pages, M., Zala, D., Humbert, S., and Saudou, F. (2006). Huntington's disease: from huntingtin function and dysfunction to therapeutic strategies. Cellular and molecular life sciences : CMLS *63*, 2642-2660.

Borroto-Escuela, D.O., Romero-Fernandez, W., Tarakanov, A.O., Ciruela, F., Agnati, L.F., and Fuxe, K. (2011). On the existence of a possible A2A-D2-beta-Arrestin2 complex: A2A agonist modulation of D2 agonist-induced beta-arrestin2 recruitment. Journal of molecular biology *406*, 687-699.

Brochier, C., Gaillard, M.C., Diguet, E., Caudy, N., Dossat, C., Segurens, B., Wincker, P., Roze, E., Caboche, J., Hantraye, P.*, et al.* (2008). Quantitative gene expression profiling of mouse brain regions

reveals differential transcripts conserved in human and affected in disease models. Physiological genomics *33*, 170-179.

Brouillet, E., Conde, F., Beal, M.F., and Hantraye, P. (1999). Replicating Huntington's disease phenotype in experimental animals. Prog Neurobiol *59*, 427-468.

Brouillet, E., Jacquard, C., Bizat, N., and Blum, D. (2005). 3-Nitropropionic acid: a mitochondrial toxin to uncover physiopathological mechanisms underlying striatal degeneration in Huntington's disease. J Neurochem *95*, 1521-1540.

Cattaneo, E., Zuccato, C., and Tartari, M. (2005). Normal huntingtin function: an alternative approach to Huntington's disease. Nat Rev Neurosci *6*, 919-930.

Cepeda, C., Andre, V.M., Yamazaki, I., Wu, N., Kleiman-Weiner, M., and Levine, M.S. (2008). Differential electrophysiological properties of dopamine D1 and D2 receptor-containing striatal medium-sized spiny neurons. Eur J Neurosci *27*, 671-682.

Cepeda, C., Wu, N., Andre, V.M., Cummings, D.M., and Levine, M.S. (2007). The corticostriatal pathway in Huntington's disease. Prog Neurobiol *81*, 253-271.

Cha, J.H. (2007). Transcriptional signatures in Huntington's disease. Prog Neurobiol *83*, 228-248.

Charvin, D., Roze, E., Perrin, V., Deyts, C., Betuing, S., Pages, C., Regulier, E., Luthi-Carter, R., Brouillet, E., Deglon, N.*, et al.* (2008). Haloperidol protects striatal neurons from dysfunction induced by mutated huntingtin in vivo. Neurobiology of disease *29*, 22-29.

Charvin, D., Vanhoutte, P., Pages, C., Borrelli, E., and Caboche, J. (2005). Unraveling a role for dopamine in Huntington's disease: the dual role of reactive oxygen species and D2 receptor stimulation. Proc Natl Acad Sci U S A *102*, 12218-12223.

Chiarlone, A., Bellocchio, L., Blazquez, C., Resel, E., Soria-Gomez, E., Cannich, A., Ferrero, J.J., Sagredo, O., Benito, C., Romero, J.*, et al.* (2014). A restricted population of CB1 cannabinoid receptors with neuroprotective activity. Proc Natl Acad Sci U S A *111*, 8257-8262.

Chou, S.Y., Lee, Y.C., Chen, H.M., Chiang, M.C., Lai, H.L., Chang, H.H., Wu, Y.C., Sun, C.N., Chien, C.L., Lin, Y.S.*, et al.* (2005). CGS21680 attenuates symptoms of Huntington's disease in a transgenic mouse model. J Neurochem *93*, 310-320.

Cowan, C.M., and Raymond, L.A. (2006). Selective neuronal degeneration in Huntington's disease. Current topics in developmental biology *75*, 25-71.

Crittenden, J.R., Dunn, D.E., Merali, F.I., Woodman, B., Yim, M., Borkowska, A.E., Frosch, M.P., Bates, G.P., Housman, D.E., Lo, D.C.*, et al.* (2010). CalDAG-GEFI down-regulation in the striatum as a neuroprotective change in Huntington's disease. Hum Mol Genet *19*, 1756-1765.

Cyr, M., Sotnikova, T.D., Gainetdinov, R.R., and Caron, M.G. (2006). Dopamine enhances motor and neuropathological consequences of polyglutamine expanded huntingtin. FASEB journal : official publication of the Federation of American Societies for Experimental Biology *20*, 2541-2543.

Damiano, M., Diguet, E., Malgorn, C., D'Aurelio, M., Galvan, L., Petit, F., Benhaim, L., Guillermier, M., Houitte, D., Dufour, N.*, et al.* (2013). A role of mitochondrial complex II defects in genetic models of Huntington's disease expressing N-terminal fragments of mutant huntingtin. Hum Mol Genet *22*, 3869-3882.

Damiano, M., Galvan, L., Deglon, N., and Brouillet, E. (2010). Mitochondria in Huntington's disease. Biochim Biophys Acta *1802*, 52-61.

de Chaldee, M., Brochier, C., Van de Vel, A., Caudy, N., Luthi-Carter, R., Gaillard, M.C., and Elalouf, J.M. (2006). Capucin: a novel striatal marker down-regulated in rodent models of Huntington disease. Genomics *87*, 200-207.

de Chaldee, M., Gaillard, M.C., Bizat, N., Buhler, J.M., Manzoni, O., Bockaert, J., Hantraye, P., Brouillet, E., and Elalouf, J.M. (2003). Quantitative assessment of transcriptome differences between brain territories. Genome Res *13*, 1646-1653.

Desplats, P.A., Kass, K.E., Gilmartin, T., Stanwood, G.D., Woodward, E.L., Head, S.R., Sutcliffe, J.G., and Thomas, E.A. (2006). Selective deficits in the expression of striatal-enriched mRNAs in Huntington's disease. J Neurochem *96*, 743-757.

Desplats, P.A., Lambert, J.R., and Thomas, E.A. (2008). Functional roles for the striatal-enriched transcription factor, Bcl11b, in the control of striatal gene expression and transcriptional dysregulation in Huntington's disease. Neurobiology of disease *31*, 298-308.

Deyts, C., Galan-Rodriguez, B., Martin, E., Bouveyron, N., Roze, E., Charvin, D., Caboche, J., and Betuing, S. (2009). Dopamine D2 receptor stimulation potentiates PolyQ-Huntingtin-induced mouse striatal neuron dysfunctions via Rho/ROCK-II activation. PLoS One *4*, e8287.

Dhaenens, C.M., Burnouf, S., Simonin, C., Van Brussel, E., Duhamel, A., Defebvre, L., Duru, C., Vuillaume, I., Cazeneuve, C., Charles, P.*, et al.* (2009). A genetic variation in the ADORA2A gene modifies age at onset in Huntington's disease. Neurobiology of disease *35*, 474-476.

Diguet, E., Petit, F., Escartin, C., Cambon, K., Bizat, N., Dufour, N., Hantraye, P., Deglon, N., and Brouillet, E. (2009). Normal aging modulates the neurotoxicity of mutant huntingtin. PLoS ONE *4*, e4637.

Ermak, G., Hench, K.J., Chang, K.T., Sachdev, S., and Davies, K.J. (2009). Regulator of calcineurin (RCAN1-1L) is deficient in Huntington disease and protective against mutant huntingtin toxicity in vitro. The Journal of biological chemistry *284*, 11845-11853.

Feigin, A., Ghilardi, M.F., Huang, C., Ma, Y., Carbon, M., Guttman, M., Paulsen, J.S., Ghez, C.P., and Eidelberg, D. (2006). Preclinical Huntington's disease: compensatory brain responses during learning. Annals of neurology *59*, 53-59.

Ferre, S., Quiroz, C., Woods, A.S., Cunha, R., Popoli, P., Ciruela, F., Lluis, C., Franco, R., Azdad, K., and Schiffmann, S.N. (2008). An update on adenosine A2A-dopamine D2 receptor interactions: implications for the function of G protein-coupled receptors. Current pharmaceutical design *14*, 1468-1474.

Finkbeiner, S., and Mitra, S. (2008). The ubiquitin-proteasome pathway in Huntington's disease. ScientificWorldJournal *8*, 421-433.

Galvan, L., André V.M., Wang E., Cepeda C., Levine M.S. (2012). Indirect striatal output pathways in Huntington's disease. J Huntington Dis *1*, 17-25.

Galvan, L., Lepejova, N., Gaillard, M.C., Malgorn, C., Guillermier, M., Houitte, D., Bonvento, G., Petit, F., Dufour, N., Hery, P.*, et al.* (2012). Capucin does not modify the toxicity of a mutant Huntingtin fragment in vivo. Neurobiology of aging *33*, 1845 e1845-1846.

Gauthier, L.R., Charrin, B.C., Borrell-Pages, M., Dompierre, J.P., Rangone, H., Cordelieres, F.P., De Mey, J., MacDonald, M.E., Lessmann, V., Humbert, S.*, et al.* (2004). Huntingtin controls neurotrophic support and survival of neurons by enhancing BDNF vesicular transport along microtubules. Cell *118*, 127-138.

Gertler, T.S., Chan, C.S., and Surmeier, D.J. (2008). Dichotomous anatomical properties of adult striatal medium spiny neurons. J Neurosci *28*, 10814-10824.

Giampa, C., Laurenti, D., Anzilotti, S., Bernardi, G., Menniti, F.S., and Fusco, F.R. (2010). Inhibition of the striatal specific phosphodiesterase PDE10A ameliorates striatal and cortical pathology in R6/2 mouse model of Huntington's disease. PLoS One *5*, e13417.

Gladding, C.M., Fan, J., Zhang, L.Y., Wang, L., Xu, J., Li, E.H., Lombroso, P.J., and Raymond, L.A. (2014). Alterations in STriatal-Enriched protein tyrosine Phosphatase expression, activation, and downstream signaling in early and late stages of the YAC128 Huntington's disease mouse model. J Neurochem.

Glass, M., Dragunow, M., and Faull, R.L. (2000). The pattern of neurodegeneration in Huntington's disease: a comparative study of cannabinoid, dopamine, adenosine and GABA(A) receptor alterations in the human basal ganglia in Huntington's disease. Neuroscience *97*, 505-519.

Glass, M., and Felder, C.C. (1997). Concurrent stimulation of cannabinoid CB1 and dopamine D2 receptors augments cAMP accumulation in striatal neurons: evidence for a Gs linkage to the CB1 receptor. J Neurosci *17*, 5327-5333.

Goto, S., Matsukado, Y., Mihara, Y., Inoue, N., and Miyamoto, E. (1986). Calcineurin in human brain and its relation to extrapyramidal system. Immunohistochemical study on postmortem human brains. Acta neuropathologica *72*, 150-156.

Harper, P.S. (1991). Huntington's disease.

Hebb, A.L., Robertson, H.A., and Denovan-Wright, E.M. (2004). Striatal phosphodiesterase mRNA and protein levels are reduced in Huntington's disease transgenic mice prior to the onset of motor symptoms. Neuroscience *123*, 967-981.

Hodges, A., Strand, A.D., Aragaki, A.K., Kuhn, A., Sengstag, T., Hughes, G., Elliston, L.A., Hartog, C., Goldstein, D.R., Thu, D.*, et al.* (2006). Regional and cellular gene expression changes in human Huntington's disease brain. Hum Mol Genet *15*, 965-977.

Humbert, S., Bryson, E.A., Cordelieres, F.P., Connors, N.C., Datta, S.R., Finkbeiner, S., Greenberg, M.E., and Saudou, F. (2002). The IGF-1/Akt pathway is neuroprotective in Huntington's disease and involves Huntingtin phosphorylation by Akt. Developmental cell *2*, 831-837.

Jakel, R.J., and Maragos, W.F. (2000). Neuronal cell death in Huntington's disease: a potential role for dopamine. Trends Neurosci *23*, 239-245.

Kawasaki, H., Springett, G.M., Toki, S., Canales, J.J., Harlan, P., Blumenstiel, J.P., Chen, E.J., Bany, I.A., Mochizuki, N., Ashbacher, A.*, et al.* (1998). A Rap guanine nucleotide exchange factor enriched highly in the basal ganglia. Proc Natl Acad Sci U S A *95*, 13278-13283.

Kehrl, J.H., and Sinnarajah, S. (2002). RGS2: a multifunctional regulator of G-protein signaling. The international journal of biochemistry & cell biology *34*, 432-438.

Kreitzer, A.C., and Malenka, R.C. (2007). Endocannabinoid-mediated rescue of striatal LTD and motor deficits in Parkinson's disease models. Nature *445*, 643-647.

Kuhn, A., Goldstein, D.R., Hodges, A., Strand, A.D., Sengstag, T., Kooperberg, C., Becanovic, K., Pouladi, M.A., Sathasivam, K., Cha, J.H.*, et al.* (2007). Mutant huntingtin's effects on striatal gene expression in mice recapitulate changes observed in human Huntington's disease brain and do not differ with mutant huntingtin length or wild-type huntingtin dosage. Hum Mol Genet *16*, 1845-1861.

Laprairie, R.B., Kelly, M.E., and Denovan-Wright, E.M. (2013). Cannabinoids increase type 1 cannabinoid receptor expression in a cell culture model of striatal neurons: implications for Huntington's disease. Neuropharmacology *72*, 47-57.

Li, S.H., and Li, X.J. (2004a). Huntingtin-protein interactions and the pathogenesis of Huntington's disease. Trends in genetics : TIG *20*, 146-154.

Li, S.H., and Li, X.J. (2004b). Huntingtin and its role in neuronal degeneration. The Neuroscientist : a review journal bringing neurobiology, neurology and psychiatry *10*, 467-475.

885 Marion, S., Urs, N.M., Peterson, S.M., Sotnikova, T.D., Beaulieu, J.M., Gainetdinov, R.R., and Caron,
886 M.G. (2014). Dopamine D2 receptor relies upon PPM/PP2C protein phosphatases to dephosphorylate
887 huntingtin protein. The Journal of biological chemistry *289*, 11715-11724.

888 Martin, B., Golden, E., Keselman, A., Stone, M., Mattson, M.P., Egan, J.M., and Maudsley, S. (2008).
889 Therapeutic perspectives for the treatment of Huntington's disease: treating the whole body. Histol
890 Histopathol *23*, 237-250.

891 Martin, E., Betuing, S., Pages, C., Cambon, K., Auregan, G., Deglon, N., Roze, E., and Caboche, J.
892 (2011). Mitogen- and stress-activated protein kinase 1-induced neuroprotection in Huntington's
893 disease: role on chromatin remodeling at the PGC-1-alpha promoter. Hum Mol Genet *20*, 2422-2434.

894 Martire, A., Calamandrei, G., Felici, F., Scattoni, M.L., Lastoria, G., Domenici, M.R., Tebano, M.T., and
895 Popoli, P. (2007). Opposite effects of the A2A receptor agonist CGS21680 in the striatum of
896 Huntington's disease versus wild-type mice. Neuroscience letters *417*, 78-83.

897 Masuo, Y., Ogura, A., Kobayashi, M., Masaki, T., Furuta, Y., Ono, T., and Takamatsu, K. (2007).
898 Hippocalcin protects hippocampal neurons against excitotoxin damage by enhancing calcium
899 extrusion. Neuroscience *145*, 495-504.

900 Mazarei, G., Budac, D.P., Lu, G., Adomat, H., Tomlinson Guns, E.S., Moller, T., and Leavitt, B.R.
901 (2013a). Age-dependent alterations of the kynurenine pathway in the YAC128 mouse model of
902 Huntington disease. J Neurochem *127*, 852-867.

903 Mazarei, G., Budac, D.P., Lu, G., Lee, H., Moller, T., and Leavitt, B.R. (2013b). The absence of
904 indoleamine 2,3-dioxygenase expression protects against NMDA receptor-mediated excitotoxicity in
905 mouse brain. Experimental neurology *249*, 144-148.

906 Mazarei, G., Neal, S.J., Becanovic, K., Luthi-Carter, R., Simpson, E.M., and Leavitt, B.R. (2010).
907 Expression analysis of novel striatal-enriched genes in Huntington disease. Hum Mol Genet *19*, 609-
908 622.

909 Mealer, R.G., Murray, A.J., Shahani, N., Subramaniam, S., and Snyder, S.H. (2014). Rhes, a striatal-
910 selective protein implicated in Huntington disease, binds beclin-1 and activates autophagy. The
911 Journal of biological chemistry *289*, 3547-3554.

912 Menalled, L., Zanjani, H., MacKenzie, L., Koppel, A., Carpenter, E., Zeitlin, S., and Chesselet, M.F.
913 (2000). Decrease in striatal enkephalin mRNA in mouse models of Huntington's disease. Experimental
914 neurology *162*, 328-342.

915 Menalled, L.B. (2005). Knock-in mouse models of Huntington's disease. NeuroRx *2*, 465-470.

916 Menalled, L.B., and Chesselet, M.F. (2002). Mouse models of Huntington's disease. Trends
917 Pharmacol Sci *23*, 32-39.

918 Mievis, S., Blum, D., and Ledent, C. (2011a). A2A receptor knockout worsens survival and motor
919 behaviour in a transgenic mouse model of Huntington's disease. Neurobiology of disease *41*, 570-576.

920 Mievis, S., Blum, D., and Ledent, C. (2011b). Worsening of Huntington disease phenotype in CB1
921 receptor knockout mice. Neurobiology of disease *42*, 524-529.

922 Mochel, F., Durant, B., Meng, X., O'Callaghan, J., Yu, H., Brouillet, E., Wheeler, V.C., Humbert, S.,
923 Schiffmann, R., and Durr, A. (2012a). Early alterations of brain cellular energy homeostasis in
924 Huntington disease models. The Journal of biological chemistry *287*, 1361-1370.

925 Mochel, F., N'Guyen, T.M., Deelchand, D., Rinaldi, D., Valabregue, R., Wary, C., Carlier, P.G., Durr,
926 A., and Henry, P.G. (2012b). Abnormal response to cortical activation in early stages of Huntington
927 disease. Mov Disord *27*, 907-910.

928 Myers, R.H., Vonsattel, J.P., Stevens, T.J., Cupples, L.A., Richardson, E.P., Martin, J.B., and Bird,
929 E.D. (1988). Clinical and neuropathologic assessment of severity in Huntington's disease. Neurology
930 *38*, 341-347.

931 Nemeroff, C.B., Youngblood, W.W., Manberg, P.J., Prange, A.J., Jr., and Kizer, J.S. (1983). Regional
932 brain concentrations of neuropeptides in Huntington's chorea and schizophrenia. Science (New York,
933 NY *221*, 972-975.

934 Obeso, J.A., Rodriguez-Oroz, M.C., Stamelou, M., Bhatia, K.P., and Burn, D.J. (2014). The expanding
935 universe of disorders of the basal ganglia. Lancet.

936 Oyama, F., Miyazaki, H., Sakamoto, N., Becquet, C., Machida, Y., Kaneko, K., Uchikawa, C., Suzuki,
937 T., Kurosawa, M., Ikeda, T.*, et al.* (2006). Sodium channel beta4 subunit: down-regulation and
938 possible involvement in neuritic degeneration in Huntington's disease transgenic mice. J Neurochem
939 *98*, 518-529.

940 Paoletti, P., Vila, I., Rife, M., Lizcano, J.M., Alberch, J., and Gines, S. (2008). Dopaminergic and
941 glutamatergic signaling crosstalk in Huntington's disease neurodegeneration: the role of p25/cyclin-
942 dependent kinase 5. J Neurosci *28*, 10090-10101.

943 Pardo, R., Colin, E., Regulier, E., Aebischer, P., Deglon, N., Humbert, S., and Saudou, F. (2006).
944 Inhibition of calcineurin by FK506 protects against polyglutamine-huntingtin toxicity through an
945 increase of huntingtin phosphorylation at S421. J Neurosci *26*, 1635-1645.

946 Petersen, A., and Bjorkqvist, M. (2006). Hypothalamic-endocrine aspects in Huntington's disease. Eur
947 J Neurosci *24*, 961-967.

948 Pineda, J.R., Pardo, R., Zala, D., Yu, H., Humbert, S., and Saudou, F. (2009). Genetic and
949 pharmacological inhibition of calcineurin corrects the BDNF transport defect in Huntington's disease.
950 Molecular brain *2*, 33.

951 Popoli, P., Blum, D., Martire, A., Ledent, C., Ceruti, S., and Abbracchio, M.P. (2007). Functions,
952 dysfunctions and possible therapeutic relevance of adenosine A2A receptors in Huntington's disease.
953 Prog Neurobiol *81*, 331-348.

954 Ravikumar, B., and Rubinsztein, D.C. (2006). Role of autophagy in the clearance of mutant huntingtin:
955 a step towards therapy? Mol Aspects Med *27*, 520-527.

956 Raymond, L.A., Andre, V.M., Cepeda, C., Gladding, C.M., Milnerwood, A.J., and Levine, M.S. (2011).
957 Pathophysiology of Huntington's disease: time-dependent alterations in synaptic and receptor function.
958 Neuroscience *198*, 252-273.

959 Reiner, A., Jiao, Y., Del Mar, N., Laverghetta, A.V., and Lei, W.L. (2003). Differential morphology of
960 pyramidal tract-type and intratelencephalically projecting-type corticostriatal neurons and their
961 intrastriatal terminals in rats. The Journal of comparative neurology *457*, 420-440.

962 Reynolds, D.S., Carter, R.J., and Morton, A.J. (1998). Dopamine modulates the susceptibility of striatal
963 neurons to 3-nitropropionic acid in the rat model of Huntington's disease. J Neurosci *18*, 10116-10127.

964 Ritter, S.L., and Hall, R.A. (2009). Fine-tuning of GPCR activity by receptor-interacting proteins.
965 Nature reviews Molecular cell biology *10*, 819-830.

966 Robinson, P., Lebel, M., and Cyr, M. (2008). Dopamine D1 receptor-mediated aggregation of N-
967 terminal fragments of mutant huntingtin and cell death in a neuroblastoma cell line. Neuroscience *153*,
968 762-772.

969 Roze, E., Betuing, S., Deyts, C., Marcon, E., Brami-Cherrier, K., Pages, C., Humbert, S., Merienne, K.,
970 and Caboche, J. (2008a). Mitogen- and stress-activated protein kinase-1 deficiency is involved in
971 expanded-huntingtin-induced transcriptional dysregulation and striatal death. FASEB journal : official
972 publication of the Federation of American Societies for Experimental Biology *22*, 1083-1093.

Roze, E., Saudou, F., and Caboche, J. (2008b). Pathophysiology of Huntington's disease: from huntingtin functions to potential treatments. Current opinion in neurology *21*, 497-503.

Rudinskiy, N., Kaneko, Y.A., Beesen, A.A., Gokce, O., Regulier, E., Deglon, N., and Luthi-Carter, R. (2009). Diminished hippocalcin expression in Huntington's disease brain does not account for increased striatal neuron vulnerability as assessed in primary neurons. J Neurochem *111*, 460-472.

Rue, L., Alcala-Vida, R., Lopez-Soop, G., Creus-Muncunill, J., Alberch, J., and Perez-Navarro, E. (2014). Early down-regulation of PKCdelta as a pro-survival mechanism in Huntington's disease. Neuromolecular medicine *16*, 25-37.

Saavedra, A., Giralt, A., Rue, L., Xifro, X., Xu, J., Ortega, Z., Lucas, J.J., Lombroso, P.J., Alberch, J., and Perez-Navarro, E. (2011). Striatal-enriched protein tyrosine phosphatase expression and activity in Huntington's disease: a STEP in the resistance to excitotoxicity. J Neurosci *31*, 8150-8162.

Seredenina, T., Gokce, O., and Luthi-Carter, R. (2011). Decreased striatal RGS2 expression is neuroprotective in Huntington's disease (HD) and exemplifies a compensatory aspect of HD-induced gene regulation. PLoS One *6*, e22231.

Seredenina, T., and Luthi-Carter, R. (2012). What have we learned from gene expression profiles in Huntington's disease? Neurobiology of disease *45*, 83-98.

Stack, E.C., Dedeoglu, A., Smith, K.M., Cormier, K., Kubilus, J.K., Bogdanov, M., Matson, W.R., Yang, L., Jenkins, B.G., Luthi-Carter, R.*, et al.* (2007). Neuroprotective effects of synaptic modulation in Huntington's disease R6/2 mice. J Neurosci *27*, 12908-12915.

Sturrock, A., and Leavitt, B.R. (2010). The clinical and genetic features of Huntington disease. Journal of geriatric psychiatry and neurology *23*, 243-259.

Subramaniam, S., Sixt, K.M., Barrow, R., and Snyder, S.H. (2009). Rhes, a striatal specific protein, mediates mutant-huntingtin cytotoxicity. Science (New York, NY *324*, 1327-1330.

Tabrizi, S.J., Scahill, R.I., Owen, G., Durr, A., Leavitt, B.R., Roos, R.A., Borowsky, B., Landwehrmeyer, B., Frost, C., Johnson, H.*, et al.* (2013). Predictors of phenotypic progression and disease onset in premanifest and early-stage Huntington's disease in the TRACK-HD study: analysis of 36-month observational data. Lancet Neurol *12*, 637-649.

Tang, B., Becanovic, K., Desplats, P.A., Spencer, B., Hill, A.M., Connolly, C., Masliah, E., Leavitt, B.R., and Thomas, E.A. (2012). Forkhead box protein p1 is a transcriptional repressor of immune signaling in the CNS: implications for transcriptional dysregulation in Huntington disease. Hum Mol Genet *21*, 3097-3111.

Tang, B., Di Lena, P., Schaffer, L., Head, S.R., Baldi, P., and Thomas, E.A. (2011). Genome-wide identification of Bcl11b gene targets reveals role in brain-derived neurotrophic factor signaling. PLoS One *6*, e23691.

Tang, T.S., Chen, X., Liu, J., and Bezprozvanny, I. (2007). Dopaminergic signaling and striatal neurodegeneration in Huntington's disease. J Neurosci *27*, 7899-7910.

The-Huntington's-Disease-Collaborative-Research-Group (1993). A novel gene containing a trinucleotide repeat that is expanded and unstable on Huntington's disease chromosomes. The Huntington's Disease Collaborative Research Group. Cell *72*, 971-983.

Thevandavakkam, M.A., Schwarcz, R., Muchowski, P.J., and Giorgini, F. (2010). Targeting kynurenine 3-monooxygenase (KMO): implications for therapy in Huntington's disease. CNS & neurological disorders drug targets *9*, 791-800.

Thomas, E.A. (2006). Striatal specificity of gene expression dysregulation in Huntington's disease. J Neurosci Res *84*, 1151-1164.

Tkac, I., Henry, P.G., Zacharoff, L., Wedel, M., Gong, W., Deelchand, D.K., Li, T., and Dubinsky, J.M. (2012). Homeostatic adaptations in brain energy metabolism in mouse models of Huntington disease. J Cereb Blood Flow Metab.

Van Laere, K., Casteels, C., Dhollander, I., Goffin, K., Grachev, I., Bormans, G., and Vandenberghe, W. (2010). Widespread decrease of type 1 cannabinoid receptor availability in Huntington disease in vivo. Journal of nuclear medicine : official publication, Society of Nuclear Medicine *51*, 1413-1417.

Vermeulen, L., De Wilde, G., Van Damme, P., Vanden Berghe, W., and Haegeman, G. (2003). Transcriptional activation of the NF-kappaB p65 subunit by mitogen- and stress-activated protein kinase-1 (MSK1). The EMBO journal *22*, 1313-1324.

Walker, F.O. (2007). Huntington's disease. Lancet *369*, 218-228.

Xifro, X., Giralt, A., Saavedra, A., Garcia-Martinez, J.M., Diaz-Hernandez, M., Lucas, J.J., Alberch, J., and Perez-Navarro, E. (2009). Reduced calcineurin protein levels and activity in exon-1 mouse models of Huntington's disease: role in excitotoxicity. Neurobiology of disease *36*, 461-469.

Zabel, C., Mao, L., Woodman, B., Rohe, M., Wacker, M.A., Klare, Y., Koppelstatter, A., Nebrich, G., Klein, O., Grams, S.*, et al.* (2009). A large number of protein expression changes occur early in life and precede phenotype onset in a mouse model for huntington disease. Mol Cell Proteomics *8*, 720-734.

Zhang, N., Li, B., Al-Ramahi, I., Cong, X., Held, J.M., Kim, E., Botas, J., Gibson, B.W., and Ellerby, L.M. (2012). Inhibition of lipid signaling enzyme diacylglycerol kinase epsilon attenuates mutant huntingtin toxicity. The Journal of biological chemistry *287*, 21204-21213.

Zuccato, C., and Cattaneo, E. (2007). Role of brain-derived neurotrophic factor in Huntington's disease. Prog Neurobiol *81*, 294-330.

Zuccato, C., and Cattaneo, E. (2014). Huntington's Disease. Handbook of experimental pharmacology *220*, 357-409.

Acknowledgments

LG was supported by the « Neuropôle de Recherche Francilien » and the « Fondation pour la Recherche Médicale ». LF was supported by the French Research Ministry.

Conflicts of interest

The authors declare no conflict of interest

2.2.Thesis objectives

All the striatal selective gene products that have not yet been explored represent a pool of potential candidate modifiers of mHtt, relevant to striatal vulnerability. Although the list of these "unexplored" striatal markers is debatable since the "cutoff" to define a gene product as "striatal selective" is subjective, currently available data point to more than 100 striatal gene products which remains to be studied to determine their potential impact in mHtt toxicity ((Francelle et al 2014), Supplementary table).

In collaboration with Michel de Chaldée and Jean-Marc Elalouf (Ibitecs, CEA), our laboratory used Serial Analysis of Gene Expression (SAGE) to generate a library of striatal gene products and compared to the library of other brain regions, identify novel "striatal gene products" or "striatal markers". More specifically, these markers are selectively expressed and enriched in the brain compared to peripheral system, and more particularly in the striatum (at least 5 fold-time more expression than in 2 others brains structures. To address the question if some of these striatal markers could have an impact against mHtt, the laboratory used the following criteria to select a short list of striatal markers over hundreds:

- high level of enrichment of the markers in the striatum of adult mice,
- enrichment in the striatum validated in the human caudate and/or putamen,
- preference for unknown or ill-defined function of the gene products,
- down-regulation of the transcript markers in HD mouse models and HD patients,
- diversity of the potential biological function of these markers.

Among these ten markers, Laurie Galvan (Thesis defense 2011) has studied the effects of five striatal markers on mHtt toxicity using the *in vivo* HD lentiviral model (see chapter Introduction 1.2.7.5. paragraph), chosen according to the easiness of study depending on the techniques we had in the laboratory. These markers were Capucine, Gpr88, Abhd11os, µ-crystallin (CRYM) and Doublecortin-like kinase 3 (DCLK3). Results of these pioneering studies showed that in this particular model Abhd11os and DCLK3 have neuroprotective effects against mHtt. The results on CRYM were difficult to interpret and needed further studies.
The work on Capucine leaded to a publication, showing that the overexpression or silencing of this striatal marker didn't change the toxicity of mHtt (Htt 171-82Q) (Galvan et al 2012). According to preliminary data from the laboratory, Gpr88 did not seem to modify mHtt toxicity either.

The objectives of my thesis were to further characterize three of these striatal markers (Abhd11os, CRYM and DCLK3) and to better understand the putative molecular mechanisms underlying their neuroprotective effects against mHtt.
While results on CRYM and Abhd11os were interesting, we chose at the beginning of my thesis to keep a strong focus on DCLK3.

The results we obtained are reported in the 3 publications that follow. The two first manuscripts on Abhd11os and CRYM are in press respectively in Neurobiology of Aging journal and Human Molecular Genetics journal, whereas the manuscript on DCLK3 is a draft version presenting most of the data we obtained. This work should be soon submitted.

PART3 RESULTS

3. Disease modifiers

Results will present the study of the three striatal markers Abhd11os, CRYM and DCLK3.

3.1. Article #1

The long non-coding RNA Abhd11os is neuroprotective against an N-terminal Fragment of Mutant Huntingtin in vivo.

The striatal long non-coding RNA Abhd11os is neuroprotective against an N-terminal Fragment of Mutant Huntingtin *in vivo.*

Laetitia Francelle [a,b (*)], Laurie Galvan [a,b (*)], Marie-Claude Gaillard [a,b], Fanny Petit [a,b], Benoît Bernay [c,d,e], Martine Guillermier [a,b], Gilles Bonvento [a,b], Noëlle Dufour [a,b], Jean-Marc Elalouf [c,d,e], Philippe Hantraye [a,b], Nicole Déglon [a,b], Michel de Chaldée [c,d,e], and Emmanuel Brouillet [a,b]

[a] *CEA, DSV, I²BM, Molecular Imaging Research Center (MIRCen), F-92265 Fontenay-aux-Roses, France*

[b] *CNRS CEA URA 2210, F-92265 Fontenay-aux-Roses, France*

[c] *CEA, iBiTecS, F-91191 Gif-sur-Yvette Cedex, France*

[d] *CNRS, FRE 3377, F-91191 Gif-sur-Yvette Cedex, France*

[e] *Université Paris-Sud, FRE 3377, F-91191 Gif-sur-Yvette Cedex, France*

(*) first co-authors, equally contributed to the work.

ABSTRACT

A large number of gene products that are enriched in the striatum have ill-defined functions, although they may have key roles in age-dependent neurodegenerative diseases affecting the striatum, especially Huntington's disease (HD). In the present study we focused on Abhd11os, (called ABHD11-AS1 in human) which is a putative long non-coding RNA (lncRNA) whose expression is enriched in the mouse striatum. We confirm that despite the presence of two small ORFs in its sequence, Abhd11os is not translated into a detectable peptide in living cells. We demonstrate that Abhd11os levels are markedly reduced in different mouse models of HD. We performed *in vivo* experiments in mice using lentiviral vectors encoding either Abhd11os or a shRNA targeting Abhd11os. Results show that Abhd11os overexpression produces neuroprotection against an N-terminal fragment of mutant huntingtin whereas Abhd11os knockdown is protoxic. These novel results indicate that the loss lncRNA Abhd11os likely contribute to striatal vulnerability in HD. Our study emphasizes that lncRNA may play crucial roles in neurodegenerative diseases.

Key words

Huntington's disease; striatum; neurodegeneration; non-coding RNA; Neuroprotection; gene regulation

1. Introduction

Comprehensive analysis of the molecular “complexity” of the adult striatum has shown that many of the gene products preferentially expressed in this brain region have a poorly characterized function [e.g.(Brochier et al., 2008)]. Amongst these “striatal” gene products, a non-negligible fraction has never been studied experimentally. However, their enrichment in the striatum as compared to other brain regions, suggests they are involved in the functions of the striatum such as implementation of motor and cognitive behaviors. It is conceivable that they could also play a key role in the preferential degeneration of the striatum in a number of neurological diseases and, as such, they constitute potential therapeutic targets.

Several disorders (e.g. Huntington’s disease [HD], Huntington’s disease type 2, Multiple System Atrophy, acute poisoning with mitochondrial toxins, inherited mitochondrial defects…) are primarily associated with striatal degeneration (Damiano et al., 2010) or secondarily lead to striatal dysfunctions (Parkinson’s disease, L-dopa-induced dyskinesia, drug addiction, schizophrenia, among others). HD is a dominantly inherited disorder with an onset during adulthood. Symptoms include involuntary abnormal movements (chorea, dyskinesia, dystonia), frontal cognitive deficits and psychiatric disturbances (Harper, 1991; Walker, 2007). The disease is fatal approximately 15 years after the onset of symptoms. There is no effective treatment to slow the progression of HD. HD is caused by a mutation in the gene encoding the protein huntingtin (Htt) that consists in a CAG triplet repeat expansion translated into an abnormal poly-glutamine (polyQ) tract within the N-terminal region of the protein (The-Huntington's-Disease-Collaborative-Research-Group, 1993). This polyQ expansion produces a gain-of-function that is toxic to neurons through unclear mechanisms, but it is likely that many different cellular pathways are implicated (Roze et al., 2008). One major early event in HD is the alteration of transcription (Cha, 2007; Seredenina and Luthi-Carter, 2012). Other early alterations include intracellular signaling defects, axonal transport alterations (Borrell-Pages et al., 2006), deregulated autophagy (Winslow and Rubinsztein, 2008), defects in BDNF transcription, secretion and transport (Zuccato and Cattaneo, 2014), perturbation of calcium homeostasis (Cowan and Raymond, 2006) and mitochondrial defects (Damiano et al., 2010).

While mutant Htt (mHtt) protein is ubiquitously expressed in the brain, degeneration primarily affects the striatum (Tabrizi et al., 2013). This particular vulnerability may be conferred by factors that are enriched in the striatum (Brouillet et al., 2005; Desplats et al., 2006; Thomas, 2006). So far, only a limited list of gene products preferentially expressed in the striatum have been found to promote mHtt toxicity, notably the small GTPase Rhes (Subramaniam et al., 2009), the dopamine type 2 receptor (D2R) (Benchoua et al., 2008; Charvin et al., 2005), and the RGS2 protein (Seredenina et al., 2011). Alternatively, striatum-enriched neuroprotective factors may be down-regulated during HD pathogenesis. For instance, A(2A) adenosine receptors, whose expression is early impaired in HD (Blum et al., 2003), have been shown to be neuroprotective (Mievis et al., 2011). However all striatal-specific gene products with reduced expression in HD have not an effect against mHtt (Galvan et al., 2012).

We previously reported that 2010001M06Rik transcript, one of those we have identified as striatal “markers”, shows markedly reduced expression in the striatum of the R6/2 mouse model of HD

(Brochier et al., 2008). It has been annotated as a long intergenic non-protein coding RNA (LINC00035) by *in silico* analysis. It has been renamed ABHD11-AS1 in human, and Abhd11os in mouse (for abhydrolase domain containing 11, opposite strand). The potential roles of long non-coding RNA in neurobiological regulatory mechanisms and neurological and psychiatric diseases have been recently underlined (Tan et al., 2013; Wu et al., 2013). Thus, we aimed at exploring the potential role of Abhd11os in HD.

Here we provide experimental evidence that Abhd11os is non-coding. We next examined its expression in the striatum of two additional mouse models of HD that are characterized by a slow progressing disease phenotype without major neurodegeneration. Finally, using lentiviral vectors, we tested whether overexpression or knock-down of Abhd11os could modify mHtt toxicity in the mouse striatum. Results indicate that Abhd11os is neuroprotective against mHtt *in vivo*.

2. Materials and methods

2.1. Animals

Mice were housed in a temperature-controlled room maintained on a 12 hr light/dark cycle. Food and water were available ad libitum. All animal studies were conducted according to the French regulation (EU Directive 86/609 – French Act Rural Code R 214-87 to 131). The animal facility was approved by veterinarian inspectors (authorization n°A 92-032-02) and complies with Standards for Humane Care and Use of Laboratory Animals of the Office of Laboratory Animal Welfare (OLAW – n°#A5826-01). All procedures received approval from the ethical committee. Adult male C57BL/6J mice (25 g each; Charles River, Saint Germain sur l'Arbresle, France) were used for lentiviral infections.

For endogenous Abhd11os mRNA levels study, we used the transgenic mouse model of HD generated and maintained in the FvB inbred background, the BACHD mice, that express full-length human mHtt from its own regulatory elements on a 240-kb BAC, which contains the intact 170-kb human htt locus plus about 20 kb of 5′ flanking genomic sequence and 50 kb of 3′. We used 9 month-old male BACHD mice for the study as previously described (Gray et al., 2008).

We also studied 13 month-old knock-in mice expressing chimeric mouse/human exon 1 containing 140 CAG repeats inserted in the murine Htt gene (KI140) and their littermate controls. KI140 colony was maintained by breeding heterozygotes KI140 males and females (Menalled et al., 2003). Mice were N3 (B6) on a 129 Sv×C57BL/6 J background. The resulting different genotypes mice were used for the study and showed no overt abnormalities.

Genotyping was determined from PCR of tail snips taken at 10–15 days of age for BACHD and KI140 mice.

2.2. Lentiviral vector construction, production and infection

DNA sequences coding for green fluorescent protein (GFP) and mouse Abhd11os (2010001M06rik) were cloned into the SIN-W-PGK lentiviral vector (LV) to generate LV-GFP and LV-Abhd11os, respectively (de Almeida et al., 2002). An Abhd11os -directed shRNA (target sequence: 5' GGGATGAAGCCATTGCTAA 3') and a Luciferase-targeted shRNA (target sequence: 5'

CGTACGCGGAATACTTCGA 3') were cloned into a bicistronic LV vector (Drouet et al., 2009), in such a way that the infected cells expressed the reporter protein GFP. The resulting constructs were designated as LV-shAbhd11os and LV-shLuc, respectively. The Abhd11os sequence targeted by the shRNA (GGGATGAAGCCATTGCTAA) is located in the second exon of the Abhd11os gene. From the ESTs and cDNA sequences available in the public databases, this exon is present in all splice variants.

The lentiviral vectors expressing a wild-type Htt fragment (LV-Htt171-18Q), a mHtt fragment (LV-Htt171 82Q) or beta-galactosidase (LV-LacZ) have been described previously (Diguet et al., 2009; Faideau et al., 2010). Viral particles were produced as described elsewhere (Hottinger et al., 2000). The particle content of the viral batches was determined by ELISA for the p24 antigen (Gentaur, Paris, France). LV-Htt171 18Q and LV-Htt171-82Q were used at a concentration of 150 ng/µl of p24, LV-Abhd11os and LV-LacZ at a concentration of 100 ng/µl of p24. LV-shAbhd11os and LV-shLuc were used at a concentration of 100 ng/µl of p24. In experiments performed for PCR analysis, LV-GFP was mixed with LV-Abhd11os or LV-LacZ at a concentration of 50 ng/µl of p24. After being anesthetized (Ketamine/xylazine), mice received a total volume of 2 µl of lentiviral suspension into the mouse striatum as previously reported (Faideau et al., 2010; Galvan et al., 2012), using the following stereotaxic coordinates: 1.0 mm anterior and 2.0 mm lateral to the bregma, at a depth of 2.7 mm from the dura, with the tooth bar set at 0.0 mm.

2.3. Histological and cytological analyses

Brain processing

After deep anesthesia by intraperitoneal injection of a sodium pentobarbital solution (50 µg per gram of body weight), mice were transcardially perfused with 100 ml of phosphate buffer containing 4 % paraformaldehyde at 8 ml/min. The brains were removed, post-fixed overnight in the same solution, then cryoprotected by immersion in a 30 % sucrose solution for 24 hours. Free-floating 30 µm-thick serial coronal sections throughout the striatum (i.e. 210µm inter-section space) were collected using a freezing sliding microtome (SM2400; Leica Microsystems, Wetzlar, Germany).

Immunohistochemistry

Sections were treated with 0.3 % hydrogen peroxide for one hour, washed three times in phosphate-buffered saline (PBS), blocked in PBS containing 4.5 % normal goat serum for one hour, then incubated overnight at 4°C in PBS containing 3 % normal goat serum and one of the following antibodies: rabbit anti-DARPP 32 (Santa Cruz Biotechnology, Santa Cruz, CA; 1:1000), mouse anti-NeuN (Millipore, Molsheim, France; 1:200), rabbit anti-Ubiquitin (Wako Chemicals, Neuss, Germany; 1:1000), or mouse anti-HA (Covance, Princeton, NJ; 1:500). Sections were rinsed three times in PBS before incubation with the appropriate anti-IgG biotinylated antibody (Vector Laboratories, Burlingame, CA) at a 1:5000 dilution for one hour. Staining was visualized by the addition of avidin-biotinylated peroxidase and incubation with DAB or VIP substrate (Vector Laboratories, Burlingame, CA) for one minute. For NeuN immunostaining, we used the M.O.M. immunodetection kit (Vector Laboratories,

Burlingame, CA). Stained sections were mounted on microscopic slides and cover slipped using Permount.

Quantitative histological evaluation

The area of the striatal lesions resulting from LV-Htt171-82Q infection was delineated manually by identifying the border of the lesion (loss of DARPP-32 and NeuN immunolabelling). Lesion area was delineated using a 5x objective. Depending on the antero-posterior extension of the lesions, 3 to 8 coronal sections were analyzed for each mouse. Observation of sections and calculation of the surface of lesioned area were performed using a Leica DM6000 equipped with a motorized stage and an automated image acquisition and analysis system (Mercator software, Explora Nova, La Rochelle, France). The volume of the striatal lesion (V) was determined using the Cavalieri method (Damiano et al., 2013; Diguet et al., 2009; Galvan et al., 2012). The number of Ubiquitin-positive inclusions was quantified as previously described (Damiano et al., 2013; Diguet et al., 2009; Galvan et al., 2012) with the following modifications: the inter-section distance was 210 µm (i.e. one in every seven sections was used) and observations were performed using a 10X objective on an Axioplan 2 Imaging microscope (Carl Zeiss, Le Pecq, France) equipped with a motorized stage and an automated image acquisition and analysis system (Mercator software, Explora Nova). With this set-up, objects with an apparent cross-sectional area > 3 μm^2 (i.e. diameter > ~1 µm) could be reliably detected.

2.4. Real-time quantitative PCR

Adult mice were deeply anesthetized by intraperitoneal injection of a sodium pentobarbital solution (50 µg per gram of body weight) before decapitation. The brains were immediately removed and positioned in a coronal brain matrix (Ted Pella, Redding, CA).

For the quantification of overexpressed or downregulated Abhd11os mRNA levels, mice were infected with a mixture of LV-Abhd11os and LV-GFP, or LV-shAbhd11os (bicistronic for GFP) alone. Injection of LV-LacZ and LV-shLuc were used as controls for viral load. The striatal region displaying fluorescence was dissected out using a circular punch (1.5 mm diameter) from 1 mm-thick fresh coronal brain sections visualized under a fluorescence binocular microscope (Leica). Total RNA extraction and real-time quantitative RT-PCR (qRT-PCR) were performed as previously described (Drouet et al., 2009; Galvan et al., 2012), using the following primer sequences Abhd11os-U GGATTGCCTCGGACCTG and Abhd11os-L GCACCCGCTCTCGAAC. This pair of primers allows detection of all Abhd11os splice variants containing the intron.

Similar procedure was used for determination of Abhd11os RNA levels in BACHD mice and KI140 mice. In this latter case, expression levels were normalized to the geometric mean of the mRNAs (□Ct) of three housekeeping genes [PPIA (cyclophilin A), HPRT1 (hypoxanthine phosphoribosyltranferase), ACTB (beta-Actin)].

We also performed qRT-PCR to quantify Abhd11 RNA in the striatum after infection with LV-Abhd11os or its control. For this the following primer sequences Abhd11-U CACATTGGAGCCTTCATAGCAG and Abhd11-L CGCTTCCTTGACAACCGA.

2.5. Biochemical analysis

Cell culture

Human embryonic kidney 293 T (HEK293T) cells were grown at 37°C in 5% CO2 in Dulbeco's modified Eagle's medium (DMEM) supplemented with 10% bovine calf serum, 1% L-glutamine and antibiotics (50 units/ml penicillin and 50 µg/ml streptomycin).

HEK293T cells were transfected with recombinant Abhd11os vectors (coding the putative ORF1 or ORF2 sequences – see supplementary figure S1) or equivalent amount of empty vector, using the calcium phosphate method. Putative ORF1 and ORF2 were subcloned from *Abhd11os* cDNA into pcDNA3 expression vector (PGK promoter). Six nucleotides were retained 5' to the potential ATG start codon to preserve the endogenous context of translation initiation. A sequence coding for haemagglutinin (HA) was introduced immediately 5' to the stop codon. The resulting constructs have the following sequences (the putative coding sequence is in capital letters; the sequence encoding the HA tag is underlined):

ORF1: agagggATGAAGCCATTGCTAAGAAGCGCGCGGTGGAAGAGGAGCTGGACTCCTGTCGAG
CCAGGCTGCGCACAGTGGAGGCTCAGCTGCTGGAGGTCCTGCAGGAGAAACGCCTACCCATAC
GACGTGCCTGACTACGCCTCCtga;

ORF2: gaagacATGCAGCATATGGTTCGAGAGCGGGTGCGGAGTCAGCTGCAGGGAGAGCCCAGA
GGCACCCTGGGAACACACGAGAACACAAGCCCGGGCAGAAGTTCCTGGATTCAACTCTCCCGG
GGTCAGTGGGGGCGACGGTGGGCCTACCCATACGACGTGCCTGACTACGCCTCCtga;

Negative controls (ORF1ΔATG and ORF2ΔATG) were obtained by deleting the initial ATG codon and, for ORF2, by mutating the downstream ATG codon into CTG

Western blotting

Transfected cultured cells were harvested 48h after transfection and lyzed in modified RIPA buffer : 50mM Tris pH8.0, 50 mM NaCl, 1 mM EDTA, 0.5% Triton-X100, 1% NP40 and protease inhibitor cocktail (Roche). Cell lysates were centrifuged at 13,000 g for 20 min at 4°C. Total protein concentration was tested with BCA kit (Pierce).

Equal amounts of total protein extract were subjected to SDS-PAGE in precast 4-12% Bis-tris gel (NuPAGE® Novex Bis-tris midi gel 15wells, Life Technology) or in precast 4-20% Bis-glycine gel (Thermo-Fisher), and transferred to nitrocellulose membranes. Blocked membranes (5% milk in TBS-0.1% Tween-20) were incubated with primary antibodies : hemagglutinin (HA) (1:3000, mouse, Covance), actin (1:4000, rabbit, Sigma), active Caspase-3 (1:800, mouse, Millipore, AB3623); and washed three times with TBS-0.1% Tween-20 for 10 min. Membranes were then labelled with secondary IgG-HRP antibodies raised against each corresponding primary antibody. After three washes, the membranes were incubated with Immun-Star WesternC kit (BioRad) according to the instructions of the supplier. Peroxidase activity was detected with camera system Fusion TX7 (Fisher scientific).

2.6 Statistical analysis

All data were expressed as means +/- SEM. Unpaired Student's t-test was used for the comparison between two groups. When more than two groups were compared, a one-way ANOVA with multiple comparisons using the *post hoc* Bonferroni test was carried out using commercially available software (StatView® software, SAS Institute Inc., USA).

3. Results

Abhd11os RNA is not translated into a detectable peptide in living cells

ABHD11-AS1 RNA is a ~473-base-long transcript processed from four exons in human. ABHD11-AS1 and its mouse homolog Abhd1os contain two small potential ORFs (ORF1, 105 nucleotides and, ORF2, 138 nucleotides in mouse), which are conserved across mammals. It has been shown that small ORFs can be translated into functional peptides *in vivo* [e.g.(Galindo et al., 2007)]. Furthermore, Abhd11os transcript has been detected in the polysomal fraction of mouse striatal neurons (Heiman et al., 2008) (see table S5 of this reference). Thus, the possibility that Abhd11os may be coding for peptides could not be ruled out.

We therefore experimentally examined whether plasmids expressing either putative ORFs of Abhd11os (ORF1 or ORF2) tagged with C-terminal hemagglutinin (HA) could generate a detectable peptide after transfection in HEK293T cells (supplementary Figure S1). As negative controls, ATG sites of each ORF were deleted (ORF1-ΔATG and ORF2-ΔATG). The transcripts of ORF1 and ORF2 (with or without ATG) could be readily detected by RT-qPCR 24 hours after transfection. As expected, Western blot analysis of protein extracts from cells transfected with ORF1-ΔATG or ORF2-ΔATG did not reveal the presence of an HA tag peptide (supplementary Fig.1S). As positive control, in cells transfected with a plasmid coding the mouse striatal protein Dclk3 tagged with HA, a band at 90 kDa corresponding to full length mouse Dclk3 could be detected. In contrast, cell transfected with plasmids coding ORF1 or ORF2 did not reveal the presence of HA-containing low molecular weight peptides. Consistent with this, no specific fluorescent signal was observed in transfected cells subjected to immunofluorescence detection of the HA tag. These results support the hypothesis that, even when overexpressed, Abhd11os RNA does not lead to the production of a peptide. Thus as predicted, Abhd11os is a non-coding RNA.

Abhd11os expression is downregulated in HD mouse models

A major reduction in Abhd11os RNA levels was noted in the striatum of R6/2 mice, which express *exon 1* of the human *HD* gene, containing 150 CAG repeats [the non-coding RNA Abhd11os was named 2010001M06rik (Brochier et al., 2008)]. To check that this loss of expression was not specific to the R6/2 model, we asked whether a similar change could be seen in the BACHD mouse model, which expresses human full-length mHtt (Gray et al., 2008). We also characterized Abhd11os RNA levels in a knock-in (KI140CAG) mouse model of HD (Menalled et al., 2003). A significant 33% reduction in Abhd11os RNA level was found in the striatum of 9 month-old BACHD mice as compared

to control age-matched littermates (Fig. 1A). In heterozygous and homozygous KI140CAG mice a significant ~70% reduction was found at 13 months of age (Fig. 1B) as compared to age-matched wild type littermates (Fig. 1B).

Lentiviral vector approach to modulate Abhd11os expression in vivo

In order to study how Abhd11os expression could change the neurotoxicity of mHtt in striatal neurons *in vivo*, we chose to use a lentiviral model of HD. In this model stereotaxic injection of LV encoding a short fragment of mHtt (LV-Htt171-82Q) produces a progressive loco-regional cell dysfunction and degeneration characterized by mHtt- and ubiquitin-containing inclusions, loss of markers linked to neuronal integrity and astrogliosis within 6 weeks (Damiano et al., 2013; Faideau et al., 2010; Galvan et al., 2012; Ruiz and Deglon, 2012). This versatile model is particularly suitable to assess *in vivo* how mHtt toxicity can be modified by different proteins or RNA that can be co-expressed with the mutant protein using injection of a mixture of lentiviral vectors in the striatum [for a review (Ruiz and Deglon, 2012)].

For lentiviral-mediated overexpression of Abhd11os *in vivo*, we constructed a lentiviral vector expressing full-length mouse Abhd11os (LV-Abhd11os). To assess its efficiency, we injected it stereotaxically into the mouse striatum together with a lentiviral vector expressing GFP (LV-GFP). Six weeks after injection, brains were collected and the fluorescent region expressing GFP (and thus Abhd11os) was dissected out for RT-qPCR expression analysis. Results showed that LV- Abhd11os produced a 30-fold increase in Abhd11os expression compared to control (Fig.2).

For Abhd11os knock-down, we designed a shRNA targeting Abhd11os. The efficacy of the shRNA was first tested in transfected HEK cells overexpressing Abhd11os. In this condition, expression of Abhd11os was reduced by ~85% by the shRNA targeting Abhd11os (Fig.S1E). We inserted the corresponding DNA sequence into a bicistronic lentiviral backbone allowing co-expression with GFP (Drouet et al., 2009). The resulting lentiviral vector (LV-shAbhd11os) was stereotaxically injected in the striatum of adult C57Bl/6 mice. Six weeks after the infection, the brains were collected and fresh coronal slices encompassing the striatum were prepared. Since LV-shAbhd11os is bicistronic for the GFP, the transduced region was visible using a fluorescence binocular microscope and could be precisely resected and processed for RNA extraction. RT-qPCR analysis showed that LV-shAbhd11os produced a significant 75 % reduction in the expression of endogenous Abhd11os as compared to control (Fig. 2).

Absence of toxicity of LV-Abhd11os and LV-shAbhd11os was verified by histological evaluation 6 weeks after infection. Staining for NeuN and DARPP32, which are well-known markers of neuronal integrity in the striatum (de Almeida et al., 2002; Diguet et al., 2009; Drouet et al., 2009; Faideau et al., 2010; Galvan et al., 2012), revealed no degeneration in the infected striata (Fig.3 and Fig.4).

Thus, the LV- Abhd11os and LV-shAbhd11os are not neurotoxic *per se* and are effective to modulate Abhd11os expression in the mouse striatum.

Overexpression of Abhd11os *protects against mHtt toxicity*

To study the effects of Abhd11os overexpression on mHtt toxicity, we stereotaxically injected a mixed suspension of LV-Htt171-82Q and LV-Abhd11os into the mouse striatum. At 6 weeks post infection, LV-Htt171-82Q produced, a loss of NeuN and DARPP32 labelling in vicinity of the injection site, indicating overt neurodegeneration (Fig.3). In separate experiments we checked that co-infection with LV-LacZ (control) did not change the size of the lesion seen using NeuN immunohistochemistry as compared to LV-Htt171-82Q alone [not shown; mean+/-SEM; NeuN, Htt171-82Q (n=8 mice/group): 0.440+/-0.043 mm^3; Htt171-82Q/LacZ (n=6 mice/group) : 0.526+/-0.088 mm^3; Student *t* test, non-significant]. Quantitative histological evaluation using NeuN immunohistochemistry showed that the striatal lesions produced by a mixture of LV-Htt171-82Q and LV-Abhd11os were significantly smaller than those produced by LV-Htt171-82Q mixed with LV-LacZ (Fig.3) [mean NeuN-depleted volume +/-SEM; Htt171-82Q/ Abhd11os (n=6 mice/group): 0.236+/-0.062 mm^3; Htt171-82Q/LacZ (n=9 mice/group): 0.573+/-0.086 mm^3; Student *t* test, $p<0.02$]. In line with this, analysis of striatal degeneration using DARPP32 immunohistochemistry also showed that the overexpression of Abhd11os reduced the lesions produced by LV-Htt171-82Q (Fig.3) [mean DARPP32-depleted volume+/-SEM; Htt171-82Q/ Abhd11os (n=11 mice/group): 0.289+/-0.046 mm^3; Htt171-82Q/LacZ (n=11 mice/group) : 0.438+/-0.048 mm^3; Student *t* test, $p<0.04$].

These results indicate that overexpression of Abhd11os can reduce the neurotoxicity of Htt171-82Q.

We then assessed the number and size of ubiquitin-positive nuclear inclusions in mice (Fig.3) injected with a mixture of LV-Htt171-82Q and LV-Abhd11os or a mixture of LV-Htt171-82Q and LV-LacZ. Microscopic quantitative analysis of the sections processed by anti-ubiquitin-immunohistochemistry showed that overexpression of LV-Abhd11os changed neither the number of ubiquitin-containing inclusions [mean inclusion number+/-SEM; Htt171-82Q/ Abhd11os (n=8 mice/group): 10,189+/-1,597; Htt171-82Q/LacZ (n=8 mice/group) : 11,141+/-1,330; Student *t* test, p=0.654] nor their mean sizes [Inclusion size, Htt171-82Q/ Abhd11os (n=8 mice/group): 13.049+/-1.266 μm^2; Htt171-82Q/LacZ (n=8 mice/group) : 13.875+/-1.059 μm^2; Student *t* test, p=0.624].

Knock-down of Abhd11os *exacerbates mHtt toxicity*

The effects of Abhd11os knock-down on mHtt toxicity were studied in the same mouse model. Co-infection with LV-Htt171-82Q and LV-sh Abhd11os produced NeuN-negative striatal lesions that were significantly larger than those produced by co-infection with LV-Htt171-82Q and control LV-shLuc (Fig.4) [mean NeuN-depleted volume+/-SEM; Htt171-82Q/shAbhd11os (n=7 mice/group): 0.541+/-0.124 mm^3; Htt171-82Q/shLuc (n=7): 0.253+/-0.0.043 mm^3; Student *t* test, $p<0.05$], indicating that Abhd11os depletion may enhance mHtt toxicity. However, the volume of DARPP32-depleted area was similar in mice co-infected with LV-Htt171-82Q and LV-shAbhd11os as compared to LV-shLuc [mean+/-SEM; Htt171-82Q/shAbhd11os (n=12 mice/group): 0.488+/-0.054 mm^3; Htt171-82Q/LacZ (n=10 mice/group): 0.454+/-0.046 mm^3; Student *t* test, p=0.64]. The number of ubiquitin-positive nuclear inclusions in LV-shAbhd11os infected striata compared to control showed a trend toward reduction although it did not reach statistical significance [mean inclusion number+/-SEM; Htt171-82Q/shAbhd11os (n=8 mice/group): 7,861+/-1,283; Htt171-82Q/shLuc (n=10 mice/group) : 11,221+/-

1,497; Student *t* test, p=0.118]. The mean size of inclusions in LV-shAbhd11os infected striata was slightly (-18.5%) but significantly smaller as compared to LV-shLuc infected striata (Fig.4) [mean inclusion size+/-SEM, Htt171-82Q/shAbhd11os (n=9 mice/group): 8.661+/-0.544 μm^2; Htt171-82Q/shLuc (n=10 mice/group): 10.638+/-0.630 μm^2; Student *t* test, p<0.04].
Altogether, these results suggest that Abhd11os exerts a neuroprotective effect against the striatal toxicity of mHtt *in vivo*, whereas its down-regulation exacerbates the toxicity of mHtt.

Abhd11os does not directly down-regulate expression of Abhd11 mRNA
The underlying mechanism of the effect of Abhd11os towards mHtt toxicity is unknown. Since Abhd11os gene overlaps the antisense 3'UTR region of the Abhd11 gene, we asked whether Abhd11os could directly regulate Abhd11 mRNA expression through an antisense-like effect where Abhd11os hybridizing to Abhd11 mRNA and accelerating its degradation could negatively regulate Abhd11 expression. We performed qRT-PCR to quantify Abhd11 RNA in the striatum after infection with LV-Abhd11os or its control. Results showed that overexpression of Abhd11os produced a slight increase (+25) in Abhd11 mRNA expression (Supplemental Figure 2). This indicated that Abhd11os did not directly down-regulate Abhd11 mRNA.

4. Discussion

Different systematic studies aimed at providing a comprehensive view of the molecular "complexity" of the striatum have shown that many of the preferential gene products of this brain region have a totally unknown function. However, their particular presence in the striatum as compared to other brain region, suggests that they play a key role in striatal function such as motor behavior and cognition. Depending on the datasets considered and methods used, numbers can vary substantially, but a large number of gene products show preferential expression in the striatum. Using a SAGE-based method, we previously identified 120 gene products whose expression levels are at least five times higher in the striatum than in other brain regions (Brochier et al., 2008). Amongst these "striatal" gene products, a large proportion are poorly characterized (<100 entries in PubMed), especially in terms of neurobiological functions/roles and for a non-negligible fraction of these gene products, experiments have never been reported (0 entry in PubMed). In comparison, well-known specific striatal gene products, considered as striatal markers, such as the phosphatase DARPP32 have hundreds of entries in public bibliographic databases.

In the present study we focused on the newly identified striatal marker Abhd11os and found that its expression is significantly reduced in the striatum of two mouse models of HD that express full length Htt with a pathological expansion (BACHD and KI140CAG), which is consistent with the major loss of Abhd11os we previously found in the R6/2 model (Brochier et al., 2008). We asked whether experimental modification of Abhd11os expression in the mouse striatum could change the toxicity of mHtt. For this purpose, we designed lentiviral vectors encoding Abhd11os and a shRNA targeting Abhd11os. Results showed that these vectors were effective in increasing and reducing Abhd11os

expression respectively. The level of overexpression was limited (1.5 fold) using our system. Possibly, this suggests endogenous mechanisms of regulation, as Abhd11os has a weak basal RNA expression in healthy organisms. Indeed, using the very same strategy (same lentiviral vector backbone and promoter) for overexpression, we were able to express more strongly other recombinant transcripts such as mitochondrial complexes subunits and the striatal protein Capucin (Damiano et al., 2013; Galvan et al., 2012).

To test the effects of Abhd11os on mHtt, we used a lentiviral model of HD *in vivo*, which is a highly flexible approach for the targeted overexpression of a disease-causing gene, with rapid and progressive phenotypes (Ruiz and Deglon, 2012). This HD model has already been used to test new experimental therapeutics targeting protein misfolding, mitochondrial defects, cell signalling and mHtt itself (Damiano et al., 2013; Drouet et al., 2009; Galvan et al., 2012; Perrin et al., 2009; Perrin et al., 2007) [review in (Ruiz and Deglon, 2012)]. Histological evaluation showed that Abhd11os overexpression, although limited, produces a significant protective effect, reducing the volume of striatal lesions as seen using two different markers of striatal neuron integrity (NeuN and DARPP32). Conversely, the down-regulation of Abhd11os was found to be pro-toxic, increasing the size of the striatal lesions produced by mHtt as seen using the neuronal marker NeuN. Lesions as seen by DARPP32 were not increased. The likely explanation for this is that at six weeks post-infection mHtt produced its maximal loss of DARPP32 neurons. In this model, loss of DARPP32 appears early after infection (de Almeida et al., 2002) and corresponds to a dysfunction of striatal neurons at first while NeuN immunoreactivity is spared. At later time points after infection, the loss of DARPP32 achieves its maximum while NeuN loss which represents actual degeneration is still at its initial stage (Diguet et al., 2009). The number and size of ubiquitin (positive inclusions in the striatum, a neuropathological hallmark of HD), was not changed by increased expression of Abhd11os. The shRNA targeting Abhd11os produced a significant but small (15%) reduction in the number and size of ubiquitin-positive inclusions. This small reduction might be attributed to the enhancement of neuronal cell death, leaving alive neurons that have the lowest levels of mHtt. These data suggest that the neuroprotective/protoxic effects resulting from the increased/decreased expression of Abhd11os is likely independent from a direct effect on mHtt expression/elimination and aggregation in neurons.

In parallel to the *in vivo* rescue experiments, we examined whether Abhd11os is truly a non-coding RNA (NCBI Reference Sequence: NR_026688). Our experiments showed that expression of the putative ORFs of Abhd11os in HEK293T cells could not reveal the existence of translated peptides. This correlates with the information provided by bioinformatics databases on the Abhd11os gene. Of course, we cannot rule out the possibility that the HA tag would be lost during transgene expression by the cells, but it would then be possible to detect this detached tag by Western blot, which was not the case. Thus it is highly probable that the neuroprotective effect of Abhd11os against mHtt is mediated by its RNA transcript.

Major efforts have been made to identify and explore the various roles of non-coding RNAs. For example the ENCODE project has identified 9,600 long non-coding RNAs (lncRNAs) (>200 nt) and some hints about their localization and roles in the cells have emerged (Cech and Steitz, 2014; Wu et

al., 2013). Current hypotheses about the mechanisms of action of lncRNA (Vucicevic et al., 2014) include interactions with proteins to bring along regulatory functions (Lai et al., 2013); and binding, guidance and organization of chromatin domains to coordinate gene activation (Wang et al., 2011). They have been described to influence mRNA processing and post-transcriptional regulation (Geisler and Coller, 2013) and to play direct and indirect roles on modulation of epigenetic regulation (Peschansky and Wahlestedt, 2014). The majority of lncRNAs expressed in the brain are thought to be brain region specific, and could even be cell-specific and subcellular compartment-specific (ENCODE project). Increasing number of lncRNAs are being identified as interacting with genes or proteins implicated in neurodegenerative and psychiatric disorders but only a few lncRNAs have so far been implicated in HD, as compared to others neurodegenerative diseases (Bhan and Mandal, 2014; Tan et al., 2013; Wu et al., 2013). Some lncRNAs seem to directly act on mHtt, as HTTAS_v1 whose overexpression specifically reduces endogenous Htt transcript levels (Chung et al., 2011), or DGCR5, a downstream target of REST in HD that exacerbates the toxicity of mHtt (Johnson et al., 2009). Considering the diverse mechanisms proposed for lincRNA function (see as reviews Guttman et al, 2009; Khalil et al, 2009; Ulitsky & Bartel 2013), it would be tempting to think that Abhd11os could produce neuroprotective effects acting on transcriptional control, for example guiding chromatin remodelling proteins to target loci, or acting with transcriptional factors, where the latter activate transcriptional program and Abhd11os could repress previous unstable transcriptional program. Or, it could also regulate gene expression of down-regulated or upregulated genes that are known to be modified by mHtt (see as reviews Zuccato et al, 2010; Seredenina & Luthi-Carter, 2012). Abhd11os could also pair with other RNAs to trigger post-transcriptional regulation known to be altered in HD. Abhd11os could directly scaffold nuclear or cytoplasmic complexes. These different mechanisms are essential for the cells to function properly and may reduce damages induced by mHtt. If Abhd11os is implicated in some of these functions, its down regulation would amplify transcriptional dysregulation induced by mHtt, leading to cell dysfunction and death. As previously said, lincRNAs, as lncRNAs, are aimed to be brain region specific, cell-specific and subcellular compartment-specific, and depending on the function of Abhd11os, the elucidation of the mechanisms underlying the neuroprotective effects of Abhd11os over-expression against mHtt toxicity will require further studies. In this respect, it would be interesting to determine the localization of Abhd11os RNA in subcellular compartments with regard to functions that are most likely altered by mHtt. In particular it would be tempting to speculate that Abhd11os could produce a neuroprotective effect by regulating the expression of a gene particularly important for neuronal survival. In line with this, we examined whether Abhd11os could directly regulate expression of Abhd11 mRNA, since Abhd11os gene is antisense with the 3'UTR region of Abhd11. Our results showed that overexpression of Abhd11os produces a slight increase in Abhd11 RNA expression, and not a downregulation. In line with this, bioinformatics search indicates slight down-regulation Abhd11 expression in HD mouse models. Thus Abhd11os does not seem to directly regulate expression of Abhd11 mRNA levels.

In conclusion, since Abhd11os has a preferential expression in the striatum and its levels are early reduced in different HD models, it is possible that this down-regulation may be involved in the preferential degeneration of the striatum in HD. Using an *in vivo* lentiviral model of HD, we showed

that Abhd11os has a neuroprotective effect against mHtt. It should be emphasized that not all striatal markers deregulated in HD can modulate the toxicity of N-terminal fragments of mHtt in this model, and that even fewer candidates have been found to produce significant effects in both overexpression and down-regulation experiments (Galvan et al., 2012; Ruiz and Deglon, 2012).

The present study therefore identifies a new potential modifier of mHtt toxicity and as such may help in future works to define novel therapeutic targets to slow disease progression.

Figures and figure legends

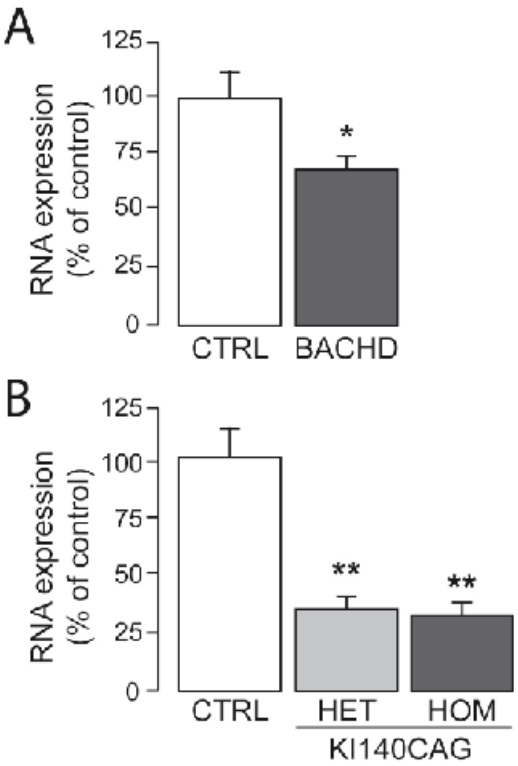

Figure 1. Down regulated expression of Abhd11os in genetic mouse models of HD. Expression of Abhd11os was measured by RT-qPCR in 9 month-old BACHD mice (A) and 13 month-old KI140CAG (B). Controls (CTRL) are age-matched wild type littermates. Results are presented as mean +/- standard error of the mean. HET, heterozygous (140Q/+); HOM, homozygous (140Q/140Q) knock-in mice carrying an expanded CAG repeat. *, $p<0.05$, n=6 mice per group, unpaired Student-t test. **, $p<0.001$, n=5 mice per group, One way ANOVA and Bonferroni *post hoc*.

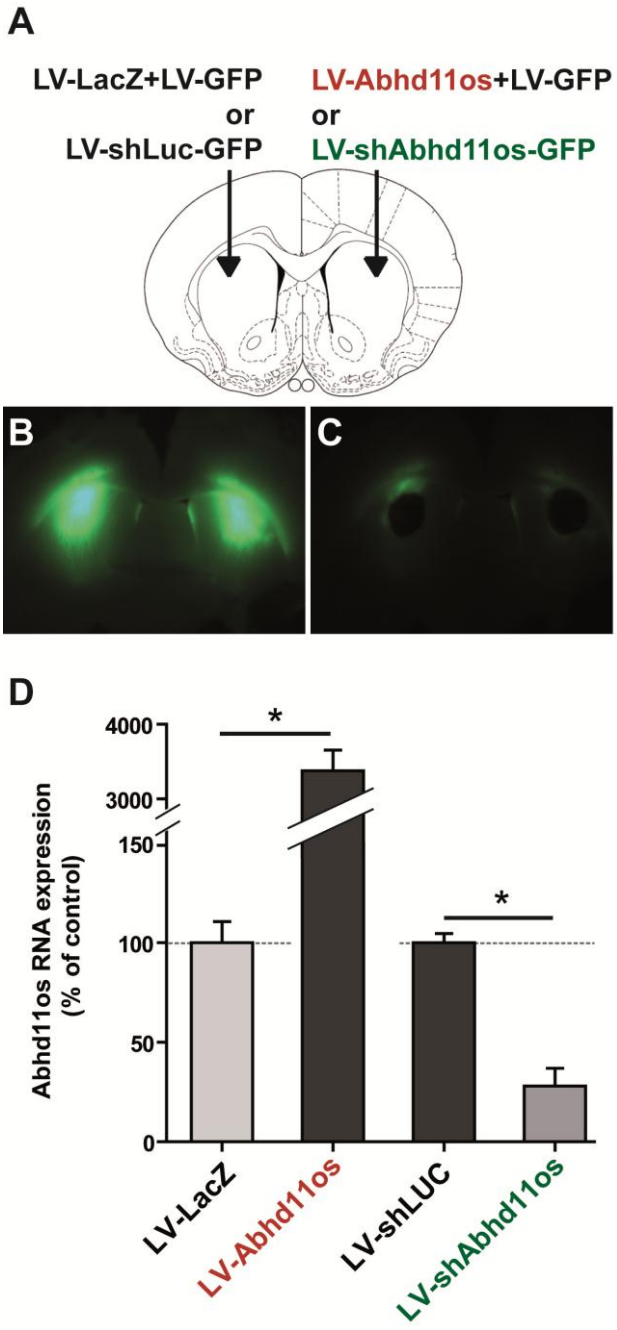

Figure 2. Efficiency of the lentiviral vectors (LV) developed for Abhd11os overexpression and knock-down. (A) Mice were injected with LV- Abhd11os mixed with LV-GFP in a 4:1 ratio in the right striatum, and with a lentiviral vector expressing beta-galactosidase (LV-LacZ; control) mixed with LV-GFP in the left striatum. A second group of mice was injected with LV-shAbhd11os-GFP (bicistronic construct also expressing GFP) in the right striatum, and with a lentiviral vector expressing a shRNA directed against Luciferase (LV-shLuc-GFP; control) in the left striatum. Six weeks later, the striatal regions expressing GFP (B) were dissected out from fresh slices using a punch (C) and analyzed by RT-qPCR (D). Results are expressed relative to controls as mean +/- standard error of the mean (n=5 to 7 mice per group). *, $p<0.0001$, paired Student *t* test.

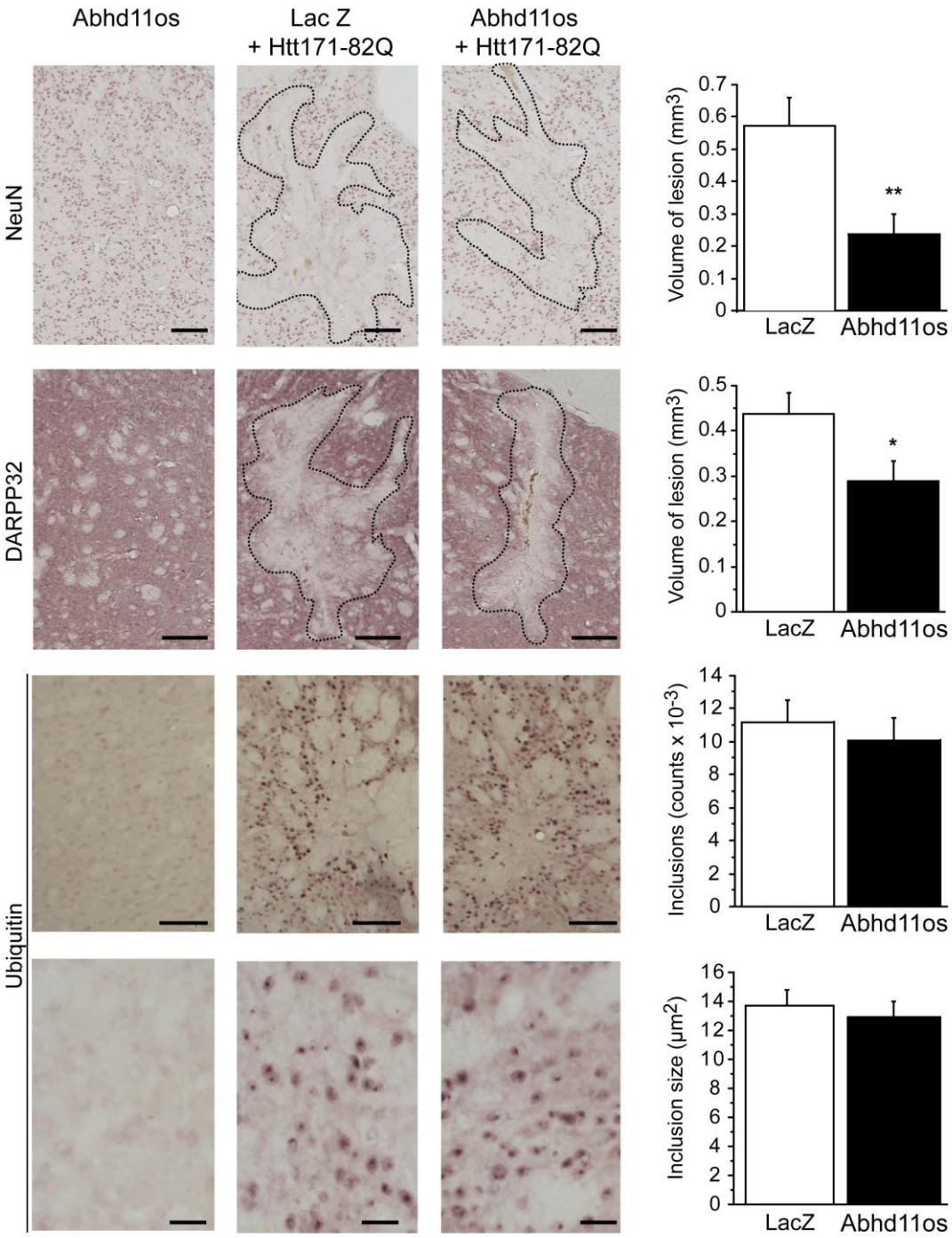

Figure 3. Effect of the overexpression of Abhd11os on the toxicity induced by mHtt. Adult male mice received a bilateral intrastriatal injection of a mixture containing LV-Htt171-82Q with either LV-LacZ (LacZ, control) or LV-Abhd11os. Six weeks after infection, brains were processed for histological evaluation using anti-DARPP32, anti-NeuN, and anti-ubiquitin-immunohistochemistry. Left panel: typical coronal mouse brain sections displaying representative areas with depleted staining. Right panel: histograms representing quantitative determination of the volume with depleted staining in the striatum. Results are expressed as mean +/- standard error of the mean (n=6-11 mice/group). *, $p<0.05$; **, $p<0.02$, unpaired Student *t* test. Scale bars : NeuN, DARPP32, 100 µm; ubiquitin, 50 µm and (lower images) 20µm.

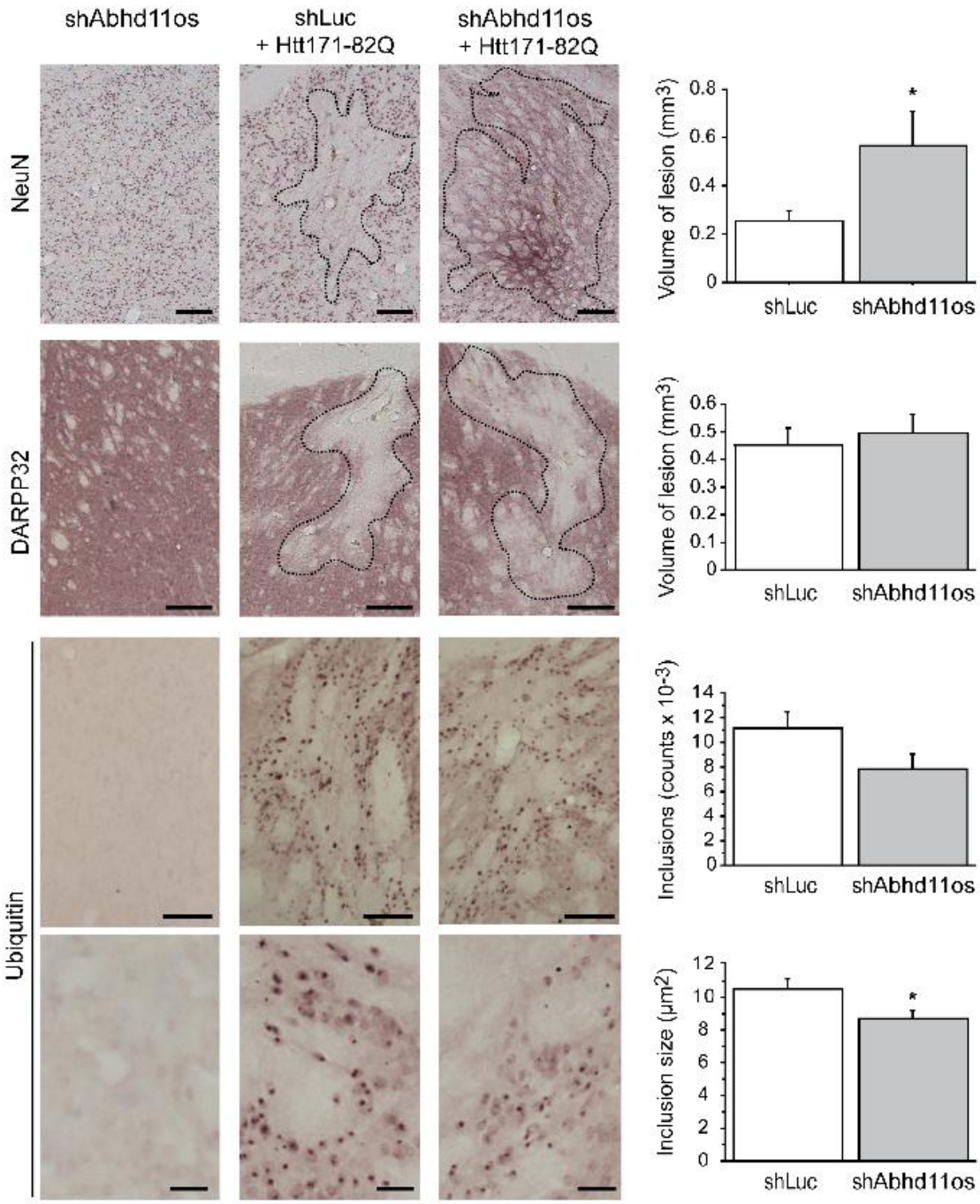

Figure 4. Effect of the knock-down of Abhd11os on the toxicity induced by mHtt. Adult male mice received a bilateral intrastriatal injection of a mixture containing LV-Htt171-82Q with either LV-shLuc (control), or LV-shAbhd11os. Six weeks after infection, brains were processed for histological evaluation using anti-DARPP32, anti-NeuN, and anti-ubiquitin-immunohistochemistry. Left panel: typical coronal mouse brain sections displaying representative areas with depleted staining. Right panel: histograms representing quantitative determination of the volume with depleted staining in the striatum. Results are expressed as mean +/- standard error of the mean (n=7-12 mice/group). *, $p<0.05$, unpaired Student *t* test. Scale bars: NeuN, DARPP32, 100 µm; ubiquitin, 50 µm and (lower images) 20µm.

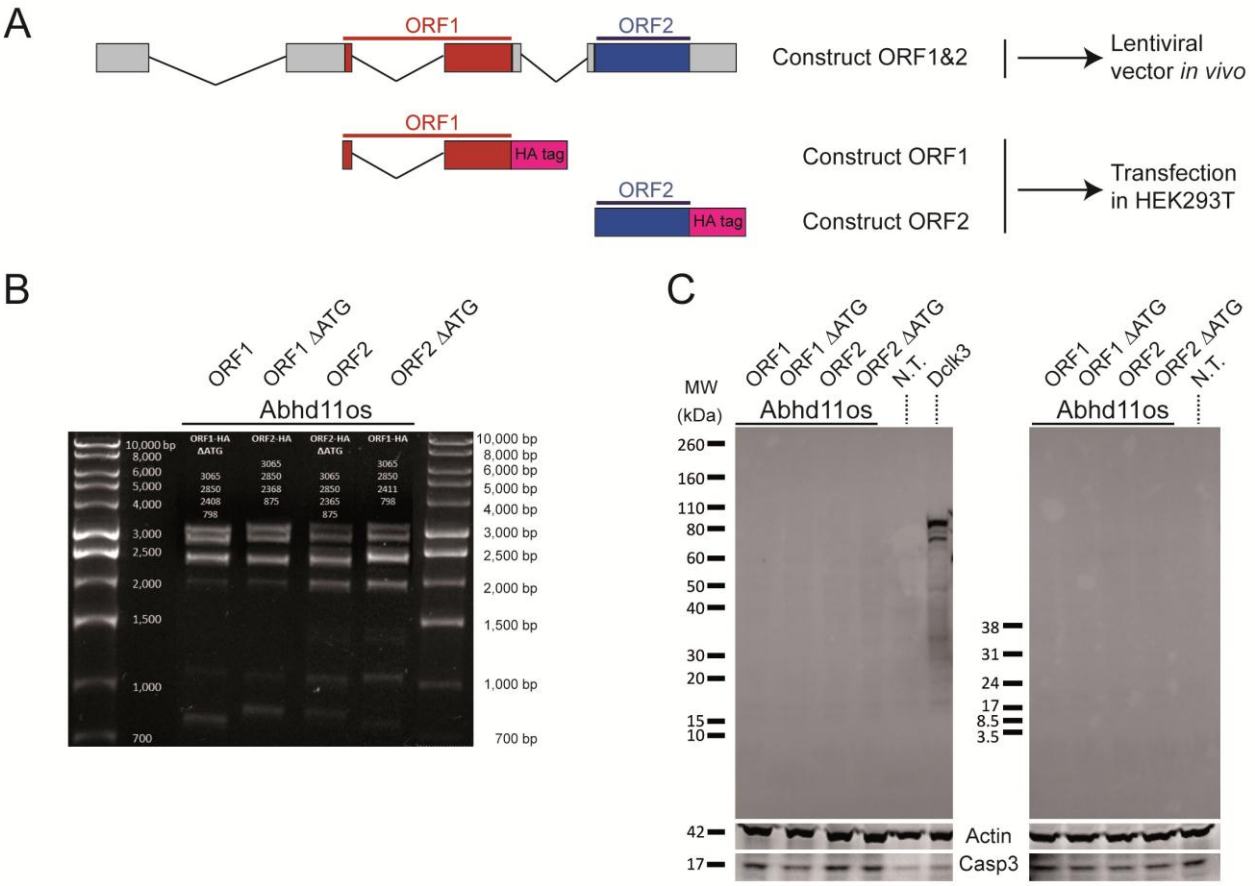
A
ORF1
ORF2
Construct ORF1&2
Lentiviral vector *in vivo*
ORF1
HA tag
ORF2
HA tag
Construct ORF1
Construct ORF2
Transfection in HEK293T
B
ORF1
ORF1 ΔATG
ORF2
ORF2 ΔATG
Abhd11os
ORF1-HA ΔATG
ORF2-HA
ORF2-HA ΔATG
ORF1-HA
10,000 bp
8,000
6,000
5,000
4,000
3,000
2,500
2,000
1,500
1,000
700
3065
2850
2408
798
2368
875
2365
2411
C
MW (kDa)
ORF1
ORF1 ΔATG
ORF2
ORF2 ΔATG
N.T.
Dclk3
Abhd11os
260
160
110
80
60
50
40
30
20
15
10
42
17
38
31
24
8.5
3.5
Actin
Casp3
D
(-) control: empty vector
(+) control: Dclk3-HA
ORF1
ORF1 ΔATG
ORF2
ORF2 ΔATG
HA / DAPI
x20
x40
E
RNA expression (% of control)
160
140
120
100
80
60
40
20
0
**
*
N.T.
Abhd11os
Abhd11os +shAbhd11os

Supplementary Figure 1. Abhd11os RNA expression in HEK293T cells does not lead to a peptide production.

A, Representation of DNA constructs containing the full-length sequence of Abhd11os, for lentiviral-mediated expression in mice (Construct ORF1&2) or containing either ORF1 (construct ORF1) or ORF2 (construct ORF2) and a C-terminal HA tag to permit their potential detection in transfected HEK293T.

B, Validation of the plasmids used for biochemical studies done by molecular biology analysis. Construct ORF1 and ORF2 with or without ATG start codon (-ΔATG construct without start codon is used as control of non-expression) were digested by restriction enzymes and separated in agarose gel to reveal the DNA fragments. Bands obtained correlate with the expected sizes (numbers in white upper the gel) according molecular weight marker (1kbp).

C, Attempt to detect a putative peptide corresponding to Abhd11os by western blot analysis of total protein extracts in HEK293T cells transfected with plasmids coding ORF1 and ORF2 constructs, with or without ATG start codon. Compared to protein expression of a control plasmid (Dclk3-HA), Abhd11os plasmids did not lead to the production of a detectable peptide. N.T., non-transfected cells; actin and active caspase 3 were used to control protein load in each lane. Duplicate experiments are presented with medium (left) and low (right) molecular weights markers.

D, Detection of a putative peptide corresponding to Abhd11os by immunofluorescence of the HA tag in HEK293T cells. ORF1 and ORF2 constructs, with or without ATG start codon were used for transfection. As negative control, HEK293T cells were transfected with an empty vector. As positive control, HEK293T cells were transfected with a plasmid expressing the striatal protein Dclk3 with an HA tag. These immunofluorescence experiments don't permit to detect a coding peptide corresponding to Abhd11os protein expression.

E, *In vitro* assessment of the efficiency of the constructs used for Abhd11os overexpression and down-regulation. Transfection of HEK293T cells with full-length Abhd11os resulted in a significant overexpression of Abhd11os (taken as 100% of expression in these experiments) as compared to non-transfected cells. Co-transfection with sh-Abhd11os led to a significant down-regulation of Abhd11os RNA expression as compared to cells transfected with Abhd11os alone.

**, $p<0.01$, n=3, as compared to N.T. *, $p>0.05$, n=3, as compared to Abhd11os, One way ANOVA and Bonferroni *post hoc*.

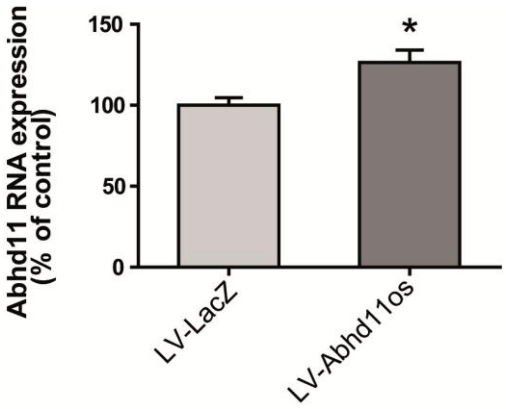

Supplementary Figure 2. Impact of overexpression of Abhd11os on endogenous Abhd11 expression.

Mice were injected with a lentiviral vector expressing beta-galactosidase (LV-LacZ; control) mixed with LV-GFP in the left striatum, and with LV-Abhd11os mixed with LV-GFP in the right striatum. Results are expressed relative to controls as mean +/- standard error of the mean (Lacz n=5; Abhd11os n=7). Endogenous Abhd11 level expression in mice injected with LacZ compared to mice injected with Abhd11os. *, $p<0.02$, n=7 mice/group, paired Student *t* test.

Acknowledgments

This work was supported by the “Commissariat à l’Energie Atomique et aux Energies Alternatives” (CEA) and “Centre National de la Recherche Scientifique” (CNRS). LG was supported by the Neuropôle de Recherche Francilien and the Fondation pour la Recherche Médicale. LF was supported by the French Research Ministry. The research leading to these results has received funding from the European Community's Seventh Framework Program FP7/2007-2013 under grant agreement no. HEALTH-F5-2008-222925. We also received financial support from the IMAGEN European integrated project (EUR617037286).

Potential Conflicts of interest

The authors of the present manuscript declare to have no Conflict of Interest.

5. References

Benchoua, A., Trioulier, Y., Diguet, E., Malgorn, C., Gaillard, M.C., Dufour, N., Elalouf, J.M., Krajewski, S., Hantraye, P., Deglon, N.*, et al.* (2008). Dopamine determines the vulnerability of striatal neurons to the N-terminal fragment of mutant huntingtin through the regulation of mitochondrial complex II. Hum Mol Genet *17*, 1446-1456.

Bhan, A., and Mandal, S.S. (2014). Long Noncoding RNAs: Emerging Stars in Gene Regulation, Epigenetics and Human Disease. ChemMedChem.

Blum, D., Hourez, R., Galas, M.C., Popoli, P., and Schiffmann, S.N. (2003). Adenosine receptors and Huntington's disease: implications for pathogenesis and therapeutics. Lancet Neurol *2*, 366-374.

Borrell-Pages, M., Zala, D., Humbert, S., and Saudou, F. (2006). Huntington's disease: from huntingtin function and dysfunction to therapeutic strategies. Cellular and molecular life sciences : CMLS *63*, 2642-2660.

Brochier, C., Gaillard, M.C., Diguet, E., Caudy, N., Dossat, C., Segurens, B., Wincker, P., Roze, E., Caboche, J., Hantraye, P.*, et al.* (2008). Quantitative gene expression profiling of mouse brain regions reveals differential transcripts conserved in human and affected in disease models. Physiological genomics *33*, 170-179.

Brouillet, E., Jacquard, C., Bizat, N., and Blum, D. (2005). 3-Nitropropionic acid: a mitochondrial toxin to uncover physiopathological mechanisms underlying striatal degeneration in Huntington's disease. J Neurochem *95*, 1521-1540.

Cech, T.R., and Steitz, J.A. (2014). The noncoding RNA revolution-trashing old rules to forge new ones. Cell *157*, 77-94.

Cha, J.H. (2007). Transcriptional signatures in Huntington's disease. Prog Neurobiol *83*, 228-248.

Charvin, D., Vanhoutte, P., Pages, C., Borrelli, E., and Caboche, J. (2005). Unraveling a role for dopamine in Huntington's disease: the dual role of reactive oxygen species and D2 receptor stimulation. Proc Natl Acad Sci U S A *102*, 12218-12223.

Chung, D.W., Rudnicki, D.D., Yu, L., and Margolis, R.L. (2011). A natural antisense transcript at the Huntington's disease repeat locus regulates HTT expression. Hum Mol Genet *20*, 3467-3477.

Cowan, C.M., and Raymond, L.A. (2006). Selective neuronal degeneration in Huntington's disease. Curr Top Dev Biol *75*, 25-71.

Damiano, M., Diguet, E., Malgorn, C., D'Aurelio, M., Galvan, L., Petit, F., Benhaim, L., Guillermier, M., Houitte, D., Dufour, N.*, et al.* (2013). A role of mitochondrial complex II defects in genetic models of Huntington's disease expressing N-terminal fragments of mutant huntingtin. Hum Mol Genet *22*, 3869-3882.

Damiano, M., Galvan, L., Deglon, N., and Brouillet, E. (2010). Mitochondria in Huntington's disease. Biochim Biophys Acta *1802*, 52-61.

de Almeida, L.P., Ross, C.A., Zala, D., Aebischer, P., and Deglon, N. (2002). Lentiviral-mediated delivery of mutant huntingtin in the striatum of rats induces a selective neuropathology modulated by polyglutamine repeat size, huntingtin expression levels, and protein length. J Neurosci *22*, 3473-3483.

Desplats, P.A., Kass, K.E., Gilmartin, T., Stanwood, G.D., Woodward, E.L., Head, S.R., Sutcliffe, J.G., and Thomas, E.A. (2006). Selective deficits in the expression of striatal-enriched mRNAs in Huntington's disease. J Neurochem *96*, 743-757.

Diguet, E., Petit, F., Escartin, C., Cambon, K., Bizat, N., Dufour, N., Hantraye, P., Deglon, N., and Brouillet, E. (2009). Normal aging modulates the neurotoxicity of mutant huntingtin. PLoS ONE *4*, e4637.

Drouet, V., Perrin, V., Hassig, R., Dufour, N., Auregan, G., Alves, S., Bonvento, G., Brouillet, E., Luthi-Carter, R., Hantraye, P.*, et al.* (2009). Sustained effects of nonallele-specific Huntingtin silencing. Ann Neurol *65*, 276-285.

Faideau, M., Kim, J., Cormier, K., Gilmore, R., Welch, M., Auregan, G., Dufour, N., Guillermier, M., Brouillet, E., Hantraye, P.*, et al.* (2010). In vivo expression of polyglutamine-expanded huntingtin by mouse striatal astrocytes impairs glutamate transport: a correlation with Huntington's disease subjects. Hum Mol Genet *19*, 3053-3067.

Galindo, M.I., Pueyo, J.I., Fouix, S., Bishop, S.A., and Couso, J.P. (2007). Peptides encoded by short ORFs control development and define a new eukaryotic gene family. PLoS biology *5*, e106.

Galvan, L., Lepejova, N., Gaillard, M.C., Malgorn, C., Guillermier, M., Houitte, D., Bonvento, G., Petit, F., Dufour, N., Hery, P.*, et al.* (2012). Capucin does not modify the toxicity of a mutant Huntingtin fragment in vivo. Neurobiology of aging *33*, 1845 e1845-1846.

Geisler, S., and Coller, J. (2013). RNA in unexpected places: long non-coding RNA functions in diverse cellular contexts. Nature reviews Molecular cell biology *14*, 699-712.

Gray, M., Shirasaki, D.I., Cepeda, C., Andre, V.M., Wilburn, B., Lu, X.H., Tao, J., Yamazaki, I., Li, S.H., Sun, Y.E.*, et al.* (2008). Full-length human mutant huntingtin with a stable polyglutamine repeat can elicit progressive and selective neuropathogenesis in BACHD mice. J Neurosci *28*, 6182-6195.

Harper, P.S. (1991). Huntington's disease.

Heiman, M., Schaefer, A., Gong, S., Peterson, J.D., Day, M., Ramsey, K.E., Suarez-Farinas, M., Schwarz, C., Stephan, D.A., Surmeier, D.J.*, et al.* (2008). A translational profiling approach for the molecular characterization of CNS cell types. Cell *135*, 738-748.

Hottinger, A.F., Azzouz, M., Deglon, N., Aebischer, P., and Zurn, A.D. (2000). Complete and long-term rescue of lesioned adult motoneurons by lentiviral-mediated expression of glial cell line-derived neurotrophic factor in the facial nucleus. J Neurosci *20*, 5587-5593.

Johnson, R., Teh, C.H., Jia, H., Vanisri, R.R., Pandey, T., Lu, Z.H., Buckley, N.J., Stanton, L.W., and Lipovich, L. (2009). Regulation of neural macroRNAs by the transcriptional repressor REST. Rna *15*, 85-96.

Lai, F., Orom, U.A., Cesaroni, M., Beringer, M., Taatjes, D.J., Blobel, G.A., and Shiekhattar, R. (2013). Activating RNAs associate with Mediator to enhance chromatin architecture and transcription. Nature *494*, 497-501.

Menalled, L.B., Sison, J.D., Dragatsis, I., Zeitlin, S., and Chesselet, M.F. (2003). Time course of early motor and neuropathological anomalies in a knock-in mouse model of Huntington's disease with 140 CAG repeats. The Journal of comparative neurology *465*, 11-26.

Mievis, S., Blum, D., and Ledent, C. (2011). A2A receptor knockout worsens survival and motor behaviour in a transgenic mouse model of Huntington's disease. Neurobiology of disease *41*, 570-576.

Perrin, V., Dufour, N., Raoul, C., Hassig, R., Brouillet, E., Aebischer, P., Luthi-Carter, R., and Deglon, N. (2009). Implication of the JNK pathway in a rat model of Huntington's disease. Experimental neurology *215*, 191-200.

Perrin, V., Regulier, E., Abbas-Terki, T., Hassig, R., Brouillet, E., Aebischer, P., Luthi-Carter, R., and Deglon, N. (2007). Neuroprotection by Hsp104 and Hsp27 in lentiviral-based rat models of Huntington's disease. Mol Ther *15*, 903-911.

Peschansky, V.J., and Wahlestedt, C. (2014). Non-coding RNAs as direct and indirect modulators of epigenetic regulation. Epigenetics : official journal of the DNA Methylation Society *9*, 3-12.

Roze, E., Saudou, F., and Caboche, J. (2008). Pathophysiology of Huntington's disease: from huntingtin functions to potential treatments. Curr Opin Neurol *21*, 497-503.

Ruiz, M., and Deglon, N. (2012). Viral-mediated overexpression of mutant huntingtin to model HD in various species. Neurobiology of disease *48*, 202-211.

Seredenina, T., Gokce, O., and Luthi-Carter, R. (2011). Decreased striatal RGS2 expression is neuroprotective in Huntington's disease (HD) and exemplifies a compensatory aspect of HD-induced gene regulation. PLoS One *6*, e22231.

Seredenina, T., and Luthi-Carter, R. (2012). What have we learned from gene expression profiles in Huntington's disease? Neurobiology of disease *45*, 83-98.

Subramaniam, S., Sixt, K.M., Barrow, R., and Snyder, S.H. (2009). Rhes, a striatal specific protein, mediates mutant-huntingtin cytotoxicity. Science (New York, NY *324*, 1327-1330.

Tabrizi, S.J., Scahill, R.I., Owen, G., Durr, A., Leavitt, B.R., Roos, R.A., Borowsky, B., Landwehrmeyer, B., Frost, C., Johnson, H.*, et al.* (2013). Predictors of phenotypic progression and disease onset in premanifest and early-stage Huntington's disease in the TRACK-HD study: analysis of 36-month observational data. Lancet Neurol *12*, 637-649.

Tan, L., Yu, J.T., Hu, N., and Tan, L. (2013). Non-coding RNAs in Alzheimer's disease. Molecular neurobiology *47*, 382-393.

The-Huntington's-Disease-Collaborative-Research-Group (1993). A novel gene containing a trinucleotide repeat that is expanded and unstable on Huntington's disease chromosomes. The Huntington's Disease Collaborative Research Group. Cell *72*, 971-983.

Thomas, E.A. (2006). Striatal specificity of gene expression dysregulation in Huntington's disease. J Neurosci Res *84*, 1151-1164.

Vucicevic, D., Schrewe, H., and Orom, U.A. (2014). Molecular mechanisms of long ncRNAs in neurological disorders. Frontiers in genetics *5*, 48.

Walker, F.O. (2007). Huntington's disease. Lancet *369*, 218-228.

Wang, K.C., Yang, Y.W., Liu, B., Sanyal, A., Corces-Zimmerman, R., Chen, Y., Lajoie, B.R., Protacio, A., Flynn, R.A., Gupta, R.A.*, et al.* (2011). A long noncoding RNA maintains active chromatin to coordinate homeotic gene expression. Nature *472*, 120-124.

Winslow, A.R., and Rubinsztein, D.C. (2008). Autophagy in neurodegeneration and development. Biochim Biophys Acta *1782*, 723-729.

Wu, P., Zuo, X., Deng, H., Liu, X., Liu, L., and Ji, A. (2013). Roles of long noncoding RNAs in brain development, functional diversification and neurodegenerative diseases. Brain research bulletin *97*, 69-80.

Zuccato, C., and Cattaneo, E. (2014). Huntington's Disease. Handbook of experimental pharmacology *220*, 357-409.

3.2. Article #2

Loss of the thyroid hormone binding protein Crym renders striatal neurons more vulnerable to mutant huntingtin in Huntington's disease.

Loss of the thyroid hormone binding protein Crym renders striatal neurons more vulnerable to mutant huntingtin in Huntington's disease

Laetitia Francelle[1,2,*], Laurie Galvan[1,2,*], Marie-Claude Gaillard[1,2], Martine Guillermier[1,2], Diane Houitte[1,2], Gilles Bonvento[1,2], Fanny Petit[1,2], Caroline Jan[1,2], Noëlle Dufour[1,2], Philippe Hantraye[1,2], Jean-Marc Elalouf[3,4,5], Michel de Chaldée[3,4,5], Nicole Déglon[1,2,6], Emmanuel Brouillet[1,2]

[1] *CEA, DSV, I²BM, Molecular Imaging Research Center (MIRCen), F-92265 Fontenay-aux-Roses, France*

[2] Neurodegenerative Diseases Laboratory, *CNRS CEA URA 2210, F-92265 Fontenay-aux-Roses, France*

[3] *CEA, iBiTecS, F-91191 Gif-sur-Yvette Cedex, France*

[4] *CNRS, FRE 3377, F-91191 Gif-sur-Yvette Cedex, France*

[5] *Université Paris-Sud, FRE 3377, F-91191 Gif-sur-Yvette Cedex, France*

[6] *Lausanne University Hospital, Department of Clinical Neurociences, Laboratory of Cellular and Molecular Neurotherapies, Lausanne, Switzerland*

(*) first co-authors, equally contributed to the work.

Abstract

The mechanisms underlying preferential atrophy of the striatum in Huntington's disease (HD) are unknown. One hypothesis is that a set of gene products preferentially expressed in the striatum could determine the particular vulnerability of this brain region to mutant huntingtin (mHtt). Here, we studied the striatal protein Crym (μ-crystallin). Crym is the NADPH-dependent p38 cytosolic T3-binding protein (p38CTBP), a key regulator of thyroid hormone T3 (3,5,3′-triiodo-L-thyronine) transportation. It has been also recently identified as the enzyme that reduces the sulphur-containing cyclic ketimines, which are potential neurotransmitters. Here, we confirm the preferential expression of the Crym protein in the rodent and macaque striatum. Crym expression was found to be higher in the macaque caudate than in the putamen. Expression of Crym was reduced in the BACHD and Knock-in 140CAG mouse models of HD before onset of striatal atrophy. We show that overexpression of Crym in striatal medium-size spiny neurons using a lentiviral-based strategy in mice is neuroprotective against the neurotoxicity of an N-terminal fragment of mHtt *in vivo*. Thus, reduction of Crym expression in HD could render striatal neurons more susceptible to mHtt suggesting that Crym may be a key determinant of the vulnerability of the striatum. In addition our work points to Crym as a potential molecular link between striatal degeneration and the thyroid hormones deregulation reported in HD patients.

INTRODUCTION

The protein mu-Crystallin (Crym) has been discovered as a highly enriched lens component in Marsupials (1). Crym was identified as the NADPH-dependent p38 cytosolic T3-binding protein (p38CTBP, also known as THBP for thyroid hormone (TH)-binding protein) which is likely a key regulator of the thyroid hormone T3 (3,5,3′-triiodo-L-thyronine) transportation in cytoplasm and nucleus, a mechanism through which it is involved in regulating thyroid-hormone-related gene expression (2). Indeed, in the nucleus T_3 binds to THR (thyroid hormone receptor)-containing dimers, which bind to genomic TREs (thyroid responsive elements) to regulate gene transcription (3). Although Crym expression in the brain is high (4), its neurobiological function is unknown. Several observations indirectly suggest that Crym could be a crucial determinant of neuronal cell death/survival. Crym has been reported to be an actor of macular degeneration in non-human primates (5). Mutations in the Crym gene lead to non syndromic deafness, possibly by the incapacity of the resulting mutants to be involved in the potassium ion recycling system with Na, K-ATPase (6, 7). Recently mutations in *CRYM* have been tentatively related to amyotrophic lateral sclerosis (ALS) (8). Given that many species-specific crystallins with NADPH binding properties are protective against oxidation in the lens (2), upregulated Crym in microglia cells in late stages of ALS may have a protective effect against neurodegeneration as do other NADPH requiring enzymes such as thioredoxin (9). Further supporting the view that Crym plays a central role in the central nervous system, Hallen and collaborators recently demonstrated using purification and MS/MS identification that the enzyme ketimine reductase (E.C. 1.5.1.25) is actually Crym (10). Thus Crym catalyzes the reduction of sulphur-containing substrates known as cyclic ketimines which derive from sulfur containing amino-acids and may play a potential role as neurotransmitters (10). Interestingly, the enzymatic activity of ketimine reductase is regulated by T3 levels. Thus, Crym may play a key role at the interface between metabolism, neurotransmission and cell survival.

We recently focused our interest on Crym because of its preferential expression in the striatum and its possible involvement in the pathogenesis of Huntington's disease (HD) (11, 12). HD is an autosomal dominant hereditary neurodegenerative disorder characterized by a preferential atrophy of the striatum associated with cognitive, psychiatric and motor symptoms (13). HD is caused by an abnormal CAG repeat expansion in the huntingtin (*htt*) gene (14). Mutant huntingtin (mHtt) is neurotoxic to neurons, especially toward neurons of the striatum, through both a gain-of-function and loss of function (15). Mutant Htt produces anomalies in energy production and oxidative stress (16), Ca^{2+} deregulation and excitotoxicity (17), abnormal trophic factor expression, trafficking and release (15), alterations of cytoskeleton-mediated transport machinery (18), and defects in signaling pathways involved in cell survival (19). However, none of these mechanisms can explain *per se* the preferential vulnerability of the striatum in HD. One hypothesis is that a set of factors, selectively expressed in the striatum may confer to striatal GABAergic projection neurons their particular susceptibility in HD [for a review (20)]. For example, the presence of the dopamine subtype 2 receptors (D2R) (21-23), the small GTPase Rhes through its E3-ubiquitin ligase activity (24) and the RGS2 protein (25) in striatal neurons have been shown to increase their susceptibility to mHtt in HD. On the contrary, the reduced expression of

several proteins with preferential expression in the striatum, and shown to possess neuroprotective properties may also increase the vulnerability of striatal neurons, such as for example adenosine type 2 receptors (A2A-R) (26), cannabinoid type 1 receptors (CB1-R) (27, 28), and Mitogen and stress-activated kinase-1 (MSK-1) (29, 30).

We previously found that the level of mRNA expression of Crym, that we identified for its enriched expression in the striatum and accumbens, is significantly reduced by 50 % in the striatum of R6/2 mice (11), a widely used transgenic model of HD. Retrospective analysis of gene array datasets of the striatum of HD patients and transgenic mouse models of HD confirms that Crym mRNA levels are reduced in HD (31, 32). Thus it is possible that Crym may be involved in striatal vulnerability through two possible ways: reduction of Crym expression could be a causal event leading to death/dysfunction, pointing to Crym as a neuroprotective/pro-survival protein. On the opposite, decreased expression of Crym in HD could be a regulatory/compensatory mechanism, if the presence Crym (like Rhes for instance) contributes to the vulnerability of striatal neurons.

The objective of the present study was to investigate whether the levels of Crym expression in the mouse striatum could change the toxicity of mHtt. We first characterized the enrichment of the protein Crym in the striatum in mouse, rat and cynomolgus monkey. Secondly, we examined the expression of Crym mRNA and protein in genetic mouse models of HD in absence of major striatal degeneration (BACHD transgenic mice and Knock-in 140CAG mice). Finally, we used a lentiviral vector approach (33) to overexpress recombinant Crym in striatal neurons and directly determine whether the protein could modulate mHtt toxicity *in vivo* in mice.

RESULTS

Crym is expressed preferentially in the striatum and localized in the cytosol

While the expression of Crym mRNA was shown to be highly enriched in the striatum and accumbens, the expression of the protein had been rarely assessed. For this reason, a chicken IgY antibody was raised against Crym (anti-Crym). Western blot analysis of striatal and cortical extracts (total protein extracts) prepared from adult rats, mice and a male adult non-human primate (macaca fascicularis) showed that endogenous Crym, appearing at an apparent molecular weight of ~37kDa was preferentially expressed in the striatum (caudate/putamen) as compared to cerebral cortex (Fig. 1A,B). In a non-human primate, Crym expression was markedly higher in the caudate than in the putamen (Fig. 1B,C).

Experiments using differential centrifugation of rat brain samples followed by Western blot analysis showed that Crym was mainly localized in the cytosol with low expression in the membrane fraction (Fig.2). Similar results were obtained in mouse cerebral cortex and striatum (not shown). Thus, these results confirmed that Crym is a cytosolic protein preferentially expressed in the striatum as compared to cerebral cortex in the adult brain. In the primate striatum, levels of the protein are higher in caudate than in putamen, consistent with mRNA levels described for the macaque and human brain (see Allen Brain Atlas).

Recombinant Crym protein is localized in the cytoplasm and nucleus

Little is known about the expression of Crym in cells, especially neurons. The cDNA for mouse Crym was cloned and a sequence encoding an HA (hemagglutinin) tag was added to its 3' end. After transfection of HEK293T cell using this construct, expression of the recombinant protein was assessed by western blot using an anti-HA antibody. A single band migrating at ~37 kDa was detected, which is consistent with the theoretical apparent molecular weight of full length Crym and with the signal obtained using the anti-Crym antibody (Fig. 3A). Confocal microscopy analysis of HEK cells transfected with the Crym-HA construct using immunofluorescence detection of the HA tag indicated that Crym was located ubiquitously throughout the cell, including the nucleus and cell processes (Fig.3B). Transfection of primary cultures of striatal neurons was also performed with a construct expressing Crym fused to the Green fluorescent protein (GFP-Crym). Confocal microscopy analysis of the transfected neurons also indicated that GFP-Crym was located ubiquitously throughout the soma, the distal portions of neurites and within the nucleus (Fig.3C).

Finally, to study the subcellular localization of recombinant Crym *in vivo*, we generated a lentiviral vector encoding Crym-HA (LV-Crym-HA) driven by the mouse PGK promoter. The lentiviral vectors that we use almost exclusively transduce neurons *in vivo* and *in vitro* (21, 34, 35). Adult C57Bl/6 mice received intrastriatal injection of the LV-Crym-HA and six weeks later, brains were processed for histochemical evaluation. Immunohistochemical detection of the HA tag showed that the recombinant protein filled the entire soma and dendrites of neurons (Fig. 4). The nucleus was also stained. Confocal analysis of the striatum in mice injected with LV-Crym-HA confirmed that indeed, striatal neurons displayed high levels of Crym in the cytoplasm and dendrites branches and spines as well as in the nucleus (not shown).

Crym expression is reduced in HD models

Crym mRNA expression has been found to be reduced in HD models and patients (11, 31, 32). Here, we studied its expression in two additional genetic mouse models of HD. Analysis with qRT-PCR showed that Crym mRNA levels were significantly reduced by 43% in the striatum of heterozygous BACHD mice at 6 months of age (mean mRNA expression +/- SEM, wild type littermates (n=5): 5.96 +/- 0.186; BACHD (n=6): 3.38 +/- 0.41; $p<0.0005$, unpaired Student *t*-test; not shown). Similarly, significant decrease in Crym mRNA levels was found in homozygous and to a lesser extent in heterozygous KI140CAG mice (13 months of age) as compared to wild type mice (mean mRNA expression +/- SEM, wild type littermates (n=8): 0.090 +/- 0.009; heterozygous KI140CAG mice (n=8): 0.080 +/- 0.005; $p<0.05$; homozygous KI140CAG mice (n=8): 0.05 +/- 0.005; $p<0.01$. One way ANOVA: $p<0.0001$, $F=9.948$; *post hoc* Bonferroni's multiple comparison test: wild type littermates VS heterozygotes n.s; wild type littermates VS homozygotes $p<0.001$; heterozygotes VS homozygotes $p<0.05$) (Fig.5). Western blot analyses in KI140CAG mice showed reduced expression of Crym protein in the striatum as compared to age-matched wild type littermates in homozygous mice with a trend to decrease in heterozygous mice (mean protein expression normalized with tubulin +/- SEM, wild type littermates (n=3): 4.15 +/- 0.34; heterozygotes (n=8): 3.21 +/- 0.32 n.s.; homozygotes (n=8): 2.27 +/- 0.13 ; $p<0.01$. One way ANOVA: $p<0.01$, $F=11.13$; *post hoc* Bonferroni's multiple comparison test: wild

type littermates VS heterozygotes n.s; wild type littermates VS homozygotes p<0.01; heterozygotes VS homozygotes ns). Expression levels in the cortex were very low and could not be reliably quantified (not shown). Thus, these results show that Crym expression is down regulated in HD models at both the mRNA and protein levels.

Crym overexpression reduces the toxicity of an N-terminal fragment of mutant huntingtin

We next examined whether overexpressing Crym could modify the toxicity of an N-terminal fragment of mHtt. We first designed and characterized a lentiviral vector to increase Crym expression *in vivo* (LV-Crym-HA). For the quantitative analysis of Crym-HA mRNA expression as compared to endogenous Crym, LV-Crym-HA was mixed with a lentiviral vector expressing GFP (LV-GFP) to allow dissection of the infected region under fluorescence binoculars. A lentivirus encoding □-Galactosidase (LV-LacZ) was used as a control of viral load. The fluorescent region expressing GFP (and thus Crym-HA) was dissected out for mRNA expression analysis. Results of the qRT-PCR showed that LV-Crym-HA produced a 14.6 fold increase of Crym expression compared to control (LV-LacZ) (Mean mRNA expression +/- SEM; LacZ (n=4), 0.030 +/- 0.005; Crym-HA (n=4), 0.437 +/- 0.049; p<0.0002, unpaired Student *t*-test) (Fig.1S). Thus, the LV-Crym-HA was efficacious to increase Crym expression in the mouse striatum.

To study the effect of Crym overexpression on the neurotoxicity of m-Htt in striatal neurons *in vivo*, we used a lentiviral model of HD in which stereotaxic injection of a lentiviral vector encoding a short fragment of mHtt (LV-Htt171-82Q) produces a progressive loco-regional cell dysfunction and degeneration characterized by m-Htt- and ubiquitin-containing inclusions, loss of markers linked to neuronal integrity and astrogliosis within 6 weeks (33, 36-38). This versatile model is particularly suitable to assess *in vivo* how mHtt toxicity can be modified by different factors that can be co-expressed with the mutant protein using injection of a mixture of lentiviral vectors in mouse striatum [for a review (33)].

We stereotaxically injected a mixed suspension of LV-Htt171-82Q and LV-Crym-HA into the mouse striatum. At 6 weeks post-infection, LV-Htt171-82Q produced a loss of NeuN and DARPP32 labelling in vicinity of the injection site, indicating overt neurodegeneration (Fig.6). In separate experiments we checked that co-infection with LV-LacZ (control) did not change the size of the lesion seen using NeuN immunohistochemistry as compared to LV-Htt171-82Q alone [data not shown; mean+/-SEM; NeuN, LV-Htt171-82Q alone (n=8): 0.440+/-0.043 mm^3; LV-Htt171-82Q+LV-LacZ (n=6) : 0.526+/-0.088 mm^3; unpaired Student *t* test, non-significant (n.s.)]. Quantitative histological evaluation using NeuN immuno-histochemistry showed that the striatal lesions produced by a mixture of LV-Htt171-82Q and LV-Crym-HA were significantly smaller than those produced by LV-Htt171-82Q mixed with LV-LacZ (Fig.6) [mean NeuN-depleted volume +/-SEM; LV-Htt171-82Q+LV-Crym-HA (n=10): 0.229+/-0.033 mm^3; LV-Htt171-82Q+LV-LacZ (n=7): 0.442+/-0.095 mm^3; Student *t* test, p<0.03]. In line with this, analysis of striatal degeneration using COX histochemistry also showed that the overexpression of Crym reduced the lesions produced by LV-Htt171-82Q (Fig.6) [mean COX-depleted volume+/-SEM; LV-Htt171-82Q+LV-Crym-HA (n=10): 0.236+/-0.024 mm^3; LV-Htt171-82Q+LacZ (n=7) : 0.360+/-0.057 mm^3; unpaired Student *t* test, p<0.05]. In contrast, analysis of striatal degeneration using DARPP-32

immunohistochemistry did not show significant differences between groups (Fig.6) [mean DARPP-32-depleted volume+/-SEM; LV-Htt171-82Q+LV-Crym-HA (n=10): 0.450+/-0.043 mm^3; LV-Htt171-82Q+LV-LacZ (n=7): 0.444+/-0.023 mm^3; unpaired Student *t*-test, n.s.].

We also assessed the number and size of Em48-positive nuclear inclusions in mice (Fig.6) injected with a mixture of LV-Htt171-82Q and LV-Crym-HA or a mixture of LV-Htt171-82Q and LV-LacZ. Microscopic quantitative analysis of the sections processed by Em48 antibody-immunohistochemistry showed that overexpression of Crym has a tendency to increase the number of Em48-containing inclusions [mean inclusion number+/-SEM; LV-Htt171-82Q+LV-Crym-HA (n=8): 36,306+/-4,091; LV-Htt171-82Q+LV-LacZ (n=6): 29,525+/-7,112; Student *t*-test, n.s.]. The mean size of Em48 positive inclusions did not show differences between groups [Inclusion size, LV-Htt171-82Q+ LV-Crym-HA (n=8): 19.09+/-1.48 μm^2; LV-Htt171-82Q+LV-LacZ (n=6): 18.39+/-1.86 μm^2; unpaired Student *t*-test, n.s.]. The mean density of Em48 positive inclusions/mm^2 shows a higher tendency in the LV-Crym-HA injected mice [Density inclusions/mm^2, LV-Htt171-82Q+ LV-Crym-HA (n=8): 935.42+/-62.48 μm^2; LV-Htt171-82Q+LV-LacZ (n=6): 831.63+/-48.15 μm^2; unpaired Student *t*-test, n.s.]. The number and size of Ubiquitin-positive nuclear inclusions were not different from what was observed with Em48 staining (data not shown).

DISCUSSION

The mechanisms underlying the vulnerability of the striatum in HD remain unclear. In the present study, we tested the hypothesis that the protein Crym may play a role in the susceptibility of adult striatal neurons to mHtt.

Our results show that expression of Crym mRNA is reduced in KI140 mice and BACHD mice. This is in agreement with the down regulation of its mRNA we and others previously found in different HD mouse models and HD patients (11, 31, 32, 39). In addition, we also show that the levels of the protein Crym is markedly reduced in KI140 mice, indicating that down regulation that occurs at the mRNA levels leads to loss of the protein, likely impairing its function in the striatum. We reasoned that this reduction in Crym expression could participate in the striatal vulnerability to mHtt toxicity. Results of our study indicated that Crym overexpression could reduce the susceptibility of striatal neurons *in vivo* toward the toxicity of an N-terminal fragment of human mHtt. The effect of the continuous expression of mHtt in lentiviral models has been characterized by the loss of expression of three markers, DARPP-32, NeuN and COX (33). The loss of NeuN immunoreactivity and the loss of COX histochemical labelling are associated with actual neuronal degeneration and dysfunction, as assessed using markers of cell death (40) and stereological cell counts (34). Thus, the present results indicate that overexpressing Crym reduces cell death induced by the mHtt fragment.

The number and size of Em48- and ubiquitin-positive inclusions in the striatum, a neuropathological hallmark of HD, were not significantly changed by the overexpression of Crym. This suggests that the neuroprotective effects produced by the increased expression of Crym in striatal neurons are likely independent from a direct effect on mHtt expression or aggregation. If Crym had reduced the levels of cellular mHtt, we should have observed a lower number of inclusions. Neuroprotective effects can be

produced without major change in inclusions and aggregates size or numbers. For example expression of the Ip and Fp subunits of mitochondrial complex II protects striatal neurons against mHtt *in vitro* and *in vivo*, while the number and size of inclusions remain unchanged (36).

The neuroprotective effects of Crym overexpression using a lentiviral approach in our mouse model are unlikely linked to methodological bias. Indeed we have tested different transgenes using the very same methods. Recently, we studied the striatal marker Capucin (Syndig1l) whose expression is markedly reduced in HD patients and mouse models (38). Overexpression of Capucin, using a similar LV-mediated approach produced no significant change in the toxicity of LV-Htt171-82Q in the striatum. Using similar co-infection approaches in rats, we have also identified the neuroprotective roles of some proteins against mHtt fragment, including the transcription factor CA150 (41), chaperone proteins (42), signaling proteins of the JNK pathway (43), the mitogen- and stress-activated protein kinase 1 (MSK-1) (30) and the subunits of mitochondrial complex II (36).

The mechanisms underlying reduced expression of Crym mRNA (and, as shown here, of Crym protein as well) are unknown. The downregulation of striatal transcripts in HD may result from the functional disruption of striatum-specific transcriptional activators such as Bcl11b (44). Depending on the transcript, this phenomenon can be protective, detrimental or have no effect on striatal neurons (Francelle et al., 2014). The downregulated expression of several proteins enriched in the striatum and involved in different neuronal functions such as neurotransmission, intracellular signaling, and transcription have been reported to play a role in striatal vulnerability in HD. For example, compelling experimental evidence shows that the loss of A2A-R, CB1-R, MSK-1, STEP61, Bcl11b, and Fox1b likely renders striatal cells more prone to degeneration in HD models [for a review (20, 45)].

The mechanisms of whereby Crym may reduce the vulnerability of striatal neurons to mHtt are not yet elucidated. However this may have to be associated with the possible alteration in the levels of the thyroid hormones in HD patients, given that thyroid hormones regulate multiple cellular events, including energy expenditure and cellular differentiation (46). In their pioneering studies, Aziz and collaborators showed that levels of T3, which is a ligand of Crym, are increased in a small cohort of HD patients as compared to age matched controls (47). In a larger cohort, no significant increase in T3 was shown but the hormone levels were found to be negatively correlated with severity of clinical impairments, supporting the hypothesis that the thyrotropic axis is altered in HD patients (48). In line with this, a functional interaction of mHtt with thyroid hormone receptor (TR) and the nuclear co-repressor NCor, which represses TR-mediated transcription, has been reported, suggesting that mHtt may lead to abnormal transcription of TR targets in the HD striatum (49). In the striatum, such mechanism would be exacerbated by the loss of Crym, which is normally expressed at high levels, likely facilitating the transport of T3 from the cytoplasm into the nucleus where it interacts with TR. Further studies are awaited to experimentally address these hypothetical T3-dependent mechanisms.

In summary, the present results indicate that the expression of the protein Crym in striatal neurons may be one of the important molecular determinants of the preferential vulnerability of the striatum in HD and further links HD pathogenesis with possible alterations of thyroid hormone-mediated regulation of transcription in the striatum.

MATERIALS and METHODS

Animals

Mice were housed in a temperature-controlled room maintained on a 12 hr light/dark cycle. Food and water were available ad libitum. All animal studies were conducted according to the French regulation (EU Directive 86/609 – French Act Rural Code R 214-87 to 131). The animal facility was approved by veterinarian inspectors (authorization n°A 92-032-02) and complies with Standards for Humane Care and Use of Laboratory Animals of the Office of Laboratory Animal Welfare (OLAW – n°#A5826-01). All procedures received approval from the ethical committee. Adult male C57BL/6J mice (25 g each; Charles River, Saint Germain sur l'Arbresle, France) were used for lentiviral infections and preparation of brain extracts for biochemical studies. For biochemical studies on endogenous Crym, brains of male Sprague-Dawleys rats (350g) were also used. We also had access to coronal brain slices from a control adult macaque fascicularis.

For the study of endogenous Crym mRNA levels in the context of HD, we used the transgenic mouse model of HD generated and maintained in the FvB inbred background, the BACHD mice, that express full-length human mHtt from its own regulatory elements on a 240-kb BAC, which contains the intact 170-kb human htt locus plus about 20 kb of 5′ flanking genomic sequence and 50 kb of 3′ (50). We used 6 month-old male BACHD mice for the present study, a time point where there is no detectable striatal atrophy (51).

We also studied 13 month-old knock-in mice expressing chimeric mouse/human exon 1 containing 140 CAG repeats inserted in the murine Htt gene (KI140) and their littermate controls. KI140 colony was maintained by breeding heterozygotes KI140 males and females (52). Mice were N3 (B6) on a 129 Sv×C57BL/6 J background. The resulting different genotypes were used for the present study. At this age homozygous and heterozygous KI140 mice showed no major striatal atrophy although these animals had motor deficits (Rotarod, CAtWalk, and open field) (data not shown).

Genotyping was determined from PCR of tail snips taken at 10–15 days of age for BACHD and KI140 mice.

Lentiviral vector construction, production and infection

DNA sequences coding for green fluorescent protein (GFP) and mouse Crym were cloned into the SIN-W-PGK lentiviral vector (LV) to generate LV-GFP and LV-Crym, respectively (40). The lentiviral vectors expressing a mHtt fragment (LV-Htt171 82Q) or beta-galactosidase (LV-LacZ) have been described previously (34, 37). Viral particles were produced as described elsewhere (53). The particle content of the viral batches was determined by ELISA for the p24 antigen (Gentaur, Paris, France). LV-Htt171-82Q was used at a concentration of 150 ng/µl of p24, LV-Crym and LV-LacZ at a concentration of 100 ng/µl of p24. In experiments performed for PCR analysis, LV-GFP was mixed with LV-Crym or LV-LacZ at a concentration of 50 ng/µl of p24. After being anesthetized (Ketamine/xylazine), mice received a total volume of 2 µl of lentiviral suspension into the mouse striatum as previously reported (37, 38), using the following stereotaxic coordinates: 1.0 mm anterior

and 2.0 mm lateral to the bregma, at a depth of 2.7 mm from the dura, with the tooth bar set at 0.0 mm.

Histological and cytological analyses

Animal studies. After deep anesthesia by intraperitoneal injection of a sodium pentobarbital solution (50 µg per gram of body weight), mice were transcardially perfused with 100 ml of phosphate buffer containing 4 % paraformaldehyde at 8 ml/min. The brains were removed, post-fixed overnight in the same solution, then cryoprotected by immersion in a 15 % sucrose solution for 24 hours followed by immersion in a 30 % sucrose solution for another 24 hours. Free-floating 40 µm-thick serial coronal sections throughout the striatum were collected using a freezing sliding microtome (SM2400; Leica Microsystems, Wetzlar, Germany).

Immunohistochemistry. For immunohistochemistry, sections were treated with 0.3 % hydrogen peroxide for 20 minutes, washed three times in phosphate-buffered saline (PBS), blocked in PBS containing 4.5 % normal goat serum for one hour, then incubated 48 hours at 4°C in PBS containing 3 % normal goat serum and one of the following antibodies: rabbit anti-DARPP 32 (Santa Cruz Biotechnology, Santa Cruz, CA; 1:1000), mouse anti-NeuN (Millipore, Molsheim, France; 1:1000), mouse anti-Em48 (Chemicon, MAB5374, Temecula, CA; 1:1000),rabbit anti-Ubiquitin (Wako Chemicals, Neuss, Germany; 1:1000), or mouse anti-HA (Covance, Princeton, NJ; 1:1000). Sections were rinsed three times in PBS before incubation with the appropriate anti-IgG biotinylated antibody (Vector Laboratories, Burlingame, CA) at a 1:1000 dilution for one hour. Staining was visualized by the addition of avidin-biotinylated peroxidase and incubation with DAB substrate (Vector Laboratories, Burlingame, CA) for 30 seconds to one minute. Stained sections were mounted on microscopic slides.

Quantitative histological evaluation. The area of the striatal lesions resulting from LV-Htt171-82Q infection was delineated manually by identifying the border of the lesion (loss of DARPP-32 and NeuN immunolabelling). Lesion area was delineated using 5x and 10x objectives. Depending on the antero-posterior extension of the lesions, 3 to 8 coronal sections were analyzed for each mouse. Observation of sections and calculation of the surface of lesioned area were performed using a Leica DM6000 equipped with a motorized stage and an automated image acquisition and analysis system (Mercator software, Explora Nova, La Rochelle, France). The volume of the striatal lesion (V) was determined using the Cavalieri method (34, 36, 38). The number of Ubiquitin-positive inclusions was quantified as previously described (34, 36, 38) with the following modifications: the inter-section distance was 320 µm (i.e. one in every seven sections was used) and observations were performed using a 10X objective on an Axioplan 2 Imaging microscope (Carl Zeiss, Le Pecq, France) equipped with a motorized stage and an automated image acquisition and analysis system (Mercator software, Explora Nova). With this set-up, objects with an apparent cross-sectional area > 3 μm^2 (i.e. diameter > ~1 µm) could be reliably detected.

Real-time quantitative PCR

Adult mice were deeply anesthetized by intraperitoneal injection of a sodium pentobarbital solution (50 µg per gram of body weight) before decapitation. The brains were immediately removed and positioned in a coronal brain matrix (Ted Pella, Redding, CA).

For the quantification of overexpressed Crym mRNA levels, mice were infected with a mixture of LV-Crym-HA and LV-GFP. Injection of LV-LacZ was used as controls for viral load. The striatal region displaying fluorescence was dissected out using a circular punch (1.5 mm diameter) from 1 mm-thick fresh coronal brain sections visualized under a fluorescence binocular (Leica). Total RNA extraction and real-time quantitative RT-PCR (qRT-PCR) were performed as previously described (38, 54), using the following primer sequences for Crym mRNA Crym-U CTATGAGGGCCACAGCAACA and Crym-L ATGACCGCCAGCAGGGAG. Primers recognized sequence in mouse (endogenous) Crym and recombinant Crym-HA after viral infection.

Cell studies

The primary culture of striatal neurons has been performed as previously described (21). These neurons were electroporated with the mouse striatal neuron Nucleofector® kit according to the supplier's manual (Amaxa, Biosystem, Köln, Germany) for detection of a chimeric eGFP-Crym construct.

Human embryonic kidney 293 T (HEK293T) cells were grown at 37°C in 5% CO2 in Dulbeco's modified Eagle's medium (DMEM) supplemented with 10% bovine calf serum, 1% L-glutamine and antibiotics (50 units/ml penicillin and 50 µg/ml streptomycin). For the study of recombinant Crym, cultured cells were seeded on glass coverslips, and transfected with recombinant Crym-HA vector or equivalent amount of empty vector for HEK293T cells, and 48 h later fixed with cold-ice methanol and EGTA. Cells were rinsed with TBST, and blocked with 2% BSA, 0.1% Tween-20 in TBS. Primary polyclonal antibody rabbit anti-HA (H6908, Sigma, St Louis, MO, USA; 1:800) was used at 2 µg/ml in 2% BSA, 0.1% Triton X-100, 0.1% azide in PBS and incubated for 1 h at room temperature. Similar attempt to detect native recombinant Crym protein using the affinity purified IgY chicken anti-Crym (Michel – see below for western blot) were also used unsuccessfully. Cells were washed with 0.05% Tween-20 in PBS and incubated with the appropriate fluorescent secondary antibody for 1 h. Nuclei were counterstained with Hoechst (DAPI). Coverslips were mounted in FluorSafe and examined with a Leika microscope fitted with the appropriate fluorescence filters, Retiga camera and Morphostrider imaging software prior to analysis in Confocal Zeiss LSM for eGFP-Crym in primary cultures and the SPE TCS Leica confocal with Leica LAS AF interface for the HEK experiments.

Biochemical analysis

Cell preparation. Cells were harvested 48h after transfection and lyzed in modified RIPA buffer : 50mM Tris pH8.0, 50 mM NaCl, 1 mM EDTA, 0.5% Triton-X100, 1% NP40 and protease inhibitor cocktail (Roche). Cell lysates were centrifuged at 15,000 g for 20 min at 4°C.

Brain tissue preparation. Mice and rats were euthanized by rapid decapitation and brains were removed, blocked and cut into 1-mm-thick coronal slices using brain matrices (Ted Pella, Redding, CA). On one coronal slice (+1mm from bregma), tissue punches were taken from the striatum using a

tissue corer (1.5-mm in diameter) and the cerebral cortex was dissected out using scalpel blades under binoculars.

Cortical and striatal (caudate and putamen) tissue samples were prepared from a control non-human primate (macaca fascicularis, #2055, male ~7years old). Briefly, the animal received a lethal dose of pentobarbital, brain was rapidly removed from the skull and cut into 5 mm-thick coronal slabs. Slabs were put on ice-cooled Petri dish and the pre-commisural putamen, caudate, and a piece of cerebral cortex (grey matter ribbon) in the somato-sensori cortex were dissected out using a scalpel blade.

For determination of total level of Crym expression in brain tissue, punches were lysed in 50 mM Tris pH8, 150 mM NaCl, 1 mM EDTA, 0.5% Triton X-100, and 1% NP40, with protease inhibitor cocktail (Complete, Roche) and phosphatase inhibitor cocktail 2 (Sigma) using glass/glass pestle potters.

Differential centrifugation experiments were performed to determine the cytosolic levels of Crym in comparison with cell membranes, tissue punches were homogenized in solution A containing 50 mM Tris pH 7.4, 100 mM NaCl, 0.25 M sucrose with protease inhibitor cocktail (Complete, Roche) using a Teflon pestle and Thomas potter. After 10 min centrifugation at 10,000 g, the supernatant S2 was collected and centrifuged at 135,000 g, 30 min 4°C. The corresponding supernatant (S_0) contained the cytosolic fraction, which was mixed in Laemli. The pellet P2 (containing membranes) was re-suspended to further remove cytosolic contaminants, placed on a 1.7 M sucrose cushion and centrifuged at 135,000g for 30 min at 4°C. The material (membranes) blocked at the 0.25 /1.7 M sucrose interface was collected and re-suspended in solution A, then centrifuged again 30 min at 135,000g, 4°C to remove sucrose; Pellet was re-suspended in Laemli before electrophoresis.

Western blotting. Total protein concentrations were determined using the BCA kit (Pierce). Equal amounts of total protein extract were subjected to SDS-PAGE in 4%-12% Bis-tris gels (NuPAGE® Novex Bis-tris midi gel 15wells, Invitrogen) and transferred to nitrocellulose membranes. Blocked membranes (5% milk in TBS-0.1% Tween-20) were incubated with primary antibodies : Crystalline μ [1:500, chicken IgY directed against AVGASRPDWRELDDE and affinity purified (AgroBio)], actin (1:2000, mouse, Sigma), hemagglutinin (HA) (1:3000, mouse, Covance), Dopamine- and cAMP-regulated PhosphoProtein 32 kDa (DARPP-32, 1:3000, rabbit, Cell Signaling), α-tubulin (1:3000, mouse, Sigma); and washed three times with TBS-0.1% Tween-20 (TBST) for 10 min. Membranes were then labelled with secondary IgG-HRP antibodies raised against each corresponding primary antibody. After three washes with TBST, the membranes were incubated with ECL chimioluminescent reagent (Clarity Western ECL substrate; Biorad or Immun-Star WesternC kit, BioRad) according to the instructions of the supplier. Peroxydase activity was detected with camera system Fusion TX7 (Fisher scientific). Normalization was done by densitometry analysis with Bio1D software.

FIGURE LEGENDS

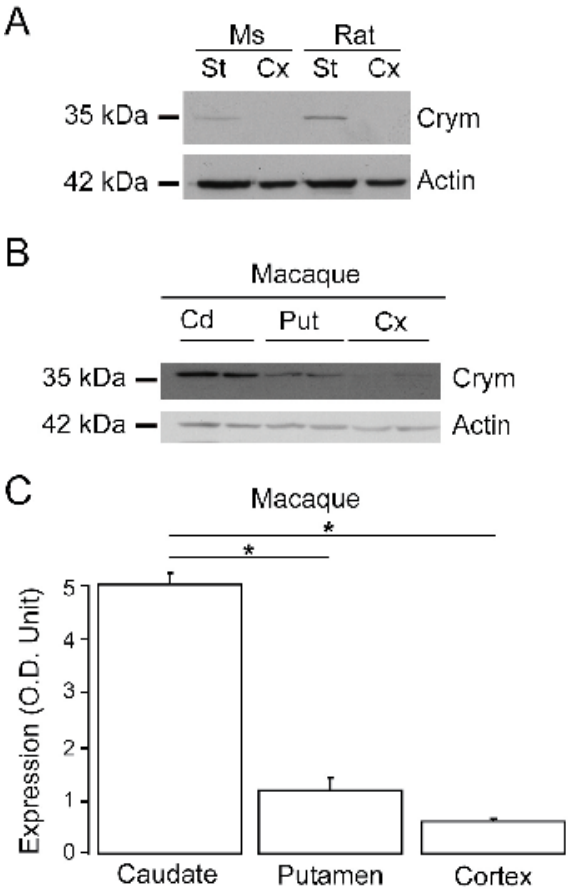

Figure 1. Western blot analysis of the expression of Crym protein in the mammalian brain. Representative western blots of total protein extracts prepared from adult mouse (Ms) and rat striatum (St) and cerebral cortex (Cx) (parietal) (**A**) and from macaque caudate (Cd), putamen (Put) and cerebral cortex (motor cortex) (**B**). **C,** semi-quantitative analysis of western blots of macaque brain extracts indicating preferential expression of Crym in caudate and putamen as compared with cerebral cortex.

*, $p<0.006$, One-way ANOVA ($p<0.01$) and *post hoc* Bonferroni test.

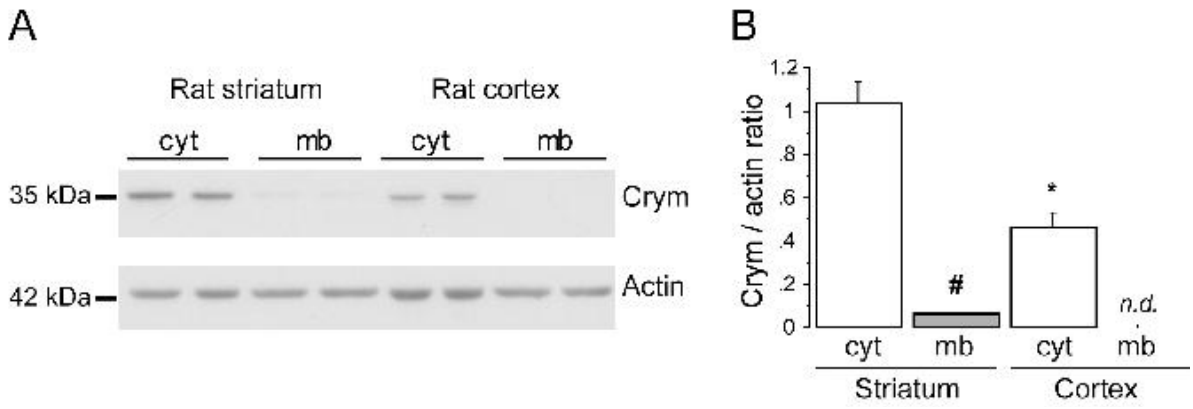

Figure 2. Cytosolic localization of Crym in neurons.

Western blot analysis of the cytosolic (cyt) and membrane (mb) fractions after differential centrifugation of homogenates prepared from the rat striatum and cerebral cortex (parietal). **A**, representative western blot. **B**, quantitative analysis of western blots. Results are expressed as mean +/- standard error of the mean.

#, $p<0.004$; *, $p<0.003$; One way ANOVA ($p<0.001$) and *post hoc* Bonferroni test.

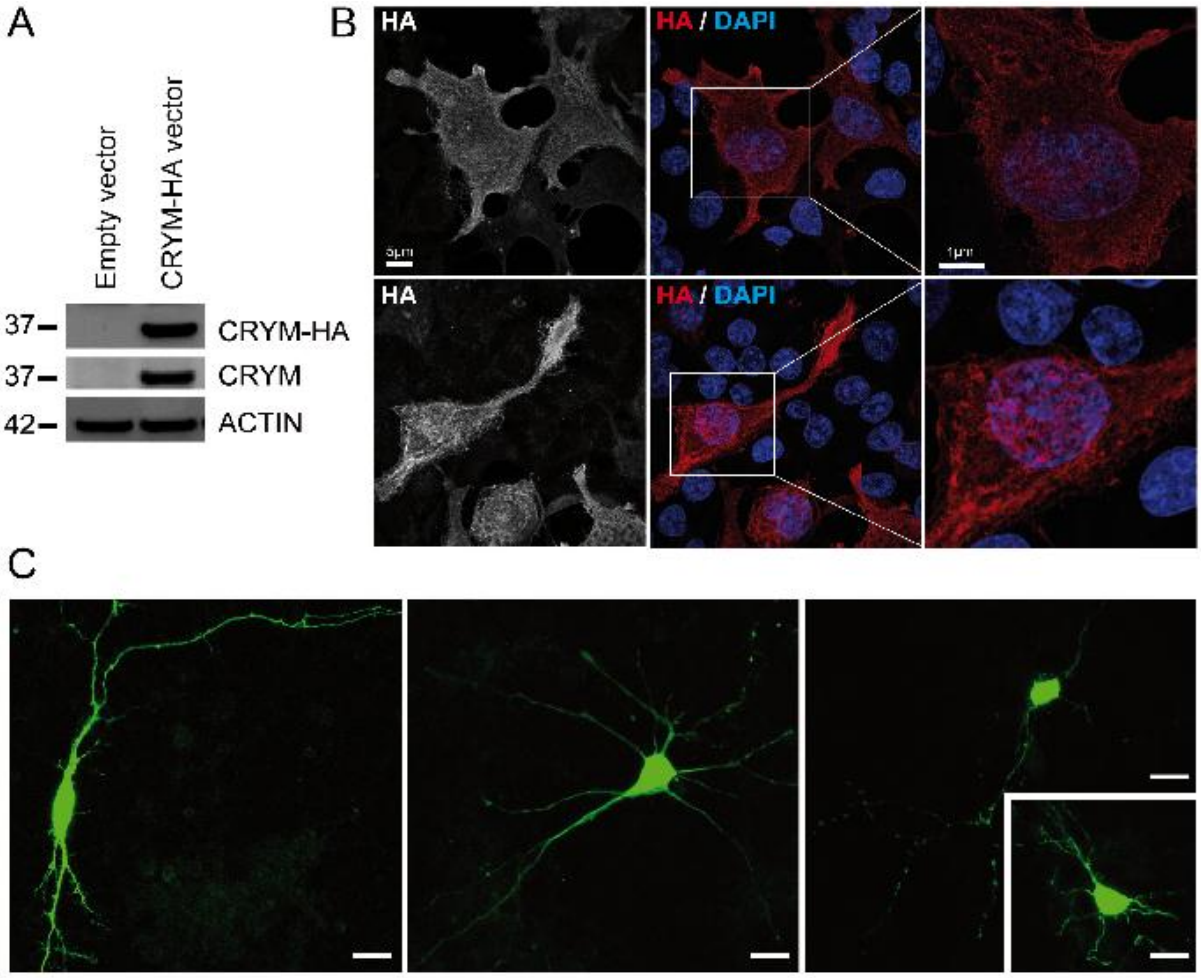

Figure 3. Recombinant Crym in cultured cells.

HEK293T cells were transfected with a Crym-HA vector (A, B). Neurons were transfected with eGFP-Crym construct. **A**, western blot showing the detection of recombinant Crym-HA protein as a single band using either an anti-HA or an anti-Crym antibody. **B**, immunofluorescence detection of Crym-HA in HEK293T cells. **C**, expression of the eGFP-Crym protein in striatal neurons in primary culture. Images were obtained using confocal microscopy. Scale bars, 5 and 1 µm in left and right image respectively; 10 µm in C.

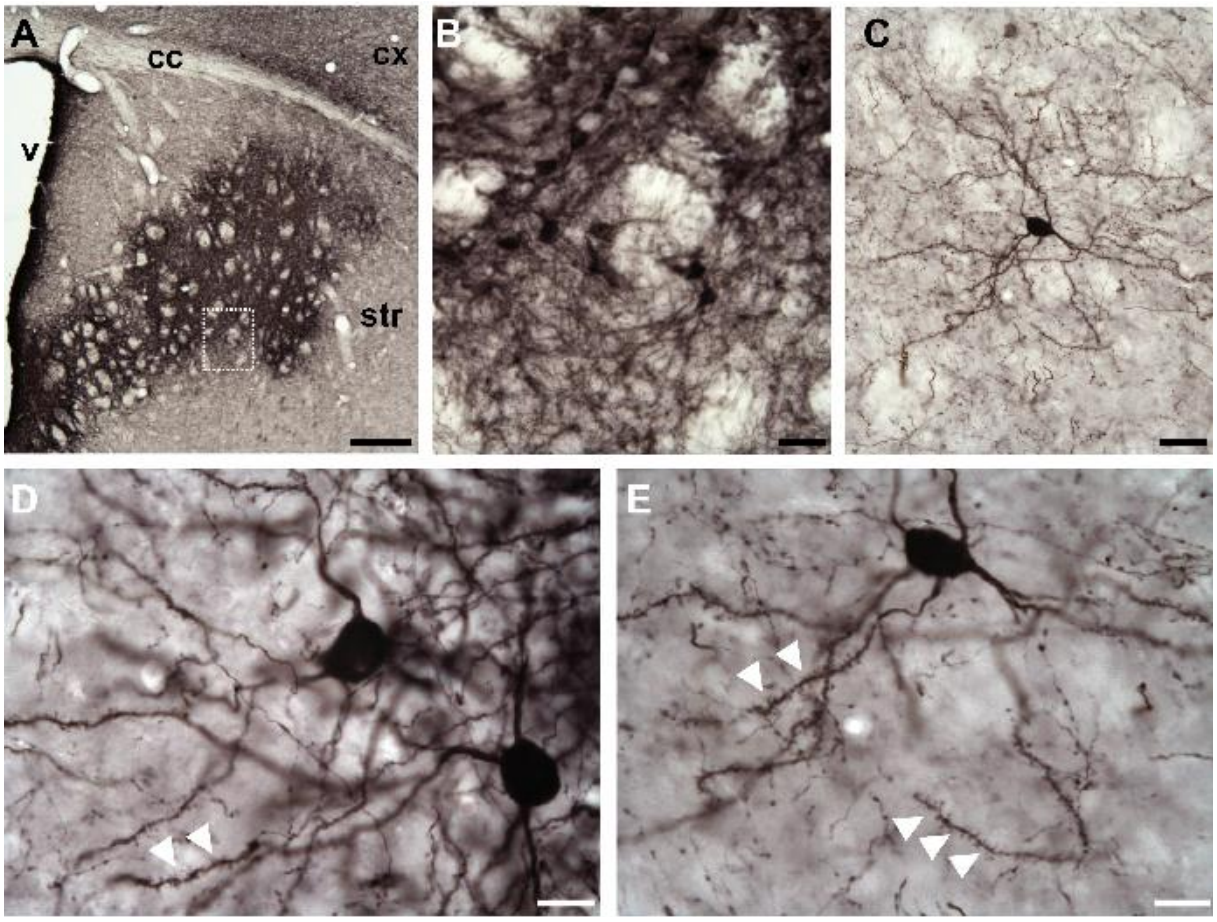

Figure 4. Recombinant Crym-HA expression in neurons after lentiviral infection of the mouse striatum.

Photomicrographs showing the expression of Crym-HA 6 weeks after intrastriatal injection of LV-Crym-HA as revealed using anti-HA immunohistochemistry. **A**, low power magnification showing the expression in the anterior striatum. **B**, higher magnification showing densely labelled /compact neurons expressing Crym-HA. **C-E**, typical isolated striatal neurons expressing Crym-HA at distance from the core of the infection showing typical medium size spiny neurons morphology. Note in D and E the dense labelling in the entire soma, and the presence of immuno-positive dendritic spines (white arrowheads). Scale bars: 200 µm in A, 20 µm in B and C, 10 µm in D and E.

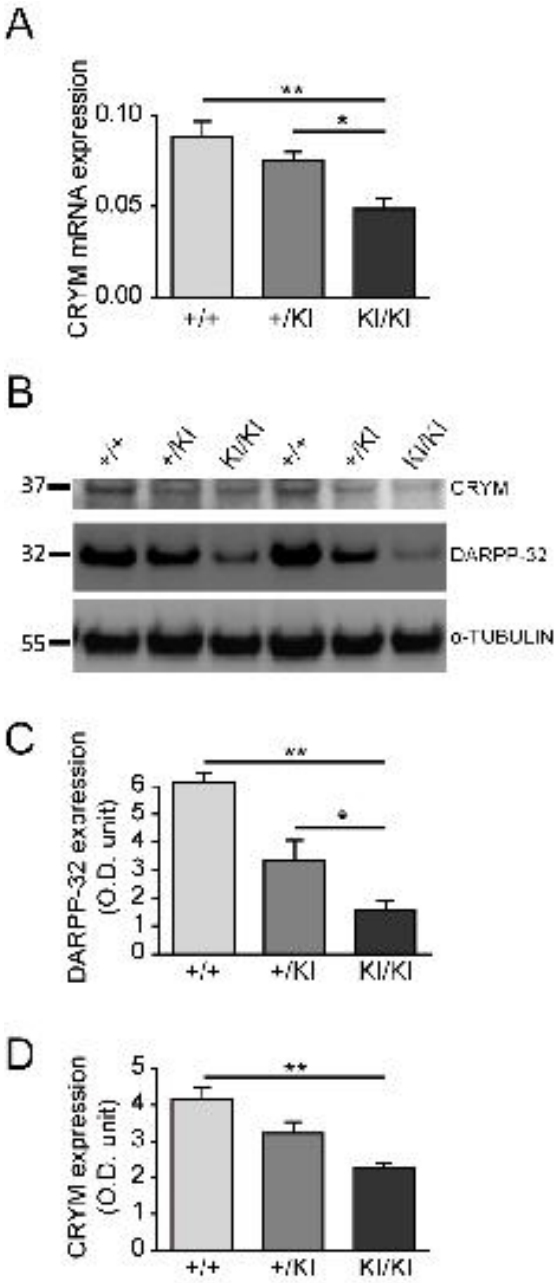

Figure 5. Crym expression in the KI140CAG mouse model of HD.

Endogenous Crym expression was characterized by qRT-PCR (A) in the striatum and by western blot (B, C and D) in the striatum and cerebral cortex of knock in heterozygous (+/KI) and homozygous (KI/KI) 140CAG mice and wild type littermates (+/+). Results are expressed as mean +/- standard error of the mean (n=3-8).

*, $p<0.05$; **$p<0.01$, one-way ANOVA, and *post hoc* Bonferroni test.

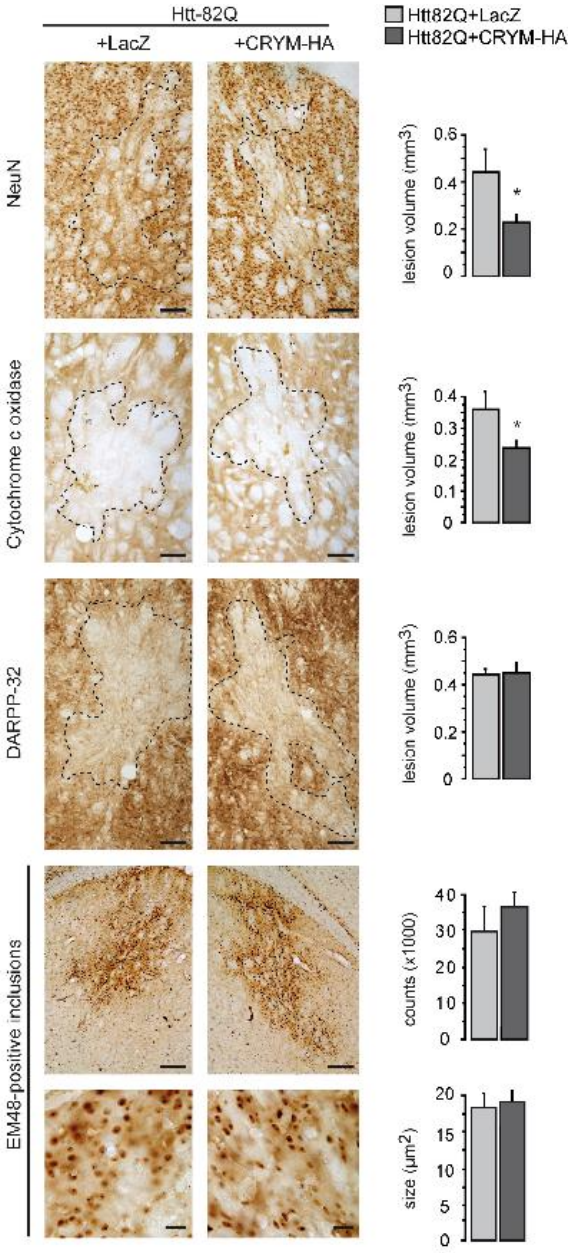

Figure 6. Effects of Crym-HA overexpression in the striatum on the neurotoxicity of an N-terminal fragment of mHtt.

Adult male mice received a bilateral intrastriatal injection of LV-Htt171-82Q mixed with either LV-LacZ (control) or a lentiviral vector coding for Crym-HA (LV-Crym-HA). Six weeks after infection, brains were processed for histological evaluation using NeuN, DARPP-32 and Cytochrome oxidase (COX) histochemistry to assess the mHtt171-82Q toxicity. Left panel: typical coronal mouse brain sections where areas with depleted staining are delineated. Right panel: histograms representing quantitative determination of the volume of the striatum with depleted staining in the different groups and the number of ubiquitin-positive inclusions. Results are expressed as mean (n=7-10/group) +/- standard error of the mean. Scale bars: Neun, Cox, DARPP32, 100µm; EM48 upper images, 200µm; EM48 lower images, 20 µm.

*, $p<0.05$, unpaired Student *t* test.

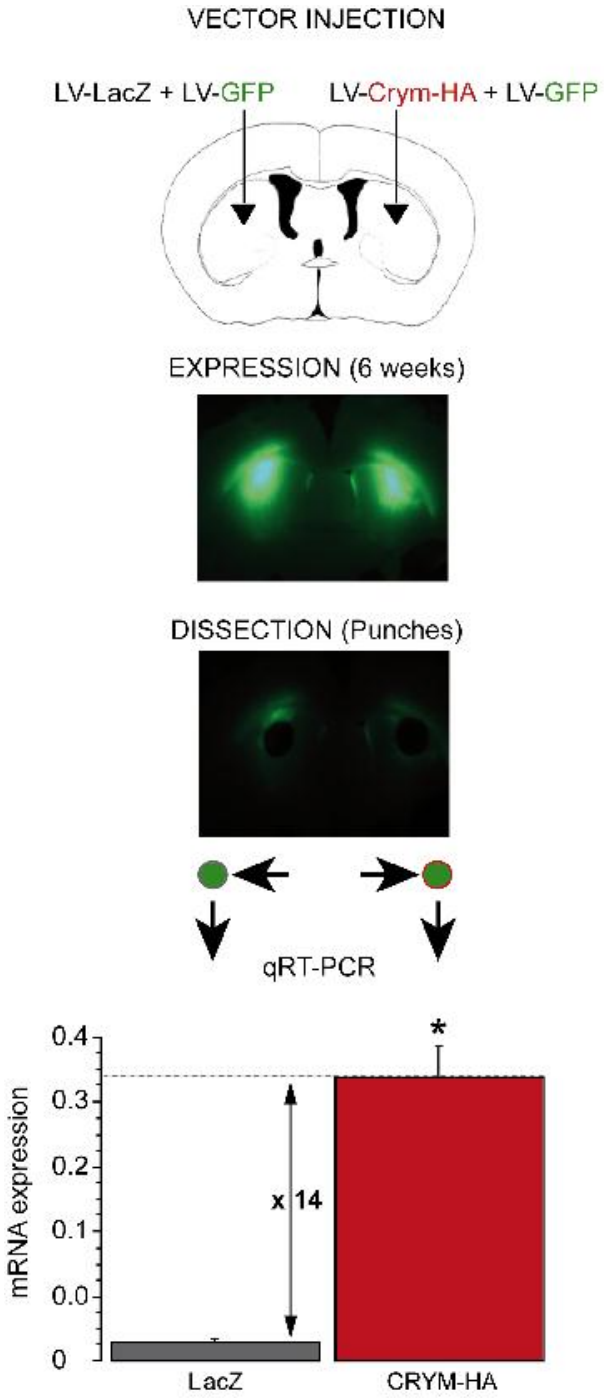

Figure 1S. Overexpression of Crym-HA in the striatum using lentiviral vectors. A mixture of a lenti-viral vector encoding Crym-HA (LV-Crym-HA) mixed with a vector encoding GFP was stereotaxically injected into the striatum of adult mice. At 6 weeks post-surgery, fluorescent striatal tissue was dissected out for mRNA extraction and qRT-PCR analysis. Results are expressed as mean +/- standard error of the mean, (n=4 per group). *, $p<0.002$, unpaired Student *t* test.

ACKNOWLEDGEMENTS

We thank Dr William Yang for his help to set up the BACHD mice colony. We are also grateful to Scott Zeitlin and Sandrine Humbert for their help to start the KI140CAG mice colony. This work was supported by the “Commissariat à l’Energie Atomique et aux Energies Alternatives” (CEA) and “Centre National de la Recherche Scientifique” (CNRS). LG was supported by the Neuropôle de Recherche Francilien and the Fondation pour la Recherche Médicale. LF was supported by the French Research Ministry. The research leading to these results has received funding from the European Community's Seventh Framework Program FP7/2007-2013 under grant agreement no. HEALTH-F5-2008-222925. We also received financial support from the IMAGEN European integrated project (EUR617037286).

POTENTIAL CONFLICTS OF INTEREST

The authors of the present manuscript declare to have no Conflict of Interest.

References

1 Wistow, G. and Kim, H. (1991) Lens protein expression in mammals: taxon-specificity and the recruitment of crystallins. *J Mol Evol*, **32**, 262-269.

2 Vie, M. P., Evrard, C., Osty, J., Breton-Gilet, A., Blanchet, P., Pomerance, M., Rouget, P., Francon, J. and Blondeau, J. P. (1997) Purification, molecular cloning, and functional expression of the human nicodinamide-adenine dinucleotide phosphate-regulated thyroid hormone-binding protein. *Mol Endocrinol*, **11**, 1728-1736.

3 Ortiga-Carvalho, T. M., Sidhaye, A. R. and Wondisford, F. E. (2014) Thyroid hormone receptors and resistance to thyroid hormone disorders. *Nature reviews. Endocrinology*, 10.1038/nrendo.2014.143.

4 Suzuki, S., Suzuki, N., Mori, J., Oshima, A., Usami, S. and Hashizume, K. (2007) micro-Crystallin as an intracellular 3,5,3'-triiodothyronine holder in vivo. *Mol Endocrinol*, **21**, 885-894.

5 Umeda, S., Suzuki, M. T., Okamoto, H., Ono, F., Mizota, A., Terao, K., Yoshikawa, Y., Tanaka, Y. and Iwata, T. (2005) Molecular composition of drusen and possible involvement of anti-retinal autoimmunity in two different forms of macular degeneration in cynomolgus monkey (Macaca fascicularis). *FASEB journal : official publication of the Federation of American Societies for Experimental Biology*, **19**, 1683-1685.

6 Abe, S., Katagiri, T., Saito-Hisaminato, A., Usami, S., Inoue, Y., Tsunoda, T. and Nakamura, Y. (2003) Identification of CRYM as a candidate responsible for nonsyndromic deafness, through cDNA microarray analysis of human cochlear and vestibular tissues. *Am J Hum Genet*, **72**, 73-82.

7 Oshima, A., Suzuki, S., Takumi, Y., Hashizume, K., Abe, S. and Usami, S. (2006) CRYM mutations cause deafness through thyroid hormone binding properties in the fibrocytes of the cochlea. *Journal of medical genetics*, **43**, e25.

8 Daoud, H., Valdmanis, P. N., Gros-Louis, F., Belzil, V., Spiegelman, D., Henrion, E., Diallo, O., Desjarlais, A., Gauthier, J., Camu, W. *et al.* (2011) Resequencing of 29 candidate genes in patients with familial and sporadic amyotrophic lateral sclerosis. *Archives of neurology*, **68**, 587-593.

9 Fukada, Y., Yasui, K., Kitayama, M., Doi, K., Nakano, T., Watanabe, Y. and Nakashima, K. (2007) Gene expression analysis of the murine model of amyotrophic lateral sclerosis: studies of the Leu126delTT mutation in SOD1. *Brain research*, **1160**, 1-10.

10 Hallen, A., Cooper, A. J., Jamie, J. F., Haynes, P. A. and Willows, R. D. (2011) Mammalian forebrain ketimine reductase identified as mu-crystallin; potential regulation by thyroid hormones. *J Neurochem*, **118**, 379-387.

11 Brochier, C., Gaillard, M. C., Diguet, E., Caudy, N., Dossat, C., Segurens, B., Wincker, P., Roze, E., Caboche, J., Hantraye, P. *et al.* (2008) Quantitative gene expression profiling of mouse brain regions reveals differential transcripts conserved in human and affected in disease models. *Physiological genomics*, **33**, 170-179.

12 de Chaldee, M., Gaillard, M. C., Bizat, N., Buhler, J. M., Manzoni, O., Bockaert, J., Hantraye, P., Brouillet, E. and Elalouf, J. M. (2003) Quantitative assessment of transcriptome differences between brain territories. *Genome Res*, **13**, 1646-1653.

13 Walker, F. O. (2007) Huntington's disease. *Lancet*, **369**, 218-228.

14 The-Huntington's-Disease-Collaborative-Research-Group. (1993) A novel gene containing a trinucleotide repeat that is expanded and unstable on Huntington's disease chromosomes. The Huntington's Disease Collaborative Research Group. *Cell*, **72**, 971-983.

15 Zuccato, C. and Cattaneo, E. (2014) Huntington's Disease. *Handbook of experimental pharmacology*, **220**, 357-409.

16 Damiano, M., Galvan, L., Deglon, N. and Brouillet, E. (2010) Mitochondria in Huntington's disease. *Biochim Biophys Acta*, **1802**, 52-61.

17 Fan, M. M. and Raymond, L. A. (2007) N-methyl-D-aspartate (NMDA) receptor function and excitotoxicity in Huntington's disease. *Prog Neurobiol*, **81**, 272-293.

18 Hinckelmann, M. V., Zala, D. and Saudou, F. (2013) Releasing the brake: restoring fast axonal transport in neurodegenerative disorders. *Trends in cell biology*, **23**, 634-643.

19 Roze, E., Saudou, F. and Caboche, J. (2008) Pathophysiology of Huntington's disease: from huntingtin functions to potential treatments. *Current opinion in neurology*, **21**, 497-503.

20 Francelle, L., Galvan, L. and Brouillet, E. (2014) Possible involvement of self-defense mechanisms in the preferential vulnerability of the striatum in Huntington's disease. *Frontiers in Cellular Neuroscience*, **8 (295)**, 1-13.

21 Benchoua, A., Trioulier, Y., Diguet, E., Malgorn, C., Gaillard, M. C., Dufour, N., Elalouf, J. M., Krajewski, S., Hantraye, P., Deglon, N. *et al.* (2008) Dopamine determines the vulnerability of striatal neurons to the N-terminal fragment of mutant huntingtin through the regulation of mitochondrial complex II. *Hum Mol Genet*, **17**, 1446-1456.

22 Charvin, D., Roze, E., Perrin, V., Deyts, C., Betuing, S., Pages, C., Regulier, E., Luthi-Carter, R., Brouillet, E., Deglon, N. *et al.* (2008) Haloperidol protects striatal neurons from dysfunction induced by mutated huntingtin in vivo. *Neurobiology of disease*, **29**, 22-29.

23 Charvin, D., Vanhoutte, P., Pages, C., Borrelli, E. and Caboche, J. (2005) Unraveling a role for dopamine in Huntington's disease: the dual role of reactive oxygen species and D2 receptor stimulation. *Proc Natl Acad Sci U S A*, **102**, 12218-12223.

24 Subramaniam, S., Sixt, K. M., Barrow, R. and Snyder, S. H. (2009) Rhes, a striatal specific protein, mediates mutant-huntingtin cytotoxicity. *Science (New York, N.Y*, **324**, 1327-1330.

25 Seredenina, T., Gokce, O. and Luthi-Carter, R. (2011) Decreased striatal RGS2 expression is neuroprotective in Huntington's disease (HD) and exemplifies a compensatory aspect of HD-induced gene regulation. *PLoS One*, **6**, e22231.

26 Blum, D., Hourez, R., Galas, M. C., Popoli, P. and Schiffmann, S. N. (2003) Adenosine receptors and Huntington's disease: implications for pathogenesis and therapeutics. *Lancet Neurol*, **2**, 366-374.

27 Mievis, S., Blum, D. and Ledent, C. (2011) Worsening of Huntington disease phenotype in CB1 receptor knockout mice. *Neurobiology of disease*, **42**, 524-529.

28 Chiarlone, A., Bellocchio, L., Blazquez, C., Resel, E., Soria-Gomez, E., Cannich, A., Ferrero, J. J., Sagredo, O., Benito, C., Romero, J. *et al.* (2014) A restricted population of CB1 cannabinoid receptors with neuroprotective activity. *Proc Natl Acad Sci U S A*, **111**, 8257-8262.

29 Roze, E., Betuing, S., Deyts, C., Marcon, E., Brami-Cherrier, K., Pages, C., Humbert, S., Merienne, K. and Caboche, J. (2008) Mitogen- and stress-activated protein kinase-1 deficiency is involved in expanded-huntingtin-induced transcriptional dysregulation and striatal death. *FASEB journal : official publication of the Federation of American Societies for Experimental Biology*, **22**, 1083-1093.

30 Martin, E., Betuing, S., Pages, C., Cambon, K., Auregan, G., Deglon, N., Roze, E. and Caboche, J. (2011) Mitogen- and stress-activated protein kinase 1-induced neuroprotection in Huntington's disease: role on chromatin remodeling at the PGC-1-alpha promoter. *Hum Mol Genet*, **20**, 2422-2434.

31 Hodges, A., Strand, A. D., Aragaki, A. K., Kuhn, A., Sengstag, T., Hughes, G., Elliston, L. A., Hartog, C., Goldstein, D. R., Thu, D. *et al.* (2006) Regional and cellular gene expression changes in human Huntington's disease brain. *Hum Mol Genet*, **15**, 965-977.

32 Kuhn, A., Goldstein, D. R., Hodges, A., Strand, A. D., Sengstag, T., Kooperberg, C., Becanovic, K., Pouladi, M. A., Sathasivam, K., Cha, J. H. *et al.* (2007) Mutant huntingtin's effects on striatal gene expression in mice recapitulate changes observed in human Huntington's disease brain and do not differ with mutant huntingtin length or wild-type huntingtin dosage. *Hum Mol Genet*, **16**, 1845-1861.

33 Ruiz, M. and Deglon, N. (2012) Viral-mediated overexpression of mutant huntingtin to model HD in various species. *Neurobiology of disease*, **48**, 202-211.

34 Diguet, E., Petit, F., Escartin, C., Cambon, K., Bizat, N., Dufour, N., Hantraye, P., Deglon, N. and Brouillet, E. (2009) Normal aging modulates the neurotoxicity of mutant huntingtin. *PLoS ONE*, **4**, e4637.

35 Regulier, E., Pereira de Almeida, L., Sommer, B., Aebischer, P. and Deglon, N. (2002) Dose-dependent neuroprotective effect of ciliary neurotrophic factor delivered via tetracycline-regulated lentiviral vectors in the quinolinic acid rat model of Huntington's disease. *Hum Gene Ther*, **13**, 1981-1990.

36 Damiano, M., Diguet, E., Malgorn, C., D'Aurelio, M., Galvan, L., Petit, F., Benhaim, L., Guillermier, M., Houitte, D., Dufour, N. *et al.* (2013) A role of mitochondrial complex II defects in genetic models of Huntington's disease expressing N-terminal fragments of mutant huntingtin. *Hum Mol Genet*, **22**, 3869-3882.

37 Faideau, M., Kim, J., Cormier, K., Gilmore, R., Welch, M., Auregan, G., Dufour, N., Guillermier, M., Brouillet, E., Hantraye, P. *et al.* (2010) In vivo expression of polyglutamine-expanded huntingtin by mouse striatal astrocytes impairs glutamate transport: a correlation with Huntington's disease subjects. *Hum Mol Genet*, **19**, 3053-3067.

38 Galvan, L., Lepejova, N., Gaillard, M. C., Malgorn, C., Guillermier, M., Houitte, D., Bonvento, G., Petit, F., Dufour, N., Hery, P. *et al.* (2012) Capucin does not modify the toxicity of a mutant Huntingtin fragment in vivo. *Neurobiology of aging*, **33**, 1845 e1845-1846.

39 Desplats, P. A., Kass, K. E., Gilmartin, T., Stanwood, G. D., Woodward, E. L., Head, S. R., Sutcliffe, J. G. and Thomas, E. A. (2006) Selective deficits in the expression of striatal-enriched mRNAs in Huntington's disease. *J Neurochem*, **96**, 743-757.

40 de Almeida, L. P., Ross, C. A., Zala, D., Aebischer, P. and Deglon, N. (2002) Lentiviral-mediated delivery of mutant huntingtin in the striatum of rats induces a selective neuropathology modulated by polyglutamine repeat size, huntingtin expression levels, and protein length. *The Journal of neuroscience : the official journal of the Society for Neuroscience*, **22**, 3473-3483.

41 Arango, M., Holbert, S., Zala, D., Brouillet, E., Pearson, J., Regulier, E., Thakur, A. K., Aebischer, P., Wetzel, R., Deglon, N. *et al.* (2006) CA150 expression delays striatal cell death in overexpression and knock-in conditions for mutant huntingtin neurotoxicity. *J Neurosci*, **26**, 4649-4659.

42 Perrin, V., Regulier, E., Abbas-Terki, T., Hassig, R., Brouillet, E., Aebischer, P., Luthi-Carter, R. and Deglon, N. (2007) Neuroprotection by Hsp104 and Hsp27 in lentiviral-based rat models of Huntington's disease. *Molecular therapy : the journal of the American Society of Gene Therapy*, **15**, 903-911.

43 Perrin, V., Dufour, N., Raoul, C., Hassig, R., Brouillet, E., Aebischer, P., Luthi-Carter, R. and Deglon, N. (2009) Implication of the JNK pathway in a rat model of Huntington's disease. *Experimental neurology*, **215**, 191-200.

44 Desplats, P. A., Lambert, J. R. and Thomas, E. A. (2008) Functional roles for the striatal-enriched transcription factor, Bcl11b, in the control of striatal gene expression and transcriptional dysregulation in Huntington's disease. *Neurobiology of disease*, **31**, 298-308.

45 Seredenina, T. and Luthi-Carter, R. (2012) What have we learned from gene expression profiles in Huntington's disease? *Neurobiology of disease*, **45**, 83-98.

46 Zhang, C. Y., Kim, S., Harney, J. W. and Larsen, P. R. (1998) Further characterization of thyroid hormone response elements in the human type 1 iodothyronine deiodinase gene. *Endocrinology*, **139**, 1156-1163.

47 Aziz, N. A., Pijl, H., Frolich, M., Roelfsema, F. and Roos, R. A. (2010) Altered thyrotropic and lactotropic axes regulation in Huntington's disease. *Clinical endocrinology*, **73**, 540-545.

48 Saleh, N., Moutereau, S., Durr, A., Krystkowiak, P., Azulay, J. P., Tranchant, C., Broussolle, E., Morin, F., Bachoud-Levi, A. C. and Maison, P. (2009) Neuroendocrine disturbances in Huntington's disease. *PLoS One*, **4**, e4962.

49 Yohrling, G. J., Farrell, L. A., Hollenberg, A. N. and Cha, J. H. (2003) Mutant huntingtin increases nuclear corepressor function and enhances ligand-dependent nuclear hormone receptor activation. *Molecular and cellular neurosciences*, **23**, 28-38.

50 Gray, M., Shirasaki, D. I., Cepeda, C., Andre, V. M., Wilburn, B., Lu, X. H., Tao, J., Yamazaki, I., Li, S. H., Sun, Y. E. *et al.* (2008) Full-length human mutant huntingtin with a stable polyglutamine repeat can elicit progressive and selective neuropathogenesis in BACHD mice. *J Neurosci*, **28**, 6182-6195.

51 Boussicault, L., Herard, A. S., Calingasan, N., Petit, F., Malgorn, C., Merienne, N., Jan, C., Gaillard, M. C., Lerchundi, R., Barros, L. F. *et al.* (2014) Impaired brain energy metabolism in the BACHD mouse model of Huntington's disease: critical role of astrocyte-neuron interactions. *J Cereb Blood Flow Metab*, **34**, 1500-1510.

52 Menalled, L. B., Sison, J. D., Dragatsis, I., Zeitlin, S. and Chesselet, M. F. (2003) Time course of early motor and neuropathological anomalies in a knock-in mouse model of Huntington's disease with 140 CAG repeats. *The Journal of comparative neurology*, **465**, 11-26.

53 Hottinger, A. F., Azzouz, M., Deglon, N., Aebischer, P. and Zurn, A. D. (2000) Complete and long-term rescue of lesioned adult motoneurons by lentiviral-mediated expression of glial cell line-derived neurotrophic factor in the facial nucleus. *J Neurosci*, **20**, 5587-5593.

54 Drouet, V., Perrin, V., Hassig, R., Dufour, N., Auregan, G., Alves, S., Bonvento, G., Brouillet, E., Luthi-Carter, R., Hantraye, P. *et al.* (2009) Sustained effects of nonallele-specific Huntingtin silencing. *Annals of neurology*, **65**, 276-285.

3.3. Article #3

Role of Doublecortin-like kinase 3 (DCLK3) in the preferential vulnerability of the striatum in Huntington's disease (draft).

Role of Doublecortin-like kinase 3 (Dclk3) in the preferential vulnerability of the striatum in Huntington's disease

Laurie Galvan[1,2*], Laetitia Francelle[1,2*], Marie-Claude Gaillard[1,2], Julien Flament[1], Julien Valette[1,2], Géraldine Liot[4,5,6], Michel de Chaldée[3], Alex Fayel[1,2], Martine Guillermier[1,2], Gwenaëlle Auregan[1,2], Gilles Bonvento[1,2], Carole Malgorn[1,2], Fanny Petit[1,2], Caroline Jan[1,2], Pauline Gipchtein[1,2], Noëlle Dufour[1,2], Jean-Marc Elalouf[3], Sandrine Humbert[4,5,6], Alexis Bemelmans[1,2], Philippe Hantraye[1,2], Frédéric Saudou[4,5,6], Anselme Perrier[7], Nicole Déglon[1,2,8,9], Emmanuel Brouillet[1,2]

[1] CEA, DSV, I²BM, Molecular Imaging Research Center (MIRCen), F-92265 Fontenay-aux-Roses, France

[2] CNRS, CEA URA 2210, F-92265 Fontenay-aux-Roses, France

[3] Commissariat à l'Energie Atomique (CEA), Institut de Biologie et de Technologies de Saclay (iBiTec-S), Service de Biologie Intégrative et Génétique Moléculaire (SBIGeM), F-91191 Gif-sur-Yvette Cedex, France

[4] Institut Curie, Orsay F-91405, France

[5] CNRS UMR 3306, Orsay F-91405, France

[6] INSERM U1005, Orsay F-91405, France

[7] I-Stem, INSERM U861, Evry, F-91030, France

[8]Lausanne University Medical School (CHUV), Department of Clinical Neurosciences (DNC), Laboratory of Cellular and Molecular Neurotherapies (LNCM), Lausanne, Switzerland

[9]Lausanne University Medical School (CHUV), Neuroscience Research Center (CRN), Laboratory of Cellular and Molecular Neurotherapies (LNCM), Lausanne, Switzerland

*****, co first authors equally contributed to this work.

Abstract

Doublecortin-like protein kinase 3 (Dclk3) is enriched in the striatum in mammals and its expression is reduced in Huntington's disease (HD) patients and HD mouse models. We demonstrate that overexpression of Dclk3 decreases mutant huntingtin-induced neurotoxicity *in vivo* in a lentiviral mouse model of HD. Knock down of Dclk3 in this model aggravated striatal degeneration. Overexpression of Dclk3 using adeno-associated viral vectors in a knockin mouse model of HD tended to improve motor signs. MRI examination also shows beneficial effects of Dclk3 in these mice. We show that the expression of the kinase domain through its catalytic activity is sufficient to protect against mutant huntingtin. A dead kinase mutant (K543M) was unable to protect in vivo. Dclk3 and its breakdown products (BP) containing the kinase binds to microtubules and are also present in the nucleus. Preliminary data indicate an abnormal Dclk3 cleavage and nuclear localization in the HD striatum. A yeast two-hybrid screen identified potential protein partners of the kinase domain that are known to be involved in regulation of transcription. These novel results indicate that mutant huntingtin-induced defects in Dclk3-dependent neuronal survival pathway could participate in the preferential susceptibility of the striatum in HD.

Introduction

Huntington's disease (HD) is an inhereted neurodegenerative disorder caused by a mutation in HD gene. The main HD hallmark is an early loss of medium spiny neurons (MSNs) in the striatum followed by massive neurodegeneration through the whole brain. Defects in many cellular functions and pathways have been suggested to play a role in HD pathogenesis. (Milnerwood and Raymond, 2010; Ross and Tabrizi, 2010). None of these mechanisms can explain the preferential early vulnerability of the striatum in HD.

One hypothesis is that some factors, selectively expressed in the striatum may confer to GABAergic projection neurons (MSNs) their particular sensitivity to degeneration (Brouillet et al., 2005; Han et al., 2010). Dopamine and its subtype 2 membrane receptors (D2R) as well as the small GTPase Rhes have been shown to be preferentially expressed in the striatum and rendered striatal neurons highly vulnerable to mutant Htt (Charvin et al., 2005; Benchoua et al., 2008; Charvin et al., 2008; Subramaniam et al., 2009). On the contrary, neuroprotective factors, which expression is reduced in the HD striatum would also contribute to rendering striatal neurons more vulnerable to mHtt (Francelle et al., 2014). To date, there are only a few of these striatal markers that have been experimentally identified as real modifiers of mHtt. In this context, we performed a transcriptome SAGE analysis of 11 regions in the mouse brain identified approximately 120 genes with preferential expression in the striatum (de Chaldee et al., 2003; Brochier et al., 2008). Many gene products show a significantly reduced expression in the brain of HD patients or HD mouse models but their function are unfortunately totally unknown.

Dclk3 is one of these striatal markers. It is a third member of a new family of kinases named "Double Cortin like Kinase" (Ohmae et al., 2006b). Dclk3 displays a conserved C-terminal "serine/threonine kinase" domain similar to Ca^{2+}/calmodulin kinase IV (CaMKIV) and a possible Double Cortin" (DC) domain anchoring Dclk proteins to microtubules (supplemental **Fig.S0**). Dclk3 displays a higly conserved kinase domain and a poorly conserved DC domain as compared to Dclk1 and Dclk2. Striatal expression of Dclk3 is decreased in R6/2 (Brochier et al., 2008), and knock-in mouse models of HD (Kuhn et al., 2007). We hypothesized that loss of Dclk3 may precipitate striatal degeneration and its restauration could contribute to MSN survival in HD.

Results

Preliminary Dclk3 characterization in neurons indicate perturbation in HD

Mouse Dclk3 primary sequence suggests two Open Reading Frames (ORF) possible leading to a large (L-Dclk3, 3498 base) and a short (S-Dclk3, 2800 base) form mRNAs of Dclk3. Both forms (L-Dclk3 and S-Dclk3) conserve the full conserved kinase sequence but only L-Dclk3 has the full putative DC domain.

Northern blot analysis using wild type (WT) mouse mRNA preparation from different brain regions (Cortex, Hippocampus, Striatum, Thalamus, Cerebellum, whole brain) showed the prominent Dclk3 form in the brain is L-Dclk3, leading theoretically to a 823 aa protein in mouse (790aa in human) (**Fig. 1S**).

A lesser expressed S-Dclk3 (652aa in mouse) could however be detected in the striatum (**Fig. 1S**). The blot also showed both forms were highly expressed in the striatum when compared to the others brain areas tested.

Several dataset indicated a reduced Dclk3 mRNA expression in various HD mouse models (Kuhn et al., 2007). We could check in the striatum of 12 month-old heterozygous and homozygous knock-in 140CAG HD mice that Dclk3 mRNA expression was significantly reduced in comparison with wild type littermates (**Fig. S2).**

We next studied Dclk3 protein expression using different approaches. Since no commercially antibody is available to detect mouse Dclk3, a hemagglutin tag (HA) was added at the C-terminus of the recombinant protein to more easily detect the proteins. L-Dclk3 and S-Dclk3 were cloned in lentiviral vectors (LV). Primary culture of neurons and striatum of WT mice were infected with either LV-L-Dclk3-HA or LV-S-Dclk3-HA and analyzed in Western blot to determine the size of L- and S-Dclk3 proteins. Surprisingly, full length and cleaved forms of Dclk3 were found (**Fig. 1, A**). All the HA-positive bands corresponded to the C-terminal part of the protein containing the kinase domain. In neurons in culture, infection with LV-L-Dclk3-HA and LV-S-Dclk3 led to the detection of the full length proteins at 100 kDa and 75 kDa band respectively (**Fig. 1, A**). In addition, bands at ~70, ~55, and ~42 kDa were found. Similar bands were found in the adult mouse striatum after infection but, in addition, a fainter band at 23 kDa was also seen when S-Dclk3 was expressed (**Fig. 1, A**).

To better characterize the cellular localization of Dclk3, HEK were transfected with L-and S-Dclk3-HA constructs. Dclk3-HA co-localized with microtubules (alpha-tubulin) with the strongest expression in the perinuclear area (**Fig.1, B**). S-Dclk3-HA localization was also mainly cytoplasmic. Cytoplasmic localization of L-Dclk3-HA was also confirmed in primary culture of rat striatal cells and differentiated Neural stem cell (NSC) derived from human Induced pluripotent stem cell (IPSC) after LV-mediated overexpression. Biochemical experiments confirmed that L- and S-Dclk3-HA could bind to microtubules prepared from primary culture of neurons (not shown).

A similar cytoplasmic localization of Dclk3-HA was also seen in striatal neurons in mice using the anti-HA antibody after infection with LV-Dclk3-HA (**Fig. 2**). This could be also seen using an antibody directed against human Dclk3 (ab21890002, central region a.a. 200-500). However, this antibody also detected a nuclear signal as seen using confocal microscopy (**Fig. 2, B**). This nuclear signal was absent when the primary antibody was omitted. Since the nuclear signal was not seen with the anti-HA antibody, this suggested that a cleaved product of Dclk3 (from which the HA tag has been removed) could be present in the nucleus.

Since the anti-hDclk3 antibody weakly cross-reacts with mouse Dclk3, we performed immunochemical detection of endogenous Dclk3 in the brain of a macaca fascicularis (**Fig. 2, C**). In fixed brain sections, the anti-hDclk3 antibody labelled striatal neurons. To a lesser extent cortical neurons could be also detected (supplemental **Fig. S3**). In the striatum, immunohistochemical labelling suggested that the protein (and/or one of its fragments) was not exclusively in the perinuclear region of neurons but also in the nucleus (**Fig. 2**).

The cellular localization of endogenous Dclk3 was assessed after differential centrifugation of tissue homogenates prepared from macaque putamen samples (**Fig.3, B**).

Fractions enriched in cytoplasm or nuclei were prepared. Western blot analysis of the cytoplasmic fraction showed a band at the apparent molecular weight compatible with macaque full length Dclk3 protein (~70kDa) and another lower molecular weight band (~38 kDa) (**Fig.3, B**). These bands were weaker in the nucleus, while bands at lower molecular weight (~26 and 20 kDa) could be seen.

A similar approach was conducted in control human striatal samples (**Fig.3, C**). The profile of anti-hDCLK3 immunoreactivity seen in the cytoplasmic and nuclear fraction was very similar to that seen in the macaque brain. We next asked in a pilot experiment whether Dclk3 expression could be affected in striatal samples from HD patients (grade 1 and 2) in comparison with controls. Western blot analyses indicated a global reduction of the bands revealed with the anti-hDclk3 antibody as compared to controls. However, we noticed an elevation of the levels of one band (~52 kDa) in the nuclear fraction in the HD samples as compared to controls where this band was barely seen (**Fig. 3**).

Since it was difficult to ascertain the specificity of the bands we observed in human samples (which are likely Dclk3 cleavage products but can also be unrelated proteins cross-reacting with the antibody), we examined the pattern of cleavage of recombinant S-Dclk3 in BACHD mice that express full length mHtt with 97 glutamines (Gray et al., 2008). BACHD mice were infected at 6 months of age with LV-S-Dclk3-HA and 4 weeks later the striatum was analysed. Western blot analysis using the anti-HA antibody showed a general change in the proportion of Dclk3-HA breakdown products (**Fig. 3, D**), the 57 and 25 kDa bands been reduced while the ~48 kDa band was increased, reminiscent of that seen in HD patients (red arrows).

Thus these results indicate that Dclk3 and its cleavage products are mainly cytoplasmic with a smaller proportion present in the nucleus. In HD, Dclk3 expression is reduced and its cleavage appears changed, expecially in the nucleus.

Neuroprotection of Dclk3 in HD models

We examined whether Dclk3 (L and S-Dclk3) expression could change the toxicity induced by the expression of mutant huntingtin (mHtt) *in vivo* using lentivrial vectors (LV). LV-Htt171-82Q was used to overexpress an N-terminal fragment of mHtt and produce striatal lesions (Galvan et al., 2012; Ruiz and Deglon, 2012). A lentival vector coding for βgalactosidase (LV-βgal) was used as a control. We injected LV-βgal, LV-S-Dclk3-HA and LV-L-Dclk3-HA with LV-Htt171-82Q in the mouse striatum. We checked that Dclk3 levels were increased after infection with LV coding Dclk3 (supplemental **Fig. S4).** At 6 weeks post-infection, the lesion was evaluated by immunostaining and immunoshistochemical labeling (**Fig.4**). The expression of Htt171-82Q and gal (control group) produced a consistent lesion size characterized by the loss of the Neuronal marker (NeuN), cytochrome c oxidase (COX) and DARPP-32 stainings. The lesion induced by the co-expression of Htt171-82Q and both froms of Dclk3-HA (L- and S-Dclk3-HA) were significantly smaller as it was visualized by the NeuN and COX staining compared to control group (**Fig. 4**). Ubiquitin-positive agregages were visualized and quantified in the infected region in all groups. No significant differences were found indicating that neuroprotection is not directly related to modification of mHtt accumulation/aggregation.

We also generated a lentiviral vector expressing a shRNA targeting both L-and S-Dclk3 (LV-shDclk3) to determine if loss of Dclk3 could exacerbate mHtt toxicity *in vivo* (**Fig.5, A**) As a control, we used the shRNA targeting luciferase mRNA, a non mammalian gene. Analysis using qRT-PCR of the infected striatal region showed that LV-shDclk3 produced a significant 75% reduction of Dclk3 mRNA expression (supplemental **Fig.S4**). In these ShRNA constructs, GFP is also expressed as a reporter gene of shRNA expression under the mouse PGK promoter. The GFP intensity measured after infection with the two LVs coding the shRNAs was similar suggesting equal levels of expression (**Fig.5, B**). LV-shLuc and LV-shDclk3 injected alone in the mouse striatum did not create a lesion by themselves (not shown). The same amount of either LV-sLuc or LV-shDclk3 was mixed with LV-Htt171-82Q and injected into the striatum. Since in these experiments, we anticipated an acceleration of mHtt-induced neurodegeneration by LV-shDclk3, we used GFP expression levels as readout of neuronal integrity at 3 and 6 weeks post-infection (**Fig.5, C**). LV-Htt171-82Q produced a reduction in the levels of GFP in the striatum at 3 weeks post infection that was more pronounced at 6 weeks in the shLuc control group. In the shDclk3 group, this loss was significantly more profound. Analysis of the striatum using DARPP-32 immunohistochemistry at 6 weeks confirmed that lesions produced by mHtt in presence of shDclk3 were larger than those found in controls injected with LV-shLuc (**Fig.5, D**). Thus, Dclk3 downregulation facilitates mHtt toxicity in MSN.

These experiments show that overexpresion of Dclk3 is neuroprotective against mHtt toxicity *in vivo*, while knockdown of Dclk3 seems to facilitate mHtt.

Study of Dclk3 overexpression using AAV2/10 in knockin 140CAG mice

We next investigated if the restauration of Dclk3 expression in the striatum could improve their phenotype in HD mice. We used AAV2/10 vector coding for L-Dclk3 (AAV-L-Dclk3) and tested whether infection of the striatum with this AAV could produce beneficial effects in the HD mouse models of HD. This vector allows wide diffusion in the striatum, which was prerequisite to express Dclk3 in a large proportion of the striatum and expect detectable functional effects (**Fig.6, A**). In a pilot experiment in a few controls and N171-82Q transgenic mice (supplemental **Fig. S5, A; B**), we observed that the AAV-L-Dclk3 was well tolerated (supplemental **Fig. S5, C**) and tended to produce a beneficial effect in female HD mice when testing their motor performance as seen in the Rotarod (supplemental **Fig. S5, D**).

We then launched a study using the KI140CAG mouse model of HD (Menalled et al., 2003). Homozygous KI140 mice were injected stereotaxically with AAV-L-Dclk3 or AAV-GFP at 5-6 months of age (**Fig.6, A**). At this age, homozygous KI140 mice show no major neurological signs. Behavioral evaluation was performed at 8 and 12 months of age in the infected mice. In vivo brain imaging was also conducted at 12 months of age (**Fig.6, B**).

KI140 homozygous mice showed significant deficits in the rotarod test (redued latency to fall) at 12 months and the open field test (reduced rearing behavior) as compared to wildtype littermate controls (supplemental **Fig. S6, A-E**). The deficits were lighter in heterozygous KI140 mice.

In the present experiment, analysis of the wildtype littermates using the rotarod test showed that AAV-Dclk3 and its control AAV-Dclk3 produced behavioral perturbations, the animal displaying poorer performance when compared to uninjected mice of the same colony. KI140 mice infected with AAV-GFP showed rotaror performance similar to the wildtype mice infected with AAV-GFP or AAV-Dclk3. However, the homozygous KI140 mice infected with AAV-L-Dclk3 performed significantly better in the rotarod test when tested at 8 months of age (i.e. 4 month post surgery) as compared to AAV-L-Dclk3 (**Fig. 6, C**). This effect was milder at 12 months of age and was not significant. In the open field test, non-significant trend were seen when considering the distance traveled, the mean velocity of the animal displacements and the time spent in groaming behavior. However, the rearing behavior, which is decrease in HD mice as compared to control, was normalized by AAV-L-Dclk3 (**Fig.6, D**). We also analysed the gait and walk of the mice using the CatWalk apparatus. In this test, mice are trained to cross a bridge and foot prints are videorecorded for kinetic image analysis. Analysis showed that the displacement of the HD mice as compared to wildtype mice was mildly but significantly altered (**Fig.6, F**). In particular, body velocity of KI140 mice infected with AAV-GFP was slower than wild type mice injected with the same vector. Velocity tended to be improved in KI140 mice infected with AAV-L-Dclk3. Interestingly, the mean variation of velocity when crossing the bridge was significantly increased by almost two fold in KI140 mice infected with AAV-GFP as compared to wild type mice, suggestive of saccaded displacements in HD mice. This was fully corrected in HD mice infected with AAV-Dclk3. KI140 mice infected with AAV-GFP also showed deficit in the forelimb grip strength test as compared to infected wildtype littermates. KI140 mice injected with AAV-L-Dclk3 showed better performances than KI140 mice infected with AAV-GFP (**Fig.6, E**).

A few wild type and homozygous KI140 mice injected with AAVs were examined at 12 month old using 1H-proton NMR spectroscopy and MRI at 11.75 teslas to characterize the striatum *in vivo*. Volumetric analysis of the striatum showed a trend to striatal atrophy in KI140 mice infected with AAV-GFP as compared to wild type mice (**Fig.7, A**). This trend to atrophy was not seen in KI140 mice infected with AAV-Dclk3. Neurochemical profile seen by NMR spectroscopy showed significant changes in homozygous KI140 mice infected with AAV-GFP as compared to wild type mice (**Fig.7, A**). Concentrations in “neuronal” related metabolites GABA, NAA and glutamate were decreased in KI140/AAV-GFP mice (**Fig.7, B; C**). An increase in glutamine and a loss of choline and taurine were observed. In the KI140 mice infected with AAV-L-Dclk3, these changes were not significantly changed. However, elevation of glutamine seen in KI1140/GFP mice as compared to controls was partially diminished in KI140/AAV-L-Dclk3 mice (**Fig.7, B; C**).

These results showed that restauration of Dclk3 expression in KI140 mouse can ameliorate some of their motor sign and neurochemical changes.

Kinase domain of Dclk3 underlies neuroprotection

To better understand the possible mechanisms underlying the neuroprotective effects of Dclk3, we studied the role of its kinase domain. Kinase protein activation and regulation follow a relatively well described pathway. Based on the homology of Dclk3 with CaMKII, we investigated if Dclk3 followed its same pattern of activaton. CaMKII requires an initial autophosphorylation of its threonine 286, for the activation of the kinase catalytic site. A similar threonine in S-Dclk3 and Kin-Dclk3 (i.e. Threonine 457 of L-Dclk3) are conserved within a motif of charged amino acids reminiscent of that existing in vicinity of CaMKII threonine 286. Site directed mutagenesis was used to create the substitution Th289>Ala (T289A) in S-Dclk3 (supplemental **Fig.S7, A**). We assesed if this mutation of S-Dclk3 could modifiy the neuroprotection *in vitro*. Overexpression of mHtt (Htt171-82Q) in primary culture of neurons produced degeneration of transfected neurons, increasing the number of fragmented nuclei. Co-infection with wild type S-Dclk3 showed a neuronal neuroprotective effect against mutant Htt toxicity. The T286A Dclk3 mutant showed no protective effects when wo-infected with mHtt. (supplemental **Fig.S7, B**). This indicated that perturbating kinase activation could disturb its capability to produce protection against mHtt.

To assess the role of the kinase domain *in vivo*, we cloned a Dclk3 domain containing only the kinase domain without the N-terminal DC domain (LV-Kin-Dclk3-HA). Wild type mice were infected with LV-Kin-Dclk3 or LV-βGal (control) and LV-Htt171-82Q. Histological evaluation of NeuN and Cox staining showed striatal lesions were significantly reduced by overexpression of Kin-Dclk3 as compared to controls (t-test, $p<0.05$) (supplemental **Fig.S8**). This experiment demonstrates that the overepression of Dclk3 kinase domain is sufficient by itself to produce a neuroprotection versus mHtt.

We next generated a dead kinase mutant by point mutation at the kinase ATP binding site by searching for homologies with many other kinases. We identified K543 as highly conserved (**Fig.8, A**). Mutation of this amino acid in other kinases abrogates kinase activity. We generated a K543M substitution in Dclk3-Kin fragment. We checked that the kinase domain of wildtype mouse S- and L-Dclk3 and Dclk3-Kin fragment were functional using ^{32}P-ATP autophosphorylation assays (**Fig.8, B; C**). All three could readily autophosphorylate. We compared the autophosphorylation activity of L-Dclk3 and Dclk3-Kin with those of the K543M mutants. Results showed that the mutants were unable to autophosphorylate. In line with this, while the wild type forms could phosphorylate the pan-substrate Myelin Basic Protein (MBP) the K543M mutants were inefficient (**Fig. 8, D**). Thus the K543M mutants could be considered as “dead kinase” proteins.

We cloned the K543M Kin-Dclk3-HA mutant in a lentiviral vector and tested its potential neuroprotective effects against Htt171-82Q toxicity in mice (**Fig. 8, E**). The levels of expression of the mutant as revealed by HA immunohistochemistry was similar to that of the wild type fragment *in vivo* (not shown). Histological evaluation of the striatal lesions produced by mHtt showed that the wild type kinase domain significantly reduced the lesions as found in the experiment reported above, whereas the deadkinase domain was not protective when evaluating the lesion volume using the marker of neuronal neuclei NeuN (**Fig. 8, F; G**) and the marker of neuronal functionality Cytochrom C oxidase (COX) (**Fig. 8, H; I**). Thus these results show that the kinase domain of Dclk3 is sufficient to produce neuroprotection and this involves its catalytic activity.

Kinase Dclk3 interactors

We launched a yeast two hybrid screen using the Kin-DCLK3 as bait in brain human mRNA bank to identify potential substrates (**Fig. 9, A**). A total of 7 interactions were found pointing to TADA3, BTBD9, TRIM89, SALL1, ZNF12, ZNF292 and ZNF366 (**Fig. 9, B**). All these proteins possess zinc finger domains. Bioinformatics search for experimentally validated protein partners for these proteins indicates that they interact with partners involved in macromolecular complexes involved in regulation of transcription in human. A similar analysis using only mouse data leads to the same conclusion. Amongst the seven Dclk3 kinase domain partners, the protein TADA3 (Transcriptional adapter 3) presents the highest number of known partners (**Fig. 9, B**). Co-immunoprecipitation experiments after transfection of HEK cells showed that TADA3 tagged with V5 could be pulled down using Kin-Dclk3-HA (**Fig. 9, C**). These preliminary results suggest that the kinase domain of Dclk3 may preferentially interact with proteins involved in transcription. This may, at least in part, participate to the neuroprotective effect of the kinase.

Discussion

The present study shows that a short and a long form of Dclk3 can be identified in the mouse striatum, the long form appearing to be the most prominent specie. We verified that, consistent with previous observations, the level of Dclk3 expression is reduced in the striatum of KI140CAG mice, a genetic mouse model of HD characterized by slow progression of symptoms and neurodegeneration. We cloned the two mouse forms of Dclk3 in lentiviral vectors that correspond to two ORF. Results showed that the increased expression of the two froms of Dclk3 using these lentiviral vectors protects striatal neurons from the toxicity of a short N-terminal fragment of mHtt. We also found that overpression of L-Dclk3 in the striatum of KI140CAG mice could provide some beneficial effects on motor symptoms. We attempted to better characterize the mechanisms underlying the protective effects of Dclk3 and demonstrated that the kinase domain of Dclk3 is sufficient to provide neuroprotection against mHtt. Two inactive mutants of the kinase were found to be inefficient to protect against mHtt, indicating that the catalytic domain of the kinase plays a role in activating neuronal survival. Protein partners of Dclk3 kinase domain were identified, pointing to a possible involvement of Dclk3 in the regulation of transcripton.

Protection of striatal neurons by Dclk3 and its breakdown fragments

The results obtained in the HD lentiviral model underscore that the overexpression of Dclk3 and its kinase domain can signiciantly block degeneration of striatal neurons that express mHtt. Consistent with this, the reduction of Dclk3 using shRNA strategy exacerbate mHtt toxicity *in vivo*. Thus, the loss of Dclk3 in HD mouse models and the striatum of HD patients could render the striatum more vulnerable to mHtt. This may explain, at least in part, the particular susceptibility of this brain region in HD, while mHtt is ubiquitously expressed in the brain.

We challenged this idea in a more progressive mouse model of HD, the KI140CAG strain using the AAV vectors that, compared to lentiviral vectors produce a more widespread transduction of neurons, increasing the striatal territory expressing more Dclk3. The results we report show that some aspect of the disease are improved by Dclk3 expression using AAV10 especially specific motor signs examined using the openfield test, the Catwalk test and the rotarod test. The present results are however to take cautiously, since the number of animals per group is relatively low (n=5-8) and the amplitude of the effect are small, often showing encouraging trends which are not statistically significant. In addition, we found that striatal injection of AAV-GFP and AAV-Dclk3 in wild type mice likely produced disturbing effects in mice. Indeed, compared to cohort of "uninfected" mice that we characterized in our lab, infected mice showed poorer performance in the rotarod motor task. The reason for this is unclear, but is likely related to the traumatic aspect of the surgery (anaesthsia, canula insertion etc.) and /or the deposit of viral particles. Concerning the viral load, we tried to minimize the amount of AAV10 to be injected in the present experiments, in order to obtain a good level of transduction and expression of Dclk3, and avoiding an inflammation that could be detrimental for the function of the striatum. Another important aspect of the AAV experiments is that while the level of Dclk3 expression appeared satisfactory, it must be emphasized that the transduction could not be achieved in the entire striatum. Larger quantity of vectors may have reached this goal but this might have likely produced a major inflammation.

However the overexpression we produced with our paradigm may have been sufficient to produce a small but detecteable effect on the function of the striatum in KI140CAG mice (i.e. amelioration of some neurological signs) while the effect in the striatum is diluted when assessed globally using NMR spectroscopy and MRI. It would be interesting to repeat these experiments with a larger number of mice and possibly using improved, more efficacious, vectorization procedures to increase Dclk3 expression in the striatum and possibly in the cerebral cortex.

Possible mechanisms underlying neuroprotection by Dclk3

The neurobiological function of Dclk3 is totally unknown so far. Some aspects can be inferred from homology with other kinases that are better understood. Primary sequence of Dclk3 indicates that this kinase has a poorly conserved DCX domain in its N-terminal domain (Ohmae et al., 2006a). In comparison, the conservation of this domain is greater for Dclk1 and Dclk2 proteins. We found that despite this limited conservation of its N-terminal part, Dclk3 interacts with the cytoskeleton. This question was relevant to HD since, mutant Htt toxicity involves perturbation of the cytoskeleton, in particular the function of protein complexes involved in retrograde and anterograde axonal transport. Htt associates with microtubule (Tukamoto et al., 1997) and is transported retrogradely and anterogradely in neurons (Block-Galarza et al., 1997). Htt interacts with HAP1 to modulate motor complex efficacy to move along microtubules. Alteration of the huntingtin/HAP1/p150 (Glued) complex correlates with reduced association of motor proteins with microtubules, reducing transport of vesicles (including BDNF vesicles) along the cytoskeleton (Gauthier et al., 2004). Our data show co-localization of Dclk3 with the microtubules. Biochemical experiments showed that Short-Dclk3, Long-Dclk3 and Kin-Dclk3 preferentially segregate with preparations enriched in microtubules (not shown).

Thus, the localization of Dclk3 on microtubules could play a role in its neuroprotective effects against mHtt.

However the yeast two-hybrid screen we performed did not identify partner proteins known for their association with the cytoskeleton. All partners we found to interact with Dclk3 kinase domain (or adjacent to the kinase domain) are known for their interaction with proteins related to regulation of transcription. It is conceivable that Dclk3 partners identified in the yeast two-hybrid screen are also partitioned between the cytoplasm and the nucleus, and that the binding of Dclk3 to microtubules is indirectly mediated by these partners. This consists at present only a hypothesis and a better characterization of the cellular localization of the Dclk3 partners in neurons is required to further examine this hypothesis.

In line with a possible role of Dclk3 in transcription, we found that Dclk3 C-terminal part of Dclk3, likely containing the kinase domain can be found into the nucleus. This is consistent with the recent data showing that Dclk2 can be cleaved and that its kinase domain migrates from the cytoplasm to the nucleus (Nagamine et al., 2014). A similar "model" of translocation from the cytoplasm to the nucleus has been also suggested for Dclk1. From a mechanistic point of view, our data on Dclk3 are original in that they show that the kinase and one or more of its breakdown product(s) can migrate to the nucleus to interact with partners directly linked to regulation of transcription. This might be a general mechanism of action of Dclks proteins.

The preliminary analyses of the striatum in two HD patients, confirm a global loss of expression of Dclk3 proteins in the cytoplasm but intriguingly, the abnormal accumulation of a fragment of Dclk3 in the nucleus is also noticeable. This needs to be further studied in a larger cohot of HD patients. We also found that the profile of cleavage of recombinant Dclk3 in BACHD mice clearly differs from that of wildtype littermates. Thus, in addition to a transcriptional perturbation of Dclk3 expression, abnormal post-translational of the kinase may also contribute to reduce the efficacy of its pro-survival properties in HD.

The existence of the different breakdown products of Dclk3, seen endogenously or after overexpression of recombinant Dclk3 proteins, in rodent, macaque and human samples, very likely resulting from cleavages by proteases as seen for Dclk1, emphasizes the complexicity of the post-translational regulations of Dclk3. In addition, other regulations likely exist. Based on the analysis of Dclk3 sequence and the similarities with Dclk1 and CaMKs, putative caspase 4 and calpain cleavage sites can be found, and a SUMOylation site in the kinase domain can be predicted (supplemental **Fig. S9).** Another putative mechanism of post-transcriptional regulation of Dclk3 probably involves phosphorylation by upstream kinases. Those upstream regulating kinases remain to be identified.

Dclk3 loss in HD: a possible cause of striatal vulnerability to mHtt?

The present results indicate that increased expression of Dclk3 can produce a neuroprotective effect upon MSN that express mHtt. Compelling evidences indicate that Dclk3 expression is reduced in the HD striatum. Thus a loss of function of Dclk3 could render MSN more fragile, and consequently could participate in the preferential and early vulnerability of the striatum in HD.

Previous SAGE analyses of the mouse striatum showed that the level of expression of DCLKs is relatively low compared to other known striatal proteins such as preproenkephalin. Dclk3 expression is in the range of that measured for D1 receptor and A2A adenosine receptor two other well-know markers of the striatum. In addition to Dclk3, other gene products which are selectively expressed in the striatum have been shown to be involved in the selective degeneration of this structure in HD (for a review, Francelle et al., 2014).

In addition to the striatum, Dclk3 depletion (and abnormal cleavage) may lead to other consequences, underlying neurological phenotype in HD patients and HD models. Dclk3 is also expressed in other brain regions such as the cerebral cortex and the hippocampus (to lower levels as compared to striatum). In this context, although not translatable in clinical terms, the cross breeding of mice KO for Dclk3 with HD mice might be an approach to be considered to determine whether the loss of Dclk3 could broadly precipitate the disease.

Dclk3 as a potential therapeutic target

If the protective role of Dclk3 against mHtt is confirmed by future experiments, the kinase might be considered as a therapeutic target. Different strategies may be plan to do. Dclk3 regulations likely occur at different levels. Selective phosphatase inhibitors or allosteric synthetic activators of Dclk3 could be developed to stimulate its activity and produce neuroprotective effects. Considering that the striatum is involved in crucial motor and cognitive processes, and that this brain structure is involved in a number of neurological / psychiatric illnesses, it is conceivable that Dclk3 may represent a therapeutic target for other diseases, beyong HD.

Materials and Methods

Animal

Mice were housed in a temperature-controlled room maintained on a 12 hr light/dark cycle. Food and water were available ad libitum. All animal studies were conducted according to the French regulation (EU Directive 86/609 – French Act Rural Code R 214-87 to 131). The animal facility was approved by veterinarian inspectors (authorization n°A 92-032-02) and complies with Standards for Humane Care and Use of Laboratory Animals of the Office of Laboratory Animal Welfare (OLAW – n°#A5826-01). All procedures received approval from the ethical committee. Adult male C57BL/6J mice (25 g each; Charles River, Saint Germain sur l'Arbresle, France) were used for lentiviral infections.

For endogenous DCLK3 mRNA levels study, we used the transgenic mouse model of HD generated and maintained in the FvB inbred background, the BACHD mice, that express full-length human mHtt from its own regulatory elements on a 240-kb BAC, which contains the intact 170-kb human htt locus

plus about 20 kb of 5′ flanking genomic sequence and 50 kb of 3′. We used 9 month-old male BACHD mice for the study as previously described (Gray et al., 2008).

We also studied knock-in mice expressing chimeric mouse/human exon 1 containing 140 CAG repeats inserted in the murine Htt gene (KI140) and their littermate controls. KI140 colony was maintained by breeding heterozygotes KI140 males and females (Menalled et al., 2003). Mice were N3 (B6) on a 129 Sv×C57BL/6 J background. The resulting different genotypes mice were used for the study and showed no overt abnormalities.

Genotyping was determined from PCR of tail snips taken at 10–15 days of age for BACHD and KI140 mice.

Lentiviral vector construction, production and infection

DNA sequences coding for green fluorescent protein (GFP) and for C-terminal hemagglutinin (HA)-tagged mouse short and long forms of Dclk3 were cloned into the SIN-W-PGK lentiviral vector (de Almeida et al., 2002) to generate lenti-GFP and lenti-S-Dclk3-HA and lenti-L-Dclk3-HA, respectively. The following probes were used to generate S-Dclk3-HA:

5' CACCATGGGCAAAGAGCCGCTGAC 3' et 5' CTAGGAGGCGTAGTCAGGCAC

GTCGTATGGGTAGGCACTGTTGGGGGACTCCTC 3'.

In addition the C-terminal domain of Dclk3 was also cloned (from aa 330 to the Cterm extremity) to only express the kinase domain. The vectors were designated as lenti-Kin-Dclk3-HA. The lenti-L-Dclk3-HA and lenti-Kin-Dclk3 have been cloned and produced by Genart followed RNA sequence provided in GENE database. An addition of Hemmaglutinin sequence has been added before STOP codon.

A Dclk3-directed shRNA (target sequence: 5’ GAGAAGTGTAAGAGAGAAA 3’) and a Luciferase-targeted shRNA (target sequence: 5’ CGTACGCGGAATACTTCGA 3’) were cloned into a bicistronic lentiviral vector (Drouet et al., 2009), in such a way that the infected cells expressed the reporter protein GFP. The resulting constructs were designated as lenti-Dclk3-shRNA and lenti-Luc-shRNA, respectively. The lentiviral vectors expressing a wild-type Htt fragment (lenti-Htt171-18Q), a mutant Htt fragment (lenti-Htt171-82Q) or beta-galactosidase (lenti-βgal) have been described previously (Diguet et al., 2009; Faideau et al., 2010). Viral particles were produced as described elsewhere (Hottinger et al., 2000). The particle content of the viral batches was determined by ELISA for the p24 antigen (Gentaur, Paris, France).

Lenti-Htt171-18Q and lenti-Htt171-82Q were used at a concentration of 150 ng/µl of p24, lenti-Dclk3-HA, lenti-Dclk3-shRNA, lenti-Luc-shRNA and lenti-βgal at a concentration of 100 ng/µl of p24, and lenti-GFP at a concentration of 50 ng/µl of p24. A total volume of 2 µl of lentiviral suspension was injected into the mouse striatum as previously reported (Faideau et al., 2010), using the following stereotaxic coordinates: 1.0 mm anterior and 2.0 mm lateral to the bregma, at a depth of 2.7 mm from the dura, with the tooth bar set at 0.0 mm.

Directed Mutagenesis of Dclk3

S-Dclk3-HA has been mutated on the threonine (286) (i.e. Threonine 457 of L-Dclk3) into Alanine (T286A) and Aspartate (T286D) using the followed probes:

T286A : 5'CCACAGCTACCTAGAGCCCGAGGGGAGGAG 3'

5' CTCCTCCCCTCGGGCTCTAGGTAGCTGTGG 3'

T286D: 5' CCACAGCTACCTAGAGCCCGAGGGGAGGAG 3' and

5' CTCCTCCCCTCGGTCTCTTGGTAGCTGTGG 3'

L-Dclk3-HA and Kin-Dclk3 has been mutated on the lysine (543) into Methionine (K543M) using the followed probes:

Dclk3-K543M-F GACAAAGCAGGCATATGCCATGATGATGATTGACAAGAGC

Dclk3-K543M-R GCTCTTGTCAATCATCATCATGGCATATGCCTGCTTTGTC

45% GC N=40 %mismatch=3/40

Tm = 81,5+0,41(%GC)-675/N-%mismatch = 81,5+0,41*45-675/40-(3/40)*100 Tm=75,58°C

A restriction site has been added to facilitate the verification of the sequence (NdeI site).

Primary culture of neurons and transfection

The primary culture of striatals neurons has been performed as previously described (Benchoua et al., 2008). These neurons were electroporated with the mouse striatal neuron Nucleofector® kit according to the supplier's manual (Amaxa, Biosystem, Köln, Germany).

Human Embryonic Kidney (HEK) 293T cells and transfection

HEK293T cells were cultured in Dulbecco's Modified Eagle's Medium (DMEM, Wako) containing 10% fetal bovine serum and 1% phenylalanine-streptamicine (Sigma). Cells were grown at 37 °C in a humidified incubator with a 5% CO2/95% air atmosphere. Transfection of HEK293T cells was performed using ref. HEK293T cells were plated at 7,5 × 105 in 6 wells plaques or at 10 × 104 in 24 wells plaques. After 48 h of culture, cells were transfected with 5 µg of plasmid DNA by incubation for 4 to 6 h in DMEM containing 10% fetal bovine serum and 1% phenylalanine-streptamicine.

Immunocytochemistry of DCLK3 in HEK293T cells

Transfected cells were cultured on poly-l-lysine coated cover glass and treated with 100% ice-cold methanol and 5mM EGTA,to preserve microtubular network, for 3 minutes. After being rinsed with TBS (Trizma (Sigma), NaCl 1mM), methanol-fixed cells were permeabilized with 0.1% Triton X-100 in blocking solution (TBS, 1% bovine serum albumin +?) for 30 min. The cells were then incubated with anti-HA-11 antibody (mouse IgG, Covance) diluted 1:1000 or anti-tubulin α antibody (rabbit IgG, Millipore?) diluted 1:500 with 1% bovine serum albumin in PBS at room temperature for 1 h. The cell samples were then incubated with Alexa 594-labelled anti-mouse IgG or Al488-labeled anti-rabbit IgG (Invitrogen), respectively, at room temperature for 30 minutes. Subsequently, the cells were rinced in TBS and treated with DAPI (Wako) diluted 1:10'000 in TBS at room temperature for 3 minutes and observed by a confocal laser-scanning microscope (SPE and SP8 Leica).

Immunoprecipitation

Cells were collected at 48 h after transfection and lysed with modified-RIPA buffer [10 mM Tris–HCl (pH 8.0), 1% NP-40, 150 mM NaCl, 1 mM EDTA, 10 µg/ml protease inhibitors (Mini-Complete, Roche) and phosphatase inhibitor cocktail 2 (Sigma?)]. The homogenates were centrifuged at 13,000*g* for 20 min, and the supernatants were collected.

BCA protein dosage was used.

To perform immunoprecipitation, IP/co-IP kit based on magnetic beads coupled protein A & &G was used (ThermoFisher). Briefly, 50µl of magnetic beads were rinced and incubated 2 hours with antibodies (0.5 µg of anti- HA-11 or 0.5 µg of anti-DCLK3 : 21890002 (Novus)).

500µg of total protein extracts were mixed with the complex antibodies-beads 4 °C for 1 h. Beads were then rinced with kinase assay buffer [40 mM Hepes-NaOH (pH 8.0), 2 mM dithiothreitol, 0.1 mM EGTA and 5 mM ?], and then determined protein kinase activity using 100 µM [γ-32P]ATP or eluted with SDS–PAGE sample buffer for SDS–PAGE analysis.

SDS–PAGE and Western blotting

SDS–PAGE was performed on NuPAGE® Novex® 4-12% Bis-Tris pre-cast polyacrylamide gels. To transfer proteins, iBlot® Transfer Stacks was used using the iBlot® Gel Transfer Device.

Protein kinase assay

The protein kinase activities of DCLK3 were determined as previously described. Phosphorylation of proteins was carried out at 30 °C for 10 min in a standard reaction mixture (10 µl) consisting of 40 mM Hepes-NaOH (pH 8.0), 2 mM dithiothreitol (DTT), 0.1 mM EGTA, 5 mM Mg(CH3COO)2, 100 µM [γ-32P]ATP and the indicated concentration of protein substrates. After incubation, the reaction was stopped by the addition of 10 µl of 2 × SDS–PAGE sample buffer. Phosphorylated proteins were resolved by SDS–PAGE and detected by film exposition and revelation with a PhosphorImager apparatus (modele).

Immunoblotting

Mice were sacrificed by dislocation without anesthesia and tissue processed as previously described. Tissues were homogenized in 200 ml Tris buffer pH 7.4 containing protease inhibitors (MiniComplete, Roche) and phosphoatase inhibitors (Phosphatase Cocktail 2, Sigma), sonicated and kept at -20°Cfor biochemical experiments. Protein dosage and processing were performed as previously described.

Histological analyses

After deep anesthesia by intraperitoneal injection of a sodium pentobarbital solution (50 µg per gram of body weight), mice were transcardially perfused with 100 ml of phosphate buffer containing 4 % paraformaldehyde at 8 ml/min.

The brains were removed, post-fixed overnight in the same solution, then cryoprotected by immersion in a 15 % sucrose solution for 24 hours followed by immersion in a 30 % sucrose solution for another 24 hours. Free-floating 30-µm-thick serial coronal sections throughout the striatum were collected using a freezing sliding microtome (SM2400; Leica Microsystems, Wetzlar, Germany).

For immunohistochemistry, sections were treated with 0.3 % hydrogen peroxide for one hour, washed three times in phosphate-buffered saline (PBS), blocked in PBS containing 4.5 % normal goat serum for one hour, then incubated overnight at 4°C in PBS containing 3 % normal goat serum and one of the following antibodies: rabbit anti-DARPP-32 (Santa Cruz Biotechnology, Santa Cruz, CA; 1:1000), mouse anti-NeuN (Millipore, Molsheim, France; 1:200), rabbit anti-Ubiquitin (Wako Chemicals, Neuss, Germany; 1:1000), or mouse anti-HA (Covance, Princeton, NJ; 1:500). Sections were rinsed three times in PBS before incubation with the appropriate anti-IgG biotinylated antibody (Vector Laboratories, Burlingame, CA) at a 1:5000 dilution for one hour. Staining was visualized by the addition of avidin-biotinylated peroxidase and incubation with DAB or VIP substrate (Vector Laboratories, Burlingame, CA) for one minute. For NeuN immunostaining, we used the M.O.M. immunodetection kit (Vector Laboratories, Burlingame, CA). Stained sections were mounted on microscopic slides.

The area of the striatal lesions resulting from lenti-Htt171-82Q infection was delineated manually by identifying the border of the lesion on each coronal brain section. The corresponding surface was calculated using the MCID image analysis software (InterFocus Imaging, Cambridge, UK). The volume of the striatal lesion was determined using the Cavalieri method (Diguet et al., 2009). The number of Ubiquitin-positive inclusions was quantified as previously described (Diguet et al., 2009) with the following modifications: the inter-section distance was 210 µm (i.e. one in every seven sections was used) and observations were performed using a 10X objective on an Axioplan 2 Imaging microscope (Carl Zeiss, Le Pecq, France). With this set-up, objects with an apparent cross-sectional area of over 5 μm^2 could be reliably detected.

For GFP fluorescence analysis, equidistant 30-µm-thick coronal brain sections (intersection distance: 210 µm) were randomly sampled throughout the striatum. Observations were performed using a 10X objective on a motorized Axioplan 2 Imaging microscope (Carl Zeiss, Le Pecq, France) equipped with an X-Cite 120PC Q fluorescence excitation system (Lumen Dynamics, Mississauga, Canada) allowing controlled excitation intensity and homogeneity throughout the field of view.

Images were automatically acquired and analyzed using Fluo'Up and Mercator softwares (Explora Nova, La Rochelle, France). Care was taken to optimize image acquisition and avoid image saturation. On each section, the fluorescence level of each lenti-GFP-infected striatum was determined by subtracting the background fluorescence level measured outside the infection site from the mean fluorescence level within the infected area. A mean fluorescence level was then calculated across sections for each striatum.

Real-time quantitative RT-PCR and Northern blot analysis

Adult mice were deeply anesthetized by intraperitoneal injection of a sodium pentobarbital solution (50 µg per gram of body weight) before decapitation. The brains were immediately removed and positioned in a coronal brain matrix (Ted Pella, Redding, CA). For Dclk3 mRNA level measurements in knockdown experiments, 1-mm-thick brain sections were examined under a fluorescence microscope (DM6000 M; Leica Microsystems) and the striatal area expressing the GFP reporter protein was sampled using a 1.5-mm-diameter punch (Ted Pella, Redding, CA). For the quantification of Dclk3 levels in mice, the striatum was dissected out using a scalpel from 1-mm-thick brain sections. Total RNA extraction and real-time quantitative RT-PCR (qRT-PCR) were carried out according to standard procedures, using the primers 5' TGGGCGGCAGGTGTGAT 3' and 5' GCTCGTCTTGGTCCCTCTCAG 3' for Dclk3.

For Northern blot analysis, a 5-mm-thick block containing the entire striatum (between grooves 3 and 8 of the matrix, groove 1 being the most anterior; Brochier et al., 2008) was removed from each brain and processed for mRNA extraction. Twenty-five-microgram total RNA samples were denatured in a glyoxal-dimethylsulfoxide solution, electrophoresed on a 1 % agarose gel, and then transferred onto a Hybond-XL nylon membrane (GE Healthcare, Little Chalfont, UK). Hybridization was carried out at 65°C in Rapid-Hyb buffer (GE Healthcare, Little Chalfont, UK) using an [α-^{32}P]dCTP random prime-labeled (Prime-It II; Agilent Technologies, Santa Clara, CA) 788-bp-long *Pst* I fragment of the Dclk3 transcribed DNA sequence as a probe (Fig. 1A)..

Yeast Two-Hybrid Analysis

Yeast two-hybrid screening was performed by Hybrigenics Services, S.A.S., Paris, France (http://www.hybrigenics-services.com). The coding sequence for Human DCLK3 (GenBank accession number gi: 149589020) was PCR-amplified and cloned into pB29 as an N-terminal fusion to LexA (N-DCLK3-LexA-C). The construct was checked by sequencing the entire insert and used as a bait to screen a random-primed human adult brain cDNA library constructed into pP6. pB29 and pP6 derive from the original pBTM116 (Vojtek and Hollenberg, 1995; Béranger et al., 1997) and pGADGH (Bartel et al., 1993) plasmids, respectively.

110 million clones (11-fold the complexity of the library) were screened using a mating approach with YHGX13 (Y187 ade2-101::loxP-kanMX-loxP, mat□) and L40□Gal4 (mata) yeast strains as previously described (Fromont-Racine et al., 1997). 36 His+ colonies were selected on a medium lacking tryptophan, leucine and histidine. The prey fragments of the positive clones were amplified by PCR and sequenced at their 5' and 3' junctions. The resulting sequences were used to identify the corresponding interacting proteins in the GenBank database (NCBI) using a fully automated procedure. A confidence score (PBS, for Predicted Biological Score) was attributed to each interaction as previously described (Formstecher et al., 2005).

Statistical analysis

All data were expressed as means +/- SEM. Unpaired Student's t-test was used for the comparison between two groups. When more than two groups were compared, a one-way ANOVA with multiple comparisons using the post hoc Bonferroni test was carried out using commercially available software (StatView® software, SAS Institute Inc., USA).

Acknowledgments

The research leading to these results has received funding from the European Community's Seventh Framework Programme FP7/2007-2013 under grant agreement no. HEALTH-F5-2008-222925. L.G. was supported by the Neuropôle de Recherche Francilien and the Fondation pour la Recherche Médicale. LF was supported by the French Research Ministry.

References

Benchoua A, Trioulier Y, Diguet E, Malgorn C, Gaillard MC, Dufour N, Elalouf JM, Krajewski S, Hantraye P, Deglon N, Brouillet E (2008) Dopamine determines the vulnerability of striatal neurons to the N-terminal fragment of mutant huntingtin through the regulation of mitochondrial complex II. Hum Mol Genet 17:1446-1456.

Block-Galarza J, Chase KO, Sapp E, Vaughn KT, Vallee RB, DiFiglia M, Aronin N (1997) Fast transport and retrograde movement of huntingtin and HAP 1 in axons. Neuroreport 8:2247-2251.

Brochier C, Gaillard MC, Diguet E, Caudy N, Dossat C, Segurens B, Wincker P, Roze E, Caboche J, Hantraye P, Brouillet E, Elalouf JM, de Chaldee M (2008) Quantitative gene expression profiling of mouse brain regions reveals differential transcripts conserved in human and affected in disease models. Physiol Genomics 33:170-179.

Brouillet E, Jacquard C, Bizat N, Blum D (2005) 3-Nitropropionic acid: a mitochondrial toxin to uncover physiopathological mechanisms underlying striatal degeneration in Huntington's disease. J Neurochem 95:1521-1540.

Charvin D, Vanhoutte P, Pages C, Borrelli E, Caboche J (2005) Unraveling a role for dopamine in Huntington's disease: the dual role of reactive oxygen species and D2 receptor stimulation. Proc Natl Acad Sci U S A 102:12218-12223.

Charvin D, Roze E, Perrin V, Deyts C, Betuing S, Pages C, Regulier E, Luthi-Carter R, Brouillet E, Deglon N, Caboche J (2008) Haloperidol protects striatal neurons from dysfunction induced by mutated huntingtin in vivo. Neurobiol Dis 29:22-29.

de Almeida LP, Ross CA, Zala D, Aebischer P, Deglon N (2002) Lentiviral-mediated delivery of mutant huntingtin in the striatum of rats induces a selective neuropathology modulated by polyglutamine repeat size, huntingtin expression levels, and protein length. J Neurosci 22:3473-3483.

de Chaldee M, Gaillard MC, Bizat N, Buhler JM, Manzoni O, Bockaert J, Hantraye P, Brouillet E, Elalouf JM (2003) Quantitative assessment of transcriptome differences between brain territories. Genome Res 13:1646-1653.

Diguet E, Petit F, Escartin C, Cambon K, Bizat N, Dufour N, Hantraye P, Deglon N, Brouillet E (2009) Normal aging modulates the neurotoxicity of mutant huntingtin. PLoS One 4:e4637.

Drouet V, Perrin V, Hassig R, Dufour N, Auregan G, Alves S, Bonvento G, Brouillet E, Luthi-Carter R, Hantraye P, Deglon N (2009) Sustained effects of nonallele-specific Huntingtin silencing. Ann Neurol 65:276-285.

Faideau M, Kim J, Cormier K, Gilmore R, Welch M, Auregan G, Dufour N, Guillermier M, Brouillet E, Hantraye P, Deglon N, Ferrante RJ, Bonvento G (2010) In vivo expression of polyglutamine-expanded huntingtin by mouse striatal astrocytes impairs glutamate transport: a correlation with Huntington's disease subjects. Hum Mol Genet 19:3053-3067.

Francelle L, Galvan L, Brouillet E (2014) Possible involvement of self-defense mechanisms in the preferential vulnerability of the striatum in Huntington’s disease. Frontiers in Cellular Neuroscience in press.

Galvan L, Lepejova N, Gaillard MC, Malgorn C, Guillermier M, Houitte D, Bonvento G, Petit F, Dufour N, Hery P, Gerard M, Elalouf JM, Deglon N, Brouillet E, de Chaldee M (2012) Capucin does not modify the toxicity of a mutant Huntingtin fragment in vivo. Neurobiol Aging 33:1845 e1845-1846.

Gauthier LR, Charrin BC, Borrell-Pages M, Dompierre JP, Rangone H, Cordelieres FP, De Mey J, MacDonald ME, Lessmann V, Humbert S, Saudou F (2004) Huntingtin controls neurotrophic support and survival of neurons by enhancing BDNF vesicular transport along microtubules. Cell 118:127-138.

Gray M, Shirasaki DI, Cepeda C, Andre VM, Wilburn B, Lu XH, Tao J, Yamazaki I, Li SH, Sun YE, Li XJ, Levine MS, Yang XW (2008) Full-length human mutant huntingtin with a stable polyglutamine repeat can elicit progressive and selective neuropathogenesis in BACHD mice. J Neurosci 28:6182-6195.

Han I, You Y, Kordower JH, Brady ST, Morfini GA (2010) Differential vulnerability of neurons in Huntington's disease: the role of cell type-specific features. J Neurochem 113:1073-1091.

Hottinger AF, Azzouz M, Deglon N, Aebischer P, Zurn AD (2000) Complete and long-term rescue of lesioned adult motoneurons by lentiviral-mediated expression of glial cell line-derived neurotrophic factor in the facial nucleus. J Neurosci 20:5587-5593.

Kuhn A, Goldstein DR, Hodges A, Strand AD, Sengstag T, Kooperberg C, Becanovic K, Pouladi MA, Sathasivam K, Cha JH, Hannan AJ, Hayden MR, Leavitt BR, Dunnett SB, Ferrante RJ, Albin

R, Shelbourne P, Delorenzi M, Augood SJ, Faull RL, Olson JM, Bates GP, Jones L, Luthi-Carter R (2007) Mutant huntingtin's effects on striatal gene expression in mice recapitulate changes observed in human Huntington's disease brain and do not differ with mutant huntingtin length or wild-type huntingtin dosage. Hum Mol Genet 16:1845-1861.

Menalled LB, Sison JD, Dragatsis I, Zeitlin S, Chesselet MF (2003) Time course of early motor and neuropathological anomalies in a knock-in mouse model of Huntington's disease with 140 CAG repeats. J Comp Neurol 465:11-26.

Milnerwood AJ, Raymond LA (2010) Early synaptic pathophysiology in neurodegeneration: insights from Huntington's disease. Trends Neurosci 33:513-523.

Nagamine T, Nomada S, Onouchi T, Kameshita I, Sueyoshi N (2014) Nuclear translocation of doublecortin-like protein kinase and phosphorylation of a transcription factor JDP2. Biochem Biophys Res Commun 446:73-78.

Ohmae E, Ouchi Y, Oda M, Suzuki T, Nobesawa S, Kanno T, Yoshikawa E, Futatsubashi M, Ueda Y, Okada H, Yamashita Y (2006a) Cerebral hemodynamics evaluation by near-infrared time-resolved spectroscopy: correlation with simultaneous positron emission tomography measurements. Neuroimage 29:697-705.

Ohmae S, Takemoto-Kimura S, Okamura M, Adachi-Morishima A, Nonaka M, Fuse T, Kida S, Tanji M, Furuyashiki T, Arakawa Y, Narumiya S, Okuno H, Bito H (2006b) Molecular identification and characterization of a family of kinases with homology to Ca2+/calmodulin-dependent protein kinases I/IV. J Biol Chem 281:20427-20439.

Ross CA, Tabrizi SJ (2010) Huntington's disease: from molecular pathogenesis to clinical treatment. Lancet Neurol 10:83-98.

Ruiz M, Deglon N (2012) Viral-mediated overexpression of mutant huntingtin to model HD in various species. Neurobiol Dis 48:202-211.

Subramaniam S, Sixt KM, Barrow R, Snyder SH (2009) Rhes, a striatal specific protein, mediates mutant-huntingtin cytotoxicity. Science 324:1327-1330.

Tukamoto T, Nukina N, Ide K, Kanazawa I (1997) Huntington's disease gene product, huntingtin, associates with microtubules in vitro. Brain Res Mol Brain Res 51:8-14.

Figures

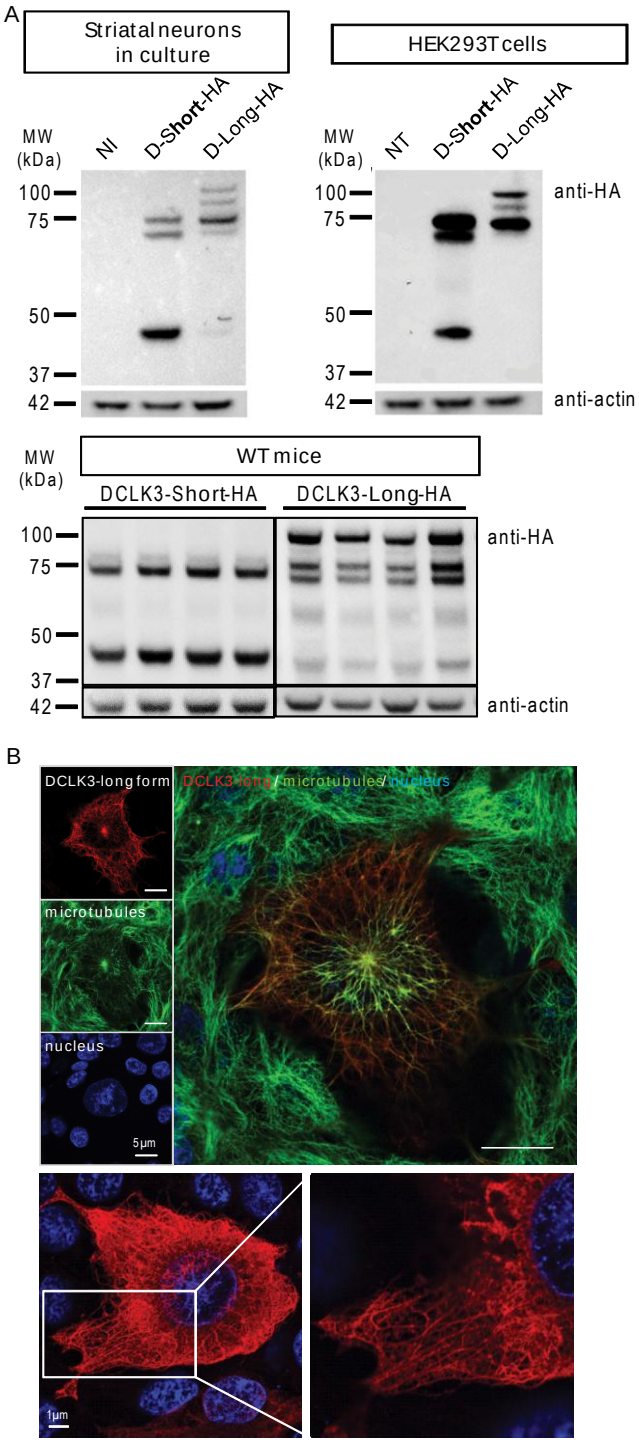

Figure 1: Studies of the cellular localisation of recombinant DCLK3-HA in cultured cells. A, biochemical analysis of overexpressed DCLK3 Short and Long forms in striata neurons in primary culture of rat embryos (upper left), in HEK293T cells (upper right) and in littermate mice, actin as charge control. **B,** immunoflurescence and confocal microscopy of overexpression of Long-DCLK3 in HEK293T cells, detected with anti-HA antibody and Alexa 594 (red), co-staining of microtubules with anti-α-tubulin antibody and Alexa 488 (green) (upper panel), and nucleus of cells with DAPI (blue).

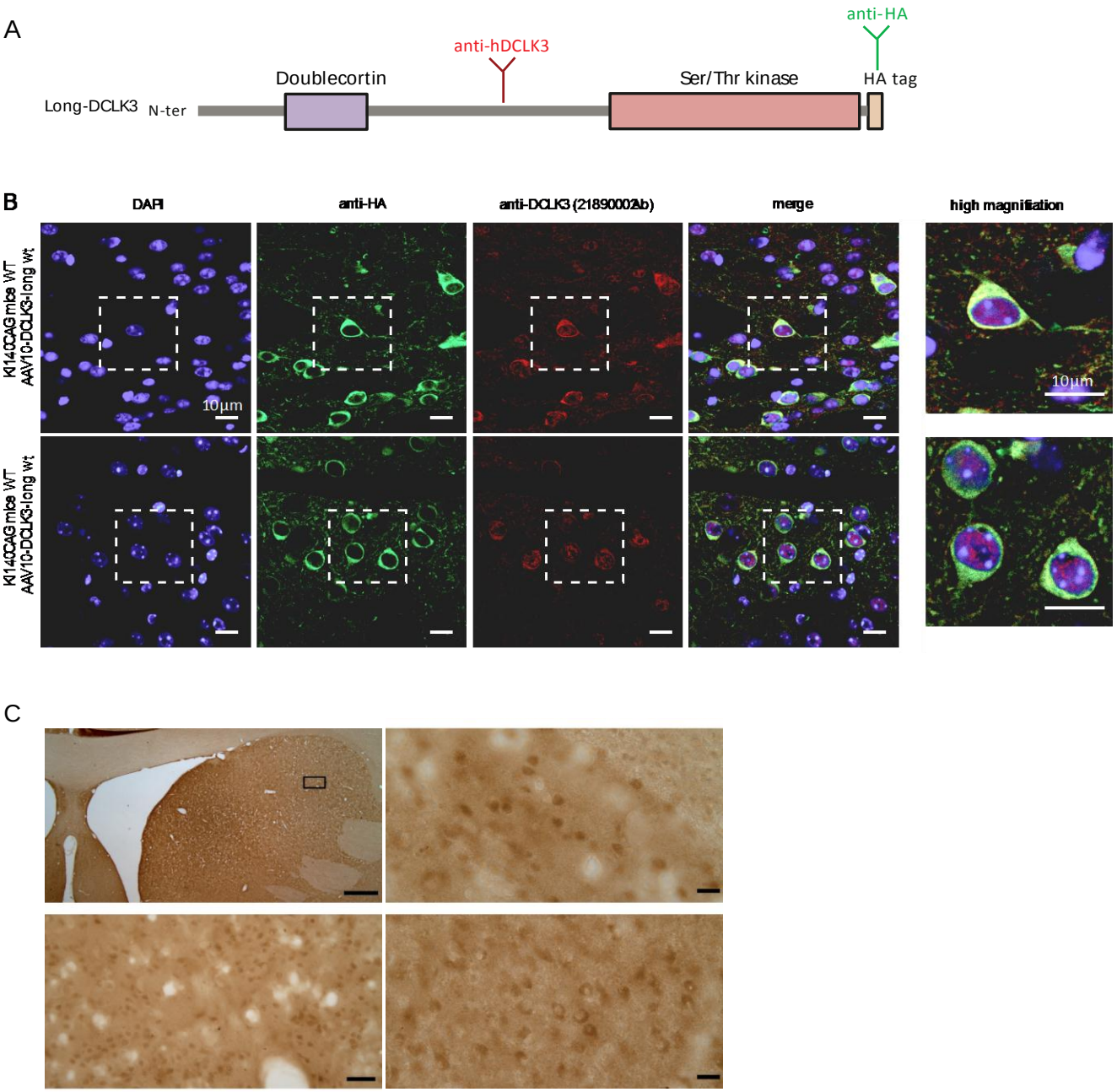

Figure 2: Study of the cellular expression of DCLK3 *in vivo.*

A, Schematic representation of Long-DCLK3-HA tagged sequence construct used to inject mice, and approximate localization of antibodies used to detect DCLK3, with its HA tag (green) or with a small sequence between the doublecortin and the kinase domains (red). **B,** immunoflurescence confocal microscopy SP8 Leica of overexpressed Long-DCLK3 in WT mice. Detection of cell nucleus with DAPI (blue), DCLK3-HA with anti-HA antibody (green), overexpressed and/or endogenous DCLK3 with anti-DCLK3 (21890002 antibody). Merge is the superposition of the DAPI, anti-HA and anti-DCLK3 staining. High magnification is a 40Xobjective picture of the cell boxed in the merge picture. Scale bar 10µm. **C,** Detection of endogenous DCLK3 protein expression in macaque caudate tissue by immunohistochemistry with anti-hDCLK3 antibody. Scale bar: upper left, 1mm; lower left, 50µm; right images, 20µm.

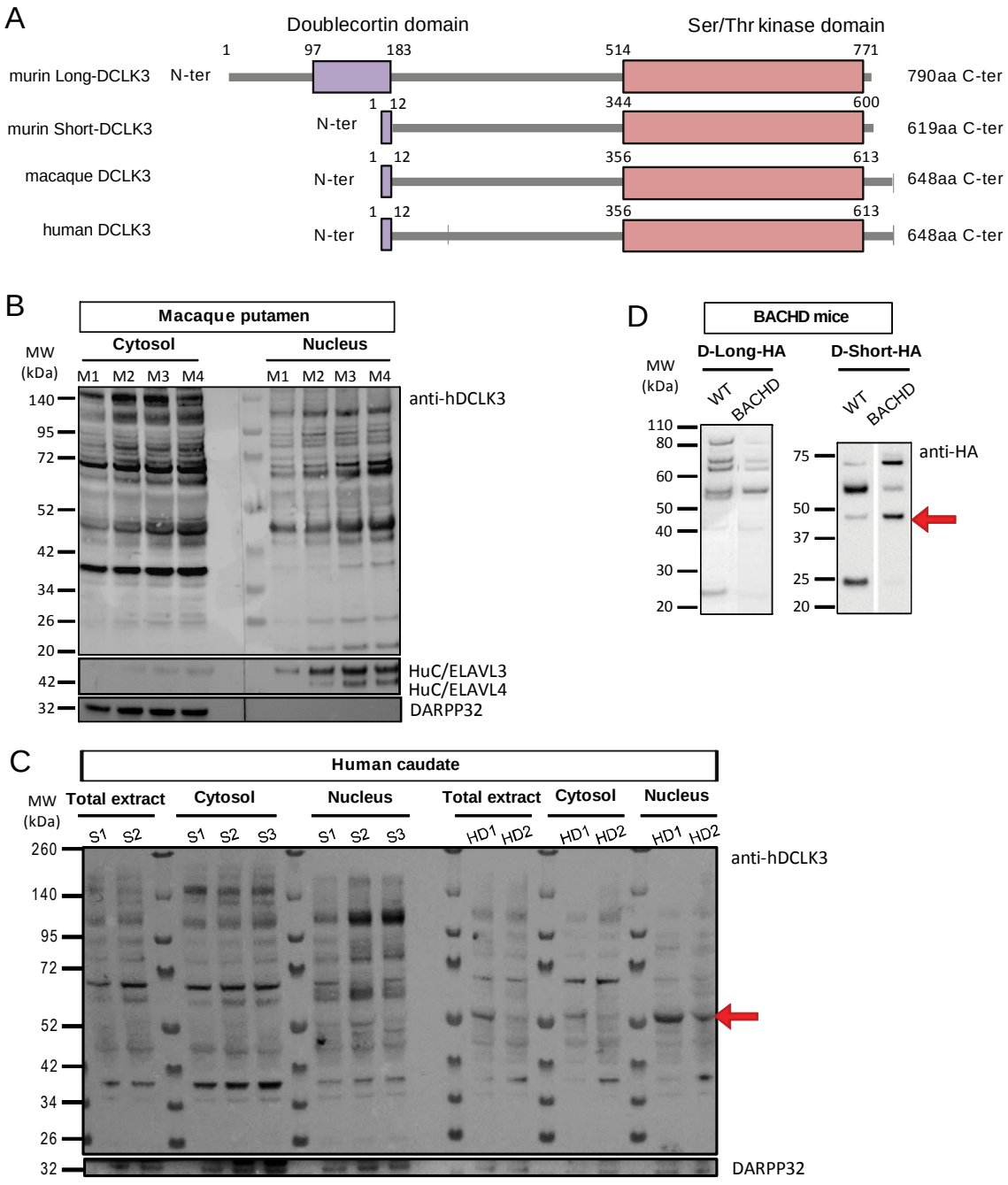

Figure 3: DCLK3 and its cleavage products in normal and HD conditions. A, Schematic representation of DCLK3 sequence in different species according to bioinformatics (Accession number: mouse Q8BWQ5, macaque H9FMA9, human Q9C098). B-D, biochemical analysis of endogenous DCLK3 protein expression in macaque putamen extracts (B) and human caudate extrats (C), and overexpressed DCLK3 Long and Short forms in BACH mice striata after 6 weeks of infection by LV-mediated vectors (D). Red arrows show the similar species between the human mHtt forms from BACHD mice and nuclear HD patients protein extracts (around 50kDa).

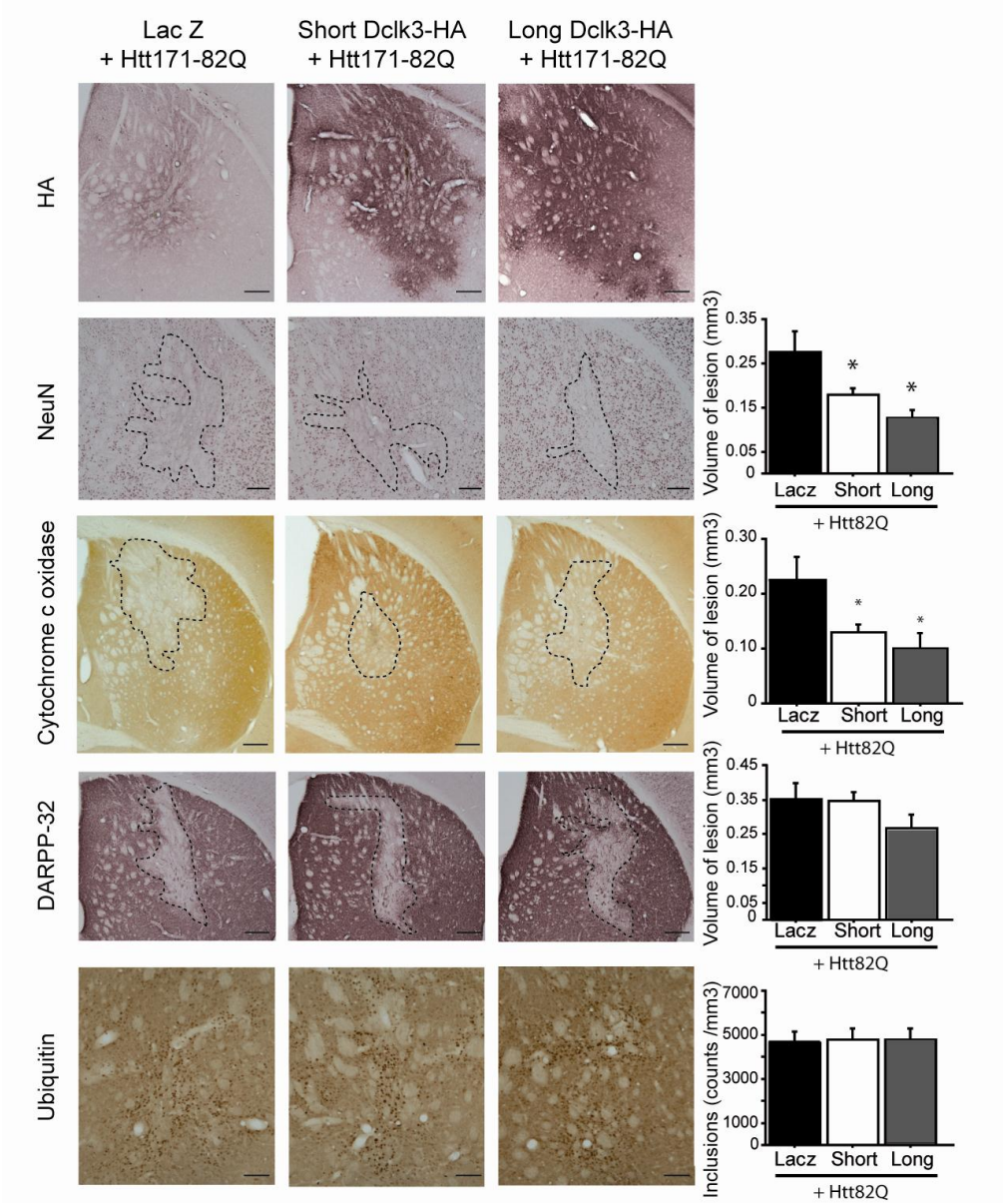

Figure 4: Effect of the overexpression of DCLK3-HA against toxicity induced by m-Htt. Adult male mice received a bilateral intrastriatal injection of a mixture of two lentiviral vectors containing lenti-Htt171-82Q with either lenti-LacZ (control), lenti-S-Dclk3-HA or lenti-L-Dclk3-HA. Six weeks after infection, brains were processed for histological evaluation using DARPP-32-, NeuN- ,Ubiquitin-immunostaining and COX histochemistry to detect Htt171-82Q toxicity. Left panel: typical coronal mouse brain sections display representative area with depleted staining in the different groups. Right panel: histograms representing quantitative determination of the volume of the striatum with depleted staining in the different groups. Immunohistochemical detection of HA-tag indicates the presence of recombinant Dclk3 proteins after infection with lenti-S-Dclk3-HA and lenti-L-Dclk3-HA. The number of Ubiquitin-positive inclusions remains unchanged. Scale bars: 0.2 mm. Results are expressed as mean (n=7-10/group) +/- standard error of the mean. *, p<0.01, One way ANOVA and Fisher PLSD *post hoc* test. Scale bars: HA 0.2mm, NeuN 0.1mm, DARPP32 and Cox 0.5mm and ubiquitin 0.125mm.

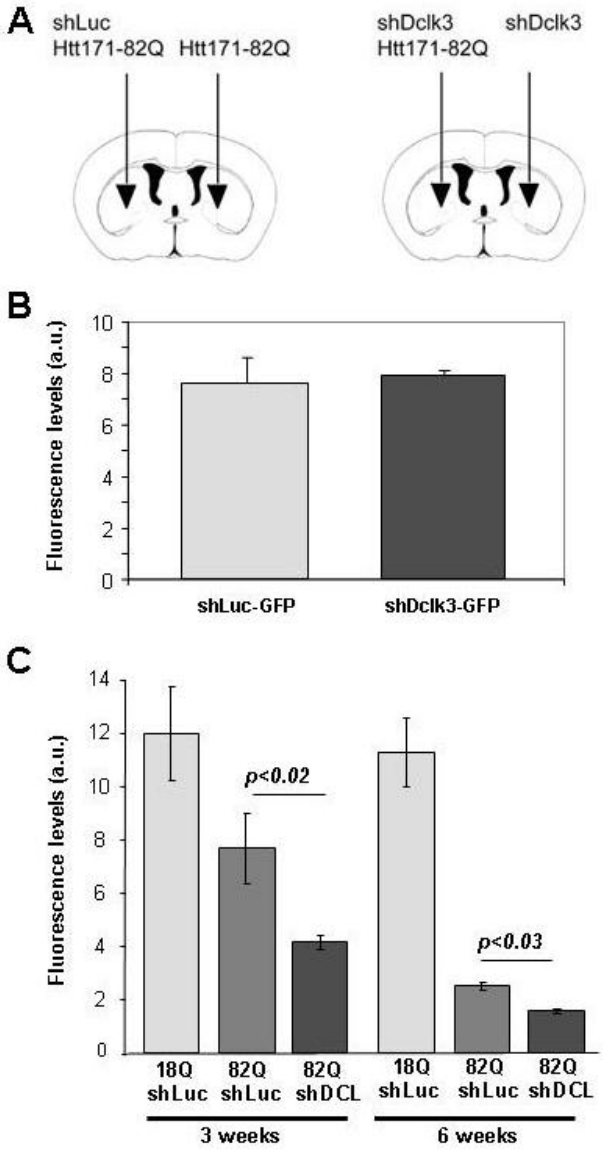
A
shLuc
Htt171-82Q
Htt171-82Q
shDclk3
Htt171-82Q
shDclk3
B
Fluorescence levels (a.u.)
0
2
4
6
8
10
shLuc-GFP
shDclk3-GFP
C
Fluorescence levels (a.u.)
0
2
4
6
8
10
12
14
p<0.02
p<0.03
18Q shLuc
82Q shLuc
82Q shDCL
18Q shLuc
82Q shLuc
82Q shDCL
3 weeks
6 weeks

D

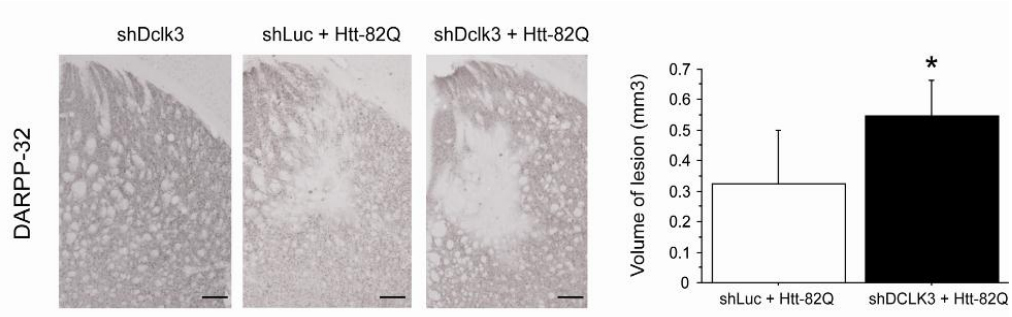
shDclk3
shLuc + Htt-82Q
shDclk3 + Htt-82Q
DARPP-32
Volume of lesion (mm3)
0
0.1
0.2
0.3
0.4
0.5
0.6
0.7
*
shLuc + Htt-82Q
shDCLK3 + Htt-82Q

Figure 5: DCLK3 knock down increases toxicity of mutant Htt *in vivo*. In **A**, mice received lentiviral vectors coding a shRNA targeting either Dclk3 (shDCLK) or luciferase (shLuc) as control. The constructs coding shRNA also code for the GFP. **B,** Three weeks later brain were removed and processed for quantification of GFP fluorescence under microscope observation image analysis. Note that both vectors alone have similar transduction efficacy, expressing same levels of GFP. In **C**, mice were infected with lenti-Htt171-18Q mixed with lenti-shLuc (control levels of GFP) or lenti-Htt171-82Q mixed with lenti-shDLK3 or lenti-shLuc. Quantification of GFP levels was performed at 3 and 6 weeks after infection. Note the levels of GFP are reduced at both time points by lenti-Htt171-82Q when compared to Htt171-18Q, suggesting toxic effect of the mutant protein. Loss of GFP is exacerbated by lenti-shDclk3. Results are expressed as mean (n=7-10/group) +/- standard error of the mean. *, $p<0.01$, One way ANOVA and Fisher PLSD *post hoc* test. **D**, Mice were also infected with lenti-shDclk3 alone (left images). Brain were processed for histological evaluation at six weeks post-infection using DARPP-32 to detect Htt171-82Q toxicity. Left panel: typical coronal mouse brain sections where areas with depleted staining can be seen when Htt171-82Q is expressed. Note that expression of shDclk3 alone produces no change in staining. Right panel: histograms representing quantitative determination of the volume of the striatum with depleted staining in the different groups. Note that shDclk3 leads to a significant increase of the lesion volume determined using DARPP-32. Scale bars = 0.2 mm. Results are expressed as mean (n=7-10/group) +/- standard error of the mean. *, $p<0.01$, Paired Student t test. Scale bars: DARPP-32 0.5mm.

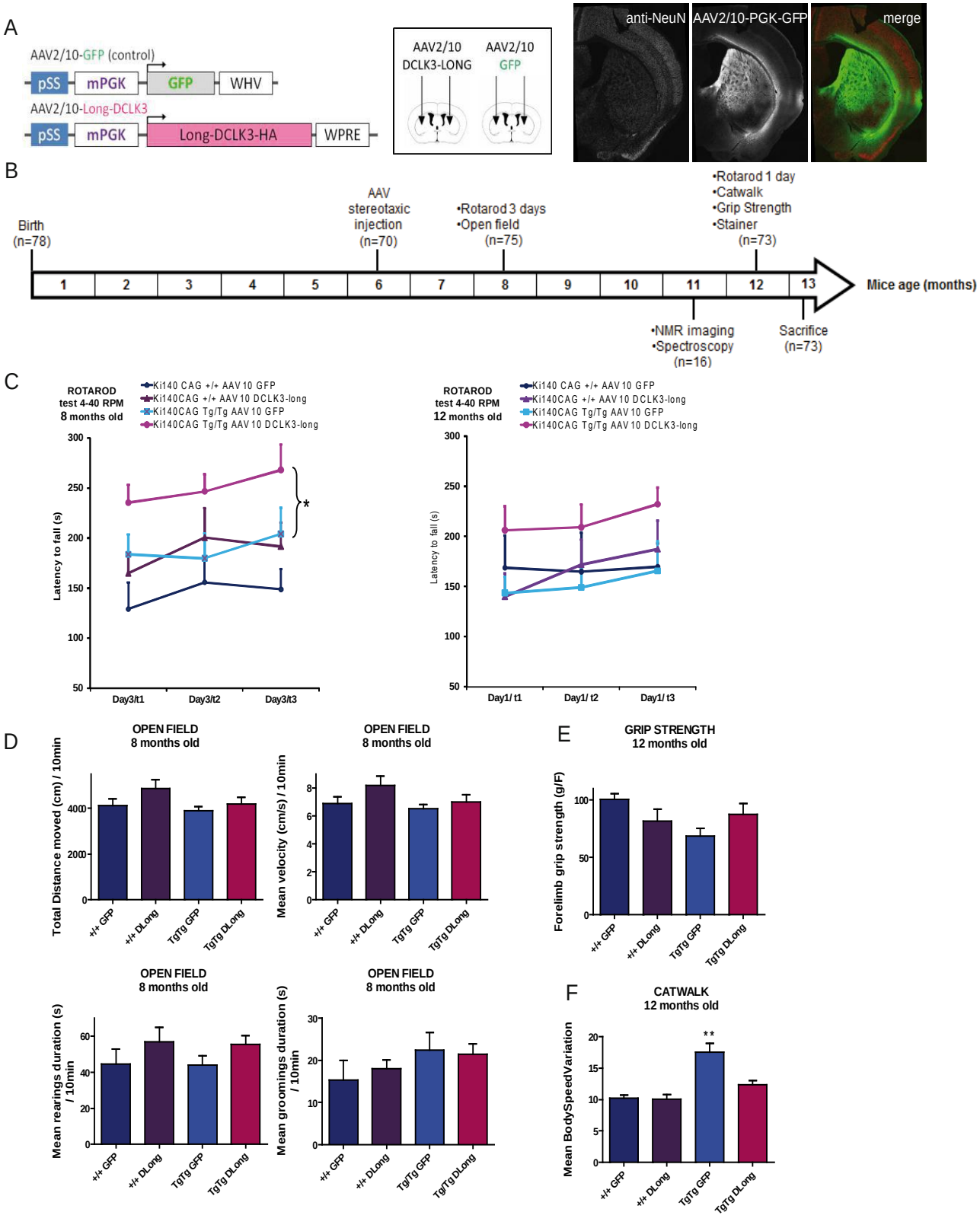
A
AAV2/10-GFP (control)
pSS
mPGK
GFP
WHV
AAV2/10-Long-DCLK3
pSS
mPGK
Long-DCLK3-HA
WPRE
AAV2/10 DCLK3-LONG
AAV2/10 GFP
anti-NeuN
AAV2/10-PGK-GFP
merge
B
Birth (n=78)
AAV stereotaxic injection (n=70)
•Rotarod 3 days
•Open field
(n=75)
•Rotarod 1 day
•Catwalk
•Grip Strength
•Stainer
(n=73)
1 2 3 4 5 6 7 8 9 10 11 12 13
Mice age (months)
•NMR imaging
•Spectroscopy
(n=16)
Sacrifice
(n=73)
C
ROTAROD
test 4-40 RPM
8 months old
Ki140 CAG +/+ AAV 10 GFP
Ki140CAG +/+ AAV 10 DCLK3-long
Ki140CAG Tg/Tg AAV 10 GFP
Ki140CAG Tg/Tg AAV 10 DCLK3-long
Latency to fall (s)
Day3/t1
Day3/t2
Day3/t3
ROTAROD
test 4-40 RPM
12 months old
Day1/ t1
Day1/ t2
Day1/ t3
D
OPEN FIELD
8 months old
Total Distance moved (cm) / 10min
Mean velocity (cm/s) / 10min
Mean rearings duration (s) / 10min
Mean groomings duration (s) / 10min
+/+ GFP
+/+ DLong
TgTg GFP
TgTg DLong
E
GRIP STRENGTH
12 months old
Forelimb grip strength (g/F)
F
CATWALK
12 months old
Mean BodySpeedVariation

Figure 6: Study of the effects of overexpression of L- DCLK3 using AAV10 in KI140 mice.

A, Schematic representation of adeno-associated-virus (AAV) constructs used to overexpressed GFP (control) or DCLK3 in mice using AAV10-GFP (left), and typical picture of GFP expression in the striatum of mice after injection of AAV10-GFP, showing that GFP in green is expressed in a wide volume of the striatum (NeuN staining in red).

B, Time course and experimental design. Mice were injected with AAV10-GFP or DCLK3 at around 6 months old performed 3 days-rotarod test and open-field test at 8 months old, spectroscopy at 11 months old, 1 day-rotarod test, catwalk and gripstrenght at 12 months old and sacrificed at 13 months old.

C, Accelerated rotarod test using procol 4-40RPM with a maximum of 5minutes on the rotarod, for three tests (t1,2,3) by day during three consecutive days (Day1,2,3) on 8 months old mice (left panel =only performances of the Day3 shown) or during one day on 12 months old mice (right panel). n=7 by group; *, $p<0.01$.

D, Open field results on 8 months old mice of total distance moved, velocity of deplacement, rearing and grooming duration (in sec) over 10 minutes of test.

E, Forelimb grip strength results in g/F of 12 months old mice. Histograms represent the mean of 3 assays.

F, Catwalk parameter “mean body speed variation”measured on 12 months old mice. This parameter is calculated by dividing the absolute difference between the body speed and the average speed of a run by the average speed.

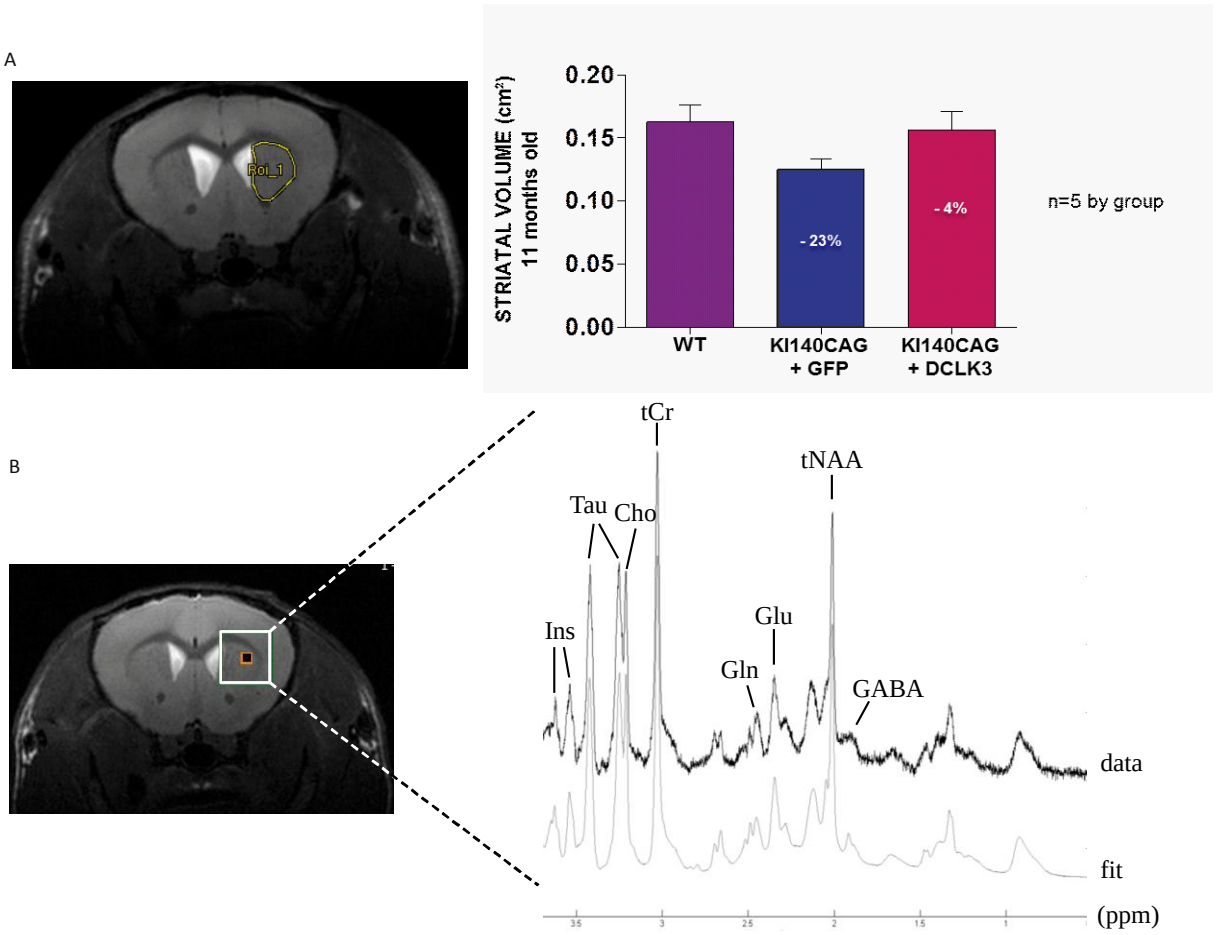

Figure 7: MRI and NMR spectroscopy analyses in KI140 mice infected with AAV10.

A, T2 MRI representative image and histogram of striatal volumes. **B,** typical spectroscopy spectrum showing brain metabolites. **C,** histograms showing changes in KI140CAG mice as compared to littermate controls and the effects of AAV-Dclk3 and AAV-GFP.

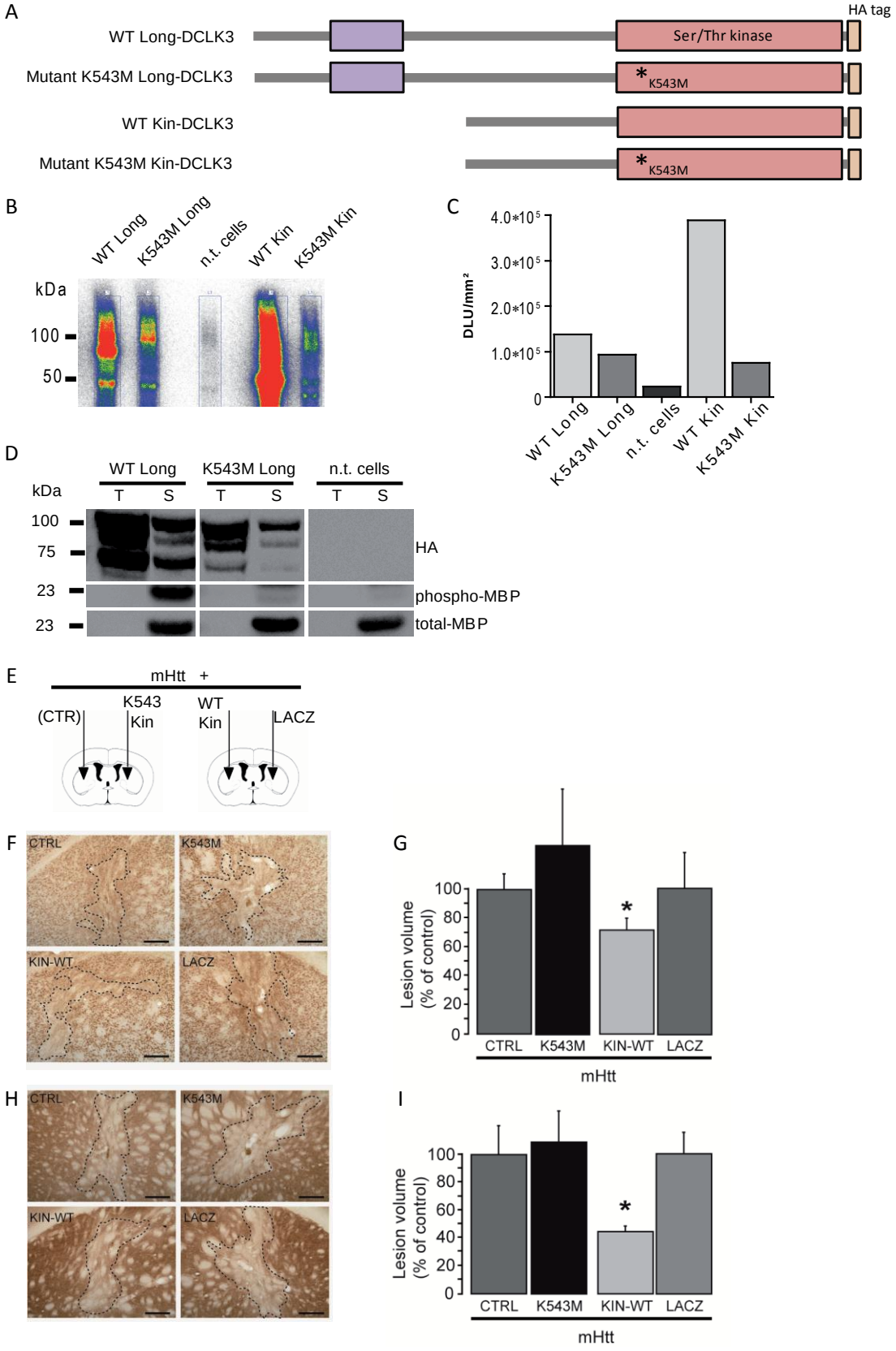
A
HA tag
WT Long-DCLK3
Ser/Thr kinase
Mutant K543M Long-DCLK3
*K543M
WT Kin-DCLK3
Mutant K543M Kin-DCLK3
*K543M
B
WT Long
K543M Long
n.t. cells
WT Kin
K543M Kin
kDa
100
50
C
DLU/mm²
4.0*10⁵
3.0*10⁵
2.0*10⁵
1.0*10⁵
0
WT Long
K543M Long
n.t. cells
WT Kin
K543M Kin
D
WT Long
K543M Long
n.t. cells
kDa
T S T S T S
100
75
23
23
HA
phospho-MBP
total-MBP
E
mHtt +
(CTR)
K543 Kin
WT Kin
LACZ
F
CTRL
K543M
KIN-WT
LACZ
G
Lesion volume (% of control)
100
80
60
40
20
0
*
CTRL
K543M
KIN-WT
LACZ
mHtt
H
CTRL
K543M
KIN-WT
LACZ
I
Lesion volume (% of control)
100
80
60
40
20
0
*
CTRL
K543M
KIN-WT
LACZ
mHtt

Figure 8: The kinase domain of DCLK3 is sufficient to protect against mHtt in vivo.

A, Schematic illustrations of Long- and Kin-DCLK3 constructs with or without the mutation K543M used in the present study.

B, Autophosphorylation experiments with incorporation of ATP [γ-32P] after co-immunoprecipitation of DCLK3-HA with anti-HA antibody, and at final detection of radioactivity with PhosphoImager apparatus. Colors represent the intensity of radioactivity signal (from white (no signal) to red (highest intensity of signal).

C, pseudo-quantification of the intensity of signal obtained after detection of radioactivity signal.

D, Activity kinase assays using myelin basic protein (MBP) as a universal kinase substrate after co-immunoprecipitation of DCLK3-HA, wt and mutant K543M forms with anti-HA constructs, and detection of phosphorylated MBP (phosphor-MBP) and total MBP. T=input (total protein extract before co-IP), S=sample test, n.t.=non transfected cells (control).

E - I, Adult male mice received a bilateral intrastriatal injection of lenti-Htt171-82Q mixed with either lenti-Lacz (control) or a lentiviral vector coding for the kinase domain of Dclk3 (lenti-KinDclk3) containing or not the mutation lysine→methionin on the position 543aa (K543M or KIN-WT) **(E)**. Six weeks after infection, brains were processed for histological evaluation using NeuN **(F)** and COX **(H)** histochemistry to assess Htt171-82Q toxicity. Histograms represent quantitative determination of the volume of the striatum with depleted staining in the different groups for NeuN **(G)** and COX **(I)**. Scale bars = 0.2 mm. Results are expressed as mean (n=7/group) +/- standard error of the mean. * Unpaired Student t-test $p<0.05$.

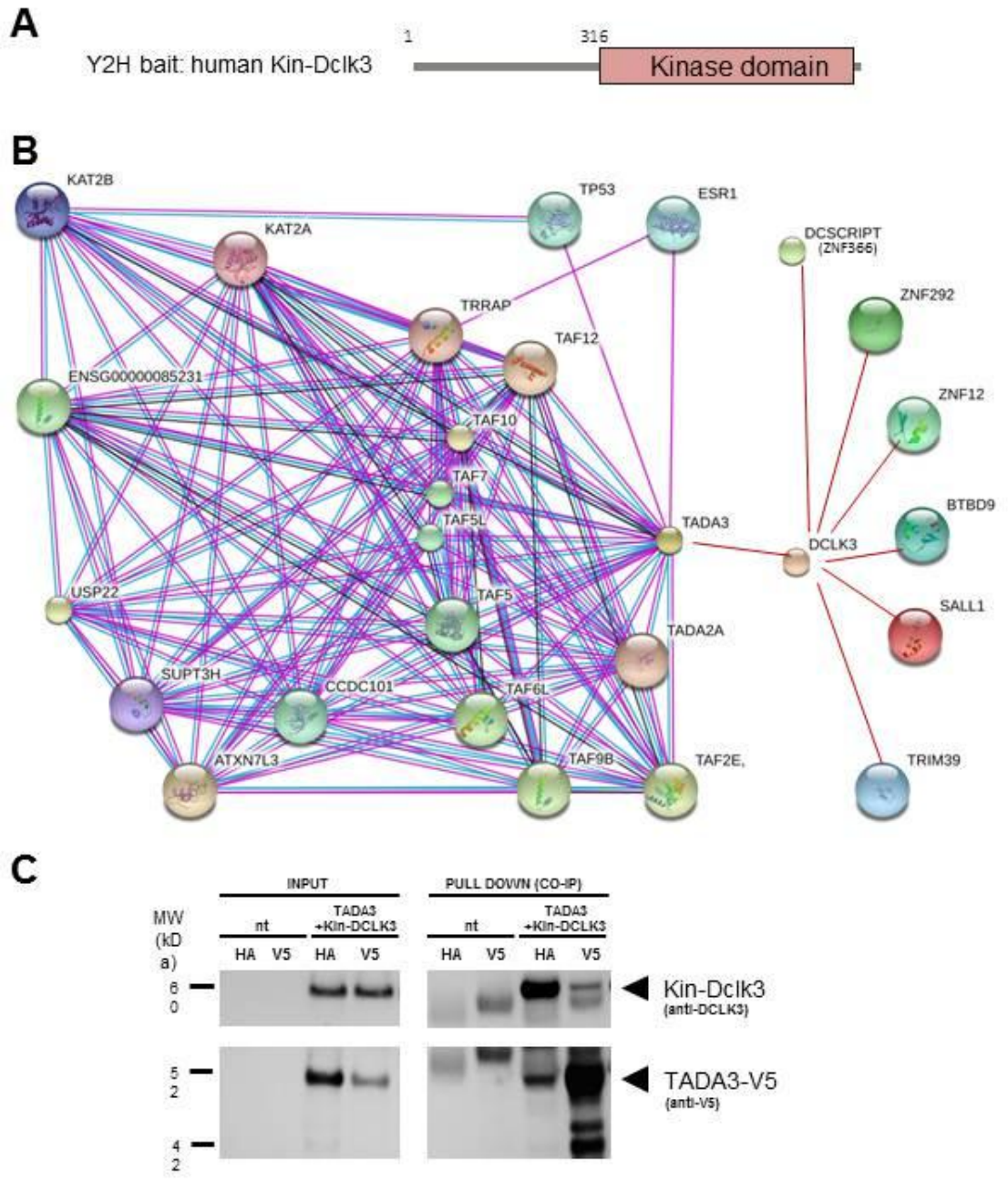

Figure 9: Yeast two-hybrid screen of interactors of the kinase domain of DCLK3.

A, The C-terminal domain of human Kin-Dclk3 was used as bait to screen a human brain mRNA library (A). Seven interactors were found to interact with Dclk3 (red link). **B**, String 9.1 bioinformatics software was used to search for secondary interactors (human only) in public databases and to schematically represent the network of interactions using only high confidence criteria. **C**, interaction between Kin-Dclk3 and TADA3 (Transcriptional adapter 3) was verified by pull-down experiments (CO-IP, Co-immunoprecipitation) after transfection of HEK cells with plasmids coding mouse Dclk3-HA and human TADA3-V5.

SUPPLEMENTARY FIGURES

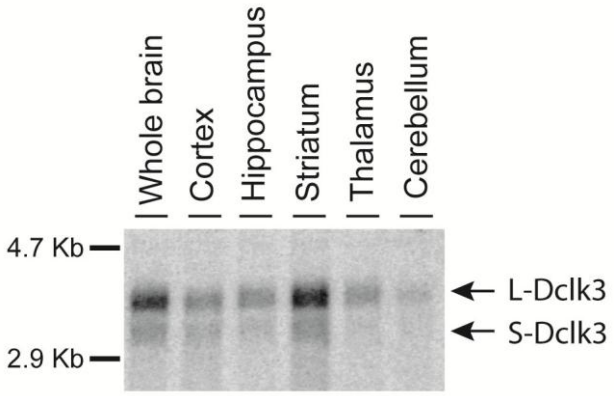

Figure S1: Expression of DCLK3 mRNAs in the brain. Northern blot analysis was performed using RNA extracts prepared from brains from wild-type mice. The membrane was hybridized with a probe corresponding to a *Pst* I fragment of the Dclk3 transcribed DNA sequence. Note the preferential expression in the striatum and the presence of two mRNA species: the upper band corresponds to the long form of Dclk3 (L-Dclk3 mRNA), the lower and fainter band corresponds to the short form of Dclk3 (S-Dclk3 mRNA).

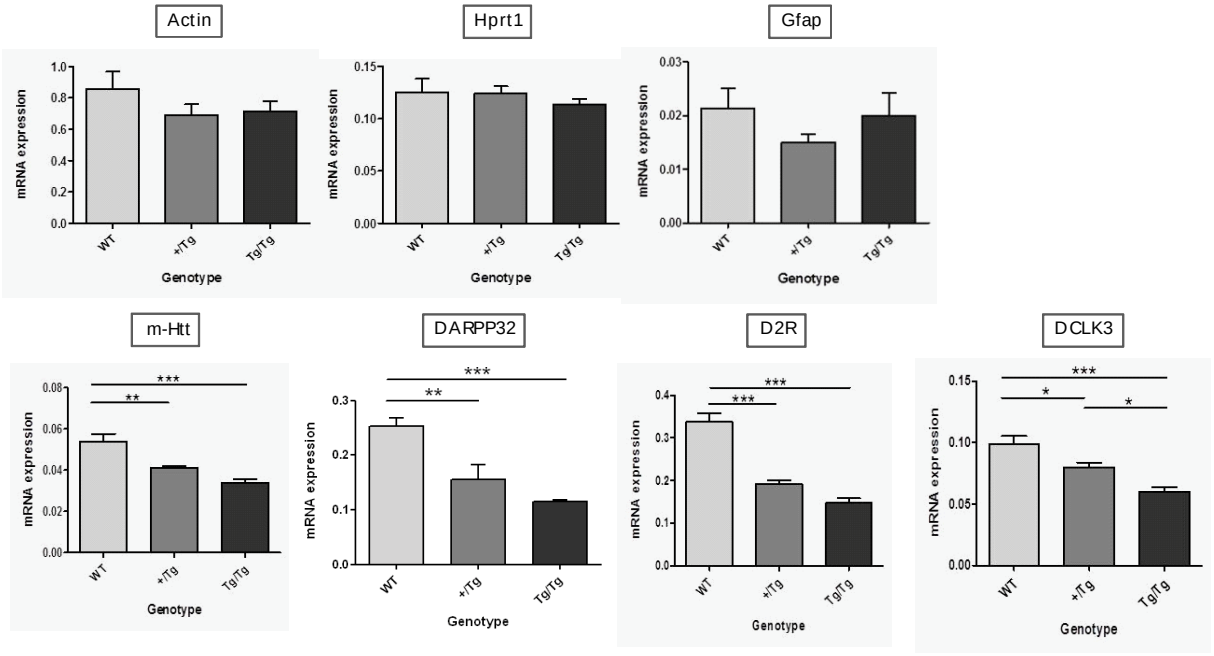

Figure S2: Loss of DCLK3 expression in adult HD KI140 mice.

Gene expression measured by RT-qPCR in 10-13 months-old Ki140CAG mice.

Results are presented as mean +/- standard error of the mean. +/+=WT littermate mice; +/Tg=heterozygous (140Q/+); Tg/Tg=homozygous (140Q/140Q) knock-in mice carrying an expanded CAG repeat.

Actin P=0.3727, F=1.040, ns; Hprt1 P=0.6523, F=0.4369, ns; GFAP P=0.44787, F=0.7659, ns.

*, p<0.05, **, p<0.001, ***, p<0.0001 n=8, One way ANOVA and Bonferroni post hoc.

m-Htt F=17.10, WTvs+/Tg t=3.488; WTvsTg/Tg t=5.775; +/Tg vs Tg/Tg t=1.858.

DARPP32 F=46.72, WTvs+/Tg t=7.058; WTvsTg/Tg t=9.249; +/Tg vs Tg/Tg t=2.191.

D2R F=29.69, WTvs+/Tg t=4.344; WTvsTg/Tg t=7.578; +/Tg vs Tg/Tg t=1.844.

DCLK3 F=15.43, WTvs+/Tg t=2.688; WTvsTg/Tg t=5.555; +/Tg vs Tg/Tg t=2.867.

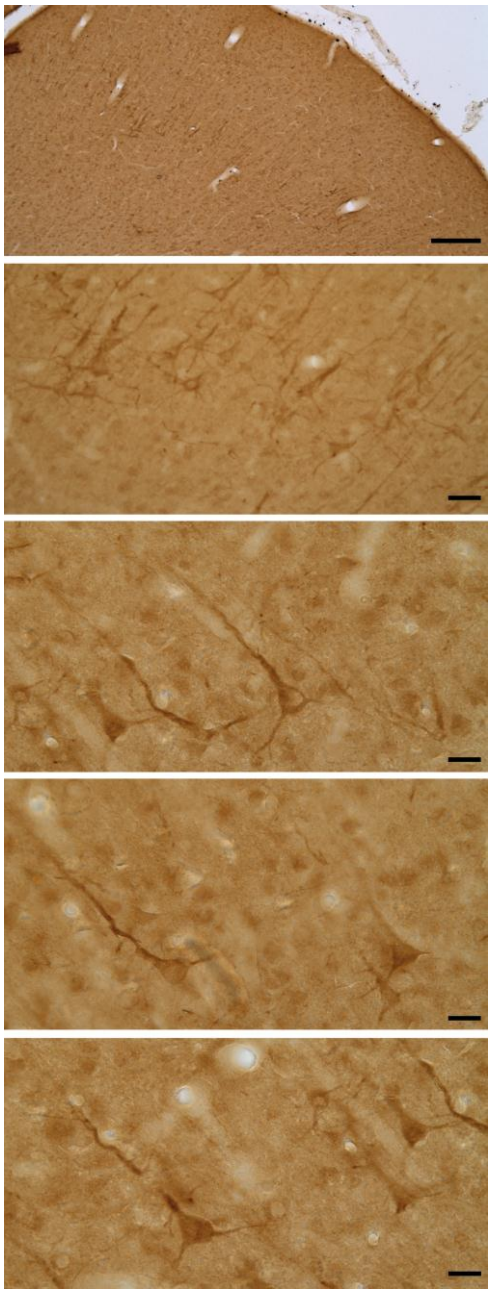

Figure S3: Expression of endogenous DCLK3 in the macaque brain.

Detection of endogenous DCLK3 expression in the cortex of macaque by immunohistochemistry using anti-DCLK3 antibody (21890002).

Scale bars, from top to bottom: 1 mm, 50 µm, 20 µm, 20 µm.

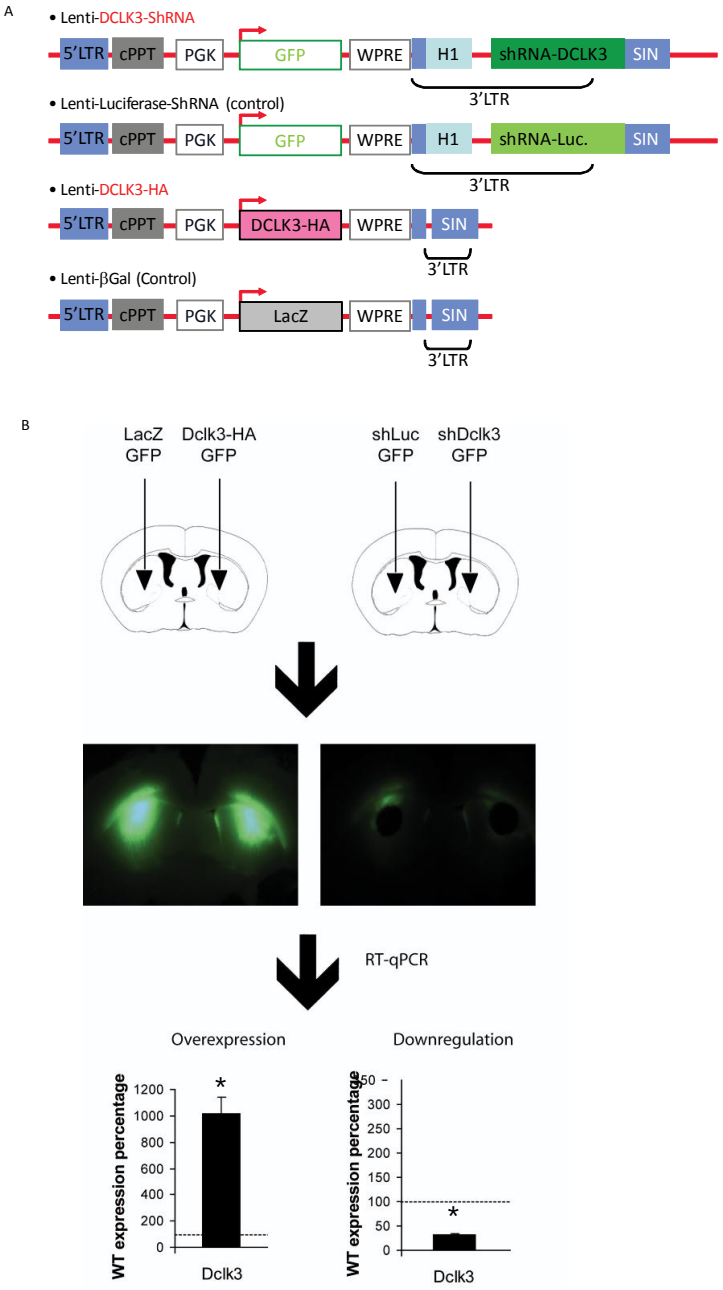

Figure S4: Efficiency of lentiviral vectors coding DCLK3-HA and its shRNA.

A, Schematic representation of lentiviral sequence used to overexpressed or silence DCLK3 expression in mice. **B,** Mice were injected in the striatum with LV-DCLK3-HA (mixed with lentiviral vector coding for GFP) or LV-shDCLK3 (biscistronic construct also coding GFP). Six weeks later the striatal region expressing GFP mice was dissected out and analyzed using qRT-PCR. Note that the level of expression using LV-Short-DCLK3-HA was approximately 10 times that of the endogenous mRNA. Similar results were obtained with Long-DCLK3-HA. LV-shDCLK3 produced a significant ~70% reduction of DCLK3 expression. Results are expressed as mean +/- standard error of the mean. *, p<0.01, Unpaired Student *t* test.

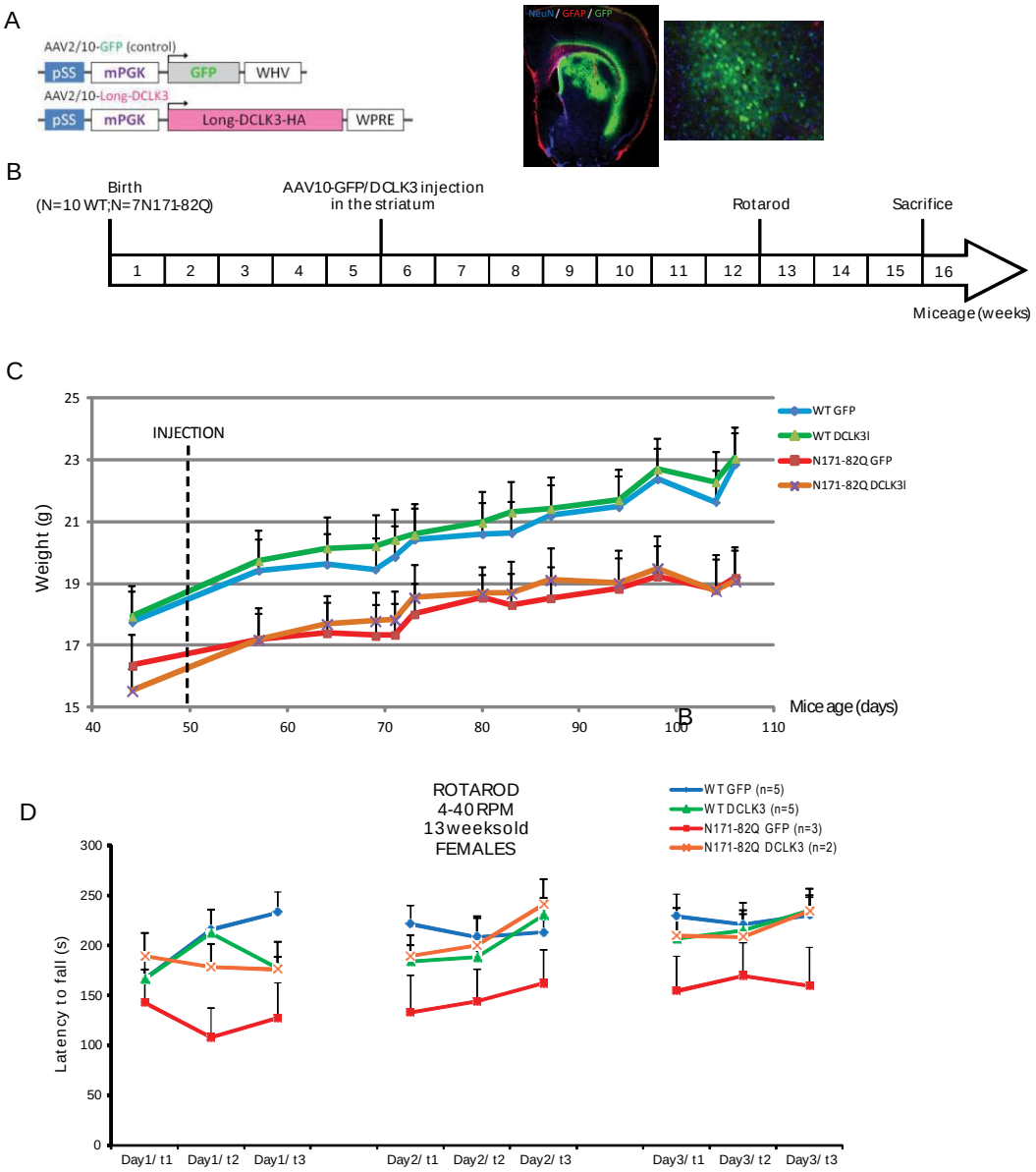

Figure S5: Pilot study in N171-82Q mice with AAV- DCLK3.

A, Schematic representation of adeno-associated-virus (AAV) constructs used to overexpressed GFP (control) or DCLK3 in mice using AAV10-GFP (left), and typical picture of GFP expression in the striatum of mice after injection of AAV10-GFP, showing that GFP in green is expressed in a wide volume of the striatum without massive inflammation (GFAP positive cells in the needle track only =yellow staining).

B, Time course and experimental design. Mice were injected with AAV10-GFP or DCLK3 at 6 weeks old, performed rotarod test at 13 weeks old and sacrificed at 16 weeks old. **C,** Weight in gram (g) of N171-82Q mice measured before and after stereotaxic injection of AAV10- GFP or DCLK3 until sacrifice. **D,** Accelerated rotarod test using procol 4-40RPM with a maximum of 5minutes on the rotarod, three tests (t1,2,3) by day during three consecutive days (Day1,2,3).

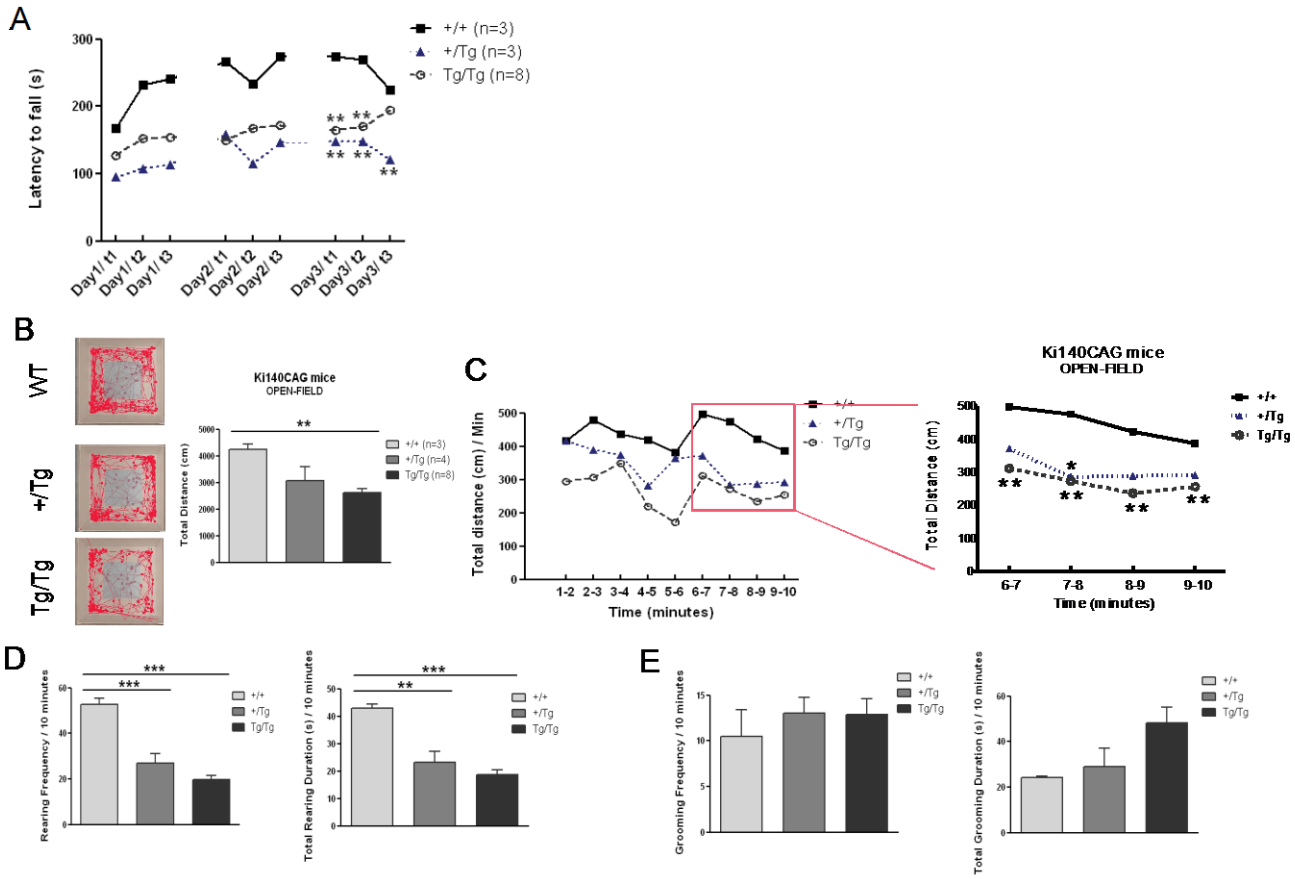

Figure S6: Characteristics of the KI140 mice and wildtype littermates in the colony.

A, Rotarod (n=3 wildtype (WT) (control), n=3 +/Tg heterozygous mice, n=8 Tg/Tg homozygous mice; Two-way ANOVA P=0,0041; F=4,712; Bonferroni *post-hoc* **P<0,01).

B, Movement tracking in red analysed with Ethovision software, and measure of the total distance moved (n=3 WT, n=4 +/Tg heterozygous, n=8 Tg/Tg homozygous; One-way ANOVA P=0,0086; F=7,257; Bonferroni *post-hoc* WT VS Tg/Tg homozygous).

C, Total distance moved by bin of one minute over 10 minutes and statistics done on the four last minutes of distance moved showing differences between WT and heterozygous/homozygous mice; Two-way ANOVA; Bonferroni *post-hoc* *P<0,05; **P<0,01. **D,** Rearing frequency and duration. **E,** Grooming frequency and duration.

A

B

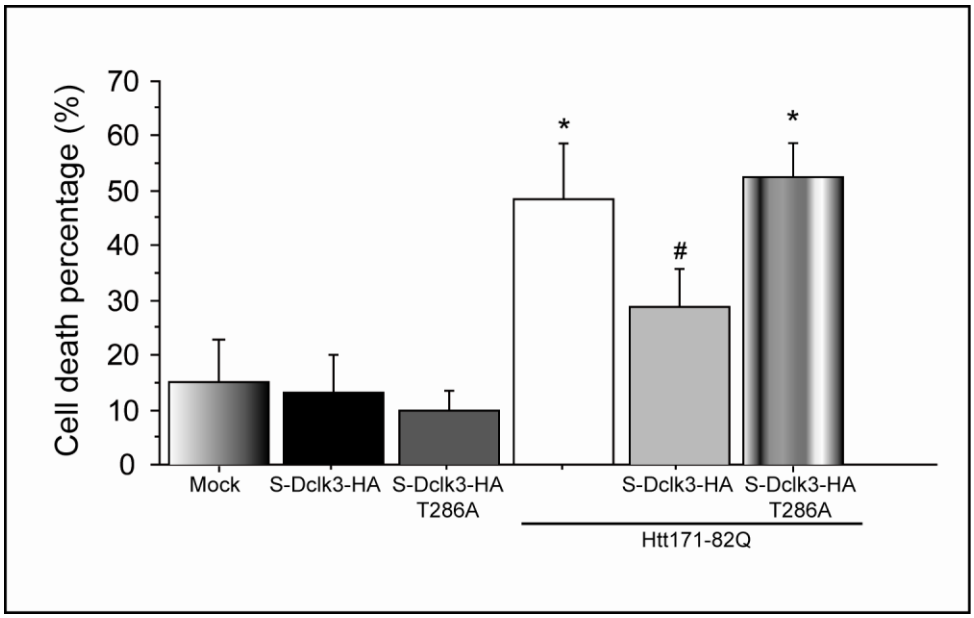

Figure S7: Mutation of Short-DCLK3 abrogates neuroprotective effects against Htt171-82Q. A, Schematic illustration of Short-DCLK3 construct and position of the T286A mutation used in the present study on the sequence. **B**, Primary culture of striatal neurons were transfected by electroporation with plasmids coding wild type S-DCLK3-HA or S- DCLK3 with T286→ Ala substitution alone or in combination with a plasmid coding Htt171-82Q. Forty eight hours later, cells were fixed and transfected neurons displaying apoptotic nuclei were counted. Note that while S-Dclk3-HA reduced Htt171-82Q-induced cell death, the T286A mutant is ineffective. Results are expressed as mean +/- standard error of the mean and correspond to three independent experiments each including 3-4 slides per experimental group. *, $p<0.01$ as compared to mock transfection, #, $p<0.01$ compared to Htt171-82Q alone. One way ANOVA and Fisher's post hoc PLSD test.

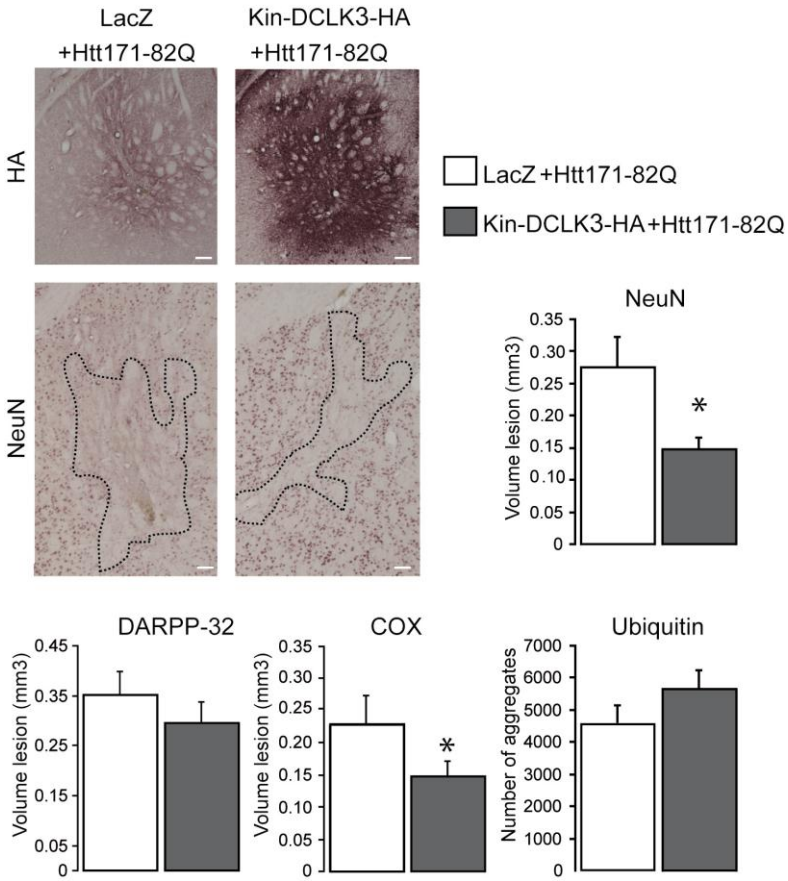

Figure S8: Overexpression of Kin-DCLK3-HA in mice protects against mutant Htt. Adult male mice received a bilateral intrastriatal injection of lenti-Htt171-82Q mixed with either lenti-Lacz (control) or a lentiviral vector coding for the kinase domain of DCLK3 (lenti-KinDclk3). Six weeks after infection, brains were processed for histological evaluation using NeuN, DARPP-32 and Ubiquitin-immunostaining and COX histochemistry to assess Htt171-82Q toxicity. Histograms represent quantitative determination of the volume of the striatum with depleted staining in the different groups. The number of Ubiquitin-positive inclusions is not significantly changed by the lenti-Kin- DCLK3 compared to control. Scale bars = 0.2 mm. Results are expressed as mean (n=7-10/group) +/- standard error of the mean. *, $p<0.01$, Paired Student t test.

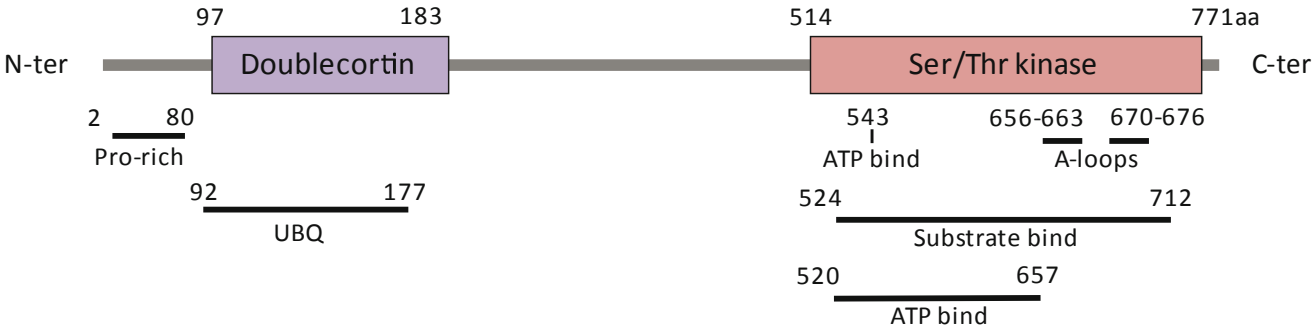

Figure S0: Dclk3 bioinformatics domain/active sites.

Using bioinformatics (mainly UniProt and NCBI Gene databases), active domain and sites are predicted in the murin sequence of Long-Dclk3 (UniProtKB/Swiss-Prot Q8BWQ5; mRNA→ protein: NM_172928.5 → NP_766516.2).

Pro-rich domain is a plateform for protein-protein interactions, particularly regulatory proteins interacting at the pro-rich domain may regulate microtubule-binding activity of Dclk3.

UBQ: ubiquitin like protein (weak description).

A-loops: activation loop (polypeptide region), that can be phosphorylated to strongly activate Dclk3.

ATP-bind: selective and non-covalently interaction site with ATP, adenosine 5'-triphosphate.

PART4 GENERAL DISCUSSION

The main objective of my thesis was to further characterize three striatal markers (Abhd11os, CRYM and DCLK3) in order to better understand the putative molecular mechanisms underlying their neuroprotective effects against a toxic fragment of mHtt.

4.1. Abhd11os

The elucidation of the mechanisms underlying the neuroprotective effects of Abhd11os overexpression against mHtt toxicity will require further studies.
However, we confirmed the bioinformatics data, i.e. Abhd11os is a long intergenic non-coding (linc) RNA, which corresponds to a long non-coding (lnc) RNA transcribed from non-coding DNA sequences between protein-coding genes. lincRNAs are an important subgroup of lncRNAs (Guttman et al 2009). Indeed, lncRNAs include heterogeneous regulatory molecules such as lincRNAs and natural antisense transcripts (NATs) (Salta & De Strooper 2012). As described in our publication, lncRNAs are un-translated transcripts with longer than 200 nucleotides, which possess many of the structural characteristics of messenger RNAs (mRNA), including a poly A tail, 5' capping, and a promoter structure, but not full or functional open reading frame (**Table 3**). Moreover, lncRNA expression patterns change during differentiation and exhibit a variety of splicing patterns. Many lncRNAs are expressed at specific times and in specific tissues during development (see as review (Kung et al 2013, Ponting et al 2009, Ulitsky & Bartel 2013)).

mRNA	lncRNA
Tissue-specific expression	Tissue-specific expression
Form secondary structure	Form secondary structure
Undergo post-transcriptional processing, i.e. 5'cap, polyadenylation, splicing	Undergo post-transcriptional processing, i.e. 5'cap, polyadenylation, splicing
Important roles in dieases and development	Important roles in diseases and development
Protein coding transcript	Non-protein coding, regulatory functions
Well conserved between species	Poorly conserved between species
Present in both nucleus and cytoplasm	Predominantly in nucleus
Total 20-24,000 mRNAs	Predicted 3-100 fold of mRNA in number
Expression level: low to high	Expression level: very low to moderate

Table 3 Similarities (gray) and differences (cyan) between mRNA and lncRNA.

Literature on lincRNAs is recent, but functional roles are predicted and for some of them already experimentally validated (**Figure 16**).

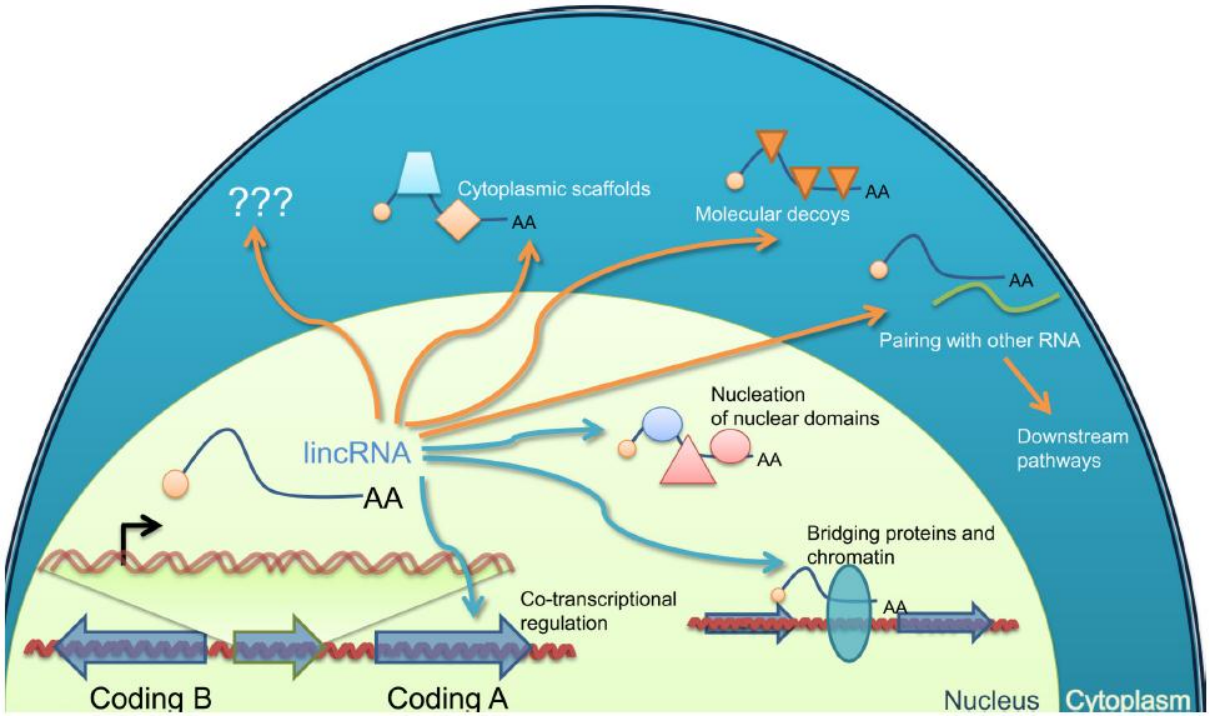

Figure 16 Diverse Mechanisms Proposed for lincRNA Function (Ulitsky & Bartel 2013).

According to the review of Ulitsky 2013, the modes of action of lincRNA include co-transcriptional regulation (e.g., through either the interaction of factors with the nascent lincRNA transcript or the act of transcribing through a regulatory region), regulation of gene expression through recruitment of proteins or molecular complexes to specific loci, scaffolding of nuclear or cytoplasmic complexes, titration of RNA-binding factors, and pairing with other RNAs to trigger post-transcriptional regulation. The two latter mechanisms take place in the cytoplasm (where they are more frequently reported) but could also occur in the nucleus. Additional mechanisms will presumably be proposed as additional functions of lincRNAs are discovered (Ulitsky & Bartel 2013).

Previously Guttman and colleagues speculated that many lincRNAs may be involved in transcriptional control—perhaps by guiding chromatin remodeling proteins to target loci—and that some transcription factors and lincRNAs may act together, with the transcription factor activating a transcriptional program and the lincRNA repressing a previous transcriptional program (Guttman et al 2009, Khalil et al 2009).
In this view, it would be tempting to speculate that Abhd11os could produce a neuroprotective effect as a negative regulator of transcription whose deregulation plays a central role in HD pathogenesis. This is in line with the current hypothesis of a central role of ncRNA in neurodegenerative disorders (Johnson & Buckley 2009, Johnson et al 2012, Johnson et al 2008, Salta & De Strooper 2012).
Testing these speculations will require biochemical and genetic studies, including gene knockdown in appropriate settings. Several techniques have been developed to identify the genomic targets of lncRNAs (Kung et al 2013).

Based on principles of both chromatin immunoprecipitation (ChIP) and RIP, chromatin RNA immunoprecipitation (ChRIP) can be used to identify RNAs associated with a particular chromatin mark (Pandey et al 2008). On the other hand, techniques such as chromatin oligo-affinity precipitation (ChOP) (Mariner et al 2008), chromatin isolation by RNA purification (ChIRP) (Chuet al.2011), and capture hybridization of RNA targets (CHART) (Simon et al 2011) use tagged complementary oligonucleotides to identify DNA loci that interact with an RNA of interest.

It would be interesting to develop this kind of techniques in the laboratory to better characterize Abhd11os and find the precise mechanisms of function of this lincRNA, first in an healthy context, then compared to an HD situation.

As Abhd11os is a rare lincRNA to have an impact on mHtt toxicity in HD, it would be necessary to overexpress it in others HD models to confirm his neuroprotective effects.

Depending on the functions of Abhd11os discovered then, it would have an impact on others diseases than neurodegenerative disorders. For example, lncRNAs play an important role in tumorigenesis (Tsai et al 2011). Indeed, ABHD11-AS1, the human related gene of Abhd11os, has been associated with gastric cancer (Lin et al 2014), but also with William-Beuren syndrome (Micale et al 2008). Overexpression or silencing of this gene in different pathologies context would bring understanding of the roles of this lincRNA.

4.2. CRYM

CRYM, also known as reduced nicotinamide adenine dinucleotide phosphate (NADPH)-dependent cytosolic T3-binding protein (CTBP) or μ-crystallin, has been first identify as a major structural component of the eye lens in Australian marsupials (Kim et al 1992). CRYM has been described as an NADPH-dependent cytosolic triiodothyronine or 3,5,3'-triiodo-L-thyronine (T3) thyroid hormone binding protein (Suzuki et al 2007b) and a key redox-dependent regulator of intracellular T3 bioavailability. Indeed, Suzuki and colleagues described the molecular functions of CRYM on thyroid hormone action (Suzuki et al 2007a, Suzuki et al 2007b) presented in **Figure 17**.

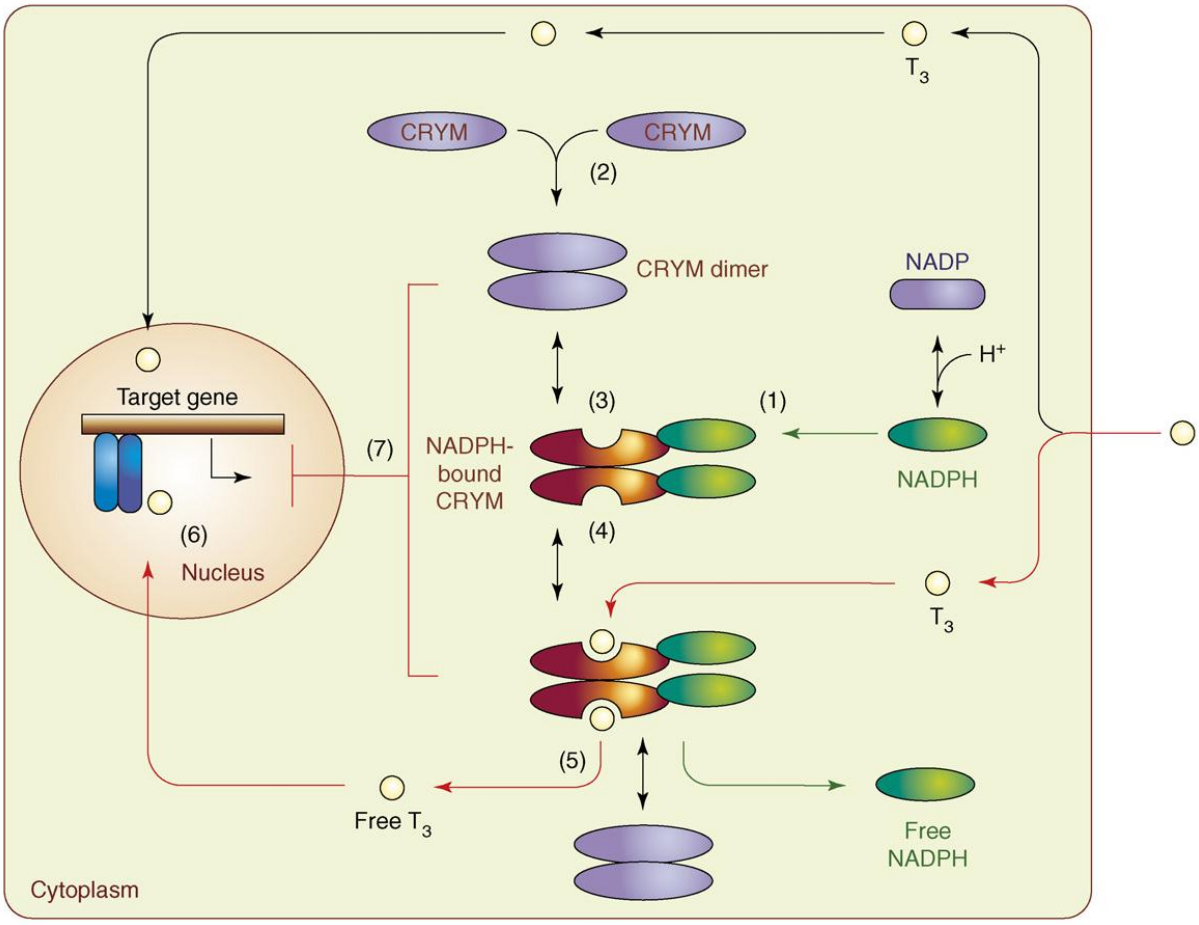

Figure 17 Molecular functions of CRYM on thyroid hormone action (Suzuki et al 2007).
Details: red arrows indicate the non-CRYM-mediated pathway (classical pathway); black arrows indicate the CRYM-mediated pathway.

The thyroid hormone T3 moves from outside the plasma membrane into the cytoplasm of the cells. Free T3 enters into the nucleus and initiates transactivation through binding to nuclear T3 receptors. CRYM forms a dimer in the cytoplasm. Each CRYM dimer binds one molecule of T3 and NADPH. In the presence of NADPH, the T3-bound form of CRYM increases the T3 concentration in the cytoplasm. Although the mechanisms have not yet been thoroughly elucidated, the expression of CRYM suppresses thyroid hormone nuclear receptor transcriptional activity.

Regulation of T3 action through CRYM is composed of binding of NADPH (**Figure 17 (1)**); dimer formation **(2)**; creation of the T3-binding site **(3)**; binding of T3 **(4)**; release of T3 caused by NADPH dissociation **(5)**; induction of transactivation **(6)**; and suppression of transactivation **(7)**.

A recent work precisely describes the crystal structure of CRYM alone or in complex with NADPH with or without T3 and suggests that CRYM would be able to recognize most of the thyroid hormone derivatives, as the thyroid hormone thyroxine or 3,5,3',5'-tetraiodo-L-thyronine (T4) (Borel et al 2014). T4 and T3 are produced by the thyroid gland. T4, the most abundant, is later converted in peripheral tissues by a selenium deiodinase into the less abundant but more potent T3 form.
Thyroid hormones play important regulatory roles in processes such as growth, metabolism, and homeostasis, and are essential for human brain development and cognitive functions (Rovet 2014, Schroeder & Privalsky 2014). Furthermore, T3 would be important for neuronal development throughout life, from early embryogenesis to the neurogenesis in the adult brain (see as review (Remaud et al 2014)). Thyroid signaling influences cellular metabolism and mitochondrial functions (Weitzel & Iwen 2011). Impaired thyroid signaling impacts mitochondrial respiration and hence reactive oxygen species (ROS) production, with either beneficial or damaging cellular effects (Long et al 2014). So, if there is a decrease of CRYM expression, as CRYM contributes to transportation or retention of T3 in the cytoplasm, it couldn't play efficiently this role, which would have several impacts on the cell, amongst others diminished neurogenesis, inefficient cellular metabolism, enhancing of ROS, and others consequences inducing death of the cells where CRYM is enriched, i.e. in MSN. This hypothesis follows what is described in HD pathogenesis. Indeed, the hormone levels were found to be negatively correlated with severity of clinical impairments, suggesting that thyrotropic axe is altered in HD patients (Saleh et al 2009).

In addition, CRYM has others roles in the cell that could explain its participation to the striatal vulnerability. Studies suggest that CRYM may therefore be a versatile enzyme with a reductase activity able to accommodate various substrates such as ketimine, thyroid hormones or AlaDH ligands pyruvate and alanine (Hallen et al 2011). Visser and colleagues suggested that CRYM could be also involved in thyroid hormone catabolism since the protein is able to bind to, and prevent the efflux of intracellular iodothyronine sulfate T3S and T4S (Visser et al 2010). Other studies have linked abnormal CRYM expression to syndromes as diverse as hyperglycemia, muscular dystrophy, deafness and prostate cancer (Abe et al 2003, Al-Kafaji & Malik 2010, Malinowska et al 2009, Oshima et al 2006, Reed et al 2007).
In HD, overexpression of CRYM would permit survival of MSN thanks to its different roles in the cells, but further studies are needed to determine by which molecular mechanisms its neuroprotective effects are mediated.
Our study points to Crym as an original link between HD pathogenesis and alterations of thyroid hormone-mediated regulation of transcription in the striatum.

4.3. DCLK3

Literature is dense concerning Doublecortin-like kinases (DCLK) 1 and 2 (Dijkmans et al 2010, Friocourt et al 2007, Tuy et al 2008, Verissimo et al 2011, Weimer & Anton 2006), part of the same kinase family than DCLK3, but a few is known on the latter member (Ohmae et al 2006, Reiner et al 2006, Wierinckx et al 2007).
Its characterization permits to better understand its neuroprotective effects.

4.3.1. Protein characterization

According to bioinformatics and experimental validation from the laboratory, this protein contains a doublecortin domain that permits to bind partially microtubules. Its subcellular localization is in the cytoplasm, but also in the nucleus. DCLK3 is processed by proteases such as calpain, which cleave it in 4 or more fragments. These breakdown products can be different depending on the species considered, which complicates the reading/understanding of the processing of this protein. We showed DCLK3 is cleaved in its Nterminal part, with the kinase domain spared, likely preserving the catalytic activity of the kinase. Indeed autophosphorylation experiments showed that the breakdown products (containing the C-terminal part of Dclk3) are still active. When the protein is cleaved, fragments containing the kinase domain may be translocated into the nucleus, but dynamic experiments would have to be assessed to confirm the nuclear translocation.
The Ser/Thr kinase domain is active according to biochemical studies. DCLK3 is neuroprotective in the *in vivo* lentiviral mouse model of HD expressing the Nterminal fragment Htt171-82Q. We showed that the activity of its kinase domain is important for the neuro-rescue of MSN when overexpressed using LV-mediated gene transfer in the striatum in LV model mice. We showed that when DCLK3 is overexpressed using AAV10 in the striatum of Ki140CAG HD mice, these mice display better locomotor performances than controls as seen in rotarod, open-field, catwalk and grip strength tests.

We conducted different approaches to explain these neuroprotective effects.

4.3.2. Disease-modifying mechanisms

Protective effects against mutant Htt
Our data show that overexpression of DCLK3 or its kinase domain only can protect striatal cells from mHtt toxicity. Several readouts support these observations including improvement of behavioral/motor performance, attenuation of neuropathological changes, and apparent preservation of striatal integrity as seen using MRI.

Because of the difficulty to have a high number of transgenic animals and the cost and heaviness of the processing of the brain slices by immunohistopathology, imaging permit to follow neurodegeneration of alive transgenic animals and to measure the effect of the treatment in the time by a translational approach.

MR spectroscopy imaging suggests that over time there are minor variations of astrocytic and neuronal metabolites concentration changes between transgenic mice injected with DCLK3 compared to control. KI140CAG mice show neurochemical changes reminiscent of neuronal and astrocytic suffering and DCLK3 overexpression tends to reduce some of these changes. The most remarkable being the recovery of GABA concentrations, the main neuromediator of MSN in the striatum. In addition, changes in glial metabolites indicate that neurons would have improved function in Ki140CAG mice infected with AAV10-DCLK3. However, a larger number of animals is required to reliably conclude on these effects.

Protein-protein interactions

Thanks to a yeast-two-hybrid screen using DCLK3 kinase domain as bait, we found seven proteins that all are potential regulator of transcription. The simple bioinformatics analysis of the network of interaction for these proteins focuses on TADA3. We presented results of stringent search criteria (avoiding text-mining, constraining to human, etc) to constrain the network to a high confidence limits. The network of interaction becomes much broader when imposing lower confidence interactions, but still point to different proteins regulating transcription factors and histone modification (methylase, acetylase, histone deacetylase).

TADA3 possesses a histone acetylase catalytic domain and is found to interact with several transcription activator factor (TAF). We checked that TADA3 is highly present in the brain, especially the striatum. Our preliminary immunoprecipitation experiments support the view that DCLK3 actually interacts with TADA3.

The network of interaction of the other potential DCLK3 partners is more limited. Data mining for these proteins provides much less information as compared to TADA3. Relatively "robust" data indicates a few binary interactions with these other DCLK3partners which each constitutes a working hypothesis to explain how DCLK3 exerts a part of its biological activity through its kinase domain. These "secondary" partners of DCLK3 also point to regulation of transcription, consistent with the fact that they all contain zinc finger motifs. Elucidation of these questions awaits further studies.

Concerning the partners of DCLK3, there is one important point which is not totally sorted out by our study. We yet do not know how the neuroprotective effects we observed when overexpressing DCLK3 or its active, fully functional kinase domain is related (or not) to the partners we identified using the Y2H screen. This question is extremely difficult to address experimentally. If we hypothesize that TADA3 plays a key role in DCLK3 effects against mHtt, knocking down TADA3 in acute cell models of mHtt overexpression should abrogate the neuroprotective effects of DCLK3. In line with this, the effect of DCLK3 may involve phosphorylation of TADA3. Site directed mutagenesis of TADA3 may also help to better decipher the link between DCLK3 neuroprotective effect and interaction with TADA3.

Model of neuroprotective effects of DCLK3

DCLK3 is downregulated in HD mouse models and HD patients. In addition, preliminary biochemical analysis indicates that in certain conditions (BACHD mice, HD patients) the cleavage of DCLK3 and its localization in the nucleus might be changes. Thus it is conceivable that its loss and perturbation could render striatal MSN more susceptible to mHtt in HD. Our data show that overexpression of DCLK3 is neuroprotective.

Our results clearly demonstrate that the kinase activity of DCLK3 is indispensable for neuroprotection. However, the step at which this kinase activity is required for protection remains elusive. According to our data, different scenario can be envisioned. When overexpressed in HD mice, DCLK3 would be cleaved, transported through microtubules, translocated to the nucleus, permitting its interaction with partners regulating transcription. Its interactions would induce pro-survival signals. It is likely that the effect of DCLK3 on transcription is relatively specific, and that it produces an "imprint" of modification rather than a broad effect. As mention above, however, we have not formally established the causal relationship between DCLK3-induced neuroprotection and the interactors we have identified using the Y2H screen. Further studies are currently on going to validate these results and permit to have a clear mechanism of action.

Another possibility is that the protective effect of DCLK3 is not mediated through these partners and regulation of transcription. Indeed, it cannot be ruled out that the Y2H screen could not picked up other partners, especially those with cytoplasmic localization. It is intriguing that while DCLK3 decorates the microtubules and can be pulled-down with microtubules, none of the interactors obtained from our Y2H screen correspond to known cytoplasmic/cytoskeleton proteins. One possibility is that the kinase domain interacts with its substrates according to a "kiss-and-run"–like weak interaction which could not be evidence in the screen. Substrates of DCLK3, once phosphorylated, could trigger survival signaling pathways opposing mHtt toxicity.
It is also conceivable that the "anchoring" of DCLK3 to the cytoskeleton is indirectly mediated by the interaction of the partners we identified. Preliminary results indicate that in cells transfected to express recombinant TADA3 and BTBD9 the proteins are found in the cytoplasm and the nucleus. Supporting this view a number of proteins that regulate transcription through direct interaction with its machinery are found in the cytoplasm and upon activation migrate to the nucleus, some examples of which are Htt, p53, NF-κB.

4.3.3. Troubleshooting

From my experience on DCLK3 project, several points have to be based in order to more efficiently keep on working on it.

- ***Specificity of antibodies used***

At the beginning of this study, we didn't have anti-DCLK3 antibodies, so the only solution was to generate and overexpress recombinant DCLK3 protein tagged in the terminus of its most conserved part (C-terminus kinase domain). This is the reason why all our constructs are HA tagged, to be able to follow the recombinant protein expression with the anti-HA antibody.
Since the beginning of my thesis, I tested 6 antibodies directed against DCLK3 in order to be able to detect the endogenous form of DCLK3. Only one antibody shows the same biochemical result of the recombinant DCLK3-HA construct cleavage than the antibody that detects the HA tag of these constructs.

This antibody recognizes a sequence located between the doublecortin domain and the kinase domain, and has been produced to detect the human sequence. As the human sequence is the same that the macaque sequence and the short-form of the rodent sequence, it seemed logical that this antibody could recognize specifically DCLK3 proteins extracted from human, macaque and in a less extent rodent tissues. The biochemical studies indicated that even if the human and macaque sequences are identical according bioinformatics, the processing of DCLK3 seems to be different. It is more obvious comparing the human/macaque and rodent extracts. This could be explained by different proteases/caspases/kinases/phosphatases environment in these species, leading to the generation of different fragments of DCLK3. When we detect DCLK3 by immunofluorescence and we compare the HA tag and the DCLK3 detection with respectively anti-HA and anti-DCLK3 antibodies in paraffin slices from Ki140CAG mice injected with DCLK3-Long and Kin forms, we see a cytoplasmic staining with the anti-HA, but a cytoplasmic AND nuclear staining with the anti-DCLK3. More observations have to be done to study more deeply this phenomenon, but two possibilities can be envisioned. Either the anti-DCLK3 is not specific of DCLK3 protein and recognizes other proteins containing the same sequence than DCLK3, for example DCLK1 or/and DCLK2, or a homologous sequence of some CaMK, but it wouldn't be coherent with the biochemical results. It is possible that when DCLK3 enters into the nucleus, it undergoes processing in its C-terminus and losses its HA-tag. In this case, the anti-HA would only recognize the HA-tag proteins in the cytoplasm. It is also possible that the HA-tag doesn't allow the recombinant protein to enter into the nucleus because of a missing signalization due to a particular conformation of the protein containing the HA tag. To address these questions, we should carry out immunodepletion using recombinant DCLK3. Another approach would be to generate knock-down DCLK3 mice and check if we still detect a signal in the nucleus with the anti-DCLK3 antibody, and validate others DCLK3 antibodies.
It would be interesting to develop anti-DCLK3 antibodies that recognize different parts of DCLK3, and more precisely study their subcellular localization, cleavage, kinase activity and interactors. This approach would bring indispensable information to understand the processing of DCLK3 and more globally its role/function in the cell. It would also lift the veil on what happens to N-terminus fragments generated by the cleavage of DCLK3.

- ***Physiological processing of the endogenous DCLK3 protein***

Based on the previous observation with the different antibodies used to detect DCLK3, and from our *in vivo* experiments, it is now asked if the overexpression of a recombinant DCLK3 protein without the HA tag could lead to a higher neuroprotective effect. Indeed, tags could change the conformation of a protein, and what is more, when targeting the highly conserved and active part of the protein. So it is possible that the observations we made when overexpressing DCLK3-HA constructs might be distorted by the possible impact of the HA tag on the conformation and activity of DCLK3.
It is necessary to generate the DCLK3 constructs without tag and study its effects against mHtt.

- ***Viral vector tools as gene therapy tools in mice***

Results from the overexpression of DCLK3 in KI140CAG mice indicate that the injection of virus by stereotaxy is not trivial and has impact on the basal behavioral performances of mice because of the chirurgical traumatism it implies. I characterized some behavioral performances of non-injected KI140CAG mice with rotarod and open-field tests. Important differences were seen between littermates, heterozygous and homozygous mice that decide us to try to treat the mice with the injection of DCLK3 in the three genotypes. After injection of AAV in the striatum of these mice, our results show that the genotype effects on locomotor performances of mice are flattened. The solutions are various. We may need to reduce the trauma produced by virus vector injection. The size of the needle/canula used for stereotaxic injection might not be a problem for rats and bigger animals, but it would be pertinent to try thinner needle for the stereotaxy method in mice or develop non-invasive techniques, particularly if these animals have to perform behavioral test. Because HD requires to target the striatum, alternatives to stereotaxy has to be developed to avoid to damage other parts of the brain, as the cortex.

In addition, we tried to reduce as much as possible the amount of viral particles to avoid neuroinflammation. However, we cannot exclude that a minor immune response would change the function of striatum in wild type animals.

- ***Controls use for preclinical therapeutic experiments***

Another recurrent difficulty encountered in our preclinical approach is to find the suitable control of the experiment, that most of the time produces undesired effects. In our neuroprotective experiment using overexpression of DCLK3 in Ki140CAG mice, we used GFP as control. Notably for behavioral tests, overexpression of GFP doesn't show toxicity, but may induce noise to our data, conjugated to Htt expression. The improvement could be to inject a non-coding GFP, or to use the dead-kinase K543M mutant construct since we showed that the activity kinase of DCLK3 is central to induce neuroprotective effects.

4.4. First conclusion

Since Abhd11os, Crym and Dclk3 have a preferential expression in the striatum and their levels are reduced in different HD models, it is possible that their down-regulation may be involved in the preferential degeneration of the striatum in HD. Using an in vivo lentiviral model of HD, we showed that they have a neuroprotective effect against N-terminal fragment of mHtt. It should be emphasized that not all striatal markers down-regulated in HD can reduce the toxicity of N-terminal fragments of mHtt when they are overexpressed. Indeed, many striatal markers are rather considered to be risk factors for MSN (see (Francelle et al 2014); **Figure 18**). At present, only few striatal markers have been experimentally tested for their capacity to change mHtt toxicity.

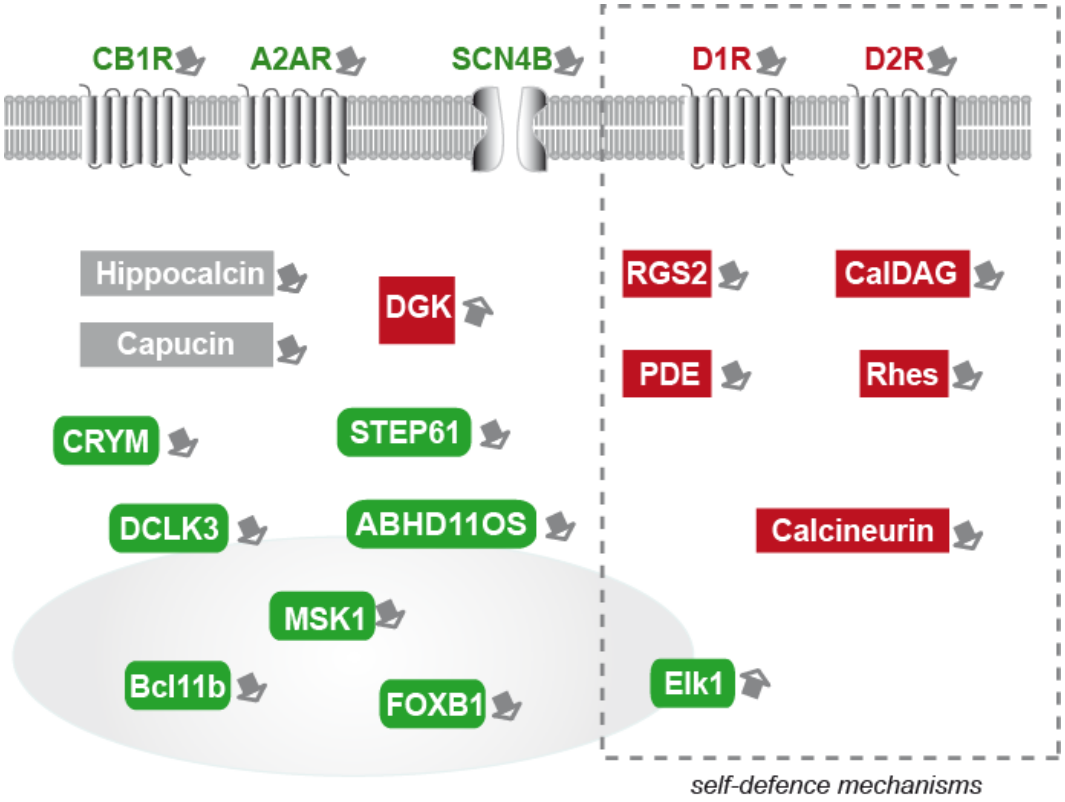

Figure 18 Schematic representation of the striatal markers that have been experimentally studied as potential modifiers of mutant huntingtin toxicity in HD (adapted from Francelle et al 2014).

Interestingly, all the striatal markers that can modulate (positively or negatively) the toxicity of mHtt could be considered as potential therapeutic targets, which pave new paths toward novel therapies.

4.5. Others models to study neuroprotective effects of striatal markers

The in vivo lentiviral (LV) mouse model of HD has been used to permit a first screening of the impact of the striatal markers on an acute and toxic fragment of mHtt, which provide rapid results concerning disease modification at the cellular level.

For DCLK3, we used the transgenic mice N171-82Q and Ki140CAG (see paragraph 1.2.7. Animal models of HD). This latter HD mouse models have been used to test potential therapeutic agents, because their advantages compared to the LV mouse model are the behavioral deficits and transcriptional dysregulation appearing with time.
The currently trendy mice model used for this purpose is zQ175 mice. This model recapitulates several features of HD (Heikkinen et al 2012, Menalled et al 2012) and is presented as the new mouse model that closely mimics the human genetic lesion and presents robust and early behavioral and molecular alterations in both homozygous and heterozygous mice. Moreover, behavioral deficits in zQ175 mice emerge at about the same age as do transcriptional abnormalities (Menalled et al 2012).
This HD mice model would permit to validate the neuroprotective effects of Abhd11os and CRYM in a proper background in a shorter time than with the Ki140CAG mice.
In parallel, it would be interesting to test the survival curve of HD mice with the three striatal markers presented here, in order to see the impact of the overexpression or silencing of these genes in a rapid HD phenotype mice model, as the R6/2 mice (Davies et al 1997, Mangiarini et al 1996) and see if neuroprotection measured at cellular level has an impact on a global improvement of survival.

Concerning our mostly advanced study on DCLK3, one interesting research direction would be to study DCLK3 effects on mHtt more broadly using a genetic strategy using backcrossing of DCLK3 KO mice (conditional) with HD mice. This could allow us to confirm that the absence of DCLK3 in the brain could exacerbate the pathology and in addition this may reveal that the "peripheral" pathological changes in HD mice may also involve DCLK3. Beyond HD, the generation of DCLK3 KO mice would also allow us to better determine the physiological role of the kinase in the basal ganglia and other part of the brain when it is highly expressed (for example hippocampus, pituitary, substantia nigra). It is conceivable that DCLK3 could constitute a therapeutic target for other neurodegenerative and psychiatric conditions involving the basal ganglia.

4.6. Impact of our study in current spotlights

Striatal markers as gene modifiers of age at onset of HD manifestations

A common feature of our studies is the potential involvement of our striatal markers on transcriptional regulation. Because the transcriptome is not limited to protein-coding genes, which represent less than 5 % of the genome, and new classes of noncoding RNAs are currently in the spotlight. The continuous development of transcriptomics technologies and concurrent bioinformatic tools is increasingly enlarging our global perspective of the transcriptional phenomenon. Currently, deep sequencing techniques coexist with newly improved array platforms to maximize coverage of the entire transcriptome, including noncoding genomic features and alternative isoforms, and to connect transcriptomics with other sources of genome-wide data related to DNA modification and the occupancy of DNA-binding proteins (histones and transcription factors) (Valor 2014).

It has a particular importance in HD, as described in the introduction of this manuscript paragraph 1.2.6.3. Molecular Mechanisms in HD.

Although neither the normal *HD* CAG allele repeat length nor its interaction with the expanded allele influenced age at motor onset, the remaining variance has been reported to be highly heritable, (Aziz et al 2012, Djousse et al 2003, Lee et al 2012, Wexler et al 2004) indicating the presence in the genome of genetic factors, called genetic modifiers, whose natural polymorphic variation contributes to altering the development of HD symptoms (Gusella & MacDonald 2009, Gusella et al 2014). Indeed, the use of RNAi screening in lower model organisms revealed that altering the expression of a surprisingly large number of genes can influence the aggregation of mHtt (Wada et al 2009).

Furthermore, early investigations showed that a gene closely linked to the HD gene may modify age of onset (Farrer et al 1993). In the HD-MAPS study, suggestive evidence for linkage was found at chromosome 4p16, adjusted for CAG repeat size in the *HD* and normal alleles (Li et al 2003). The findings of suggestive linkage to chromosomes 4 and 6, as well as marginal evidence for linkage to chromosomes 1, 2, 5 and 18, in a sample of 629 affected sibling pairs has provided a direction for the identification of candidate modifiers for onset of motor symptoms of HD.

From this knowledge, Kalathur and colleagues have generated a compendium of molecular mechanisms that might play critical roles in HD. The compendium links biological processes, molecular functions and pathways to sets of HD-relevant genes (Kalathur et al 2012). It permits to generate cartography of all HD-relevant genes to their loci on human chromosomes (Kalathur et al 2012).

Kalathur and colleagues also derived a candidate set of 24 novel genetic modifiers, including histone deacetylase 3 (HDAC3), metabotropic glutamate receptor 1 (GRM1), CDK5 regulatory subunit 2 (CDK5R2), and coactivator 1ß of the peroxisome proliferator-activated receptor gamma (PPARGC1B). The list of the HD-relevant genes and their loci is shown in **Table 4**.

	Entrez ID	Symbol	TVS	Chr.	Band
Region = 2q33-2q35	7341	SUMO1	3	2	q33.1
	9689	BZW1	3	2	q33.1
	23451	SF3B1	3	2	q33.1
HD MAPS: LOD =1.63 (at 2q33)	1385	CREB1	3.5	2	q33.3
Gayan et al: LOD =3.39 (at 2q35)	7855	FZD5	3	2	q33.3
	3300	DNAJB2	3	2	q35
	8941	CDK5R2	3	2	q35
	10109	ARPC2	3	2	q35
Region = 4p16	6286	S100P	3	4	p16.1
	9948	WDR1	3	4	p16.1
HD MAPS: LOD =1.93	118	ADD1	3	4	p16.3
Gáyan et al : LOD =1.49	3064	HTT	4	4	p16.3
	7469	WHSC2	3	4	p16.3
Region = 5q31-32	3308	HSPA4	3.5	5	q31.1
	6500	SKP1	3	5	q31.1
	2107	ETF1	3	5	q31.2
HD MAPS: LOD = 2.02 (at 5q31-32)	3313	HSPA9	3	5	q31.2
Gáyan et al: LOD =3.14 (at 5q32)	7322	UBE2D2	3	5	q31.2
	8841	HDAC3	4	5	q31.3
	10915	TCERG1	3	5	q32
	133522	PPARGC1B	3	5	q32
Region = 6q22-24	2444	FRK	3	6	q22.1
	6206	RPS12	3	6	q23.2
HD MAPS: LOD =2.28 (at 6q23-24)	9439	MED23	3	6	q23.2
Gáyan et al: LOD =2.48 (at 6q22)	4217	MAP3K5	4	6	q23.3
	2911	GRM1	3	6	q24.3

Table 4 HD-relevant genes located in the four chromosomal regions implicated by both genome-wide scans (Kalathur et al 2012).

As loci modifying age of onset, Kalathur and al. used those that were reported in the genome-wide scans by (Li et al 2003) (HD MAPS study) and by (Gayan et al 2008). The LOD score (logarithm (base 10) of odds) for suggestive evidence for linkage and exact loci localization were retrieved from the publications and indicated on the left column of **Table 4**.

This approach resulted in 26 HD-relevant genes located in the regions that were previously linked to age of onset. Interestingly, the results of their analyses reflect many discoveries that elucidated molecular mechanisms in HD. More remarkably, they also strongly support a functional relevance of processes, that have received little attention, or that have not been studied at all in the context of HD.

Pooling data of approaches like these would permit to better understand phenomenon in HD. For example, in the **Table 4** is cited CDK5 as HD-relevant gene. Yet, Varjosalo and colleagues show an interaction between DCLK3 and cyclin-dependent kinase 5 (CDK5) (Varjosalo et al 2013) tested by affinity capture-mass spectrometry. CDK5 is a member of the serine/threonine CDK family, and is associated with a wide range of cellular functions including neural development, neuromuscular development and hippocampal neurogenesis (see (Su & Tsai 2011) for a review). CDK5 activity has been found to be crucial for neuronal survival during development and disease.

Indeed, CDK5 activity is consistently found to suppress mHtt toxicity (Cheung & Ip 2012). The neuroprotective potential of CDK5 is therefore likely to be dependent on factors such as age and disease progression, or any other cellular insult resulting in DNA damage. CDK5 could be initially high in models of HD, where it may act as either a compensatory protective mechanism by phosphorylating mHtt or as a pro-apoptotic mechanism by enhancing excitotoxic vulnerability, dependent on the ratio of its activators present (Cheung & Ip 2012, Paoletti et al 2008). It is tempting to think that DCLK3 could be integrated in kinase signaling of CDK5, whose results would be pro-survival effects.

Striatal markers as neuronal identity protectors

There is one important aspect of transcriptional regulation in HD. Transcriptional deregulation of "striatal markers" seems to be more profound as compared to other gene products (Francelle et al 2014). In other words, neurodegeneration in the striatum would start by a phenomenon related to a loss of neuronal identity. Establishment of neuronal identity requires coordinated expression of specific batteries of genes (Ballas et al 2001, Belyaev et al 2004, Muhr et al 2001). According to Johnson and colleagues, neurodegeneration can be seen as an RNA disorder. They worked to demonstrate a role for microRNAs in HD, indicating that the molecular aetiology of HD is reflected in a loss of neuronal identity, caused in part by dysregulation of both transcriptional and post-transcriptional mechanisms (Johnson et al 2012, Johnson et al 2008).

Transcriptional repression is a principal path by which developmental programs of gene expression are established. One of the transcription factors proposed to play an important role in establishing and maintaining expression of neuron-specific genes is REST (Chong et al 1995, Schoenherr et al 1996). Soldati and colleagues, among others, have investigated which aspects of the transcriptional dysregulation seen in cellular models of HD can be attributed to aberrant repression of coding and non-coding REST target genes (Johnson & Buckley 2009, Soldati et al 2013). They provided evidence that REST is likely to contribute to HD gene dysregulation by direct and indirect repression of a cohort of genes, including miRNAs, many of which are responsible for regulating neuronal identity and function (Soldati et al 2013). As proof of concept, Charbord and colleagues have shown that using a chemical component that targets REST degradation, but neither REST expression, RNA splicing nor binding to RE1 sequence, promotes the expression of neuronal genes including BDNF and SNAP25 [(Charbord et al 2013); see **Annexe 6.1.**]. Confirming these results, *in vivo* delivery of dominant-negative form of REST (DN:REST) to interfering with REST function improves transcriptional changes of REST-regulated genes in HD mice (Conforti et al 2013). Indeed, delivery of DN:REST in the motor cortex restores brain-derived neurotrophic factor (BDNF) mRNA and protein levels by reducing endogenous REST occupancy at the Bdnf locus. Similarly, expression of other REST-regulated genes such as Synapsin I (Syn1), Proenkephalin (Penk1) and Cholinergic receptor muscarinic 4 (Chrm4) were restored to normal levels while non-REST-regulated genes were unaffected.

Modulation of BDNF expression is encouraging, but recovering the basal expression of genes as important as REST would bring more efficient perspectives in HD therapy. The next question would be how striatal vulnerability-relevant genes influence the striatal identity.

More globally, it is important to determine a potential role for other *cis*-factors that potentially modify age at onset of HD manifestations and cellular function and identity integrity.

As discussed in our review (Francelle et al 2014), it is possible that striatal markers are amongst genes preferentially downregulated in HD, which would contribute to render the striatum more susceptible to mHtt.

PART5 CONCLUSION AND PERSPECTIVES

There is no efficient therapies that prevent or cure HD. Current most promising strategies consist in directly decreasing mHtt expression (ASO and shRNA) and increasing wt-Htt expression, or as in our approach, playing on HD modifiers, the striatal modifiers being, as we showed by our study, relevant to the fact that although HD is not a purely striatal disease, early cellular abnormalities and symptoms are related to striatal alterations.

5.1. Therapeutic perspectives

As detailed previously, Htt is an important protein for vertebrates, which cannot be totally silenced to provide therapeutic approach. It is important to gain a better understanding of how much of a loss of wt-Htt expression can be tolerated by cells, since some of the therapeutic approaches being developed target reduction of Htt levels [(Tian et al 2014); see paragraph 1.2.8.1. Gene silencing therapy]. Indeed, one way to obviate the risk of wt-Htt knockdown is to target the mutant allele selectively (Drouet et al 2014, Ruiz & Deglon 2012, Yu et al 2014). However, this strategy presents difficulties to develop efficient techniques to this aim: targeting polymorphisms dramatically reduces the repertoire of possible RNA target sequences, increasing the chance of off-target effects (Lombardi et al 2009, Wild & Tabrizi 2014)
Furthermore, reducing mHtt expression in both cortex and striatum may be necessary for optimal suppression of relevant phenotypes in a mouse model of HD (Wang et al 2014), which poses a problem of delivery of therapeutic agents in larger animal model brain.

The only serotype so far utilized in CNS clinical trials has been AAV type 2 (AAV2), which has displayed an excellent safety profile (Mandel et al 2006). Recently, other serotypes have become available, such as AAV1, AAV5, AAV8, AAV9 and AAV10 (Sondhi et al 2007) that display greater transduction efficiency, greater diffusion in the brain parenchyma, and higher levels of transgene expression than AAV2. The large volumes of distribution of newly identified AAV serotypes favor the study of behavioral deficits. Using vascular system to major delivery is an attempt conducted by Dufour et al (Dufour et al 2014). Intrajugular vein injection of AAV9 expressing a mutant Htt-specific RNAi construct significantly reduced mHtt expression in multiple brain regions and peripheral tissues affected in HD. Correspondingly, this approach prevented atrophy and inclusion formation in the first brain regions touched by HD as well as the severe characteristic weight loss of HD YAC mice.
The group of Viviana Gradinaru has developed a methodology that uses a derivative application of CLARITY, SCALE, SeeDB, ClearT and BABB (Murray's Clear) techniques (Becker et al., 2012; Chung et al., 2013; Dodt et al., 2007; Ertu¨ rk et al., 2012a; Hama et al., 2011; Ke et al., 2013; Kuwajima et al., 2013; Susaki et al., 2014) to facilitate fast, whole-brain and whole-body clearing using systemic or cerebrospinal circulation to directly deliver clarifying agents and to immunostain intact organs. This technique can be useful to follow tropism of AAV without sectioning and can be used as a rapid tool for individual cell phenotyping and genotyping modification (Yang et al 2014).

Diffusion problem of therapeutic agents is also addressed for therapeutic agents that do not directly target mHtt.

Other ways to find therapeutic targets for HD, potentially useful for other striatal disorders are:
1) to used high throughput screening of chemical molecules in HD cellular models, which is a rapid way to identify active compounds, providing starting points for drug design and for understanding of the interaction or role of a particular biochemical process (Charbord et al 2013, Lausted et al 2014, Lazzeroni et al 2013, Lu et al 2013); In certain cases, the strategy is to screen large FDA approved drug library. Thus efficacious drug in the screen may be rapidly tested in patients, and if the drug has an impact on the disease, a "repositioning" of the drug can be obtained very rapidly;
2) to identify novel therapeutic targets based on proteins known to have neuroprotective properties against mutant Htt. There are currently hundreds of targets studied as potential target to treat HD. In this context the study of proteins that are relevant to the particular vulnerability of the striatum (i.e. the striatal markers) might be promising (Francelle et al 2014). Concerning CRYM, Abhd11os and DCLK3 much work has to be carried out to better understand their mode of action and their efficacy. In parallel, it may be important to develop strategies to target these striatal markers. For example DCLK3 could be targeted to increase its activity, to produce neuroprotection. While kinase inhibitors can be easily found, allosteric inhibitor of kinase are more difficult to discover. For example, AMPK is allosterically regulated by AMP and chemical analogues have been developed to activate the kinase, which regulates key aspect of energy metabolism (Xiao et al 2013). Another example is the case of serine which is the nature allosteric activator of pyruvate kinase 2, central in coupling metabolism and cell proliferation in cancer cells (Chaneton et al 2012, Hawley et al 2012). Some kinases have allosteric pockets (docking phosphate motif on substrates) that serve to activate phosphorylation (Hindie et al 2009).
This strategy could be developed for activation of DCLK3, however a better knowledge of the 3D structure of the protein is required, and the potential mechanisms of regulation (especially phosphorylation by upstream kinases, such as CDK5 for example) need to be identified. Another parallel strategy would be to screen large libraries of chemical compounds to identify synthetic activators using biochemical assays with recombinant DCLK3 and FRET reporter substrate.

The questions behind these approaches are:
-What to do with the few already studied striatal markers? We need to elucidate their mechanisms of action and test them in complex HD animal models.
-What to do with the hundreds striatal markers not yet experimentally studied? Identification of their function, if unknown, would permit to have a global idea of the mechanisms of action.

Characterization of novel markers can be simple when using simple HD models (cells, yeasts, Drosophila, zebrafish, C. elegans, etc.) to better apprehend their mechanisms of action. Test their impact against mHtt toxicity, first with simple but acute HD models, using for example derivatives of stem cells or the in vivo LV mouse model of HD.

Depending on the nature of the impact against mHtt toxicity, if striatal markers exacerbate cytotoxicity of mHtt, it would be interesting to find inhibitors of these markers, and test their inhibition in different HD models; if they present neuroprotective effects, the validation of their effects in others animal models of HD, chosen depending on the asked question, is essential.
As described in the introduction of the manuscript, paragraph 1.2.7. Animal models of HD, it exists a large diversity of HD animal models, but to assess the disease-modifying of a potential therapeutic agent, I would used Drosophila and R6/2 mice for a proof of feasibility and survival curve, knock-in models for long-term effects, and ultimately non-human primates for cognitive and fine motor behavior.

The designation most commonly applied to a treatment that postpones or slows the progression of a neurodegenerative disease is "neuroprotective". However, this concept is restrictive, because it describes a mechanism of action rather than a consequence of an intervention. Other similar mechanistic concepts include "neuro-rescue" (refers to the salvage of dying neurons) and "neuro-restoration" (refers to increasing the numbers of neurons by techniques such as cell implantation or nerve growth factor infusion).
Another term used in my manuscript is "disease-modifier", that implies halting or delaying the neuronal loss and therefore slowing or stopping the progression of neurological symptoms, and ultimately modifying the clinical course of the disease.

5.2. How to improve methods to optimize the testing of modifiers

Limitation of classical histological approaches, toward 3D approaches
In our approach, we used histo-neuropathology, with functional markers as DARPP32, NeuN and COX proteins to detect dysfunctional or dying neurons in the striatum. These proteins are characteristic of the loss of MSN, but it would be useful to find others functional markers to have a wider overview of the neurodegeneration (for example HDAC, autophagy functionality detection). We counted the number of aggregates thanks to Em48 antibody and ubiquitin staining, even if the way aggregates are protective or toxic is still unclear.
Protection can be functionally observed by electrophysiology experiments, to measure the connectivity between cells, receptors environment, neuronal and non-neuronal responses to stimuli/pharmacology/treatments.

In vivo imaging as a prerequisite
As in clinical studies, *in vivo* imaging in rodent models of HD is probably a key methodological approach to study modifiers of mHtt toxicity. MR-imaging is a useful tool to address functional question. For example, the remarkable longitudinal follow up of HD gene carriers in large cohorts have been performed using MRI, revealed key aspect of striatal and extrastriatal atrophy in the brain using cutting edge 3D analyses.
Cerebral white matter (WM) changes in HD have been reported in a number of studies (for reviews see (Bohanna et al 2008, Kloppel 2009)), mainly using magnetic-resonance (MR)-based diffusion weighted imaging (DWI) and diffusion tensor imaging (DTI) (Douaud et al 2009, Rosas et al 2006).

These techniques use diffusion directions of water molecules to calculate a tensor, which can be converted into metrics such as fractional anisotropy (FA) (Basser & Jones 2002, Basser & Pierpaoli 1996),In particular, DTI techniques (tractography) permit to establish the ”connectome” of the brain and identify subtle changes in HD gene carriers and later evolution in patients. So DTI has emerged as a sensitive tool for detection of altered tissue integrity at both preclinical and clinical stages of HD (Mascalchi et al 2004, Reading et al 2005). Reduced fiber connectivity between the prefrontal cortex and the caudate has been shown to reflect symptomatology in pre-HD (Kloppel et al 2008). Diffusion properties of white matter are altered across an extensive, distributed anatomical area in HD. Changes in diffusion metrics are associated with markers of HD severity (Dumas et al 2012, Novak et al 2014, Poudel et al 2014). In view of these data acquired in human, it would be interesting to study the grey and white matter connectivity of HD mice injected with DCLK3 to have an overview of grey and white matter diffusion and rely these data to literature. It may constitute one more argument of the large impact of DCLK3 neuro-rescue effects against mHtt toxicity.

Other methods need to be further developed to improve the follow-up of patients in correlation with symptom evolution. For example, the GluCEST (glutamate (Glu) chemical exchange saturation transfer) technique, developed for detecting brain Glu in millimolar concentrations (Cai et al 2012, McMahon et al 2006, Sherry & Woods 2008, Ward et al 2000). Alterations in cortical and striatal glutamate and DA neurotransmission in HD could be measured by this way in our laboratory.

5.3. Further perspectives: combinatory therapy

Finally, as long-term perspectives and ultimate goal, once striatal markers and a maximum of therapeutic agents will be discovered and experimentally tested, a way to increase disease-modifying effects of the molecules tested in HD animal models could be the combination of several neuro-rescue and neuro-restorative molecules in complement of a preventive medicine (see **Figure 19** Combinatory therapy model of HD).

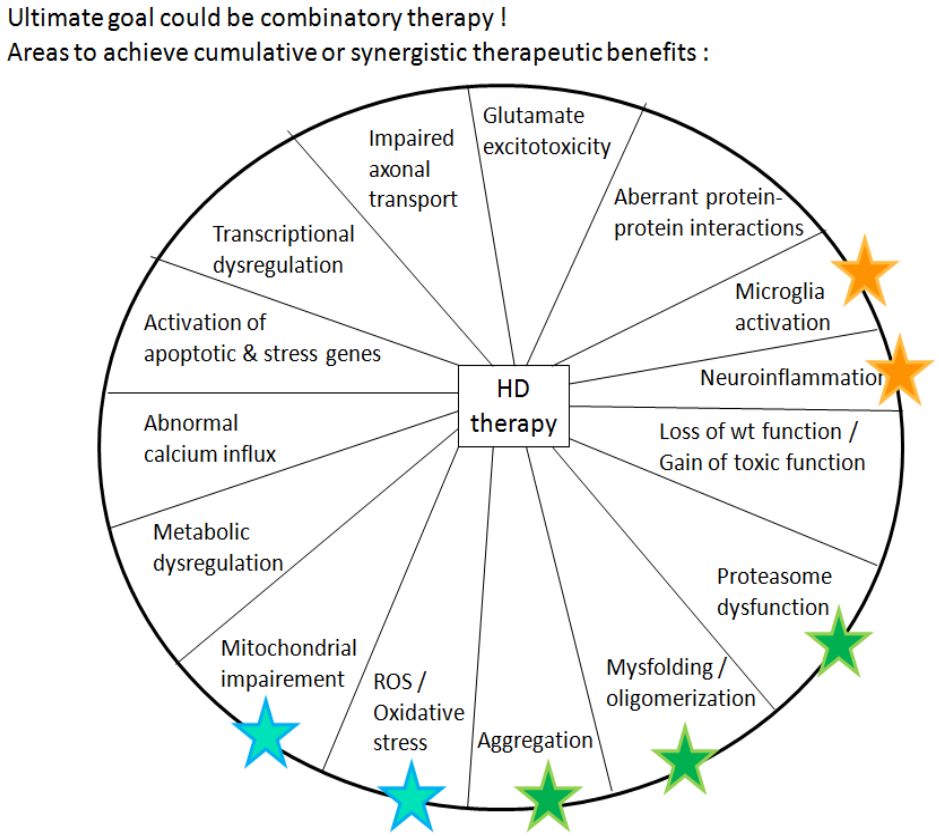

Figure 19 Combinatory therapy model of HD

Indeed, the diversity of biochemical parameters involved in neuronal death in HD (oxidative stress, mitochondrial dysfunction, protein aggregation, decreased neurotrophic factors, inflammation and activation of apoptotic enzymes) implies that a therapeutic agents targeting multiple cellular components and/ or embodying a range of different properties may be more efficacious to alleviate the various pathological features of HD disease.

PART6 ANNEXES

6.1. Collaborative work #1

High Throughput Screening for Inhibitors of REST in Neural Derivatives of Human Embryonic Stem Cells Reveals a Chemical Compound that Promotes Expression of Neuronal Genes.

STEM CELLS®

STEM CELL TECHNOLOGY: EPIGENETICS, GENOMICS, PROTEOMICS, AND METABONOMICS

High Throughput Screening for Inhibitors of REST in Neural Derivatives of Human Embryonic Stem Cells Reveals a Chemical Compound that Promotes Expression of Neuronal Genes

JÉRÉMIE CHARBORD,[a,b] PAULINE POYDENOT,[c] CAROLINE BONNEFOND,[c] MAXIME FEYEUX,[a,b] FABRICE CASAGRANDE,[c] BENJAMIN BRINON,[c] LAETITIA FRANCELLE,[d,e] GWENAELLE AURÉGAN,[d,e] MARTINE GUILLERMIER,[d,e] MICHEL CAILLERET,[a,b] PEDRO VIEGAS,[a,b] CAMILLE NICOLEAU,[a,b] CÉCILE MARTINAT,[a,b] EMMANUEL BROUILLET,[d,e] ELENA CATTANEO,[f] MARC PESCHANSKI,[a,b] MARC LECHUGA,[c] ANSELME L. PERRIER[a,b]

[a]Inserm U861, [b]UEVE U861, and [c]CECS, I-Stem, AFM Evry Cedex, France; [d]CEA, DSV, I[2]BM, Molecular Imaging Research Center (MIRCen), Fontenay aux Roses, France; [e]CNRS CEA URA 2210, Fontenay-aux-Roses, France; [f]Department of Pharmacological Sciences and Centre for Stem Cell Research, University of Milano, Milano, Italy

Key Words: Human embryonic stem cells • High throughput screening • Repressor element-1 silencing transcription factor • Neuron restrictive silencer factor • Neural stem cells

ABSTRACT

Decreased expression of neuronal genes such as brain-derived neurotrophic factor (BDNF) is associated with several neurological disorders. One molecular mechanism associated with Huntington disease (HD) is a discrete increase in the nuclear activity of the transcriptional repressor REST/NRSF binding to repressor element-1 (RE1) sequences. High-throughput screening of a library of 6,984 compounds with luciferase-assay measuring REST activity in neural derivatives of human embryonic stem cells led to identify two benzoimidazole-5-carboxamide derivatives that inhibited REST silencing in a RE1-dependent manner. The most potent compound, X5050, targeted REST degradation, but neither REST expression, RNA splicing nor binding to RE1 sequence. Differential transcriptomic analysis revealed the upregulation of neuronal genes targeted by REST in wild-type neural cells treated with X5050. This activity was confirmed in neural cells produced from human induced pluripotent stem cells derived from a HD patient. Acute intraventricular delivery of X5050 increased the expressions of BDNF and several other REST-regulated genes in the prefrontal cortex of mice with quinolinate-induced striatal lesions. This study demonstrates that the use of pluripotent stem cell derivatives can represent a crucial step toward the identification of pharmacological compounds with therapeutic potential in neurological affections involving decreased expression of neuronal genes associated to increased REST activity, such as Huntington disease. STEM CELLS *2013;31:1816-1828*

Disclosure of potential conflicts of interest is found at the end of this article.

INTRODUCTION

Several pathological states affecting the central nervous system are associated with perturbations of the expression of neuronal genes before actual neural cell loss or transformation occurs. This, for instance, is the case for Huntington disease (HD) [1–3]. One identified mechanism that leads to such phenomena is an increased activity of the repressor element-1 silencing transcription factor (REST), also known as neuron restrictive silencer factor (NRSF). Accordingly, a therapeutic avenue for those pathologies may be to interfere pharmacologically with REST inhibition of its target genes (RE1-genes) [4,5]. Indeed, REST inhibition achieved in vitro via the overexpression of a dominant-negative form of REST (D/N-REST) lifts REST-mediated repression or silencing of several hundreds of neuron-specific genes, among which, notably, the brain-derived neurotrophic factor (BDNF) [6–8]. While D/N-REST-mediated inhibition has limited clinical relevance, pharmacological intervention that would similarly increase neuroprotective gene expression through REST inhibition would open promising therapeutic perspectives. This study

Author contributions: J.C.: conception and design, collection and/or assembly of data, data analysis and interpretation, and manuscript writing; P.P. and M.L.: conception and design, collection and/or assembly of data, and data analysis and interpretation; C.B.: collection and/or assembly of data and data analysis and interpretation; M.F., F.C., B.B., L.F., G.A., M.G., M.C., P.V., C.N., and C.M.: collection and/or assembly of data; E.B.: conception and design and collection and/or assembly of data; E.C.: conception and design; M.P.: conception and design and manuscript writing; A.L.P.: conception and design, data analysis and interpretation, manuscript writing, and final approval of manuscript.

Correspondence: Anselme L. Perrier, Ph.D., 5 rue Henri Desbruères, 91030 Evry Cedex, France. Telephone: +33-1-69-90-85-23; Fax: +33-1-69-90-85-21; e-mail: aperrier@istem.fr Received October 11, 2012; accepted for publication April 9, 2013; first published online in STEM CELLS *EXPRESS* May 27, 2013. 1066-5099/2013/$30.00/0 doi: 10.1002/stem.1430

has accordingly been undertaken in a search for compounds that could meet that goal.

REST is a Krüppel-type zinc finger transcription factor that exerts its repressive *cis*-activity in the nucleus upon binding to a 21-nucleotide DNA sequence called repressor element-1 (RE1). REST is the key component of a nuclear complex consisting of associated core factors such as *SIN3A*, *SIN3B,* and *RCOR1* (a.k.a Co-Rest), and epigenetic regulators such as histone-deacetylases (HDACs), histone-methyltransferase (*EHMT2*), and histone-demethylase (*KDM1A*) that mediate chromatin compaction [9]. The composition of the nuclear complex and, as a consequence, the exact role of REST is dependent on the cell type and developmental stage [9,10]. REST has been initially described as an inhibitor of neuronal genes in non-neuronal cells [11,12], and its activity has more recently extended to several aspects of development, in particular pluripotent and neural stem cell (NSC) maintenance and commitment [13–16].

Levels of REST transcript and protein decrease during transition from mouse embryonic stem cells (ESCs) to neurons [17,18]. REST degradation leads to neural commitment and further differentiation of neural cells via the expression of critical proneural and neuronal activators containing RE1 site(s) in their promoters [13,17,19,20]. Different levels of REST may also control neuronal and glial lineage diversification [21–23] and the maintenance of the quiescent state characteristic of postmitotic neurons [24–26].

This study has been undertaken within the framework of a program seeking therapeutics for HD, using chemical compounds that may decrease the activity of REST in the human brain. Human pluripotent stem cells (hPSC: embryonic: hESC or induced: hiPSC) were used as they give access to an unlimited supply of human neural cells [27,28]. Harnessing this biological resource, we developed a cell-based reporter system to monitor REST activity in hPSC neural derivatives and carried out high throughput screening (HTS) that revealed hit compounds. The mechanism of action of the most potent of these hit compounds was subsequently determined. The activity of this compound was measured in vitro in human NSC carrying the Huntington mutation and in vivo in a phenotypic model of HD-like striatal degeneration. This work opens a potential path for the development of therapeutic agents against neurological diseases that involve loss of expression of neural genes controlled by REST.

Materials and Methods

Cell Culture

SA-01 (Cellartis) and RC9 (RoslinCells) hESC repeats lines (WT, XY) and HD1-iPS4 [29] hiPSC line (HD 72 CAG, XY) were differentiated into NSCs as described previously [27]. NSCs were grown on polyornithine/laminin-coated tissue culture plates in NSC medium containing Neurobasal, Dulbecco's modified Eagle's medium (DMEM)/F-12, N-2, and B-27 (Invitrogen, Carlsbad, CA, http://www.invitrogen.com) supplemented with 0.55 mM 2-mercaptoethanol, 10 ng/mL epidermal growth factor (EGF) (R&D Systems, Minneapolis, MN, http://www.rndsystems.com), and 10 ng/mL fibroblast growth factor 2 (FGF2) (Invitrogen). NSCs were passaged every 5–7 days up to 20 passages. To obtain neurons, confluent NSCs were grown during 7 days in NSC medium without BDNF, EGF, and FGF2. Cells were then plated at 400,000 cells per centimeter square in NSC medium supplemented with 10 μM DAPT (Sigma-Aldrich, St. Louis, http://www.sigmaaldrich.com). Cells were harvested after 14 days. Human embryonic kidney 293 (HEK) cells were passaged every 3–4 days and grown in DMEM, high glucose (Invitrogen) supplemented with 10% fetal bovine serum (Invitrogen).

Vectors

A 1,200 nucleotide (nt) fragment of the elongation factor 1 (EF1α) promoter containing the transcription start site (TSS) was blunted and cloned into HindIII-digested pGL4.82 [hRluc/Puro] luciferase reporter vector (Promega, Madison, WI, http://www.promega.com), upstream of *renilla* luciferase. Alternatively, a 540-nt fragment of phosphoglycerate kinase (PGK) containing the TSS was blunted and cloned into the NheI-digested pGL4.82 upstream of *renilla* luciferase. Sense and antisense 90 nt DNA fragment (see sequences in Supporting Information Table 3) containing three 17-nt-long RE1 or mutant RE1 sites, each one separated by 9 nt spacer, were synthesized by Invitrogen. These fragments were then annealed and cloned upstream of PGK or EF1α. Subcloning strategies for 6, 12, and 24 RE1 sites or mutantRE1 sequences were based on polymerase chain reaction (PCR) amplification of inserts with adapter primers or digestion/ligation of DNA fragments containing RE1 or mutant RE1 sequences. The D/N-REST vector was kindly provided by Dr. Noel Buckley (King's College, London). The D/N REST cassette corresponding to 234–437 amino-acid residues of mouse sequence coding for REST [30] was subcloned downstream of EF1α promoter in pIRES backbone (Clontech, Mountain View, CA, http://www.clontech.com) (pEF1α-D/N-REST: D/N-REST and pIRES: backbone vector). pMission small hairpin RNA (shRNA) plasmids (TRCN0000014785, Sigma-Aldrich) are directed against human REST gene (exon IV). Myc-DDK-tagged open reading frame (ORF) clone of Homo sapiens REST, transcript variant 1 was purchased from Origene (Rockville, MD, http://www.origene.com).

Bioluminescence Studies

Cells were transiently transfected using the Nucleofector Technology (Lonza, Basel, Switzerland, http://www.lonza.com). One and five million cells were transfected per nucleofection for HEK cells and NSCs, respectively. One microgram of reporter plasmids was used per transfection. Four microgram of D/N-REST or backbone plasmids were cotransfected with 1 μg reporter plasmids. Si-REST (Hs_REST_5) and si-RCOR1 (Hs_RCOR1_6) were purchased from Qiagen (Hilden, Germany, http://www1.qiagen.com) and were cotransfected at 100 and 10 nM, respectively, with 1 μg reporter plasmids. HEK cells and NSCs were plated in 96-well plates in 100 μL media at 350,000 and 500,000 cells per centimeter square, respectively. Cells were treated 5 hours after seeding with chemical compound or dimethyl sulfoxide (DMSO) only. Plates were then incubated for 24 hours at 37°C, with 95% humidity, and 5% CO_2. Enduren substrate (Promega) was then added in each well and the bioluminescent signal was read 90 minutes later on an AnalystGT microplate reader (Molecular devices, Union City, CA, http://www.moleculardevices.com). This measure was immediately followed by addition of CellTiter-Glo reagent (Promega) and the second bioluminescence signal (viability) was read 40 minutes later. Dual-glo luciferase assay, CellTiter-Glo, and Enduren live cell substrate experiments were done according to the manufacturer's protocols (Promega). The percentage of repression, de-repression, activity and the specificity index were calculated as follows:

- % repression = [E/CTG (mutant RE1) – E/CTG (RE1)]/[E/CTG (mutant RE1)] where E is the Enduren substrate signal, CTG is the CellTiter-Glo viability signal, and mutant RE1 or RE1 is the reporter plasmid.
- % de-repression by D/N-REST = [E/CTG(RE1 + D/N-REST) – E/CTG(RE1+backbone)]/[E/CTG(RE1+D/N-REST)].
- % de-repression by si-RNA = [E/CTG (RE1 + si-RNA) – E/CTG(RE1+ si-CTRL)]/[E/CTG (RE1 + si-RNA)] where si-RNA is si-REST or si-RCOR1. % activity = [(Sc/MN)) – 1] where Sc is the sample treated by compound and MN is the mean of samples treated by negative control (DMSO) in the same plate
- Specificity index = [% activity (RE1 + backbone) – % activity(RE1+D/N-REST)]/[% activity (RE1 + backbone)].

Primary HTS

Two chemical libraries were purchased: one from CHEM-X Infinity (Romainville, France, http://www.chem-x-infinity.com) and the other from Prestwick company (Illkirch, France, http://www.prestwickchemical.com); these libraries consisted of 5,864 compounds and 1,120 compounds, respectively. The primary screening was conducted on the Biocel1800 (Agilent, Palo Alto, CA, http://www.agilent.com) platform starting with 150 million NSCs that were transiently transfected with p12RE1-EF1α-Luc plasmids. Cells were then seeded in 44 384-well plates coated with poly-ornithine and laminin (15,000 cells per well in 38 μL of NSC medium). Five hours after seeding, each compound of Prestwick (5 μM final) or Chem-X library (2 μM final) was transferred in duplicate into wells. Positive control (valproic acid [VPA] 10 mM in DMSO 0.1% v/v) and negative control (DMSO 0.1% v/v) were added in columns 1 and 2 of each plate. Plates were then incubated for 24 hours. One day later, Enduren substrate CellTiter-Glo reagents were added and bioluminescence signals were measured as described above. Data analysis of the screening was done with Spotfire software (Tibco Co, Palo Alto, CA, http://spotfire.tibco.com/). The robustness of the HTS was evaluated using Z' factor calculated as follows: $Z' = 1 - [3(SDH + SDL)/(MH - ML)]$ where MH and ML correspond to the means of the positive and negative controls, respectively, and SDH and SDL correspond to the standard deviation of the positive and negative controls. Z-score method was applied to normalize values.

Quantitative Reverse Transcriptase PCR

RNA from NSCs SA-01, RC9, HD1-iPS4 or HEK293 cells was extracted after 1 day of treatment with DMSO (0.1% final) or with X5050 (100 μM final) in NSC medium without cytokines or HEK medium. The NSCs were lysed directly in the culture dishes, and RNA was isolated using RNeasy Mini kit (Qiagen) with DNAse I digestion. After quantification using a NanoDrop ND-1000A spectrophotometer, reverse transcription was performed with SuperScript III reverse transcriptase (Invitrogen) and random primers (Invitrogen). Gene expression was determined by quantitative reverse transcriptase PCR (QRT-PCR) performed with LC480 SYBR Green I Master mix (Roche, Basel, Switzerland, http://www.roche-applied-science.com). Primer sequences are presented in Supporting Information Table 4. For all experiments on human samples, values were related to 18S housekeeping gene then to appropriate control. For all experiments on mouse samples, values were related to β-actin housekeeping gene then to appropriate control.

Electrophoretic Mobility Shift Assay

Sense and antisense DNA fragments containing two RE1 sites separated by 9 nt spacer were synthesized (Invitrogen) and annealed (see sequences in Supporting Information Table 4). γ-dATP was incorporated by polynucleotide kinase T4 (Promega), and probes were purified on illustra MicroSpin G-50 Columns (GE Healthcare, Chalfont St Giles, United Kingdom, http://www.gehealthcare.com). Lysate from HEK cells transiently transfected with plasmids overexpressing REST (REST lysate) was purchased from Origene. Five microgram of lysate proteins were preincubated for 30 minutes at RT with or without competitor DNA (100-fold radioactive probe approximately 300 ng) in 22 μL of solution containing 0.1% DMSO (v/v) or 100 μM X5050, and the binding mix consisting of 8% (v/v) glycerol, 0.1 mM EDTA, 25 mM Hepes (pH 7.9), 5 mM $MgCl_2$, 34 mM KCl, 1 mM dithiothreitol (DTT), and 1 μg polydI-dC. Approximately 3 ng (≈40,000 cpm) of probes were then added, and the reaction mixture was incubated for another 20 minutes at RT. Reactions were run in 22.5 mM Tris-borate/0.5 mM EDTA buffer and electrophoretic mobility shift assay (EMSA) was performed using 5% polyacrylamide gels. Gels were then fixed, dried, and exposed to Biomax X-ray film (Kodak) for 72 hours.

Western Blot

Cells were resuspended in RIPA lysis buffer (Sigma-Aldrich) in the presence of Protease Inhibitor Cocktail (Sigma-Aldrich) and anti-phosphatases PhosphoSTOP (Roche). Protein concentration of cell extracts was determined using Pierce BCA Protein Assay Kit (Thermo Fisher Scientific Inc, Waltham, MA, http://www.thermofisher.com) according to the manufacturer's instructions. Proteins from each sample were mixed with NuPAGE lithium dodecyl sulfate (LDS) sample buffer 4× (Invitrogen) and DTT 1 M (Sigma-Aldrich) then heated at 70°C for 10 minutes. SDS poly-acrylamide gel electrophoresis (SDS-PAGE) was performed using NuPAGE Novex 4%–12% Bis-Tris Gels (Invitrogen) and NuPAGE 2-(N-morpholino)ethanesulfonic acid (MES) SDS running buffer (Invitrogen) with addition of NuPAGE antioxidant (Invitrogen). Twenty microgram of total proteins was loaded per well along with HiMark Pre-stained Protein Standard (Invitrogen). Protein migration was performed during 45 minutes at 200 V at RT. Proteins were transferred onto nitrocellulose membranes using the iBlot Gel Transfer Stack (Invitrogen) and the iBlot Dry Blotting System (Invitrogen). Membranes were blocked with 5% non-fat milk in phosphate-buffered saline (PBS) containing 0.1% Tween 20 (PBST) for 1 hour, then incubated overnight at 4°C with REST polyclonal antibody (Abcam, Cambridge, U.K., http://www.abcam.com). After several washes with PBST, blots were incubated for 1 hour at room temperature with rabbit horseradish peroxidase-conjugated secondary antibody. Membranes were then washed with PBST and incubated in Amersham ECL Plus Western Blotting Detection Reagents (GE Healthcare) in order to reveal immunoreactive bands by using the ImageQuant LAS 4000 mini luminescent image analyzer (GE Healthcare). Results were normalized to β-actin revealed with AC-74 antibody (Sigma-Aldrich). For myc-tagged experiments, we used anti-myc antibody (Invitrogen)

Transcriptome

RNA was extracted from six samples, corresponding to three independent cultures of NSCs SA-01, each one treated either with DMSO (0.1%) or with X5050 (100 μM). RNA was isolated using RNeasy Mini kit with DNase I digestion (Qiagen). Quality control was assessed using Agilent Bioanalyzer (Agilent Technologies, Germany) and NanoDrop spectrophotometer ND-1000A. Genome-wide gene expression profiling was performed by hybridization on oligonucleotide microarrays (in

total six GeneChips human Gene 1.0 ST) according to standards supplied by the manufacturer (Affymetrix, Santa Clara, CA, http://www.affymetrix.com). All quality controls and statistics were performed using Partek Genomic Suite. Raw data were normalized using the Robust Multichip Algorithm in Partek [32]. We first made a hierarchical clustering (Pearson's dissimilarity and average linkage) and principal component analysis for unsupervised analysis with all samples. To find differentially expressed genes, we applied a two-way ANOVA (factor treatment and factor culture) and computed the fold-change for each gene. All data obtained by microarray analysis have been submitted on gene expression omnibus (GEO) site with this accession number (GSE40695).

Gene set enrichment analysis (GSEA) was carried out using the motif database from the Broad Institute [31,33]. Genes belonging to the enrichment core of datasets with false discovery rate (FDR) < 0.05 were selected. For core enrichment genes in each dataset, gene ontology was performed using the online database DAVID (http://david.abcc.ncifcrf.gov [34,35]) and some of these genes were selected and confirmed by QRT-PCR. Hierarchical clustering with Ward method was done using JMP software.

Intraventricular Injection of X5050 in Quinolinic Acid Lesioned Mice

12-week-old male C57Bl6 mice (Charles River, France) were used in this study ($n = 14$). All experimental procedures were performed in strict accordance with the recommendations of the European Commission (86/609/EEC) concerning the care and use of laboratory animals. Mice were anesthetized with 0.1 mL/10 g of a mixture of ketamine (100 mg/mL) and 0.5 mL xylazine (20 mg/mL). Quinolinic acid was injected into the striatum, using a 34-gauge blunt-tip canula linked to a Hamilton syringe by a polyethylene catheter. A total volume of 1 μL (80 mM) was injected at 0.5 μL/minute. The stereotaxic coordinates were: anteroposterior, +1 mm; lateral, +2 mm from the bregma; and ventral, −2.7 mm from the dura, with tooth bar set at 0 mm. At the end of the injection, the needle was left in place for 5 minutes before being slowly removed. The skin was sutured and mice were allowed to recover. One week after the lesion, mice received simultaneous bilateral injection of X5050 (2× 2 μL of 20 mM in 10% DMSO in water) in the lateral ventricles (the stereotaxic coordinates were: anteroposterior, −0.46 mm; lateral, ±1 mm from the bregma; and ventral, −2.25 mm from the dura, with tooth bar set at 0 mm). An equal volume of 10% DMSO in water was injected in controls. Before injection, the needles were fully removed to allow cerebrospinal fluid (CSF) to exit from the needle tract, lower CSF pressure, and validate needle placement. At the end of the injection, the needles were left in place for 5 minutes before being slowly removed. One day after intraventricular injection, mice were killed and the brain was removed, blocked, and cut into 1-mm-thick coronal slices. On one coronal slice (+1 mm from bregma), tissue punches from the striatum were taken by using a tissue corer (1.5-mm in diameter). From the adjacent (anterior) slice, the prefrontal cortex was dissected out. RNA from all tissue punches was isolated with Trizol Reagent and RNeasy micro Kit according to the manufacturer's instructions (Qiagen).

Statistical Analysis

With the exception of the microarray analysis, all statistical analyses were performed using Graph Pad Prism5 and JMP software. For multiple comparisons we used one-way ANOVA analysis. In paired experiments, one sample *t* test or Student's *t* test were used depending on each experiment as indicated in the figure legends.

Results

Assay Development for Measuring REST Activity

REST activity was first measured during neuronal differentiation of SA-01 hESCs, in order to control the relevance of the cell model. REST mRNA levels were quantified using QRT-PCR in three cell populations: undifferentiated hESCs, hESC-derived NSCs, and neurons differentiated for 21 days from NSCs; Nestin (*NES*) and *SOX1* expression peaked in NSCs while synaptophysin (*SYP*), neural cell adhesion molecule L1 (*L1CAM*), synaptosomal-associated protein 25 (*SNAP25*), and α-synuclein (*SNCA*) were highest in neurons (Supporting Information Fig. S1A). In keeping with previous studies [13,17], the expression of the predominant and longer transcript of REST was maximal in hESCs and NSCs and decreased by 25-fold in neurons, while that of the alternatively spliced and shorter transcript *REST4* was minimal in hESCs and NSCs and increased by more than 100-fold in neurons (Supporting Information Fig. S1B) confirming observations made in rodent brain [36–38] and PC12 derivatives [39]. As a control, *RCOR1*, a core member of the REST nuclear complex, was not significantly modulated in any of the three cell populations. Western blot analyses confirmed the presence of the 122 kDa longer isoform of the REST protein in NSCs, the identity of which was further established by knocking-down REST using specific shRNA (Supporting Information Fig. S1C). The functionality of REST protein in NSCs was checked using a dominant/negative REST (D/N-REST) isoform. Expression of three RE1-genes containing two RE1 sites, *L1CAM*, *SNAP25*, and *SYP*, was significantly increased 24 hours after transfection (Fig. 1D). As control of specificity of the effects of D/N-REST, similar changes were not observed on mRNA levels of *SOX1* or *NES* that are not regulated by REST or on levels of REST itself.

Several RE1-containing reporter plasmids were designed and constructed in order to measure the activity of REST in hESC derivatives. "RE1-plasmids" included the coding sequence of *Renilla* luciferase under the control of the promoter of either EF1α or PGK, itself located downstream of 3, 6, 12, or 24 consensus RE1 sites (Fig. 1A). In control vectors ("mutant RE1-plasmids"), six nucleotides of the consensus sequence located at position with the highest position-scoring matrix (PSM) were mutated. The repressor activity of REST on luciferase expression was measured in SA-01 derived NSCs, 24 hours after transfection with either RE1-plasmids or mutant RE1-plasmids. Luciferase signals normalized to cell viability were lower in cells transfected with RE1-plasmids. This suggested the RE1-mediated repression of the luciferase expression cassette by endogenous REST in transfected cells (Fig. 1B). Additional experiments confirmed the specificity of the assay, that is, the relationship between luciferase signal and repressor activity of endogenous REST on RE1 sites upstream of PGK/EF1α promoter. RE1-plasmids were cotransfected with either D/N-REST plasmids or small interfering RNA (siRNA) targeting REST or RCOR1 to impair endogenous REST function (Fig. 1B). De-repression of these control conditions measured was found equivalent across the range of experiments. The assay specificity was further validated using reporter plasmids containing increasing numbers of RE1 or mutant RE1 sites. Repression of the activity of EF1α and PGK promoters under the control of RE1 sites increased in parallel to the number of RE1 sites. Repression curves were similar for both promoters and fitted a logarithmic model (Fig. 1C). The capacity of REST to inhibit luciferase expression of RE1-plasmids was independent of the orientation

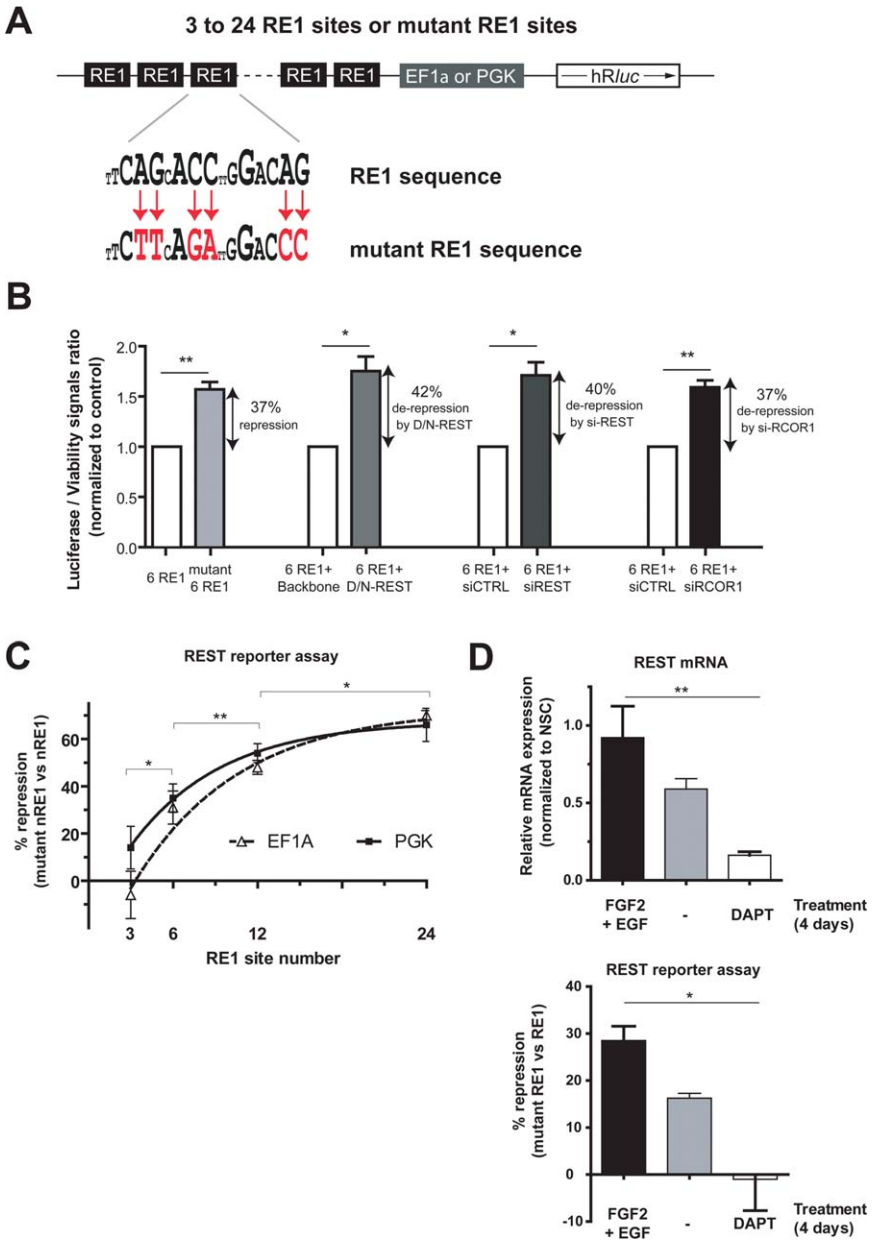

Figure 1. Luciferase-based reporter assay for REST activity in neural stem cells (NSCs). **(A):** Schematic of REST reporter cassette and RE1 consensus and mutated (red) sequences. **(B):** REST activity expressed as percentage of repression/de-repression of luciferase cassette. From left to right : Luciferase repression comparing signals with mutant 6RE1-PGK and 6RE1-PGK plasmids: luciferase de-repression by D/N-REST comparing signals with 6RE1-PGK + D/N-REST and 6RE1-PGK + backbone plasmids; luciferase de-repression by si-REST comparing 6RE1-PGK + si-REST and 6RE1-PGK + si-CTRL; luciferase de-repression by si-RCOR1 comparing 6RE1-PGK + si-RCOR1 and 6RE1-PGK + si-CTRL. Error bars: mean ± SEM ($n = 4$). One sample t test compared to 0. **(C):** Percentage of repression related to the number of RE1 sites. Experiments similar to (B) with plasmids with EF1α (continuous line) or PGK (dashed line) promoter driving luciferase. Error bars: mean ± SEM ($n = 11$). *, $p < .05$; **, $p < .01$ by unpaired two-tailed Student's t-test. Significant logarithmic fit of means ($p = .014$ for EF1α and $p = .007$ for PGK). **(D):** REST activity and REST mRNA levels in neural derivatives. Upper panel: Percentage repression quantified as in (B) but using 12RE1-EF1α and mutant 12RE1-EF1α plasmids. Lower panel: relative REST mRNA levels by quantitative reverse transcriptase polymerase chain reaction. NSCs pretreated for 7 days in medium without mitogens before being treated with one of three media (FGF2 + EGF, without cytokines, DAPT). Error bars: mean ± SEM ($n = 6$). *, $p < .05$; **, $p < .01$ by one-way ANOVA and Dunnett's multiple comparison test. Abbreviations: D/N REST, dominant-negative form of REST; DAPT, N-[N-(3,5-Difluorophenacetyl)-L-alanyl]-S-phenylglycine t-butyl ester; EGF, epidermal growth factor; EF1α, elongation factor 1α; FGF2, fibroblast growth factor; PGK, phosphoglycerate kinase; RE-1, repressor element-1; REST, repressor element-1 silencing transcription factor

(sense or reverse) of the RE1 sequences and of the normalization method (Supporting Information Fig. S1A, S1B).

In order to test the correlation between REST mRNA levels and repression of the reporter gene in cells transfected with RE1-plasmids, three neural cell populations containing different levels of REST were assayed: cells cultured with FGF2 and EGF, in which REST level is the highest, cells coaxed to neuronal differentiation by the notch inhibitor DAPT (Supporting Information Fig. S2C) that have the lowest level and cells cultured without mitogens that have

intermediate level. Levels of REST enzymatic reporter activity paralleled levels of *REST* mRNA (Fig. 1D).

HTS for REST Inhibitors

The conditions that achieved statistical robustness compatible with HTS of several thousand chemical compounds were defined in SA-01-derived NSCs. Several pharmacological inhibitors of enzymes present in the REST nuclear complex were examined in order to identify the most suitable positive control for our REST assay in NSCs. The HDAC inhibitor (VPA, 10 mM) showed the highest activity, as normalized to negative control treatment (DMSO) (Supporting Information Fig. S3A). Using these controls, the mean score of Z' factor calculated for the REST assay in NSCs on a set of five 384-well plates was 0.5 ± 0.2 (mean $\pm$ SD), a value that is appropriate for HTS (Supporting Information Fig. S3B).

The effect of 6,984 compounds was tested in duplicate in SA-01-derived NSCs transfected with 12 RE1-plasmids. Compounds were selected as primary hits—potential REST inhibitors—when viability signal was not reduced below 70% and when REST activity was above a two-sigma threshold (mean plate signal + 2 SD) (Fig. 2A). Fifty compounds matched those first selection criteria. Retest screening and counter-screening using mutant RE1-plasmid retained 23 of them (Fig. 2B) out of which 20 showed dose-dependent activity. We then applied an arbitrary threshold for maximum activity of 30% over controls (D/N-REST plasmids) and thus selected the 11 most potent compounds. These 11 compounds mostly clustered into two chemical families, namely benzoimidazole-5-carboxamide and pyrazole propionamide derivatives (Supporting Information Fig. S2C; Table 4). Properties of the two most potent and specific members of each chemical family are shown in Figure 2C, 2D, and 2E. The benzoimidazole-5-carboxamide derivative X5050 exhibited both the highest activity and specificity. Its activity was dependent on the number of RE1 sites (Fig. 2F) and was confirmed both using an alternative normalization strategy based on a firefly luciferase control plasmid and in another NSC line derived from RC9 (WT) hESCs (Supporting Information Fig. S2D). X5050 compound was therefore selected for subsequent studies.

Mechanism of Action of X5050 on REST Activity

Mechanism of action of X5050 was sought on REST binding to RE1 site, REST transcription, alternative RNA splicing, and protein degradation. EMSA with a radioactive oligonucleotide containing two RE1 sequences revealed a distinctive labeled band that disappeared after addition of 100-fold excess of unlabeled probes in extracts of HEK293 cells overexpressing REST (Fig. 3A). Addition of X5050 (100 μM) did not decrease the band intensity indicating that it did not affect the in vitro binding of endogenous REST to RE1 sites. Quantification of REST levels using primers recognizing all types of REST transcripts showed no significant change in X5050 treated cells, excluding a transcriptional effect (*REST-all* in Fig. 3C). There was no change in the titer of transcripts for the longer isoform of REST either (*REST* in Fig. 3C). However, levels of the *REST4* shorter transcripts increased twofold, which is likely associated to the initiation of neuronal commitment in treated cultures (*REST4* in Fig. 3C).

In the absence of effects of X5050 at DNA or RNA levels, the levels of REST protein were then analyzed. Western blot analyses of NSC extracts showed that 24-hour-long treatments with increasing doses of X5050 induced a dose-dependent decrease in the 122 kDa longer REST isoform (Fig. 3D). Treatment of NSCs with Bortezomib (100 nM) or MG132 (10 μM), two cell-permeable proteasome inhibitors, increased the activity of REST as measured by the repression of the reporter cassette but did not prevent X5050 dose-dependent inhibition. This result indicated that the compound does not act directly on the proteasome activity (Supporting Information Fig. S4). Although NSCs assayed are proliferative, one possible confusing parameter in these experiments could be the concomitant stimulation of neuronal differentiation in the culture, as REST levels decrease over that process. The activity of X5050 was therefore assessed in non-neural cells expressing high levels of REST in the absence of any potential neuronal differentiation. Twenty-four hours after cotransfection of HEK cells with 12RE1-plasmids and either backbone or D/N-REST plasmids in the presence of increasing concentrations of X5050, REST activity—that is, de-repression of the reporter cassette—decreased in a dose-dependent manner, similarly to results obtained in treated NSCs (Fig. 3B). As in NSCs, REST expression was not changed by X5050 treatment, the expression of the neuron-specific and shorter transcript *REST4* being below detection level (Fig. 3E). Western blot analyses of HEK extracts showed that 24-hour-long treatments with increasing doses of X5050 induced a dose-dependent decrease in the 122 kDa longer REST isoform (Fig. 3F). This was also the case for transgenic MYC-tagged-REST protein (Fig. 3G). These results altogether support the hypothesis that X5050 reverses REST repression on neuronal genes by promoting its degradation.

Functional Impact of X5050 on Gene Expression in Human NSC

The functional impact of the changes induced by X5050 was then investigated using a whole-genome differential transcriptomic approach. Changes in gene expression resulting from the treatment of NSCs with 100 μM X5050 for 24 hours were analyzed using GSEA on Affymetrix human Gene 1.0 ST array. Genes modulated by X5050 that contained a common regulatory sequence (e.g., a binding site for a transcription factor or for a micro-RNA) were identified using the analysis software and "motif" gene set database from the Broad Institute. Eight out of the 828 gene sets were over-represented in a statistically significant (FDR <0.05) manner at the top (two upregulated gene sets) or bottom (six downregulated gene sets) of the list of genes ranked according to their modulation by X5050 (Fig. 4A; Supporting Information Table 2). Gene ontology of the core enrichment group of each of these eight gene sets—that is, the list of genes that contributed most to the enrichment result—were analyzed using DAVID bioinformatics resource (Fig. 4A). Among the six downregulated gene sets, four comprised genes that encode nucleic acid-interacting proteins such as histones and proteins present in nucleosomes or spliceosomes. The last two gene sets contained genes involved in focal adhesion and cellular contractility. One of the two upregulated gene sets consisted of genes containing a consensus binding sequence for miR-380. However, the result that attracted most attention was the other upregulated gene set, V$NRSF, as it clusterized the 72 genes that display at least one validated RE1 sequence and are, accordingly, the most likely targets of REST silencing (Fig. 4B). Furthermore, gene ontology of the 26 genes that formed the core enrichment group of V$NRSF revealed a statistically significant over-representation of RE1-genes implicated in neuronal function or development ($p < 10^{-3}$ to 10^{-6}). In order to further confirm the specific impact of X5050 on RE1-genes, a larger set of 494 genes that were identified as functional RE1-genes with PSM score >0.9 (http://bioinformatics.leeds.ac.uk/RE1db_mkII/) was analyzed. Hierarchical clustering of these data segregated transcriptome observations of DMSO-treated cells from X5050-treated cultures (Fig. 4C).

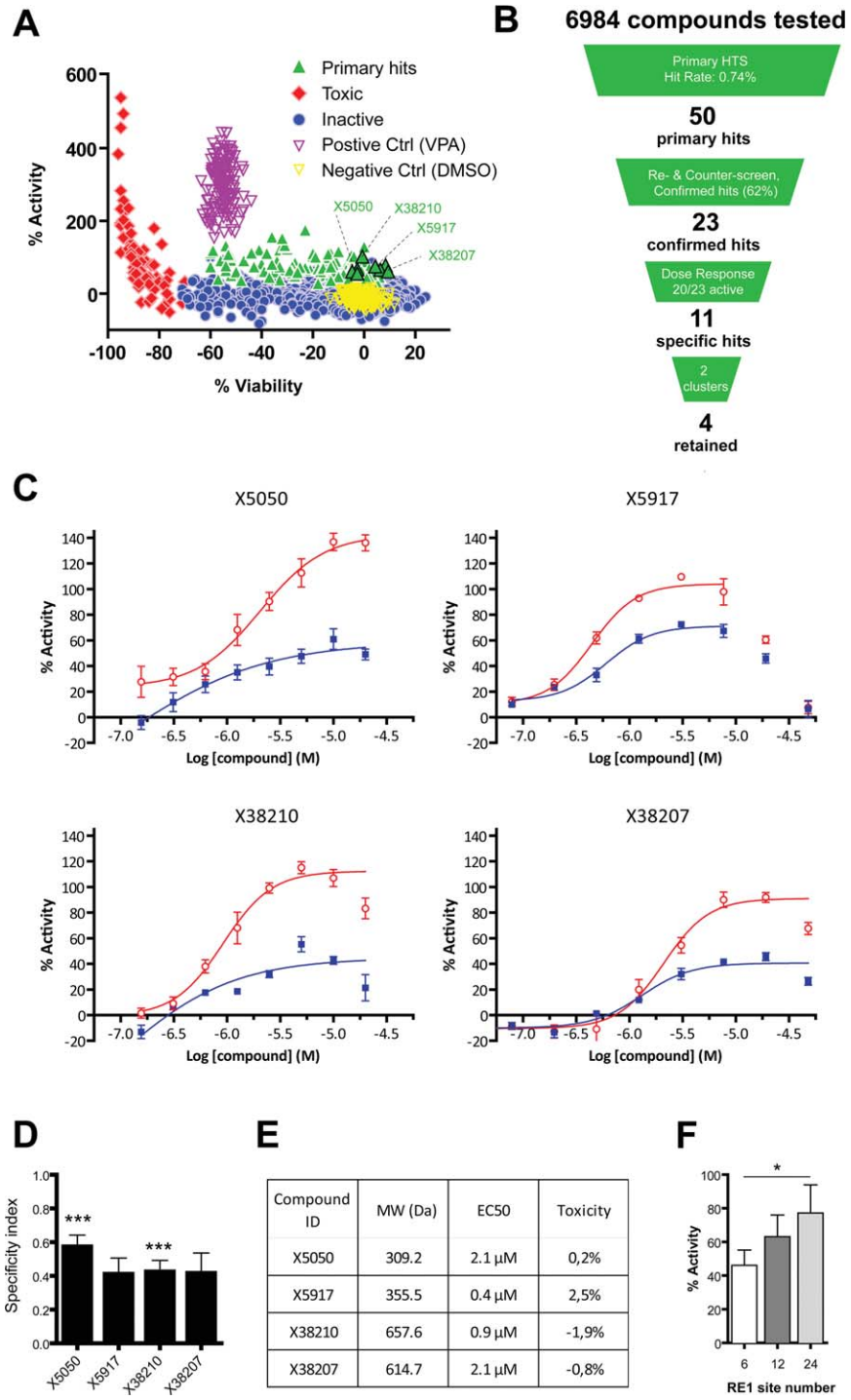

Figure 2. Identification by high throughput screening of candidate repressor element-1 silencing transcription factor (REST) inhibitors in neural stem cells (NSCs). **(A):** Primary screening and hit selection. Activity of each compound expressed as % increase in bioluminescence-to-viability ratio signal with compound normalized to bioluminescence-to-viability ratio signals obtained with DMSO. Primary hit compounds shown in green, toxic compounds in red, inactive compounds in blue, negative controls (DMSO) in yellow, and positive controls (10 mM VPA) in purple. **(B):** Attrition cascade of primary hits. **(C):** Dose-response activity for four most potent hit compounds. NSCs cotransfected with 12RE1-PGK and backbone plasmids (REST activity in red) or D/N-REST plasmids (nonspecific activity in blue). Error bars: mean ± SD of three wells. Nonlinear fit using the inhibitory dose-response curves with variable slope model with Graph pad Prism5. **(D):** Specificity index of the four selected hits. Specificity index calculated from the difference in plateau levels of dose-response REST activity related to control. Error bars: mean ± SEM ($n = 6$). ***, $p < .001$ by one sample t test compared to 0. **(E):** Characteristic parameters for the four selected hits. **(F):** Dose-dependent activity of X5050 to the number of RE1 sites. NSCs transfected with RE1 plasmids with increasing number of RE1 sites treated for 1 day with 8 μM X5050. Error bars: mean ± SEM ($n = 6$). *$p < .05$ by unpaired two-tailed Student t test. Abbreviations: DMSO, dimethyl sulfoxide; VPA, valproic acid.

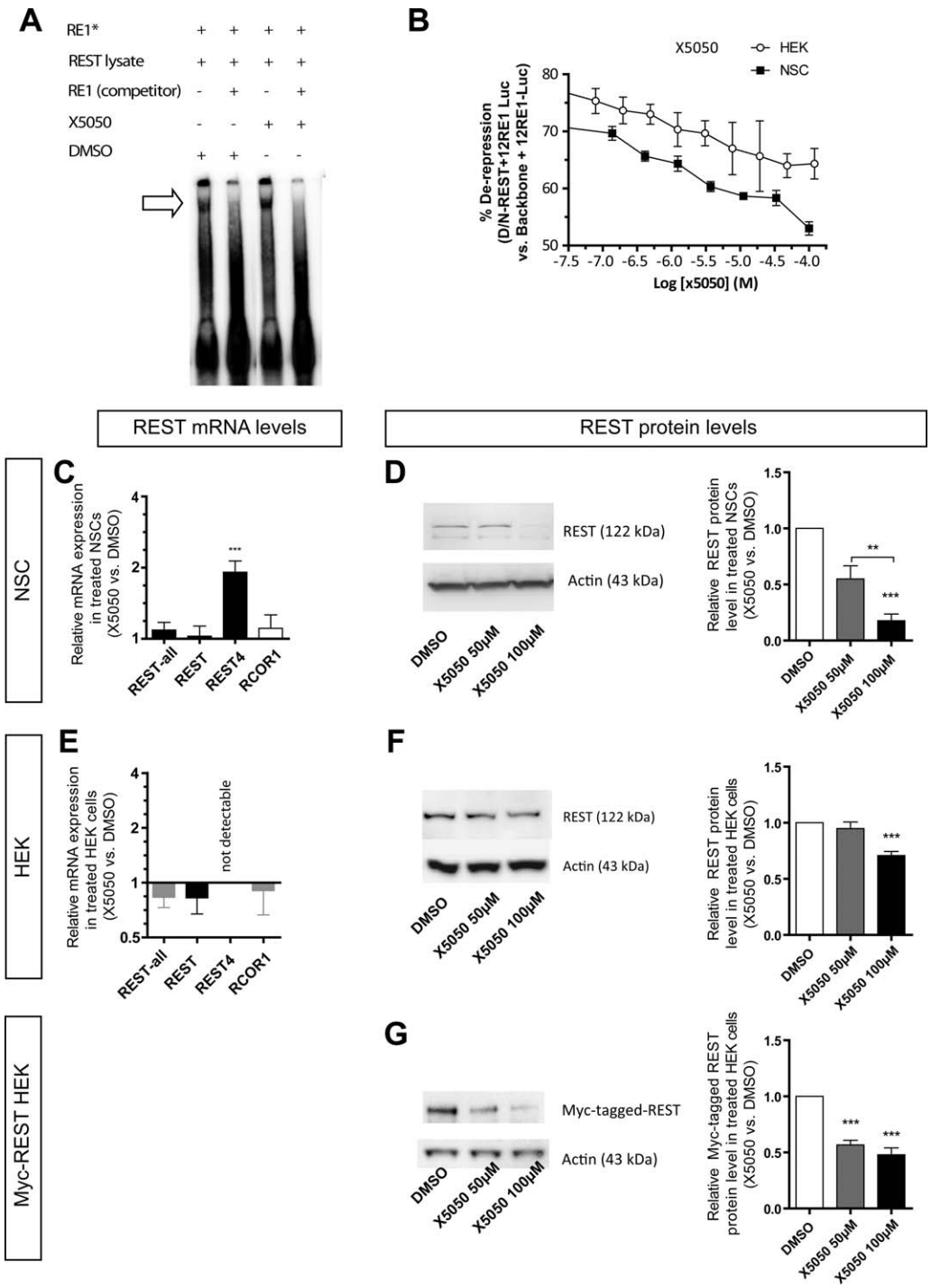

Figure 3. Mechanism of action of X5050. **(A):** Electrophoretic mobility shift assay of radiolabeled oligonucleotides with 2 RE1 sequences. Arrow corresponds to REST-RE1* complex. **(B):** Percentage of de-repression by D/N-REST with increasing X5050 concentrations in NSCs and HEK cells. Cells cotransfected with 12RE1-EF1α and backbone or D/N-REST plasmids. Values are mean ± SD (three wells). **(C, E):** Relative mRNA expression levels of REST and RCOR1 in NSCs derived from SA-01 wild-type (WT) human embryonic stem cells (C) or in HEK cells (E) treated with X5050. **(D, F):** Effect of X5050 on endogenous REST protein level in NSCs. Left panel: one representative immunoblot. SA-01 (WT)-derived NSCs (D) or HEK (F) treated 1 day before protein extraction, with 50 or 100 μM X5050 or with DMSO. β-Actin as loading control. Right panel: Densitometry (values are normalized to DMSO-treated cells). **(G):** Effect of X5050 on transgenic myc-tagged REST protein level in transfected HEK cells. Left panel: One representative immunoblot. HEK cells transfected with Myc-tagged REST plasmid 1 day before treatment. One day treatment with 50 or 100 μM X5050 or with DMSO. β-Actin as loading control. Right panel: Densitometry. One day treatment with 50 or 100 μM X5050. For (C–G): Error bars, mean ± SEM ($n = 6$). **, $p < .01$; ***, $p < .001$ by one sample t test compared to 1. Abbreviations: DMSO, dimethyl sulfoxide; HEK, human embryonic kidney; NSC, neural stem cell; REST, repressor element-1 silencing transcription factor; RE-1, repressor element-1.

A

GSEA geneset name	NES	FDR	Recognized sequence	GO analysis of enrichment core	GO p-value
KRCTCNNNNMANAGC_UNKNOWN, TTTNNANAGCYR_UNKNOWN	-2.97 -2.38	< 0.001 < 0.001	in promoter (unknown)	nucleosome, histone	10^{-11}-10^{-52}
GGAANCGGAANY_UNKNOWN	-2.17	< 0.001	in promoter (unknown)	spliceosome	10^{-3}
SGCGSSAAA_V$E2F1DP2_01	-1.79	0.029	in promoter for E2F1	chromatin, nucleosome, transcription	10^{-3}- 10^{-6}
V$SRF_Q4 V$SRF_01,	-1.78 -1.73	0.026 0.038	in promoter for SRF	actin-binding, contractile, focal adhesion	10^{-4}-10^{-8}
ATTACAT,MIR-380-3P	2.27	< 0.001	in 3'UTR for miR-380-3p	no GO	/
V$NRSF_01	1.85	0.046	in promoter for REST	nerve impulse, synapse, axonogenesis, ion channel	10^{-3}-10^{-6}

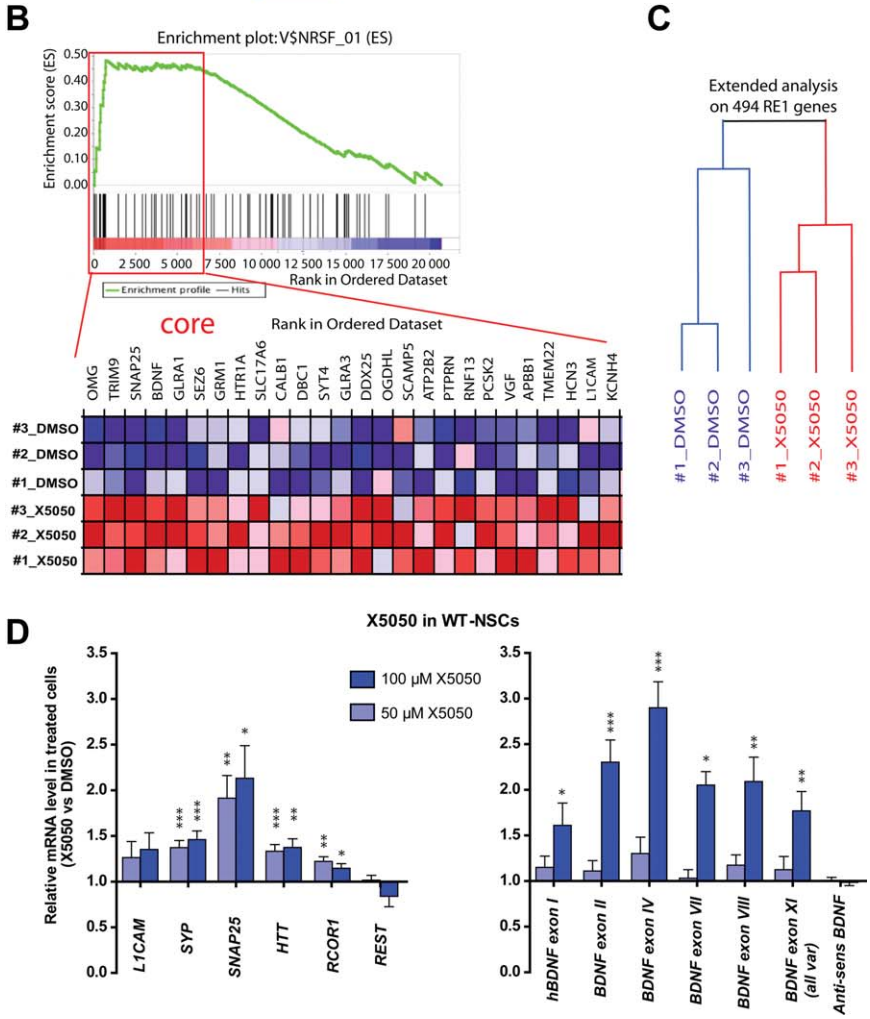

Figure 4. Transcriptome analysis of wild-type NSCs treated with X5050. **(A):** Significant motif gene sets by GSEA of SA-01 NSC samples. NES (values for genes upregulated and downregulated by X5050 in red and blue, respectively). GO analysis of enrichment core of genes in corresponding gene set. **(B):** V$NRSF gene set. Upper panel: Plot of enrichment score for genes present in the gene set. Bars underneath the plot correspond to genes of the gene set. Lower panel: Heatmap of core enrichment genes of the V$NRSF gene set. **(C):** Hierarchical clustering of experiments using 494 functionally identified RE1 genes with position-scoring matrix >0.9. **(D):** Quantitative reverse transcriptase polymerase chain reaction confirmation of transcriptome data in RC9 (WT) derived NSCs. Left panel: Expression level of RE1 genes (*L1CAM, SNAP25, SYP, HTT*) and control genes (*RCOR1, REST*), Right panel: Expression level of BDNF alternative transcripts, 1 day after treatment with 50 μM (light blue bars) or 100 μM (dark blue bars) of X5050. Values normalized to values in NSCs treated with DMSO. Error bars: mean ± SEM ($n = 12$). *, $p < .05$; **, $p < .01$; ***, $p < .001$ compared to DMSO by one sample *t* test compared to 1. Abbreviations: BDNF, brain-derived neurotrophic factor; DMSO, dimethyl sulfoxide; FDR, false discovery rate; GO, gene ontology; GSEA, gene set enrichment analysis; NES, normalized enrichment score; NSC, neural stem cell; REST, repressor element-1 silencing transcription factor; UTR, untranslated region; WT, wild type.

Analysis of upregulated genes showed the predominance of neuronal genes. Gene expression data were confirmed by QRT-PCR in another NSC line derived from RC9 wild-type (WT) hESCs on selected upregulated or downregulated transcripts. At 100 μM, X5050 upregulated by more than twofold two representative RE1 neuronal genes, *SNAP25* and *BDNF*

(Fig. 4D) while downregulating histone 1H genes (*HIST1H2BM*, *HIST1H3J*) (Supporting Information Fig. S5). Differential regulation of BDNF splice variants was measured using primers specific for upstream 5′ untranslated exons, including exon II that contains an RE1 site. Upregulation of other RE1-genes tested was less marked (*SYP*, *HTT*) or not statistically significant (*L1CAM*). Expression of REST and other control genes without known RE1 sites such as, RCOR1 or antisense BDNF was not notably upregulated. Altogether, the unbiased GSEA and the supervised analysis of a large number of RE1-genes indicated that X5050 upregulates neuronal RE1-genes in human NSCs.

Functional Impact of X5050 in HD Models

The functional impact of the changes induced by X5050 was finally investigated in HD pathological conditions. X5050 activity was measured on NSCs derived from a human induced pluripotent stem cells (HD1-iPS4 line) previously generated from somatic cells of a patient diagnosed with HD [29]. The dose-dependent effect of X5050 was tested in HD1-iPS4 derived NSCs (Fig. 5A). Dose-response curves for REST activity measured in parallel in HD-iPSC4 NSCs and RC9 (WT) NSCs showed no significant difference. Effect of X5050 on the expression levels of selected RE1- and control genes in HD-NSCs was measured by QRT-PCR. The profile of regulation by X5050 of the expression of RE1-genes and control genes was similar to that measured in WT-NSCs (Figs. 5B, 4D). The highest and most significant upregulations were those observed for *SNAP25* and *BDNF* alternative transcript containing exon II and to a lesser degree for *BDNF* transcripts containing exons IV and VIII and *SYP* (Fig. 5B). Basal levels of *BDNF II* and *BDNF IV* were lower in HD-NSCs than in WT-NSCs (Supporting Information Fig. S6), confirming previous report using similar cells derived from HD1-iPS4, WT-iPSC, and HD1-iPS4 clones genetically corrected the for CAG expansion [40].

In vivo activity of X5050 was finally measured in the brain of mice with Quinolinic Acid (QA)-induced excitotoxic striatal lesions. C56BL6 mice received unilateral injection of 80 nmol of QA to induce neurodegeneration of medium spiny striatal projection neurons (Darpp32 immunopositive), the major population of striatal neurons [41]. Although striatal QA does not produce direct excitotoxic neuronal death in the cortical regions anatomically connected to the striatum, a loss of BDNF levels has been reported in the cerebral cortex ipsilateral to the lesion [42]. Thus, we reasoned that the QA model would be appropriate to test the pharmacological efficacy of X5050 in vivo to increase BDNF expression. One week after lesioning, mice received bilateral injection of either X5050 or vehicle in the lateral ventricles in order to bypass the blood brain barrier. Effect of QA lesion and X5050 acute treatment on the expression levels of selected RE1 and control genes was measured 24 hours after X5050 injection, in striatum and in the prefrontal cortex, a cortical area spared by the direct excitotoxic effect of QA but anatomically connected to the striatum and localized near the anterior part of the lateral ventricles where X5050 was injected. A decrease in *Darpp32* and *Snap25* expression was found by QRT-PCR in the lesioned striatum as compared with the contralateral striatum. This confirmed that QA had induced significant neurodegeneration in this brain region (Fig. 5C). Expression levels in samples from prefrontal cortex from all animals were also measured by QRT-PCR (Fig. 5D). Results showed a significant ($p < .05$) upregulation of *Bdnf, Snap25*, *Trim9*, and *Omg* (the mouse homologs of the top four RE1-genes of the V$NRSF-1 core enrichment list presented in GSEA, Fig. 4B) by X5050 in the prefrontal cortex ipsilateral to the QA-lesioned striatum (Fig. 5D). Most importantly, using splice variant specific primers for *BDNF,* QRT-PCR revealed that, in QA-lesioned hemisphere, X5050 significantly increased the levels of *Bdnf II* splice variant (exon II containing variant) while *Bdnf IV* levels were not significantly changed. Altogether, the functional analysis of X5050 in HD-NSCs and QA-lesion mice suggested that this compound was active in an HD pathological context (Fig. 5D).

Discussion

The main result of this study is the identification of a benzoimidazole-5-carboxamide derivative (X5050) that promotes the expression of neuronal genes including *BDNF* and *SNAP25* via the degradation of REST in human neural stem cells. Combination of HTS and pluripotent stem cell technologies was instrumental in identifying that compound as an inhibitor of REST activity from a proprietary library of several thousand molecules and in exploring its mechanism of action in human neural stem cells. In vitro and in vivo functional analyses in HD models revealed that X5050 is active in HD pathological context. In particular, X5050 upregulated among several known REST-regulated genes, the expression of *BDNF* in the cortex of mice with striatal lesions. This study underlines the value of a strategy aimed at modulating REST in the attempt to restore key neuronal gene transcription in the brain. This may reveal valuable to tackle neurodegenerative conditions involving downregulation of BDNF in particular in the case of HD for which BDNF impairment results in part from increased REST activity.

REST transcriptional regulation of RE1-genes is modulated at multiple levels including transcription, protein degradation, intracellular localization, and REST-nuclear complex composition and binding to RE1-sequences [18]. We have developed a luciferase-based assay for REST activity on transgenic RE1 sites that could report all these types of regulation. This assay efficiently measured REST activity levels in NSCs as it successfully integrated a number of challenges against REST function including: (a) the inhibition of REST binding to RE1 either via the mutation of the RE1 sequences or via the competitive binding of D/N-REST, (b) *REST* expression knockdown by REST-targeting siRNA, (c) the combined reduction of *REST* mRNA and protein levels via induction of NSC neuronal differentiation, and finally (d) the impairment of the formation of REST nuclear complex via the knockdown of RCOR1, one of the main core cofactors of this complex.

With the ultimate goal of discovering chemical compounds that may decrease the activity of REST in the human brain, we took advantage of the specificity of this assay to identify by HTS two clusters of candidate REST inhibitors. None of the FDA-approved drugs (Prestwick library) we tested displayed a significant effect against REST activity, suggesting that drug repositioning may not be an option. All hits were identified from a proprietary chemical library of over 5,000 synthetic molecules. The most potent REST inhibitor was the benzoimidazole-5-carboxamide derivative X5050. Several compounds closely related to X5050 were active against REST, although with reduced potency.

The exploration of the mechanisms of action of X5050 in NSCs has evidenced drug-induced degradation of REST. Treatment of non-neural cells, HEK, with X5050, resulted in a similar reduction in endogenous or transgenic Myc-tagged REST levels, indicating that this reduction was not mediated by the induction of the neuronal differentiation of NSCs, also known to decrease REST bioavailability [17]. The actual

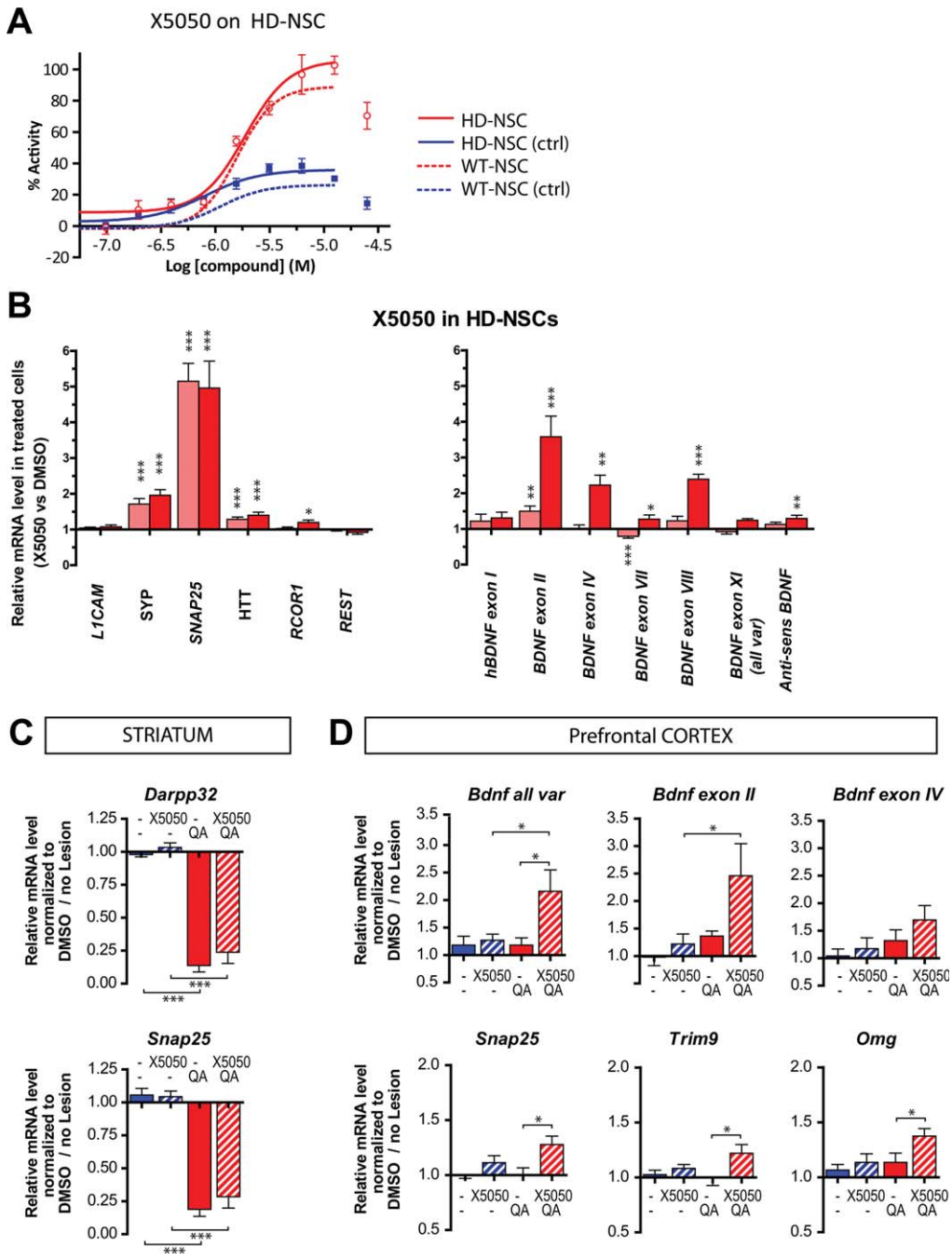

Figure 5. Functional impact of X5050 in Huntington disease models: **(A):** Dose-response activity for X5050 in NSC derived from RC9 (WT) and HD1-iPS4 (HD) pluripotent stem cells. NSCs were cotransfected with 12RE1-EF1a and backbone plasmids (REST-activity in red) or D/N-REST plasmids (nonspecific activity in blue). Nonlinear fit dose-response curves for WT-NSCs (dashed lines) and for HD-NSCs (solid lines). Error bars: mean ± SEM of four wells. **(B):** Quantitative reverse transcriptase polymerase chain reaction (QRT-PCR) analyses of X5050 activity in HD1-iPS4-derived NSCs. Left panel: Expression level of RE1 genes (*L1CAM, SNAP25, SYP, HTT*) and control genes (*RCOR1, REST*), Right panel: Expression level of BDNF alternative transcripts, 1 day after treatment with 50 μM (pink bars) or 100 μM (red bars) of X5050. Values normalized to values in HD-NSCs treated with DMSO. Error bars, mean ± SEM ($n = 12$). *, $p < .05$; **, $p < .01$; ***, $p < .001$ compared to DMSO by one sample *t* test compared to 1. **(C, D):** QRT-PCR analyses of X5050 activity in the brain of mice with QA-induced excitotoxic striatal lesions. (C) Expression level in striatal samples of striatal neurons marker (*Darpp32*, *Snap25*), 24 hours after X5050 bilateral intraventricular injection of X5050 (i.e., 1 week after QA injection). (D) Expression level in prefrontal cortex samples of selected neuronal RE1-genes [*Bdnf (variant containing exon II, IV and all variants*), *Snap25, Trim9*, and *Omg*] 24 hours after bilateral intraventricular injection of X5050. Values normalized to median of values of samples from same brain region of unlesioned hemisphere injected with vehicle. Values for samples from unlesioned brain hemisphere (blue bars), from QA-lesioned hemisphere (red bars), from X5050-treated mice (cross-hatched bars). Error bars, mean ± SEM ($n = 7$ per group). *, $p < .05$; **, $p < .01$; ***, $p < .001$ by unpaired two-tailed Student *t* test. Abbreviations: BDNF, brain-derived neurotrophic factor; DMSO, dimethyl sulfoxide; HD, Huntington disease; NSC, neural stem cell; QA, quinolinic acid; REST, repressor element-1 silencing transcription factor; WT, wild type.

target protein(s) of X5050 remain(s) to be identified. Since inhibition of proteasome did not reduce X5050 activity, good candidates may therefore be found among the enzymes that control REST ubiquitination by tagging REST for proteasome degradation. Several studies have indeed demonstrated that REST degradation in the proteasome via the SCF-βTRCP complex, which consists of Skp1, Cul1 and the F-box protein β-TrCP (β-transducin repeat containing protein), critically regulates REST activity and, consequently, neuronal commitment of NSCs [13,19,43].

BDNF deficiency in the brain has been linked to psychiatric and neurodegenerative disorders including depression, Alzheimer, Parkinson, or HD (for review see [44,45]). In the later case, reduced BDNF level in the striatum has been reported both in HD patients and in HD genetic models [46,47]. BDNF is mostly anterogradly transported to the striatal tissue from cortical neurons [48]. Studies in transgenic mice lacking cortical BDNF expression best illustrate that BDNF is required for the differentiation and long-term survival of the medium spiny neurons in the striatum, the neurons most affected in HD [49]. HTT mutation disrupts both the BDNF transport from the cortex to the striatum [50,51] and the expression of cortical BDNF via HTT mutation-mediated impairment of REST [7,52,53]. These observations have set BDNF as a promising therapeutic target for HD [54]. Along that this line, pharmacological upregulation of BDNF level in the brain through REST inhibition should open interesting perspectives. The backbone of X5050 appears of particular interest since transcriptome analysis has shown that, among RE1-genes encompassing a wide variety of organ-specific cell types, X5050 affected specifically those related to neuronal function. This included *BDNF* and most significantly the *BDNF* splice variant known to be regulated by REST containing exon II: *BDNF II*. Effect of X5050 on *BDNF* was not limited in WT-NSCs to *BDNF II* but was detectable for *BDNF I, IV, VII, VIII* mRNA variants. This could result from a positive feedback loop induced by X5050 activity on BDNF. Increased release of BDNF that may result from X5050 upregulation of *BDNF II* could activate BDNF receptor TrkB and its downstream intracellular effectors such as cyclic CREB (cAMP response element binding) in turn responsible for *BDNF I* and *IV* promoters' activation (for review see [55]). Effect of X5050 on *BDNF II* expression was as well confirmed in HD-NSCs. An et al. [40] have linked the reduced expression of *BDNF* in HD1-iPS4 derived NSCs (compared with level in WT-NSCs) to the *HTT* mutation, genetically correcting the CAG expansion (72 CAGs) in HD1-iPS4 clones. In this work, we showed that X5050 rescued *BDNF II* reduced expression in NSCs derived from the same HD1-iPS4 line.

A pilot assessment of the acute activity of the X5050 compound was conducted in mice with QA lesion of the striatum that reproduce the neuronal loss observed in the striatum of HD patient (for review see [56]). Reduced BDNF protein levels in the cortex have been reported within weeks of QA injection in the ipsilateral striatum and have been monitored to assess the efficacy of new neuroprotective approach [42,57,58]. Using the same animal model, Rite et al. [59] have also demonstrated that the expression of *BDNF* in cortical areas projecting to striatum is dependent on both target integrity and neuronal activity. We consequently explored the activity of X5050 in a cortical region known to project in the striatum, the prefrontal cortex. Neurons in this cortical region should be affected by the loss of their striatal targets. Indeed, we found that X5050 treatment impacted on *BDNF* and other RE1-neuronal gene expression in QA-lesioned hemisphere. The identification of novel chemical compounds that could lift the repression of neuronal genes such as *BDNF* mediated by pathologically over-active REST may have direct therapeutic applications. Strategies to further characterize the therapeutic potential of X5050 will involve chronic administration of this hit compound or one of its chemical derivatives in a genetic model of HD in mice and should ultimately aim at exploring the capacity of the agent injected to slow neurodegeneration and dysfunction in HD animal. Overall our data show that compounds with X5050 backbone appear as potential candidates for normalizing expression level of key neuronal genes in patients with HD and even other neurodegenerative disorders featuring alteration of BDNF level.

Acknowledgments

We thank Dr. G. Daley (Children's Hospital Boston, MA) for providing the HD1-iPS4 line; Dr. P. De Sousa (RoslinCells, U.K.) for the RC9 line; Dr. P. Charbord for helpful discussions and transcriptome analysis; Dr. J. Denis and Dr. N.J. Buckley for helpful discussions; and Dr. F. Letourneur and F. Dumont of the Genomic/transcriptomic platform (Cochin Institute, Paris, France). This work was supported by additional grants from European Union programs FP6 STEM-HD and FP7 Neurostemcell, the laboratoire d'Excellence Revive (Investissement d'Avenir; ANR-10-LABX-73) and by a FRM fellowship to J.C. J.C. is currently affiliated with Department of Cell and Molecular Biology, Karolinska Institutet, Stockholm, Sweden; P.P. is currently affiliated with CYTOO Cell Architects, Bâtiment BHT- BP 50, 7 parvis Louis Néel, Grenoble, France; F.C. is currently affiliated with Discngine-Parc Biocitech, Romainville, France; M.L. is currently affiliated with Institut de la Vision, UMRS INSERM 968, UMRS CNRS 72.10, Université Pierre et Marie Curie, Paris, France.

Disclosure of Potential Conflicts of Interest

The authors indicate no potential conflict of interest.

References

1 Zuccato C, Tartari M, Crotti A et al. Huntingtin interacts with REST/NRSF to modulate the transcription of NRSE-controlled neuronal genes. Nat Genet 2003;35:76–83.

2 Zuccato C, Belyaev N, Conforti P et al. Widespread disruption of repressor element-1 silencing transcription factor/neuron-restrictive silencer factor occupancy at its target genes in Huntington's disease. J Neurosci 2007;27:6972–6983.

3 Ravache M, Weber C, Merienne K et al. Transcriptional activation of REST by Sp1 in Huntington's disease models. Plos One 2010;5:e14311.

4 Rigamonti D, Mutti C, Zuccato C et al. Turning REST/NRSF dysfunction in Huntington's disease into a pharmaceutical target. Curr Pharm Des 2009;15:3958–3967.

5 Rigamonti D, Bolognini D, Mutti C et al. Loss of huntingtin function complemented by small molecules acting as repressor element 1/neuron restrictive silencer element silencer modulators. J Biol Chem 2007;282:24554–24562.

6 Johnson R, Teh CH, Kunarso G et al. REST regulates distinct transcriptional networks in embryonic and neural stem cells. Plos Biol 2008;6:e256.

7 Bruce AW, Donaldson IJ, Wood IC et al. Genome-wide analysis of repressor element 1 silencing transcription factor/neuron-restrictive silencing factor (REST/NRSF) target genes. Proc Natl Acad Sci USA 2004;101:10458–10463.

8 Conforti P, Mas Monteys A, Zuccato C et al. In vivo delivery of DN:REST improves transcriptional changes of REST-regulated genes in HD mice. Gene Ther 2013;20:678–685.
9 Ooi L, Wood IC. Chromatin crosstalk in development and disease: Lessons from REST. Nat Rev Genet 2007;8:544–554.
10 Lunyak VV, Burgess R, Prefontaine GG et al. Corepressor-dependent silencing of chromosomal regions encoding neuronal genes. Science 2002;298:1747–1752.
11 Chong JA, Tapia-Ramirez J, Kim S et al. REST: A mammalian silencer protein that restricts sodium channel gene expression to neurons. Cell 1995;80:949–957.
12 Schoenherr CJ, Anderson DJ. The neuron-restrictive silencer factor (NRSF): A coordinate repressor of multiple neuron-specific genes. Science 1995;267:1360–1363.
13 Ballas N, Grunseich C, Lu DD et al. REST and its corepressors mediate plasticity of neuronal gene chromatin throughout neurogenesis. Cell 2005;121:645–657.
14 Singh SK, Kagalwala MN, Parker-Thornburg J et al. REST maintains self-renewal and pluripotency of embryonic stem cells. Nature 2008; 453:223–227.
15 Bergsland M, Werme M, Malewicz M et al. The establishment of neuronal properties is controlled by Sox4 and Sox11. Genes Dev 2006;20: 3475–3486.
16 Covey MV, Streb JW, Spektor R et al. REST regulates the pool size of the different neural lineages by restricting the generation of neurons and oligodendrocytes from neural stem/progenitor cells. Development 2012;139:2878–2890.
17 Huang Z, Wu Q, Guryanova OA et al. Deubiquitylase HAUSP stabilizes REST and promotes maintenance of neural progenitor cells. Nat Cell Biol 2011;13:142–152.
18 Ballas N, Mandel G. The many faces of REST oversee epigenetic programming of neuronal genes. Curr Opin Neurobiol 2005;15:500–506.
19 Westbrook TF, Hu G, Ang XL et al. SCFbeta-TRCP controls oncogenic transformation and neural differentiation through REST degradation. Nature 2008;452:370–374.
20 Guardavaccaro D, Frescas D, Dorrello NV et al. Control of chromosome stability by the beta-TrCP-REST-Mad2 axis. Nature 2008;452:365–369.
21 Abrajano JJ, Qureshi IA, Gokhan S et al. Differential deployment of REST and CoREST promotes glial subtype specification and oligodendrocyte lineage maturation. Plos One 2009;4:e7665.
22 Abrajano JJ, Qureshi IA, Gokhan S et al. REST and CoREST modulate neuronal subtype specification, maturation and maintenance. Plos One 2009;4:e7936.
23 Kohyama J, Sanosaka T, Tokunaga A et al. BMP-induced REST regulates the establishment and maintenance of astrocytic identity. J Cell Biol 2010;189:159–170.
24 Soldati C, Bithell A, Johnston C et al. REST couples loss of pluripotency with neural induction and neural differentiation. Stem Cells 2012;30:425–434.
25 Tomasoni R, Negrini S, Fiordaliso S et al. A signaling loop of REST, TSC2 and {beta}-catenin governs proliferation and function of PC12 neural cells. J Cell Sci 2011;124:3174–3186.
26 Abrajano JJ, Qureshi IA, Gokhan S et al. Corepressor for element-1-silencing transcription factor preferentially mediates gene networks underlying neural stem cell fate decisions. Proc Natl Acad Sci USA 2010;107:16685–16690.
27 Feyeux M, Bourgois-Rocha F, Redfern A et al. Early transcriptional changes linked to naturally occurring Huntington's disease mutations in neural derivatives of human embryonic stem cells. Hum Mol Genet 2012;21:3883–3895.
28 Benchoua A, Aubry L, Perrier A. Method and medium for neural differentiation of pluripotent cells. EP2356218A1, WO/2010/063848; 2008.
29 Park IH, Arora N, Huo H et al. Disease-specific induced pluripotent stem cells. Cell 2008;134:877–886.
30 Chen ZF, Paquette AJ, Anderson DJ. NRSF/REST is required in vivo for repression of multiple neuronal target genes during embryogenesis. Nat Genet 1998;20:136–142.
31 Subramanian A, Tamayo P, Mootha VK et al. Gene set enrichment analysis: A knowledge-based approach for interpreting genome-wide expression profiles. Proc Natl Acad Sci USA 2005;102:15545–15550.
32 Irizarry RA, Hobbs B, Collin F et al. Exploration, normalization, and summaries of high density oligonucleotide array probe level data. Biostatistics 2003;4:249–264.
33 Mootha VK, Lindgren CM, Eriksson KF et al. PGC-1alpha-responsive genes involved in oxidative phosphorylation are coordinately downregulated in human diabetes. Nat Genet 2003;34:267–273.
34 Huang da W, Sherman BT, Lempicki RA. Systematic and integrative analysis of large gene lists using DAVID bioinformatics resources. Nat Protoc 2009;4:44–57.
35 Huang Da W, Sherman BT, Lempicki RA. Bioinformatics enrichment tools: Paths toward the comprehensive functional analysis of large gene lists. Nucleic Acids Res 2009;37:1–13.
36 Palm K, Belluardo N, Metsis M et al. Neuronal expression of zinc finger transcription factor REST/NRSF/XBR gene. J Neurosci 1998;18: 1280–1296.
37 Lee JH, Chai YG, Hersh LB. Expression patterns of mouse repressor element-1 silencing transcription factor 4 (REST4) and its possible function in neuroblastoma. J Mol Neurosci 2000;15:205–214.
38 Tabuchi A, Yamada T, Sasagawa S et al. REST4-mediated modulation of REST/NRSF-silencing function during BDNF gene promoter activation. Biochem Biophys Res Commun 2002;290:415–420.
39 Shimojo M, Paquette AJ, Anderson DJ et al. Protein kinase A regulates cholinergic gene expression in PC12 cells: REST4 silences the silencing activity of neuron-restrictive silencer factor/REST. Mol Cell Biol 1999;19:6788–6795.
40 An MC, Zhang N, Scott G et al. Genetic Correction of Huntington's Disease Phenotypes in Induced Pluripotent Stem Cells. Cell Stem Cell 2012;11:253–263.
41 Jacquard C, Trioulier Y, Cosker F et al. Brain mitochondrial defects amplify intracellular [Ca2+] rise and neurodegeneration but not Ca2+ entry during NMDA receptor activation. FASEB J 2006;20:1021–1023.
42 Fusco FR, Zuccato C, Tartari M et al. Co-localization of brain-derived neurotrophic factor (BDNF) and wild-type Huntingtin in normal and quinolinic acid-lesioned rat brain. Eur J Neurosci 2003;18:1093–1102.
43 Westbrook TF, Martin ES, Schlabach MR et al. A genetic screen for candidate tumor suppressors identifies REST. Cell 2005;121:837–848.
44 Hu Y, Russek SJ. BDNF and the diseased nervous system: A delicate balance between adaptive and pathological processes of gene regulation. J Neurochem 2008;105:1–17.
45 Zuccato C, Cattaneo E. Brain-derived neurotrophic factor in neurodegenerative diseases. Nat Rev Neurol 2009;5:311–322.
46 Ferrer I, Goutan E, Marin C et al. Brain-derived neurotrophic factor in Huntington disease. Brain Res 2000;866:257–261.
47 Zuccato C, Marullo M, Conforti P et al. Systematic assessment of BDNF and its receptor levels in human cortices affected by Huntington's disease. Brain Pathol 2008;18:225–238.
48 Altar CA, Cai N, Bliven T et al. Anterograde transport of brain-derived neurotrophic factor and its role in the brain. Nature 1997;389: 856–860.
49 Baquet ZC, Gorski JA, Jones KR. Early striatal dendrite deficits followed by neuron loss with advanced age in the absence of anterograde cortical brain-derived neurotrophic factor. J Neurosci 2004;24:4250–4258.
50 Gauthier LR, Charrin BC, Borrell-Pages M et al. Huntingtin controls neurotrophic support and survival of neurons by enhancing BDNF vesicular transport along microtubules. Cell 2004;118:127–138.
51 Her LS, Goldstein LS. Enhanced sensitivity of striatal neurons to axonal transport defects induced by mutant huntingtin. J Neurosci 2008; 28:13662–13672.
52 Zuccato C, Cattaneo E. Role of brain-derived neurotrophic factor in Huntington's disease. Prog Neurobiol 2007;81:294–330.
53 Johnson R, Zuccato C, Belyaev ND et al. A microRNA-based gene dysregulation pathway in Huntington's disease. Neurobiol Dis 2008; 29:438–445.
54 Nagahara AH, Tuszynski MH. Potential therapeutic uses of BDNF in neurological and psychiatric disorders. Nat Rev Drug Discov 2011;10: 209–219.
55 Zheng F, Zhou X, Moon C et al. Regulation of brain-derived neurotrophic factor expression in neurons. Int J Physiol Pathophysiol Pharmacol 2012;4:188–200.
56 Ramaswamy S, McBride JL, Kordower JH. Animal models of Huntington's disease. ILAR J 2007;48:356–373.
57 De March Z, Zuccato C, Giampa C et al. Cortical expression of brain derived neurotrophic factor and type-1 cannabinoid receptor after striatal excitotoxic lesions. Neuroscience 2008;152:734–740.
58 Giampa C, Patassini S, Borreca A et al. Phosphodiesterase 10 inhibition reduces striatal excitotoxicity in the quinolinic acid model of Huntington's disease. Neurobiol Dis 2009;34:450–456.
59 Rite I, Machado A, Cano J et al. Divergent regulatory mechanisms governing BDNF mRNA expression in cerebral cortex and substantia nigra in response to striatal target ablation. Exp Neurol 2005;192:142–155.


See www.StemCells.com for supporting information available online.

6.2. Collaborative work #2

Mutant huntingtin alters Tau phosphorylation and subcellular distribution.

HMG Advance Access published September 2, 2014

Human Molecular Genetics, 2014 **1–10**
doi:10.1093/hmg/ddu421

Mutant huntingtin alters Tau phosphorylation and subcellular distribution

David Blum[1,2,3,*], Federico Herrera[4,†], Laetitia Francelle[6,7,†], Tiago Mendes[4,*], Marie Basquin[1,2], Hélène Obriot[1,2], Dominique Demeyer[1,2], Nicolas Sergeant[1,2,3], Ellen Gerhardt[5], Emmanuel Brouillet[6,7], Luc Buée[1,2,3] and Tiago F. Outeiro[4,5]

[1]Université Lille-Nord de France, UDSL, F-59000, Lille, France, [2]Inserm U837, Jean-Pierre Aubert Research Centre, IMPRT, F-59000, Lille, France, [3]CHRU, F-59000, Lille, France, [4]Cell and Molecular Neuroscience Unit, Instituto de Medicina Molecular, Av. Prof. Egas Moniz, 1649-029 Lisboa, Portugal, [5]Department of Neurodegeneration and Restorative Research, Center for Nanoscale Microscopy and Molecular Physiology of the Brain, University Medical Center Goettingen, Waldweg 33, 37073 Goettingen, Germany, [6]CEA, DSV, I[2]BM, Molecular Imaging Research Center (MIRCen), Fontenay-aux-Roses F-92265, France and [7]CNRS, CEA URA 2210, Fontenay-aux-Roses F-92265, France

Received July 16, 2014; Revised and Accepted August 14, 2014

Tau abnormalities play a central role in several neurodegenerative diseases, collectively known as tauopathies. In the present study, we examined whether mutant huntingtin (mHtt), which causes Huntington's disease (HD), modifies Tau phosphorylation and subcellular localization using cell and mouse HD models. Initially, we used novel bimolecular fluorescence complementation assays in live cells to evaluate Tau interactions with either wild type (25QHtt) or mutant huntingtin (103QHtt). While 25QHtt and Tau interacted at the level of the microtubule network, 103QHtt and Tau interacted and formed 'ring-like' inclusions localized in the vicinity of the microtubular organizing center (MTOC). Fluorescence recovery after photobleaching experiments also indicated that, whereas homomeric 103QHtt/103QHtt pairs rapidly re-entered into inclusions, heteromeric 103QHtt/Tau pairs remained excluded from the 'ring-like' inclusions. Interestingly, *in vitro* Tau relocalization was associated to Tau hyperphosphorylation. Consistent with this observation, we found strong Tau hyperphosphorylation in brain samples from two different mouse models of HD, R6/2 and 140CAG knock-in. This was associated with a significant reduction in the levels of Tau phosphatases (PP1, PP2A and PP2B), with no apparent involvement of major Tau kinases. Thus, the present study strongly suggests that expression of mHtt leads to Tau hyperphosphorylation, relocalization and sequestration through direct protein–protein interactions in inclusion-like compartments in the vicinity of the MTOC. Likewise, our data also suggest that Tau alterations may also contribute to HD pathogenesis.

INTRODUCTION

Huntington's disease (HD) is an autosomal dominant inherited neurodegenerative disorder caused by mutations in the *IT15/HD1* gene that encodes huntingtin (Htt) protein (1). The mutation consists in a CAG triplet repeat expansion that is translated into an abnormally long polyglutamine (polyQ) tract (>39) within the N-terminal region of the protein (2). Mutant huntingtin (mHtt) leads to several neuronal and glial alterations, including notable transcriptional, mitochondrial and axonal transport defects, ultimately leading to neuronal death, primarily in striatal and cortical areas (3).

Tau is a microtubule-associated protein widely expressed in the central nervous system, playing a role in microtubule stabilization and axonal transport (4), synaptic plasticity (5) and neuronal response to stress (6). Tau hyperphosphorylation and aggregation are hallmarks of several neurodegenerative disorders referred to as Tauopathies, among which Alzheimer's

*To whom correspondence should be addressed at: Inserm U837, 'Alzheimer & Tauopathies', Place de Verdun, 59045, Lille Cedex, France. Tel: +33320298858; Fax: +33320538562; Email: david.blum@inserm.fr (D.B.); Department of Neurodegeneration and Restorative Research University Medical Center Goettingen, Waldweg 33, 37073 Goettingen, Germany. Tel: +495513913544; Email: touteiro@gmail.com (T.F.O.)
†These authors equally contributed to this work.

disease (AD) is included (7). Besides Tauopathies, Tau hyperphosphorylation has been associated with detrimental metabolic conditions as obesity and diabetes (8–11) but also impaired memory function due to chronic anesthesia (12,13).

The composition and location of protein aggregates are frequently used to diagnose and define neurodegenerative disorders. There is general consensus, for example, that α-synuclein is the main component of Parkinson's disease Lewy bodies, Tau and β-amyloid aggregate in AD, while mHtt aggregates in HD. However, α-synuclein interacts with Tau and also with Htt, possibly contributing to Alzheimer's or Huntington's pathologies, respectively (14–17). Notably, we showed that α-synuclein modifies the pattern of mHtt aggregation (18). Whether Htt mutation impacts upon Tau remains unknown so far. Previous data reported limited AD neuropathology in the brain of HD patients (19) and we reported co-aggregation of Htt and Tau in a patient exhibiting both corticobasal degeneration and huntingtin mutation (20). Altogether, these observations prompted us to evaluate the impact of mHtt upon Tau using both *in vitro* and *in vivo* HD models.

RESULTS

Tau hyperphosphorylation in HD mice

Initially, we evaluated Tau phosphorylation in two distinct HD mouse models, namely R6/2 and KI140. Given the important number of phosphorylation sites on Tau (>80; 4), we first performed a two-dimensional (2D) gel electrophoresis analysis to evaluate global changes in murine Tau protein in the cortex of HD mice. Upon membranes probing with a total Tau antibody (C-ter), we observed a significant shift of murine Tau isovariants from the basic to the acidic pH range in the cortex of R6/2 mice and KI140 (arrows, Fig. 1A and B) when compared with littermate controls, consistent with increased phosphorylation. This observation was in line with the shift of Tau isovariant following probing of 2D membranes with antibodies raised against

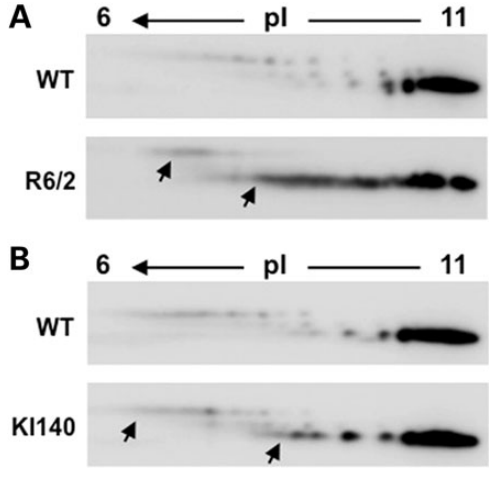

Figure 1. Global Tau phosphorylation in HD mice using Total Tau antibody. Comparison of representative two-dimensional profile of murine tau in the cortex of 10 week-old R6/2 (**A**) and 17 month-old KI140 (**B**) mice when compared with respective littermate controls. Profiles show increased Tau acidification in HD animals (arrows). The pH gradient used to resolve Tau protein is indicated at the top of 2D-western blots.

pSer404 and pSer396 (Supplementary Material, Fig. S1). Next, to confirm the occurrence of increased phosphorylation, we also performed SDS–PAGE and immunoblot analyses. In line with the 2D results, we found a significant increase in Tau phosphorylation at Ser396 and Ser404 in the cortex of R6/2 mice (Fig. 2A), while Tau-1 immunoreactivity representing unphosphorylated Tau was significantly decreased. In addition, we observed a significant shift of total Tau immunoreactive bands toward a higher apparent molecular weight (Fig. 2A). Similar changes were found in the cortex of KI140 animals (Fig. 2B) as well as in the striatum of both transgenic strains (Supplementary Material, Fig. S2). Increased phosphorylation at Ser396 was further confirmed using immunofluorescence analysis. Notably, the number of pSer396-Tau positive cells was increased in the brain of KI140 mice as shown in Supplementary Material, Figure S3.

In order to determine whether mHtt and Tau could interact, co-localize and eventually co-aggregate *in vivo*, we performed additional immunohistochemical and biochemical evaluations. Using confocal microscopy, we analyzed the expression of the two proteins in the brain of KI140 and littermate controls following immunofluorescence detection of Tau pSer396 and Htt (2B4 or Em48 antibodies). Results showed no major colocalization of the two proteins (Fig. 3). Lack of major *in vivo* interaction between Tau and Htt in the cortex HD animals was confirmed by co-immunoprecipitation studies (not shown). Finally, we failed to demonstrate the presence of Tau in cortical sarkosyl-insoluble protein fractions from R6/2 mice (Supplementary Material, Fig. S4).

Tau phosphorylation is under the tight control of several protein kinases and phosphatases (4). Here, we assessed the effects of mHtt on the expression or activation of major Tau protein kinases, such as GSK3β, CaMKII, Erk or cdk5. As shown in Figure 4A, neither expression nor activation of these kinases was found increased in R6/2 mice. Rather, we observed an increased Ser9 phosphorylation of GSK3β, reduced phosphorylation of CaMKII and reduced cdk5 expression in the cortex of R6/2 mice compared with littermate controls (Fig. 4A). Changes in CaMKII and cdk5 were also observed in the cortex of KI140 animals (Fig. 4B). These kinase changes thus fail to explain the increased Tau phosphorylation (Figs 1 and 2). In order to uncover a possible mechanism underlying Tau hyperphosphorylation in HD animals, we next assessed the expression levels of Tau protein phosphatases namely PP1, PP2A and PP2B (21). In R6/2 mice, we found an association of Tau hyperphosphorylation with a significant decrease in PP1, PP2A and PP2B expression (Fig. 4A). A trend for PP1 loss and a significant reduction in PP2B expression were also observed in KI140 animals (Fig. 4B). These results thus suggest that phosphatase dysregulation correlates with Tau phosphorylation changes in HD animals.

In vitro interaction between huntingtin and Tau

In a second series of experiments, we used an *in vitro* system to estimate the impact of mHtt on Tau phosphorylation and behavior and to evaluate a potential relationship between both proteins. We found that, as in the *in vivo* situation, mHtt expression promoted Tau hyperphosphorylation at S396 (Fig. 5B). Interestingly, using filter trap assays, we also observed that Tau inhibited 103QHtt aggregation (Fig. 5A). Wild type 25QHtt did not

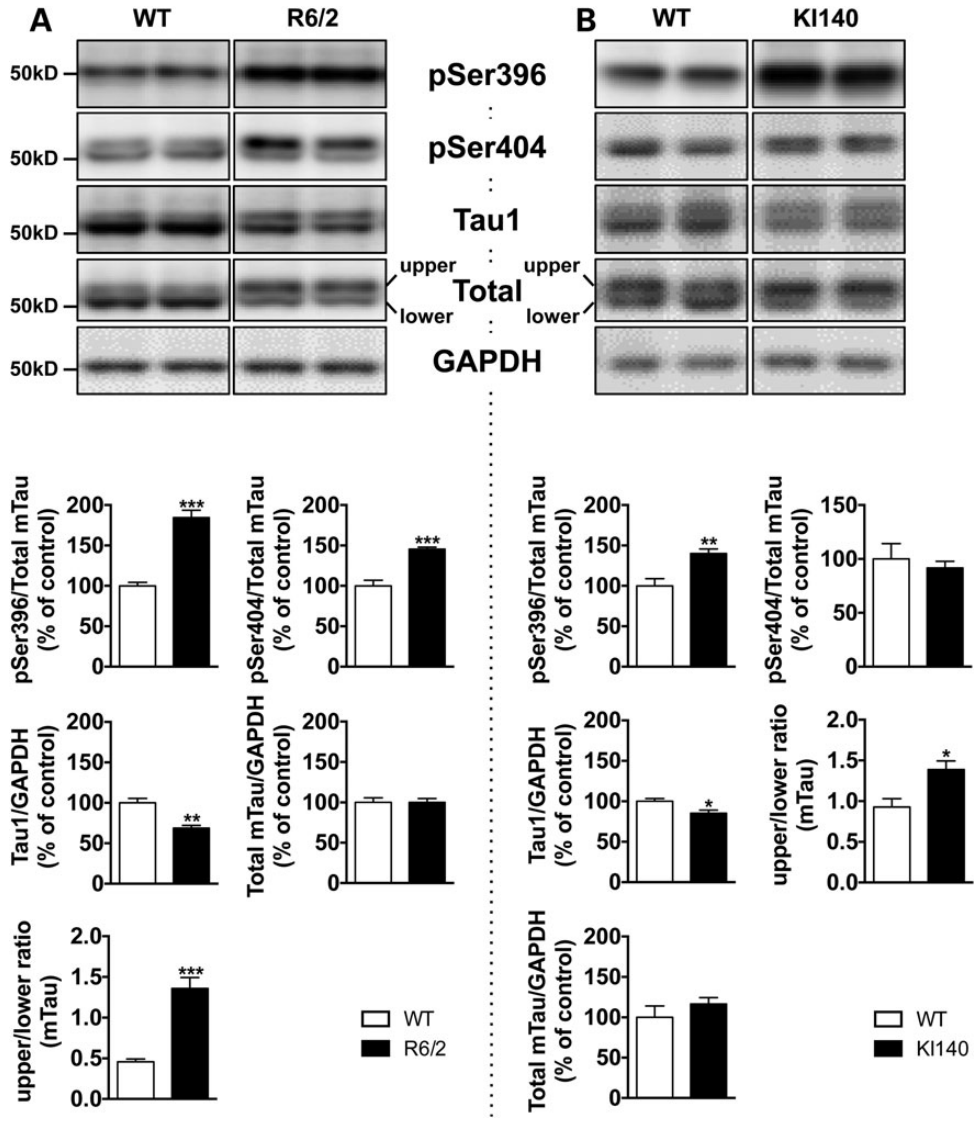

Figure 2. Immunoblot analysis of Tau phosphorylation in the cortex of HD mice. Analysis of Tau in the cortex of 10 week-old R6/2 (**A**) and 17 month-old KI140 (**B**) animals using antibodies targeting pSer396, pSer404, dephosphorylated Tau (Tau1) and Total Tau antibody (Cter). Quantifications indicate a significant enhancement of Tau phosphorylation at Ser396 and Ser404, a decreased dephosphorylated Tau using Tau1 antibody and a significant shift of Total Tau (Cter) immunoreactive bands toward a higher apparent molecular weight. Quantifications of phosphoepitopes were performed versus total Tau. Total Tau quantification was performed versus GAPDH. $^{*}P < 0.05$, $^{**}P < 0.01$, $^{***}P < 0.001$ versus littermate control using Student's *t*-test. $n = 5–6$/group.

produce SDS-insoluble aggregates in the presence or absence of Tau, while mutant 103QHtt produced more SDS-insoluble aggregates in the absence of Tau. Tau was retained in filter traps when it was co-expressed with 103QHtt, but not with 25QHtt, further indicating that mHtt and Tau co-aggregate *in vitro*. Interestingly, retained Tau was phosphorylated at S396.

In order to further evaluate the possible interaction between Htt and Tau at a cellular level, we used the bimolecular fluorescence complementation (BiFC) assay. In BiFC assays, the proteins of interest are fused to two non-fluorescent halves of a fluorescent reporter protein. When the proteins of interest dimerize/oligomerize, the two reporter halves are brought together and reconstitute the fluorophore, emitting fluorescence. Fluorescence is therefore indicative of dimerization/oligomerization. We have recently developed BiFC constructs for wild type (25Q) and mutant (103Q) Htt (22), as well as for Tau (Fig. 6A). Different combinations of 25QHtt, 103QHtt and Tau formed dimers/oligomers in human cells (Fig. 6B–G). Wild-type Htt BiFC pairs showed mostly a diffuse cytoplasmic fluorescence, indicative of the formation of dimers/oligomers (Fig. 6D), while 103QHtt BiFC pairs showed the occurrence of inclusion bodies (Fig. 6F). Tau/Tau BiFC pairs marked the microtubular network, as expected given the microtubule-binding properties of Tau (Fig. 6C and H). When 25QHtt was combined with Tau, the cellular phenotype resembled that of Tau BiFC pairs, indicating that Tau recruited 25QHtt to the microtubular network (Fig. 6E). On the other hand, combinations of 103QHtt with Tau produced a mixed phenotype. As with 25QHtt, 103QHtt was also recruited to the microtubular network, with all cells showing the microtubular cytoskeleton

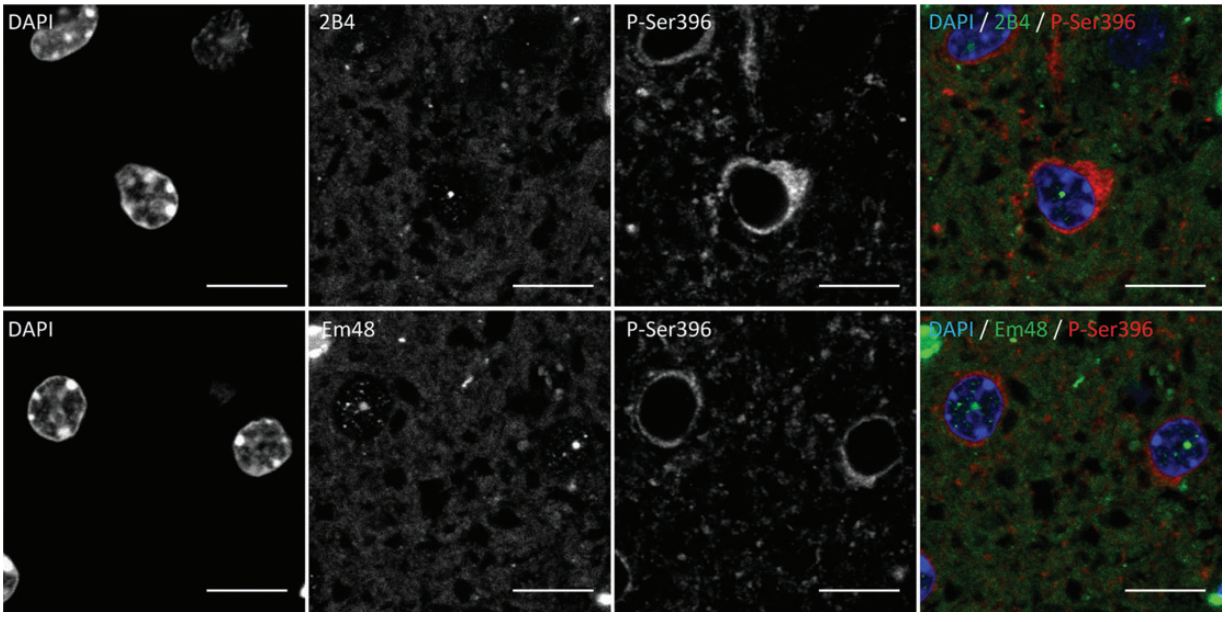

Figure 3. Absence of colocalization of pSer396 Tau and mHtt in the brain of KI140 HD mice. Confocal immunofluorescence images showing mutant Htt-containing intranuclear inclusions seen as typical round small dots in the nucleus (2B4, upper images; EM48, lower images) in the striatum of Ki140 mice. Immunofluorescence corresponding to Tau pSer369 (red) is mainly detected in the cytoplasm. No major colocalization of mutant Htt inclusions and Tau pSer396 was found. Similar results were obtained in three KI140 mice. Scale bar, 10 μm.

but, in addition, we also observed cells with large inclusions (Fig. 6G). None had the typical bright foci that characterize 103QHtt BiFC pairs (Fig. 6F). Notably, 103QHtt/Tau transfected cells often exhibited bright 'knot-like' inclusions in their microtubular cytoskeletons, close to where the microtubular organizing center (MTOC) is located (Fig. 6I). Besides BiFC experiments, we also evaluated whether mutant mHtt and Tau could colocalize in HEK293T cells following co-expression of c-myc tagged Htt171-82Q and non-tagged Tau. Confocal analysis showed that in a small proportion of transfected cells mHtt and phospho-Tau (AT8) colocalized in a perinuclear region compatible with MTOC (Supplementary Material, Fig. S5). These results are consistent with previous evidence showing that Htt binds to microtubules and localizes in the centrosome (23) and the mitotic spindle (24,25).

Mutant 103QHtt BiFC pairs characteristically produce aggregates in 30–40% of transfected cells (18,22) with an average of 14.70% ($\pm$ 5.66) aggregates per cell (Fig. 6J). 103QHtt/Tau BiFC pairs produced 'knots' in 16.21% ($\pm$ 1.27) of transfected cells. These 'knots' are larger than average 103QHtt aggregates, but are only one or two per cell (Fig. 6F versus G and J). A closer look to aggregates showed that most 103QHtt aggregates are solid (see Supplementary Material, Fig. S6), while 103QHtt/Tau aggregates had ring-like shape in their focal center, suggesting that they are hollow inclusions or complex rings (Supplementary Material, Fig. S7A; see also Supplementary Material, Figs S8 and S9 for full Z-stack videos). Furthermore, the dynamics of 103QHtt and 103QHtt/Tau aggregates, as well as of Tau dimers, were radically different (Supplementary Material, Fig. S7B and C). 103QHtt aggregates recovered relatively quickly after photobleaching (FRAP), indicating that they recruit new 103QHtt molecules to their core. The same was observed with Tau dimers, either at the MTOC or at the microtubules (Supplementary Material, Fig. S7D). On the other hand, 103QHtt/Tau aggregates did not recover after 2.5 min of monitoring (see also Supplementary Material, Figs S10 and 11 for full FRAP videos).

In summary, our *in vitro* results indicate that mHtt can interact with Tau and that this interaction interferes with the normal pattern of mHtt aggregation, favors Tau hyperphosphorylation and alters the subcellular distribution of Tau, promoting its aggregation.

DISCUSSION

The present study reports that expression of mHtt impacts on Tau cellular localization, molecular interactions and phosphorylation pattern. Strikingly, *in vitro*, Tau was found also able to modulate Htt aggregation. These results notably support a mutual relationship between mHtt and Tau proteins that might contribute to the neurodegenerative phenotype in HD.

Brain of symptomatic HD animals and cultured cells co-expressing mHtt and Tau constructs showed significant Tau hyperphosphorylation, indicating that the expression of the former is sufficient to promote hyperphosphorylation of the latter. Notably, in HD mice, we did not notice increase in the activity of the main Tau kinases. Rather, we found a congruent reduction of CaMKII and cdk5 expression in both R6/2 and KI140 mice. Reduced CamKII expression may notably rely on a reorganization of postsynaptic density as previously described (26). On the other hand, we observed significant phosphatase changes in HD lines. Both R6/2 and KI140 animals exhibited significant reduction of cortical PP2B expression, in line with previous observations in the brain of HD patients (27) and several HD models (28–30). PP2B dephosphorylates Tau at multiple

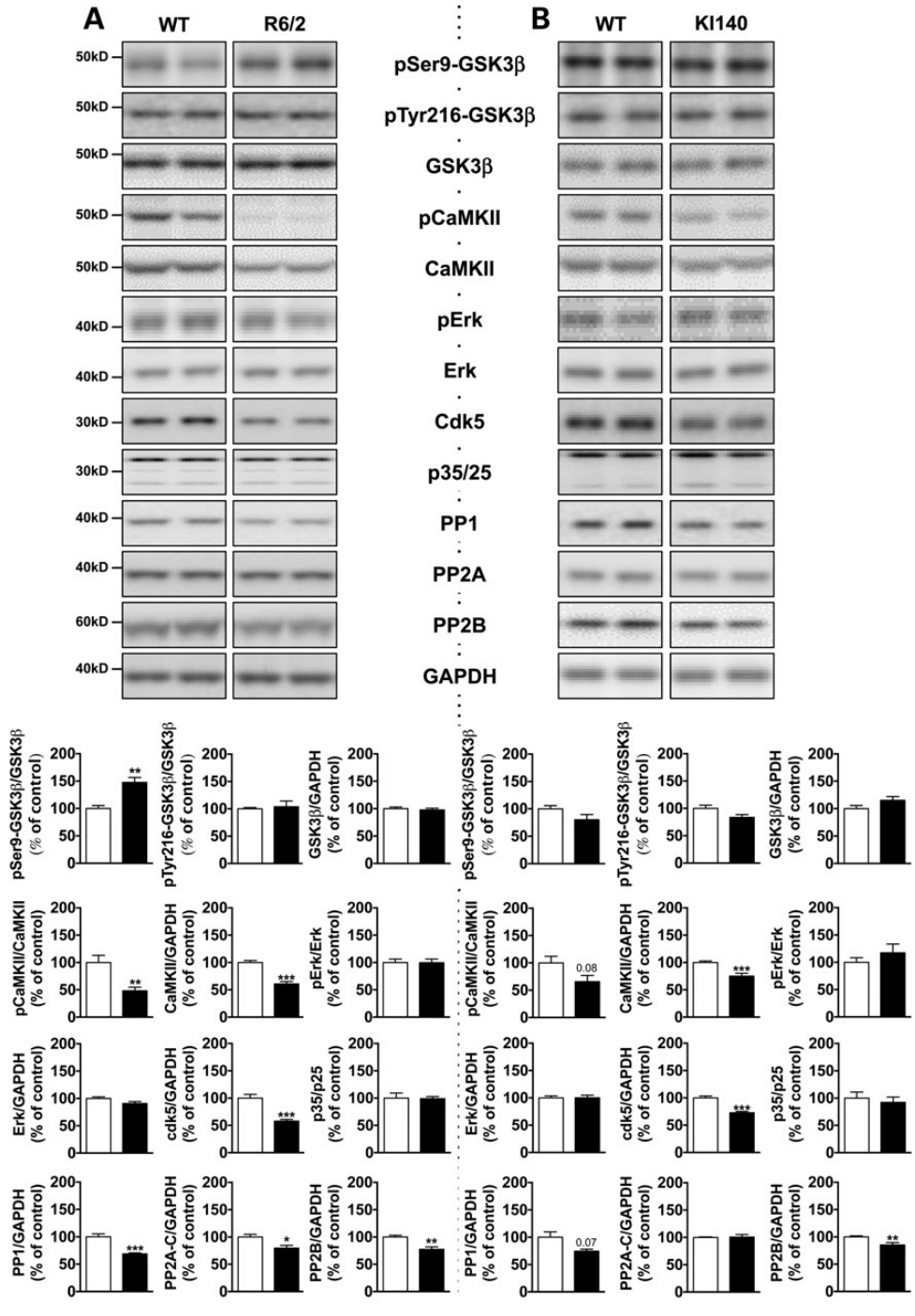

Figure 4. Tau kinases and phosphatases in HD mice. SDS–PAGE and immunoblot analysis was performed in the cortex of 10 week-old R6/2 (**A**) and 17 month-old KI140 (**B**) using antibodies raised against total and phosphorylated forms of several Tau kinases as well as phosphatases. Quantifications of phosphoepitopes were performed versus respective total protein. In other cases quantifications were performed versus GAPDH. $^{*}P < 0.05$, $^{**}P < 0.01$, $^{***}P < 0.001$ versus littermate control using Student's *t*-test. $n = 5–6$/group.

epitopes including those evaluated here (31). Therefore, a reduced PP2B expression is one possible explanation for increased Tau phosphorylation in transgenic HD mice and in cells expressing 103QHtt.

Our data indicate that expression of mHtt is associated with changes in Tau function. Indeed our *in vitro* data suggest that in addition to impact Tau hyperphosphorylation, mHtt leads to changes in its cellular distribution. Tau hyperphosphorylation is thought to impair its cellular localization (32) and its microtubule-stabilizing function (33). These observations suggest that HD would be associated with a loss of Tau function, at least regarding axonal transport, possibly contributing to the axonal transport defects previously reported in HD conditions (34). As Tau hyperphosphorylation can be associated with

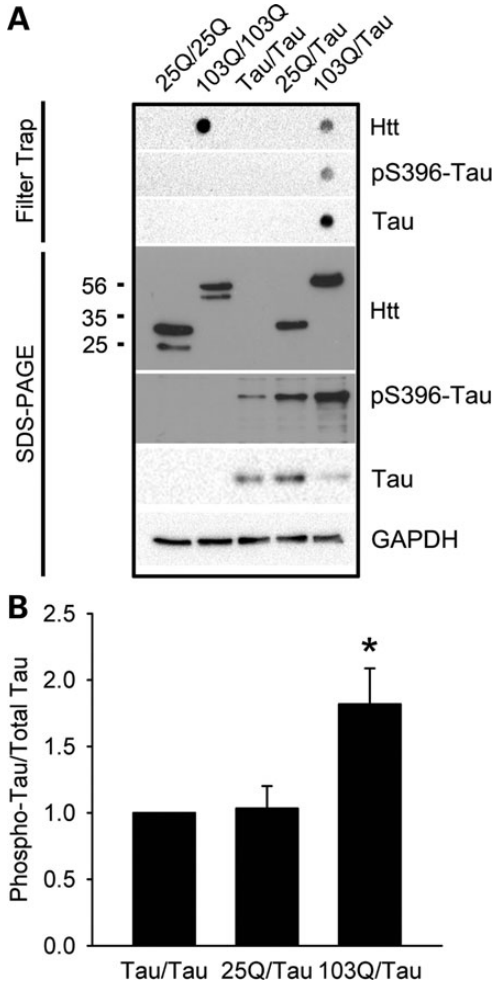

Figure 5. mHtt co-aggregates with Tau and increases the levels of Tau phosphorylation (pS396) *in vitro*. (**A**) Filter trap assays showed that mHtt, but not wild-type Htt, produced SDS-insoluble aggregates (dark dots, first line). Co-transfection of mutant Htt with Tau reduced the levels of insoluble aggregates (first line). Tau was retained in filter traps only when co-transfected with mHtt, but not wild-type Htt (second and third lines), indicating that they co-aggregate. Furthermore, retained Tau is phosphorylated at S396 (second line). SDS–PAGE immunoblots indicated that Htt/Tau co-transfection induced hyperphosphorylation of Tau at this residue (third line). Htt and GAPDH signals were used as expression and loading controls, respectively. (**B**) Quantification of Tau hyperphosphorylation see in A.

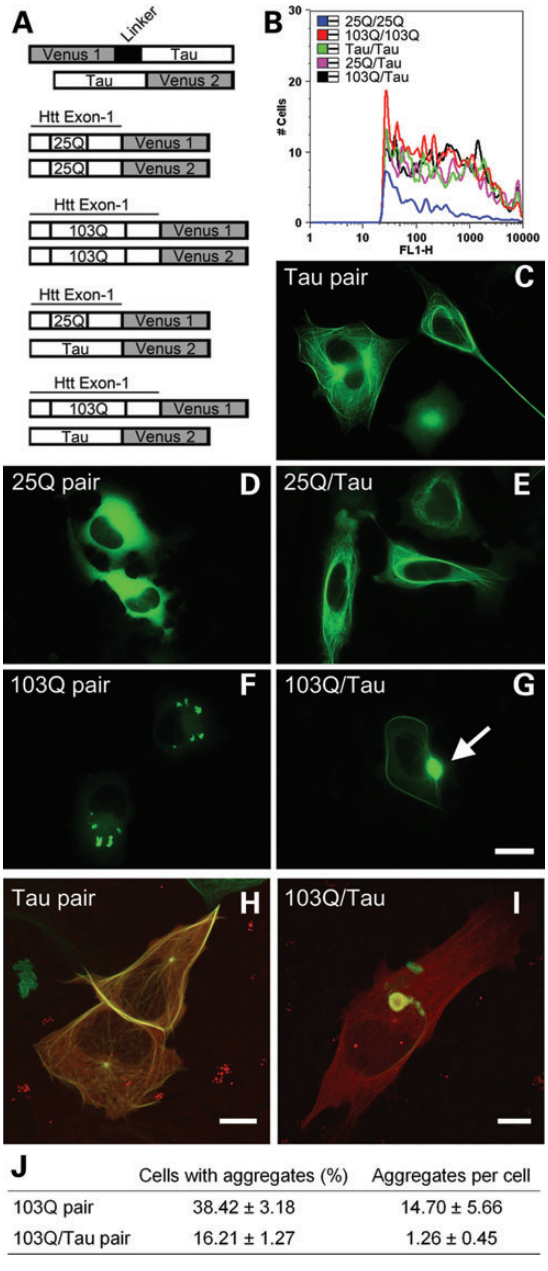

Figure 6. Mutant Htt interacts and interferes with normal Tau distribution. (**A**) Schematic of Htt- and Tau-Venus BiFC constructs. (**B**) Flow cytometry analyses of H4 cells carrying different combinations of Htt- and/or Tau-Venus BiFC constructs. (**C**–**G**) Representative pictures of the different BiFC pairs. Wild-type Htt (25Q) BiFC pairs produced most frequently a diffuse cytoplasmic fluorescence, while mutant Htt (103Q) BiFC pairs aggregated in inclusion bodies. Tau BiFC pairs showed a clearly defined microtubular localization, as expected. Combinations of 25QHtt with Tau maintained a microtubular localization, while 103QHtt disrupted Tau distribution, producing knot-like structures. No inclusion bodies are found in 103QHtt/Tau BiFC pairs. Scale bar (C–G), 20 μm. (**H** and **I**), Cells co-transfected with mCherry-Tubulin (red) and Tau/Tau or 103Q/Tau (green) pairs. Tau/Tau and 103Q/Tau dimers co-localize with the microtubular network, including MTOC, but the microtubular network of 103Q/Tau cells produced ring-like structures close to the MTOC. Co-localization of tubulin and BiFC dimers is shown in yellow. Scale bar (**H** and **I**), 5 μm. (**J**) Quantification of the frequency of cells with aggregates (percentage versus transfected cells) and the number of aggregates per cell. One hundred cells per experimental group from a total of three independent experiments were counted. Data are the average minus/plus the standard deviation.

cognitive deficits (12) and Tau loss-of-function is possibly prone to promote motor alterations in mice (35) as well as synaptic plasticity defects in the hippocampus (36), altered Tau function may underline some HD features. Whether Tau alterations precede, contribute or are concomitant to behavioral impairments and pathological features that characterize HD remains to be evaluated.

While mHtt has a clear effect on Tau phosphorylation and cellular distribution, *in vitro*, Tau also induces changes in mHtt behavior. In our cellular system, mHtt forms solid inclusions of different sizes distributed throughout the cytoplasm. These inclusions are highly dynamic, constantly recruiting new mHtt molecules to the core of the inclusion. In the presence of Tau, typical Htt aggregates almost disappear, and Htt is at least partially recruited to the microtubular network. Htt recruitment

to the microtubular network has been reported by independent laboratories (23–25). In particular, Htt is able to bind to microtubules, and has been found in the centrosome (23) and the mitotic spindle (24,25), although the biological meaning of these findings remains unclear. In a significant number of cells, one or two large ring-like inclusions are formed in the perinuclear region, where cellular quality control inclusion bodies are located. The formation of mHtt-Tau inclusions is in agreement with previous observations indicating that mHtt accumulates in cytoplasmic inclusions containing sequestrated vesicle-associated proteins, such as HSP70, dynamin or HIP1 (37). mHtt-Tau inclusions have a different morphology and are significantly less dynamic than pure mHtt inclusions or Tau dimers, indicating severe alterations in the biology of the individual proteins. Interestingly, other aggregation-prone proteins, such as transthyretin or an amyloidogenic immunoglobulin light chain, can also form ring-like inclusions (38,39). However, we are not aware of previous reports on the formation of this type of species by mHtt. Thus, our results indicate, for the first time, that at least under particular conditions, mHtt can also form this type of aggregated species. The abnormal localization/dynamics of Tau linked to its enhanced direct interaction with mHtt may also concurrently increase Tau phosphorylation. It is indeed conceivable that this interaction with mHtt would reduce the interaction of tau with its regulating phosphatase. This possibility will require further investigation in future studies.

Finally, it is noteworthy that while mHtt-induced Tau hyperphosphorylation is consistently found *in vitro* and *in vivo* using biochemical and histochemical methods, mHtt/Tau colocalization and co-aggregation is readily detected only *in vitro* using overexpression systems, but not tissue from the animal models tested. *In vitro*, under optimized conditions, co-localization was detected in ∼16% of cells. Using immunohistochemistry, we could not detect colocalization of the proteins. Since Tau hyperphosphorylation does not accumulate in mHtt-containing inclusions in mice, it is possible that the interaction between Tau and mHtt may occur before the formation of detectable/macroscopic aggregates. Together, these observations suggest that a direct mHtt/Tau interaction might be a rare phenomenon *in vivo*, and that the major impact of mHtt toward Tau is related to kinase/phosphatase imbalance.

In conclusion, our study demonstrates that mHtt expression may impact Tau functions by promoting its hyperphosphorylation. Interestingly, recent retrospective neuropathological data underlined that elderly HD demented patients exhibited AD-like lesions, supporting a relationship between mHtt and Tau (40). Moreover, another recent report demonstrated that Tau deletion improves the motor phenotype in a transgenic mouse model of HD (41). Together with our current findings, these data strongly support that Tau may play an important and understudied role in HD pathogenesis.

MATERIALS AND METHODS

In vitro experiments

Constructs and cell lines

Wild-type (25Q) and mutant (103Q) huntingtin-Venus BiFC constructs were described elsewhere (22). Tau-Venus BiFC constructs were produced by subcloning a PCR-amplified Tau gene into the Venus BiFC vectors. Tau was initially inserted in N- and C-terminal positions in order to find the combination of constructs that provides an optimal BiFC signal (22,42). Optimal Tau-Tau BiFC was obtained with a combination of constructs where Tau was located at the C-terminus of the first Venus half and the N-terminus of the second Venus half, as previously described for α-synuclein (42) (Fig. 1A). mCherry-tubulin constructs were kindly provided by Dr Domingos Henrique (Instituto de Medicina Molecular, Lisbon, Portugal).

H4 human neuroglioma cells (HTB-148, ATCC, LGC Standards, Barcelona, Spain) were maintained as described elsewhere (22,42). Cells were transfected with complementary pairs of huntingtin- and/or tau-Venus BiFC constructs using the Xtremegene reagent (Roche diagnostics, Mannheim, Germany) in a proportion 1 μg DNA: 3 μl Xtremegene. For mCherry-tubulin plus BiFC experiments (Fig. 1H and I), H4 cells were transfected first with the mCherry tubulin construct and 24 h later with the BiFC constructs. Twenty-four hours later, samples were prepared for microscopy, flow cytometry or immunoblotting and analyzed as described below.

HEK293T cells were grown in DMEM cell culture medium (Sigma-Aldrich) supplemented with 10% fetal bovine serum (Gibco) in a humidified atmosphere at 5% CO_2 at 37°C. Cells were transiently transfected 24 h after seeding with 5 μg of plasmid DNA (SIN-PGK-FLAG-htt171-82Q-myc-WHV and SIN-cPPT-PGK-human-Tau46wt-WHV), fixed 48 h after transfection with ice-cold methanol and 5 mM EGTA for 3 min, followed by permeabilization with 0.1% Triton X-100 in blocking solution (TBS, 1% bovine serum albumin) for 30 min at room temperature. Cells were then incubated with anti-c-Myc-FITC coupled (1:400, Abcam, 3G30) antibody and a Tau clone 8 antibody (AT8) (1:800, mouse, Thermo Scientific, MN1020B) with 1% bovine serum albumin in PBS at room temperature for 1 h, then incubated with Alexa Fluor 594-labeled anti-mouse IgG at room temperature for 30 min. Subsequently, cells were rinsed in TBS and treated with DAPI (Wako) diluted 1:10 000 in TBS at room temperature for 3 min and visualized by confocal microscope Leica SP8.

Flow cytometry

Cells were collected by trypsinization (5 min at 37°C), washed once with PBS and fixed in 1% (w/v) paraformaldehyde in PBS for 10 min at room temperature. Samples were analyzed by means of a FACSCalibur flow cytometer (Beckton Dickinson, Franklin Lakes, NJ, USA). Ten thousand cells were analyzed per group. Graphics and data analysis were carried out by means of the FlowJo software (Tree Star, Inc., Ahsland, OR, USA).

Fluorescence microscopy and fluorescence recovery after photobleaching experiments

Pictures were acquired from live cultures at 37°C using an Axiovert 200 M widefield fluorescence microscope or a META LSM 510 confocal microscope equipped with CCD cameras (Carl Zeiss MicroImaging GmbH, Germany). No pre-incubation at 30°C was needed, since Venus halves complement efficiently at 37°C. For fluorescence recovery after photobleaching (FRAP) experiments, protein aggregates were focused at the central focal plane and adjusted to avoid pixel saturation.

Table 1. Antibodies used in this study

Name	Abbreviation	Epitope	Type	Origin	Provider	WB
CaMKII (pThr286)	pCaMKII	pThr286	Poly	Rabbit	Cell Signaling Technology	1/1000
CaMKII	CaMKII	Human CaMKII amino-terminal region	Poly	Rabbit	Cell Signaling Technology	1/1000
Cdk5 (C-8)	Cdk5	Cdk5 COOH terminus	Poly	Rabbit	Santa Cruz Biotechnology	1/1000
Erk1/2 pThr202/Tyr204	pErk	pThr202/pTyr204	Mono	Mouse	Cell Signaling Technology	1/1000
Erk1/2 (3A7)	Erk	Mouse Erk1/2	Mono	Mouse	Cell Signaling Technology	1/1000
GAPDH	GAPDH	Human GAPDH FL 1-335	Poly	Rabbit	Santa Cruz Biotechnology	1/10 000
GAPDH	GAPDH	6C5	Mono	Mouse	Ambion	1/30 000
GSK-3β (pSer9)	pGSK3β (S9)	pSer9	Poly	Rabbit	Cell Signaling Technology	1/1000
GSK-3α/β pTyr279/Tyr216 (5G-2F)	P-GSK3β (Y216)	pTyr279/Tyr216	Mono	Mouse	Millipore	1/1000
GSK-3α/β (0011-A)	GSK3	Mouse $GSK3_{1-420}$	Mono	Mouse	Santa Cruz Biotechnology	1/2000
Huntingtin	Htt	mEM48	Mono	Mouse	Millipore	1/500
Huntingtin	Htt	2B4	Mono	Mouse	Millipore	1/500
p35 (C-19)	p35	Human P35 COOH terminus	Poly	Rabbit	Santa Cruz Biotechnology	1/1000
PP1 (E9)	PP1	Human full-length PP1	Mono	Mouse	Santa Cruz	1/1000
PP2A, C subunit, (1D6)	PP2A-C	Human PP2A C subunit 295–309	Mono	Mouse	Millipore	1/2000
PP2B (Calcineurin)	PP2B	Human Calcineurin α	Poly	Rabbit	Cell Signaling	1/1000
Tau pSer396	pSer396	pSer396	Poly	Rabbit	Invitrogen	1/10 000
Tau pSer404	pSer404	pS404	Poly	Rabbit	Invitrogen	1/10 000
Tau-1 (PC1C6)	Tau1	Non-phospho-Ser195,198,199,202	Mono	Mouse	Millipore	1/2000
Tau, Total	Cter	Cter last 15 aa of COOH terminus	Poly	Rabbit	Home-made	1/2000

Mono, monoclonal; Poly, polyclonal; WB, dilution used in western blotting.

Experiments lasted for 150 s, taking one picture every second. After five pictures to establish the basal signal, aggregates were bleached using the 488 nm laser line at 100% laser transmission on a circular region of interest with a diameter of 30 pixels (1.31 μm radius) for 5 s (10 iterations). Fluorescence recovery was then monitored for 140 s with LSM software. Data analyses were carried out on ImageJ free software (http://rsb.info.nih.gov/ij/), and represented by means of SigmaPlot 11.0 (Systat Software, Inc., Chicago, IL, USA).

Immunoblotting

Proteins were extracted in non-denaturing conditions [lysis buffer 50 mM Tris–HCl pH 7.4, 175 mM NaCl, 5 mM EDTA and a protease inhibitor cocktail tablet (Roche diagnostics, Mannheim, Germany)] as described previously (22) and quantified by the Bradford method. Twenty micrograms of protein were submitted to electrophoresis in denaturing conditions (SDS–PAGE), transferred to nitrocellulose membranes for immunoblotting. For filter trap assays, 100 mg of protein were transferred by means of a vacuum-driven dot-blot device to cellulose acetate membranes (0.2 μm pore) after addition of SDS to the samples (final concentration: 1% w/v). Membranes were washed twice with PBS plus SDS 1% (w/v) and then probed with Htt antibody as described. Only large, SDS-insoluble aggregates are retained in these membranes and, therefore, Htt signal is proportional to the amount of this type of aggregate in the samples. All antibodies used in the present manuscript are reported in Table 1. Analyses were performed using Image J Software.

Animal experiments

In the present study, we used 10-week-old R6/2 transgenic heterozygous mice overexpressing exon1 of human Huntingtin with about 120 CAG repeats and wild-type (WT) littermate controls (43). In addition, we also studied 17-month-old knock-in (KI) mice expressing chimeric mouse/human exon 1 containing 140 CAG repeats inserted in the murine huntingtin gene (KI140) and their littermate controls (44). Mice were maintained in a temperature-controlled room (~23°C) with a light/dark cycle of 12/12 h. All animals had access to food and water ad libitum. Animals were handled according to approved Animal Care procedures. Genotyping was determined from PCR of tail snips taken at 10–15 days of age. In our experiments, we used 5–6 animals per experimental group. Groups were balanced between males and females, and we did not notice gender differences regarding Tau changes as well as kinase/phosphatase modulation.

Immunoblotting

Mice were sacrificed by dislocation without anesthesia and tissue processed as described (11,12). Tissues were homogenized in 200 μl Tris buffer pH 7.4 containing 10% sucrose and protease inhibitors (Complete, Roche), sonicated and kept at −80°C for biochemical experiments. Protein dosage, processing as mono- and bi-dimensional electrophoresis, as well as sarkosyl fractionations experiments were performed as previously described (11,12).

Histological analysis

Mice brains were dissected and fixed immediately by immersion in 4% paraformaldehyde in 0.1 M phosphate buffer (pH 7.4). Samples were dehydrated in graded alcohol solutions, embedded in paraffin and cut at 5 μm using a microtome. Slices were pretreated with boiling citrate buffer, pH 6 (4 cycles of 2 min), incubated overnight in humidified chamber with anti-Htt 2B4 (mouse, 1:500, Millipore, MAB5492) or anti-Htt Em48 (mouse, 1:500, Millipore, MAB5374) and anti-Tau[pSer396] (rabbit, 1:500, Life Technologies). Samples were washed and incubated with anti-mouse IgG-Alexa Fluor 488 and anti-rabbit IgG-Alexa Fluor 594 (1:500, Life Technologies) and with DAPI,

and then subsequently washed and mounted. An inverted Leica SP8 confocal microscope was used to examine the samples.

Statistics

Results are expressed as means ± SEM. Differences between mean values were determined using the Student's *t*-test. *P*-values <0.05 were considered significant.

SUPPLEMENTARY MATERIAL

Supplementary Material is available at *HMG* online.

ACKNOWLEDGEMENTS

The authors thank the animal facility of IMPRT-IFR114 and M. Besegher, I. Brion, D. Cappe, R. Dehaynin, J. Devassine, Y. Lepage, C. Meunier and D. Taillieu for R6/2 transgenic mouse production and animal care as well as Patrizia Popoli and Alberto Martire from ISS, Roma. The authors also thank Jean-Marie Héliès and Julien Mitja (animal facility at MIRCen, CEA) for their help in developing the colony of CAG140 knock-in mice.

Conflict of Interest statement. None declared.

FUNDING

This work was supported by grants from France Alzheimer and LECMA/Alzheimer Forschung Initiative, Agence Nationale de la Recherche (ADORATAU) (D.B.). A&T laboratory is also supported by the LabEx (excellence laboratory) DISTALZ (Development of Innovative Strategies for a Transdisciplinary approach to ALZheimer's disease), Inserm, CNRS, Université Lille 2, Région Nord/Pas-de-Calais, DN2M, and FUI MEDIALZ. L.F. was the recipient of a Ph.D. fellowship from the Ministère de l'Education Nationale, de la Recherche et de la Technologie. F.H. is supported by a postdoctoral fellowship by the Portuguese Fundação para a Ciência e a Tecnologia (SFRH/BPD/63530/2009). F.H. and T.F.O. were supported by a grant from the European Huntingtoń Disease Network (EHDN). T.F.O. was supported by an EMBO Installation Grant, and is currently supported by the DFG Center for Nanoscale Microscopy and Molecular Physiology of the Brain (CNMPB).

REFERENCES

1. Walker, F.O. (2007) Huntington's disease. *Lancet*, **369**, 218–228.
2. The Huntington's Disease Collaborative Research Group. (1993) A novel gene containing a trinucleotide repeat that is expanded and unstable on Huntington's disease chromosomes. *Cell*, **72**, 971–983.
3. Brouillet, E., Jacquard, C., Bizat, N. and Blum, D. (2005) 3-Nitropropionic acid: a mitochondrial toxin to uncover physiopathological mechanisms underlying striatal degeneration in Huntington's disease. *J. Neurochem.*, **95**, 1521–1540.
4. Sergeant, N., Bretteville, A., Hamdane, M., Caillet-Boudin, M.L., Grognet, P., Bombois, S., Blum, D., Delacourte, A., Pasquier, F., Vanmechelen, E. *et al.* (2008) Biochemistry of Tau in Alzheimer's disease and related neurological disorders. *Expert Rev. Proteomics*, **5**, 207–224.
5. Burnouf, S., Martire, A., Derisbourg, M., Laurent, C., Belarbi, K., Leboucher, A., Fernandez-Gomez, F.J., Troquier, L., Eddarkaoui, S., Grosjean, M.E. *et al.* (2013) NMDA receptor dysfunction contributes to impaired brain-derived neurotrophic factor-induced facilitation of hippocampal synaptic transmission in a Tau transgenic model. *Aging Cell*, **12**, 11–23.
6. Sultan, A., Nesslany, F., Violet, M., Begard, S., Loyens, A., Talahari, S., Mansuroglu, Z., Marzin, D., Sergeant, N., Humez, S. *et al.* (2011) Nuclear tau, a key player in neuronal DNA protection. *J. Biol. Chem.*, **286**, 4566–4575.
7. Bretteville, A. and Planel, E. (2008) Tau aggregates: toxic, inert, or protective species? *J. Alzheimers Dis.*, **14**, 431–436.
8. Planel, E., Richter, K.E., Nolan, C.E., Finley, J.E., Liu, L., Wen, Y., Krishnamurthy, P., Herman, M., Wang, L., Schachter, J.B. *et al.* (2007) Anesthesia leads to tau hyperphosphorylation through inhibition of phosphatase activity by hypothermia. *J. Neurosci.*, **27**, 3090–3097.
9. Papon, M.A., El Khoury, N.B., Marcouiller, F., Julien, C., Morin, F., Bretteville, A., Petry, F.R., Gaudreau, S., Amrani, A., Mathews, P.M. *et al.* (2013) Deregulation of protein phosphatase 2A and hyperphosphorylation of tau protein following onset of diabetes in NOD mice. *Diabetes*, **62**, 609–617.
10. Planel, E., Tatebayashi, Y., Miyasaka, T., Liu, L., Wang, L., Herman, M., Yu, W.H., Luchsinger, J.A., Wadzinski, B., Duff, K.E. and Takashima, A. (2007) Insulin dysfunction induces *in vivo* tau hyperphosphorylation through distinct mechanisms. *J. Neurosci.*, **27**, 13635–13648.
11. Leboucher, A., Laurent, C., Fernandez-Gomez, F.J., Burnouf, S., Troquier, L., Eddarkaoui, S., Demeyer, D., Caillierez, R., Zommer, N., Vallez, E. *et al.* (2013) Detrimental effects of diet-induced obesity on tau pathology are independent of insulin resistance in tau transgenic mice. *Diabetes*, **62**, 1681–1688.
12. Le Freche, H., Brouillette, J., Fernandez-Gomez, F.J., Patin, P., Caillierez, R., Zommer, N., Sergeant, N., Buee-Scherrer, V., Lebuffe, G., Blum, D. and Buee, L. (2012) Tau phosphorylation and sevoflurane anesthesia: an association to postoperative cognitive impairment. *Anesthesiology*, **116**, 779–787.
13. Eckenhoff, R.G. and Planel, E. (2013) Anesthesia, surgery and neurodegeneration. *Prog. Neuropsychopharmacol. Biol. Psychiatry*, **47**, 121.
14. Badiola, N., de Oliveira, R.M., Herrera, F., Guardia-Laguarta, C., Goncalves, S.A., Pera, M., Suarez-Calvet, M., Clarimon, J., Outeiro, T.F. and Lleo, A. (2011) Tau enhances alpha-synuclein aggregation and toxicity in cellular models of synucleinopathy. *PLoS One*, **6**, e26609.
15. Clinton, L.K., Blurton-Jones, M., Myczek, K., Trojanowski, J.Q. and LaFerla, F.M. (2010) Synergistic interactions between Abeta, tau, and alpha-synuclein: acceleration of neuropathology and cognitive decline. *J. Neurosci.*, **30**, 7281–7289.
16. Charles, V., Mezey, E., Reddy, P.H., Dehejia, A., Young, T.A., Polymeropoulos, M.H., Brownstein, M.J. and Tagle, D.A. (2000) Alpha-synuclein immunoreactivity of huntingtin polyglutamine aggregates in striatum and cortex of Huntington's disease patients and transgenic mouse models. *Neurosci. Lett.*, **289**, 29–32.
17. Furlong, R.A., Narain, Y., Rankin, J., Wyttenbach, A. and Rubinsztein, D.C. (2000) Alpha-synuclein overexpression promotes aggregation of mutant huntingtin. *Biochem. J.*, **346**, 577–581.
18. Herrera, F. and Outeiro, T.F. (2012) alpha-Synuclein modifies huntingtin aggregation in living cells. *FEBS Lett.*, **586**, 7–12.
19. Jellinger, K.A. (1998) Alzheimer-type lesions in Huntington's disease. *J. Neural Transm.*, **105**, 787–799.
20. Caparros-Lefebvre, D., Kerdraon, O., Devos, D., Dhaenens, C.M., Blum, D., Maurage, C.A., Delacourte, A. and Sablonniere, B. (2009) Association of corticobasal degeneration and Huntington's disease: can Tau aggregates protect Huntingtin toxicity? *Mov. Disord.*, **24**, 1089–1090.
21. Tian, Q. and Wang, J. (2002) Role of serine/threonine protein phosphatase in Alzheimer's disease. *Neurosignals*, **11**, 262–269.
22. Herrera, F., Tenreiro, S., Miller-Fleming, L. and Outeiro, T.F. (2011) Visualization of cell-to-cell transmission of mutant huntingtin oligomers. *PLoS Curr.*, **3**, RRN1210.
23. Hoffner, G., Kahlem, P. and Djian, P. (2002) Perinuclear localization of huntingtin as a consequence of its binding to microtubules through an interaction with beta-tubulin: relevance to Huntington's disease. *J. Cell Sci.*, **115**, 941–948.
24. Godin, J.D., Colombo, K., Molina-Calavita, M., Keryer, G., Zala, D., Charrin, B.C., Dietrich, P., Volvert, M.L., Guillemot, F., Dragatsis, I. *et al.* (2010) Huntingtin is required for mitotic spindle orientation and mammalian neurogenesis. *Neuron*, **67**, 392–406.

25. Atwal, R.S., Desmond, C.R., Caron, N., Maiuri, T., Xia, J., Sipione, S. and Truant, R. (2011) Kinase inhibitors modulate huntingtin cell localization and toxicity. *Nat. Chem. Biol.*, **7**, 453–460.
26. Torres-Peraza, J.F., Giralt, A., García-Martínez, J.M., Pedrosa, E., Canals, J.M. and Alberch, J. (2008) Disruption of striatal glutamatergic transmission induced by mutant huntingtin involves remodeling of both postsynaptic density and NMDA receptor signaling. *Neurobiol. Dis.*, **29**, 409–421.
27. Hodges, A., Strand, A.D., Aragaki, A.K., Kuhn, A., Sengstag, T., Hughes, G., Elliston, L.A., Hartog, C., Goldstein, D.R., Thu, D. *et al.* (2006) Regional and cellular gene expression changes in human Huntington's disease brain. *Hum. Mol. Genet.*, **15**, 965–977.
28. Xifro, X., Giralt, A., Saavedra, A., Garcia-Martinez, J.M., Diaz-Hernandez, M., Lucas, J.J., Alberch, J. and Perez-Navarro, E. (2009) Reduced calcineurin protein levels and activity in exon-1 mouse models of Huntington's disease: role in excitotoxicity. *Neurobiol. Dis.*, **36**, 461–469.
29. Luthi-Carter, R., Strand, A., Peters, N.L., Solano, S.M., Hollingsworth, Z.R., Menon, A.S., Frey, A.S., Spektor, B.S., Penney, E.B., Schilling, G. *et al.* (2000) Decreased expression of striatal signaling genes in a mouse model of Huntington's disease. *Hum. Mol. Genet.*, **9**, 1259–1271.
30. Hernandez-Espinosa, D. and Morton, A.J. (2006) Calcineurin inhibitors cause an acceleration of the neurological phenotype in a mouse transgenic for the human Huntington's disease mutation. *Brain Res. Bull.*, **69**, 669–679.
31. Liu, F., Grundke-Iqbal, I., Iqbal, K. and Gong, C.X. (2005) Contributions of protein phosphatases PP1, PP2A, PP2B and PP5 to the regulation of tau phosphorylation. *Eur. J. Neurosci.*, **22**, 1942–1950.
32. Jenkins, S.M., Zinnerman, M., Garner, C. and Johnson, G.V. (2000) Modulation of tau phosphorylation and intracellular localization by cellular stress. *Biochem. J.*, **345**, 263–270.
33. Buee, L., Bussiere, T., Buee-Scherrer, V., Delacourte, A. and Hof, P.R. (2000) Tau protein isoforms, phosphorylation and role in neurodegenerative disorders. *Brain Res. Brain Res. Rev.*, **33**, 95–130.
34. Hinckelmann, M.V., Zala, D. and Saudou, F. (2013) Releasing the brake: restoring fast axonal transport in neurodegenerative disorders. *Trends Cell Biol.*, **23**, 634–643.
35. Morris, M., Maeda, S., Vossel, K. and Mucke, L. (2011) The many faces of tau. *Neuron*, **70**, 410–426.
36. Ahmed, T., Van der Jeugd, A., Blum, D., Galas, M.C., D'Hooge, R., Buee, L. and Balschun, D. (2014) Cognition and hippocampal synaptic plasticity in mice with a homozygous tau deletion *Neurobiol. Aging* (in press). doi: 10.1016/j.neurobiolaging.2014.05.005.
37. Qin, Z.H., Wang, Y., Sapp, E., Cuiffo, B., Wanker, E., Hayden, M.R., Kegel, K.B., Aronin, N. and DiFiglia, M. (2004) Huntingtin bodies sequester vesicle-associated proteins by a polyproline-dependent interaction. *J. Neurosci.*, **24**, 269–281.
38. Pires, R.H., Karsai, Á., Saraiva, M.J., Damas, A.M. and Kellermayer, M.S. (2012) Distinct annular oligomers captured along the assembly and disassembly pathways of transthyretin amyloid protofibrils. *PLoS One*, **7**, e44992.
39. Zhu, M., Han, S., Zhou, F., Carter, S.A. and Fink, A.L. (2004) Annular oligomeric amyloid intermediates observed by *in situ* atomic force microscopy. *J. Biol. Chem.*, **279**, 24452–24459.
40. Davis, M.Y., Keene, C.D., Jayadev, S. and Bird, T. (2014) The co-occurrence of Alzheimer's disease and Huntington's disease: a neuropathological study of 15 elderly Huntington's disease subjects. *J. Huntingtons Dis.*, **3**, 209–217.
41. Fernández-Nogales, M., Cabrera, J.R., Santos-Galindo, M., Hoozemans, J.J., Ferrer, I., Rozemuller, A.J., Hernández, F., Avila, J. and Lucas, J.J. (2014) Huntington's disease is a four-repeat tauopathy with tau nuclear rods. *Nat. Med.*, **20**, 881–885.
42. Outeiro, T.F., Putcha, P., Tetzlaff, J.E., Spoelgen, R., Koker, M., Carvalho, F., Hyman, B.T. and McLean, P.J. (2008) Formation of toxic oligomeric alpha-synuclein species in living cells. *PLoS One*, **3**, e1867.
43. Mangiarini, L., Sathasivam, K., Seller, M., Cozens, B., Harper, A., Hetherington, C., Lawton, M., Trottier, Y., Lehrach, H., Davies, S.W. *et al.* (1996) Exon 1 of the HD gene with an expanded CAG repeat is sufficient to cause a progressive neurological phenotype in transgenic mice. *Cell*, **87**, 493–506.
44. Menalled, L.B., Sison, J.D., Dragatsis, I., Zeitlin, S. and Chesselet, M.F. (2003) Time course of early motor and neuropathological anomalies in a knock-in mouse model of Huntington's disease with 140 CAG repeats. *J. Comp. Neurol.*, **465**, 11–26.

6.3. Clinical trials status report

SPONSOR	STUDY NAME/ IDENTIFIER	STUDY AGENT	PHASE	PRINCIPAL INVESTIGATOR, CONTACT	DESIGN	TRIAL LENGTH	SITES	STATUS
Omeros Corporation	NCT02074410	OMS643762	II	Albert Yu MD 206-676-5000	Randomized, double-blind, placebo-controlled, sequential cohort study to evaluate safety and efficacy of OMS643762 in subjects with HD	28 days	4 sites - U.S.	*Currently enrolling*
Teva Pharmaceutical Industries	PRIDE-HD	Pridopidine	II	Teva US Medical Information 800-896-5855	Randomized, double-blind, placebo-controlled study of safety and efficacy of pridopidine 45 mg, 67.5 mg, 90 mg, and 112.5 mg BID versus placebo for symptomatic treatment in patients with HD	26 weeks	U.S.	*Currently enrolling*
Teva Pharmaceutical Industries	OPEN-HART	Pridopidine	II	Karl Kieburtz, MD MPH	Open label, single group assignment study to assess the long-term safety of 45 mg of pridopidine in HD participants	2 years	22 sites - U.S. and Canada	*Enrollment complete, study ongoing*
Prana Biotechnology	REACH2HD	PBT2	II	Ray Dorsey, MD 800-487-7671 (U.S.) 800-794-669 (Australia)	Randomized, double-blind safety and tolerability study of PBT2 of individuals with mild to moderate HD	6 months	20 sites - Australia and U.S.	*Study complete, top line results released*
Pfizer	NCT01806896	PF-0254920	II	Pfizer CT.gov Call Center, 800-718-1021	Randomized double-blind study testing the efficacy and tolerability of PF-0254920 in changing the total motor score patients with HD	28 days	Paris, France	*Currently enrolling*
Charité University	ETON-Study	Epigallo-catechin Gallate	II	Josef Priller, MD+49 (0)30 450 617209	Randomized double blind study testing the efficacy and tolerability of (2)-epigallocatechin-3-gallate (EGCG) in changing cognitive function in patients with HD	1 year	4 sites - Germany	*Enrollment complete, study ongoing*
Charité University	Action-HD	Bupropion	II	Josef Priller, MD +49 (0)30 450 617209	Randomized double-blind study testing the efficacy and tolerability of Bupropion in changing apathy in patients with HD	10 weeks	3 sites - Germany	*Enrollment complete, study ongoing*
Raptor Pharmaceuticals	CYST-HD	Cysteamine Bitartrate Delayed release (RP103)	II/III	Christophe Verny, MD	Double-blind, placebo-controlled study to be followed by an open-label extension study	18 months	8 sites - France	*Study ongoing, preliminary results released*
National Institute of Neurological Disorders and Stroke	2CARE	Coenzyme Q10	III	Merit Cudkowicz, MD, MSc Huntington Study Group: 800-487-7671	Randomized double-blind study to see whether coenzyme Q10 is effective in slowing the worsening of symptoms of HD	5 years	49 sites - U.S., Canada, Australia	*Study concluded for futility (see p.1)*
Auspex Pharmaceuticals, Inc.	FIRST-HD	SD-809 Extended Release	III	Samuel Frank, MD Huntington Study Group: 800-487-7671	Randomized double blind study to determine whether SD-809 ER tablets are effective in the treatment of chorea associated with HD	12 weeks	7 sites - U.S.	*Enrollment complete, study ongoing*
Auspex Pharmaceuticals, Inc.	ARC-HD	SD-809 Extended Release	III	Samuel Frank, MD Huntington Study Group: 800-487-7671	Open-label, long term safety study of SD-809 ER	58 weeks	7 sites - U.S.	*Currently enrolling*
Assistance Publique - Hôpitaux de Paris	NEUROHD	Olanzapine, Tetrabenazine and Tiapride	III	Anne-Catherine Bachoud Levi, PhD +33 (0)1 49 81 23 01	Randomized controlled study to compare the beneficial and adverse effects of 3 different neuroleptics in HD	1 year	1 site - Europe	*Currently enrolling*
National Center for Complementary and Alternative Medicine	CREST-E	Creatine	III	Steven M Hersch, MD, PhD Huntington Study Group: 800-487-7671	Randomized double blind study to test whether high-dose creatine can slow the progressive functional decline that occurs in adult persons with early clinical features of HD	3 years	52 sites - U.S., Canada, Australia, New Zealand	*Currently enrolling*
New York Medical College	NCT1834911	Tetrabenazine	IV	Robert Fekete, MD 914-594-4293	Prospective case-control study to compare Stroop Visual Interference Scores while individuals who are already taking tetrabenazine are off the drug for three days and then back on the drug	6 hours	1 site - Terence Cardinal Cooke Health Care Center	*Currently enrolling*

Table 5 Current HD clinical trials (source : http://www.clinicaltrials.gov/)

PART7 BIBLIOGRAPHY

Abe S, Katagiri T, Saito-Hisaminato A, Usami S, Inoue Y, et al. 2003. Identification of CRYM as a candidate responsible for nonsyndromic deafness, through cDNA microarray analysis of human cochlear and vestibular tissues. *American journal of human genetics* 72: 73-82

Agostinho LA, Dos Santos SR, Alvarenga RM, Paiva CL. 2013. A systematic review of the intergenerational aspects and the diverse genetic profiles of Huntington's disease. *Genetics and molecular research : GMR* 12: 1974-81

Al-Kafaji G, Malik AN. 2010. Hyperglycemia induces elevated expression of thyroid hormone binding protein in vivo in kidney and heart and in vitro in mesangial cells. *Biochemical and biophysical research communications* 391: 1585-91

Albin RL, Reiner A, Anderson KD, Dure LSt, Handelin B, et al. 1992. Preferential loss of striato-external pallidal projection neurons in presymptomatic Huntington's disease. *Annals of neurology* 31: 425-30

Albin RL, Young AB, Penney JB. 1989. The functional anatomy of basal ganglia disorders. *Trends in neurosciences* 12: 366-75

Alexi T, Borlongan CV, Faull RL, Williams CE, Clark RG, et al. 2000. Neuroprotective strategies for basal ganglia degeneration: Parkinson's and Huntington's diseases. *Progress in neurobiology* 60: 409-70

Andre VM, Cepeda C, Levine MS. 2010. Dopamine and glutamate in Huntington's disease: A balancing act. *CNS neuroscience & therapeutics* 16: 163-78

Andreassen OA, Dedeoglu A, Ferrante RJ, Jenkins BG, Ferrante KL, et al. 2001. Creatine increase survival and delays motor symptoms in a transgenic animal model of Huntington's disease. *Neurobiology of disease* 8: 479-91

Andrew SE, Goldberg YP, Kremer B, Telenius H, Theilmann J, et al. 1993. The relationship between trinucleotide (CAG) repeat length and clinical features of Huntington's disease. *Nature genetics* 4: 398-403

Aoyama K, Suh SW, Hamby AM, Liu J, Chan WY, et al. 2006. Neuronal glutathione deficiency and age-dependent neurodegeneration in the EAAC1 deficient mouse. *Nature neuroscience* 9: 119-26

Arenas J, Campos Y, Ribacoba R, Martin MA, Rubio JC, et al. 1998. Complex I defect in muscle from patients with Huntington's disease. *Annals of neurology* 43: 397-400

Arrasate M, Mitra S, Schweitzer ES, Segal MR, Finkbeiner S. 2004. Inclusion body formation reduces levels of mutant huntingtin and the risk of neuronal death. *Nature* 431: 805-10

Atkin G, Paulson H. 2014. Ubiquitin pathways in neurodegenerative disease. *Frontiers in molecular neuroscience* 7: 63

Atwal RS, Xia J, Pinchev D, Taylor J, Epand RM, Truant R. 2007. Huntingtin has a membrane association signal that can modulate huntingtin aggregation, nuclear entry and toxicity. *Human molecular genetics* 16: 2600-15

Augood SJ, Faull RL, Emson PC. 1997. Dopamine D1 and D2 receptor gene expression in the striatum in Huntington's disease. *Annals of neurology* 42: 215-21

Aziz NA, Roos RA, Gusella JF, Lee JM, Macdonald ME. 2012. CAG repeat expansion in Huntington disease determines age at onset in a fully dominant fashion. *Neurology* 79: 952; author reply 52-3

Bae BI, Xu H, Igarashi S, Fujimuro M, Agrawal N, et al. 2005. p53 mediates cellular dysfunction and behavioral abnormalities in Huntington's disease. *Neuron* 47: 29-41

Ballas N, Battaglioli E, Atouf F, Andres ME, Chenoweth J, et al. 2001. Regulation of neuronal traits by a novel transcriptional complex. *Neuron* 31: 353-65

Basser PJ, Jones DK. 2002. Diffusion-tensor MRI: theory, experimental design and data analysis - a technical review. *NMR in biomedicine* 15: 456-67

Basser PJ, Pierpaoli C. 1996. Microstructural and physiological features of tissues elucidated by quantitative-diffusion-tensor MRI. *Journal of magnetic resonance. Series B* 111: 209-19

Bates GP. 2005. History of genetic disease: the molecular genetics of Huntington disease - a history. *Nature reviews. Genetics* 6: 766-73

Bauer PO, Goswami A, Wong HK, Okuno M, Kurosawa M, et al. 2010. Harnessing chaperone-mediated autophagy for the selective degradation of mutant huntingtin protein. *Nature biotechnology* 28: 256-63

Beal MF. 1992. Does impairment of energy metabolism result in excitotoxic neuronal death in neurodegenerative illnesses? *Annals of neurology* 31: 119-30

Beal MF, Brouillet E, Jenkins BG, Ferrante RJ, Kowall NW, et al. 1993. Neurochemical and histologic characterization of striatal excitotoxic lesions produced by the mitochondrial toxin 3-nitropropionic acid. *The Journal of neuroscience : the official journal of the Society for Neuroscience* 13: 4181-92

Beal MF, Ferrante RJ. 2004. Experimental therapeutics in transgenic mouse models of Huntington's disease. *Nature reviews. Neuroscience* 5: 373-84

Beal MF, Kowall NW, Ellison DW, Mazurek MF, Swartz KJ, Martin JB. 1986. Replication of the neurochemical characteristics of Huntington's disease by quinolinic acid. *Nature* 321: 168-71

Beal MF, Shults CW. 2003. Effects of Coenzyme Q10 in Huntington's disease and early Parkinson's disease. *BioFactors* 18: 153-61

Belyaev ND, Wood IC, Bruce AW, Street M, Trinh JB, Buckley NJ. 2004. Distinct RE-1 silencing transcription factor-containing complexes interact with different target genes. *The Journal of biological chemistry* 279: 556-61

Benn CL, Landles C, Li H, Strand AD, Woodman B, et al. 2005. Contribution of nuclear and extranuclear polyQ to neurological phenotypes in mouse models of Huntington's disease. *Human molecular genetics* 14: 3065-78

Bennett CF, Swayze EE. 2010. RNA targeting therapeutics: molecular mechanisms of antisense oligonucleotides as a therapeutic platform. *Annual review of pharmacology and toxicology* 50: 259-93

Berrios GE, Wagle AC, Markova IS, Wagle SA, Rosser A, Hodges JR. 2002. Psychiatric symptoms in neurologically asymptomatic Huntington's disease gene carriers: a comparison with gene negative at risk subjects. *Acta psychiatrica Scandinavica* 105: 224-30

Bjorkqvist M, Fex M, Renstrom E, Wierup N, Petersen A, et al. 2005. The R6/2 transgenic mouse model of Huntington's disease develops diabetes due to deficient beta-cell mass and exocytosis. *Human molecular genetics* 14: 565-74

Blum D, Herrera F, Francelle L, Mendes T, Basquin M, et al. 2014. Mutant huntingtin alters Tau phosphorylation and subcellular distribution. *Human molecular genetics*

Bohanna I, Georgiou-Karistianis N, Hannan AJ, Egan GF. 2008. Magnetic resonance imaging as an approach towards identifying neuropathological biomarkers for Huntington's disease. *Brain research reviews* 58: 209-25

Borel F, Hachi I, Palencia A, Gaillard MC, Ferrer JL. 2014. Crystal structure of mouse mu-crystallin complexed with NADPH and the T3 thyroid hormone. *The FEBS journal* 281: 1598-612

Borrell-Pages M, Canals JM, Cordelieres FP, Parker JA, Pineda JR, et al. 2006. Cystamine and cysteamine increase brain levels of BDNF in Huntington disease via HSJ1b and transglutaminase. *The Journal of clinical investigation* 116: 1410-24

Bose P, Dai Y, Grant S. 2014. Histone deacetylase inhibitor (HDACI) mechanisms of action: emerging insights. *Pharmacology & therapeutics* 143: 323-36

Bouchard J, Truong J, Bouchard K, Dunkelberger D, Desrayaud S, et al. 2012. Cannabinoid receptor 2 signaling in peripheral immune cells modulates disease onset and severity in mouse models of Huntington's disease. *The Journal of neuroscience : the official journal of the Society for Neuroscience* 32: 18259-68

Bowles KR, Jones L. 2014. Kinase signalling in Huntington's disease. *Journal of Huntington's disease* 3: 89-123

Brochier C, Gaillard MC, Diguet E, Caudy N, Dossat C, et al. 2008. Quantitative gene expression profiling of mouse brain regions reveals differential transcripts conserved in human and affected in disease models. *Physiological genomics* 33: 170-9

Brouillet E. 2014. The 3-NP Model of Striatal Neurodegeneration. *Current protocols in neuroscience / editorial board, Jacqueline N. Crawley ... [et al.]* 67: 9 48 1-9 48 14

Brouillet E, Hantraye P, Ferrante RJ, Dolan R, Leroy-Willig A, et al. 1995. Chronic mitochondrial energy impairment produces selective striatal degeneration and abnormal choreiform movements in primates. *Proceedings of the National Academy of Sciences of the United States of America* 92: 7105-9

Browne SE, Bowling AC, MacGarvey U, Baik MJ, Berger SC, et al. 1997. Oxidative damage and metabolic dysfunction in Huntington's disease: selective vulnerability of the basal ganglia. *Annals of neurology* 41: 646-53

Burklen TS, Schlattner U, Homayouni R, Gough K, Rak M, et al. 2006. The creatine kinase/creatine connection to Alzheimer's disease: CK-inactivation, APP-CK complexes and focal creatine deposits. *Journal of biomedicine & biotechnology* 2006: 35936

Cai K, Haris M, Singh A, Kogan F, Greenberg JH, et al. 2012. Magnetic resonance imaging of glutamate. *Nature medicine* 18: 302-6

Caine ED, Shoulson I. 1983. Psychiatric syndromes in Huntington's disease. *The American journal of psychiatry* 140: 728-33

Calabresi P, Picconi B, Tozzi A, Ghiglieri V, Di Filippo M. 2014. Direct and indirect pathways of basal ganglia: a critical reappraisal. *Nature neuroscience* 17: 1022-30

Carroll JB, Warby SC, Southwell AL, Doty CN, Greenlee S, et al. 2011. Potent and selective antisense oligonucleotides targeting single-nucleotide polymorphisms in the Huntington disease gene / allele-specific silencing of mutant huntingtin. *Molecular therapy : the journal of the American Society of Gene Therapy* 19: 2178-85

Cattaneo E, Rigamonti D, Goffredo D, Zuccato C, Squitieri F, Sipione S. 2001. Loss of normal huntingtin function: new developments in Huntington's disease research. *Trends in neurosciences* 24: 182-8

Cha JH. 2007. Transcriptional signatures in Huntington's disease. *Progress in neurobiology* 83: 228-48

Cha JH, Kosinski CM, Kerner JA, Alsdorf SA, Mangiarini L, et al. 1998. Altered brain neurotransmitter receptors in transgenic mice expressing a portion of an abnormal human huntington disease gene. *Proceedings of the National Academy of Sciences of the United States of America* 95: 6480-5

Chaneton B, Hillmann P, Zheng L, Martin AC, Maddocks OD, et al. 2012. Serine is a natural ligand and allosteric activator of pyruvate kinase M2. *Nature* 491: 458-62

Charbord J, Poydenot P, Bonnefond C, Feyeux M, Casagrande F, et al. 2013. High throughput screening for inhibitors of REST in neural derivatives of human embryonic stem cells reveals a chemical compound that promotes expression of neuronal genes. *Stem cells* 31: 1816-28

Charvin D, Vanhoutte P, Pages C, Borrelli E, Caboche J. 2005. Unraveling a role for dopamine in Huntington's disease: the dual role of reactive oxygen species and D2

receptor stimulation. *Proceedings of the National Academy of Sciences of the United States of America* 102: 12218-23

Chen N, Luo T, Wellington C, Metzler M, McCutcheon K, et al. 1999. Subtype-specific enhancement of NMDA receptor currents by mutant huntingtin. *Journal of neurochemistry* 72: 1890-8

Cheung ZH, Ip NY. 2012. Cdk5: a multifaceted kinase in neurodegenerative diseases. *Trends in cell biology* 22: 169-75

Chong JA, Tapia-Ramirez J, Kim S, Toledo-Aral JJ, Zheng Y, et al. 1995. REST: a mammalian silencer protein that restricts sodium channel gene expression to neurons. *Cell* 80: 949-57

Choo YS, Johnson GV, MacDonald M, Detloff PJ, Lesort M. 2004. Mutant huntingtin directly increases susceptibility of mitochondria to the calcium-induced permeability transition and cytochrome c release. *Human molecular genetics* 13: 1407-20

Choong PF, Mok PL, Cheong SK, Leong CF, Then KY. 2007. Generating neuron-like cells from BM-derived mesenchymal stromal cells in vitro. *Cytotherapy* 9: 170-83

Chopra V, Quinti L, Kim J, Vollor L, Narayanan KL, et al. 2012. The sirtuin 2 inhibitor AK-7 is neuroprotective in Huntington's disease mouse models. *Cell reports* 2: 1492-7

Cicchetti F, Saporta S, Hauser RA, Parent M, Saint-Pierre M, et al. 2009. Neural transplants in patients with Huntington's disease undergo disease-like neuronal degeneration. *Proceedings of the National Academy of Sciences of the United States of America* 106: 12483-8

Clabough EB. 2013. Huntington's disease: the past, present, and future search for disease modifiers. *The Yale journal of biology and medicine* 86: 217-33

Clabough EB, Zeitlin SO. 2006. Deletion of the triplet repeat encoding polyglutamine within the mouse Huntington's disease gene results in subtle behavioral/motor phenotypes in vivo and elevated levels of ATP with cellular senescence in vitro. *Human molecular genetics* 15: 607-23

Colin E, Regulier E, Perrin V, Durr A, Brice A, et al. 2005. Akt is altered in an animal model of Huntington's disease and in patients. *The European journal of neuroscience* 21: 1478-88

Conforti P, Mas Monteys A, Zuccato C, Buckley NJ, Davidson B, Cattaneo E. 2013. In vivo delivery of DN:REST improves transcriptional changes of REST-regulated genes in HD mice. *Gene therapy* 20: 678-85

Coppede F. 2014. The potential of epigenetic therapies in neurodegenerative diseases. *Frontiers in genetics* 5: 220

Cortes CJ, La Spada AR. 2014. The many faces of autophagy dysfunction in Huntington's disease: from mechanism to therapy. *Drug discovery today* 19: 963-71

Crane AT, Rossignol J, Dunbar GL. 2014. Use of Genetically Altered Stem Cells for the Treatment of Huntington's Disease. *Brain sciences* 4: 202-19

Craufurd D, Thompson JC, Snowden JS. 2001. Behavioral changes in Huntington Disease. *Neuropsychiatry, neuropsychology, and behavioral neurology* 14: 219-26

Cui L, Jeong H, Borovecki F, Parkhurst CN, Tanese N, Krainc D. 2006. Transcriptional repression of PGC-1alpha by mutant huntingtin leads to mitochondrial dysfunction and neurodegeneration. *Cell* 127: 59-69

Cummings JL. 1995. Behavioral and psychiatric symptoms associated with Huntington's disease. *Advances in neurology* 65: 179-86

Damiano M, Diguet E, Malgorn C, D'Aurelio M, Galvan L, et al. 2013. A role of mitochondrial complex II defects in genetic models of Huntington's disease expressing N-terminal fragments of mutant huntingtin. *Hum Mol Genet* 22: 3869-82

Damiano M, Galvan L, Deglon N, Brouillet E. 2010. Mitochondria in Huntington's disease. *Biochimica et biophysica acta* 1802: 52-61

Davies SW, Turmaine M, Cozens BA, DiFiglia M, Sharp AH, et al. 1997. Formation of neuronal intranuclear inclusions underlies the neurological dysfunction in mice transgenic for the HD mutation. *Cell* 90: 537-48

de Chaldee M, Gaillard MC, Bizat N, Buhler JM, Manzoni O, et al. 2003. Quantitative assessment of transcriptome differences between brain territories. *Genome research* 13: 1646-53

de la Monte SM, Vonsattel JP, Richardson EP, Jr. 1988. Morphometric demonstration of atrophic changes in the cerebral cortex, white matter, and neostriatum in Huntington's disease. *Journal of neuropathology and experimental neurology* 47: 516-25

Dedeoglu A, Kubilus JK, Jeitner TM, Matson SA, Bogdanov M, et al. 2002. Therapeutic effects of cystamine in a murine model of Huntington's disease. *The Journal of neuroscience : the official journal of the Society for Neuroscience* 22: 8942-50

Dedeoglu A, Kubilus JK, Yang L, Ferrante KL, Hersch SM, et al. 2003. Creatine therapy provides neuroprotection after onset of clinical symptoms in Huntington's disease transgenic mice. *Journal of neurochemistry* 85: 1359-67

Deglon N, Hantraye P. 2005. Viral vectors as tools to model and treat neurodegenerative disorders. *The journal of gene medicine* 7: 530-9

DeMarch Z, Giampa C, Patassini S, Bernardi G, Fusco FR. 2008. Beneficial effects of rolipram in the R6/2 mouse model of Huntington's disease. *Neurobiology of disease* 30: 375-87

Desplats PA, Kass KE, Gilmartin T, Stanwood GD, Woodward EL, et al. 2006. Selective deficits in the expression of striatal-enriched mRNAs in Huntington's disease. *Journal of neurochemistry* 96: 743-57

DiFiglia M. 1990. Excitotoxic injury of the neostriatum: a model for Huntington's disease. *Trends in neurosciences* 13: 286-9

DiFiglia M, Sapp E, Chase K, Schwarz C, Meloni A, et al. 1995. Huntingtin is a cytoplasmic protein associated with vesicles in human and rat brain neurons. *Neuron* 14: 1075-81

DiFiglia M, Sapp E, Chase KO, Davies SW, Bates GP, et al. 1997. Aggregation of huntingtin in neuronal intranuclear inclusions and dystrophic neurites in brain. *Science* 277: 1990-3

Dijkmans TF, van Hooijdonk LW, Fitzsimons CP, Vreugdenhil E. 2010. The doublecortin gene family and disorders of neuronal structure. *Central nervous system agents in medicinal chemistry* 10: 32-46

Djousse L, Knowlton B, Hayden M, Almqvist EW, Brinkman R, et al. 2003. Interaction of normal and expanded CAG repeat sizes influences age at onset of Huntington disease. *American journal of medical genetics. Part A* 119A: 279-82

Douaud G, Behrens TE, Poupon C, Cointepas Y, Jbabdi S, et al. 2009. In vivo evidence for the selective subcortical degeneration in Huntington's disease. *NeuroImage* 46: 958-66

Douaud G, Gaura V, Ribeiro MJ, Lethimonnier F, Maroy R, et al. 2006. Distribution of grey matter atrophy in Huntington's disease patients: a combined ROI-based and voxel-based morphometric study. *NeuroImage* 32: 1562-75

Dragatsis I, Levine MS, Zeitlin S. 2000. Inactivation of Hdh in the brain and testis results in progressive neurodegeneration and sterility in mice. *Nature genetics* 26: 300-6

Drouet V, Perrin V, Hassig R, Dufour N, Auregan G, et al. 2009. Sustained effects of nonallele-specific Huntingtin silencing. *Annals of neurology* 65: 276-85

Drouet V, Ruiz M, Zala D, Feyeux M, Auregan G, et al. 2014. Allele-specific silencing of mutant huntingtin in rodent brain and human stem cells. *PloS one* 9: e99341

Dufour BD, Smith CA, Clark RL, Walker TR, McBride JL. 2014. Intrajugular vein delivery of AAV9-RNAi prevents neuropathological changes and weight loss in Huntington's disease mice. *Molecular therapy : the journal of the American Society of Gene Therapy* 22: 797-810

Dumas EM, van den Bogaard SJ, Ruber ME, Reilman RR, Stout JC, et al. 2012. Early changes in white matter pathways of the sensorimotor cortex in premanifest Huntington's disease. *Human brain mapping* 33: 203-12

Dunah AW, Jeong H, Griffin A, Kim YM, Standaert DG, et al. 2002. Sp1 and TAFII130 transcriptional activity disrupted in early Huntington's disease. *Science* 296: 2238-43

Echtay KS, Roussel D, St-Pierre J, Jekabsons MB, Cadenas S, et al. 2002. Superoxide activates mitochondrial uncoupling proteins. *Nature* 415: 96-9

Ehrnhoefer DE, Sutton L, Hayden MR. 2011. Small changes, big impact: posttranslational modifications and function of huntingtin in Huntington disease. *The Neuroscientist : a review journal bringing neurobiology, neurology and psychiatry* 17: 475-92

Emson PC, Arregui A, Clement-Jones V, Sandberg BE, Rossor M. 1980. Regional distribution of methionine-enkephalin and substance P-like immunoreactivity in normal human brain and in Huntington's disease. *Brain research* 199: 147-60

Erba P, Terenghi G, Kingham PJ. 2010. Neural differentiation and therapeutic potential of adipose tissue derived stem cells. *Current stem cell research & therapy* 5: 153-60

Ernster L, Dallner G. 1995. Biochemical, physiological and medical aspects of ubiquinone function. *Biochimica et biophysica acta* 1271: 195-204

Falkenberg KJ, Johnstone RW. 2014. Histone deacetylases and their inhibitors in cancer, neurological diseases and immune disorders. *Nature reviews. Drug discovery* 13: 673-91

Farrer LA, Cupples LA, Wiater P, Conneally PM, Gusella JF, Myers RH. 1993. The normal Huntington disease (HD) allele, or a closely linked gene, influences age at onset of HD. *American journal of human genetics* 53: 125-30

Feigin A, Ghilardi MF, Huang C, Ma Y, Carbon M, et al. 2006. Preclinical Huntington's disease: compensatory brain responses during learning. *Annals of neurology* 59: 53-9

Fernandez-Ruiz J. 2009. The endocannabinoid system as a target for the treatment of motor dysfunction. *British journal of pharmacology* 156: 1029-40

Fernandez-Ruiz J, Moreno-Martet M, Rodriguez-Cueto C, Palomo-Garo C, Gomez-Canas M, et al. 2011. Prospects for cannabinoid therapies in basal ganglia disorders. *British journal of pharmacology* 163: 1365-78

Ferrante RJ, Andreassen OA, Jenkins BG, Dedeoglu A, Kuemmerle S, et al. 2000. Neuroprotective effects of creatine in a transgenic mouse model of Huntington's disease. *The Journal of neuroscience : the official journal of the Society for Neuroscience* 20: 4389-97

Ferrante RJ, Gutekunst CA, Persichetti F, McNeil SM, Kowall NW, et al. 1997. Heterogeneous topographic and cellular distribution of huntingtin expression in the normal human neostriatum. *The Journal of neuroscience : the official journal of the Society for Neuroscience* 17: 3052-63

Ferrante RJ, Kowall NW, Beal MF, Richardson EP, Jr., Bird ED, Martin JB. 1985. Selective sparing of a class of striatal neurons in Huntington's disease. *Science* 230: 561-3

Ferrante RJ, Kubilus JK, Lee J, Ryu H, Beesen A, et al. 2003. Histone deacetylase inhibition by sodium butyrate chemotherapy ameliorates the neurodegenerative phenotype in Huntington's disease mice. *The Journal of neuroscience : the official journal of the Society for Neuroscience* 23: 9418-27

Folstein SE, Franz ML, Jensen BA, Chase GA, Folstein MF. 1983. Conduct disorder and affective disorder among the offspring of patients with Huntington's disease. *Psychological medicine* 13: 45-52

Forsmark-Andree P, Lee CP, Dallner G, Ernster L. 1997. Lipid peroxidation and changes in the ubiquinone content and the respiratory chain enzymes of submitochondrial particles. *Free radical biology & medicine* 22: 391-400

Francelle L, Galvan L, Brouillet E. 2014. Possible involvement of self-defense mechanisms in the preferential vulnerability of the striatum in Huntington's disease. *Frontiers in cellular neuroscience* 8: 295

Franke TF, Hornik CP, Segev L, Shostak GA, Sugimoto C. 2003. PI3K/Akt and apoptosis: size matters. *Oncogene* 22: 8983-98

Friocourt G, Liu JS, Antypa M, Rakic S, Walsh CA, Parnavelas JG. 2007. Both doublecortin and doublecortin-like kinase play a role in cortical interneuron migration. *The Journal of neuroscience : the official journal of the Society for Neuroscience* 27: 3875-83

Gafni J, Hermel E, Young JE, Wellington CL, Hayden MR, Ellerby LM. 2004. Inhibition of calpain cleavage of huntingtin reduces toxicity: accumulation of calpain/caspase fragments in the nucleus. *The Journal of biological chemistry* 279: 20211-20

Galvan L, Lepejova N, Gaillard MC, Malgorn C, Guillermier M, et al. 2012. Capucin does not modify the toxicity of a mutant Huntingtin fragment in vivo. *Neurobiology of aging* 33: 1845 e5-6

Gardian G, Vecsei L. 2004. Huntington's disease: pathomechanism and therapeutic perspectives. *Journal of neural transmission* 111: 1485-94

Garriga-Canut M, Agustin-Pavon C, Herrmann F, Sanchez A, Dierssen M, et al. 2012. Synthetic zinc finger repressors reduce mutant huntingtin expression in the brain of R6/2 mice. *Proceedings of the National Academy of Sciences of the United States of America* 109: E3136-45

Gauthier LR, Charrin BC, Borrell-Pages M, Dompierre JP, Rangone H, et al. 2004. Huntingtin controls neurotrophic support and survival of neurons by enhancing BDNF vesicular transport along microtubules. *Cell* 118: 127-38

Gayan J, Brocklebank D, Andresen JM, Alkorta-Aranburu G, Group US-VCR, et al. 2008. Genomewide linkage scan reveals novel loci modifying age of onset of Huntington's disease in the Venezuelan HD kindreds. *Genetic epidemiology* 32: 445-53

Gerfen CR, Engber TM, Mahan LC, Susel Z, Chase TN, et al. 1990. D1 and D2 dopamine receptor-regulated gene expression of striatonigral and striatopallidal neurons. *Science* 250: 1429-32

Giampa C, Laurenti D, Anzilotti S, Bernardi G, Menniti FS, Fusco FR. 2010. Inhibition of the striatal specific phosphodiesterase PDE10A ameliorates striatal and cortical pathology in R6/2 mouse model of Huntington's disease. *PloS one* 5: e13417

Gibrat C, Cicchetti F. 2011. Potential of cystamine and cysteamine in the treatment of neurodegenerative diseases. *Progress in neuro-psychopharmacology & biological psychiatry* 35: 380-9

Goebel HH, Heipertz R, Scholz W, Iqbal K, Tellez-Nagel I. 1978. Juvenile Huntington chorea: clinical, ultrastructural, and biochemical studies. *Neurology* 28: 23-31

Goldberg YP, Nicholson DW, Rasper DM, Kalchman MA, Koide HB, et al. 1996. Cleavage of huntingtin by apopain, a proapoptotic cysteine protease, is modulated by the polyglutamine tract. *Nature genetics* 13: 442-9

Goula AV, Stys A, Chan JP, Trottier Y, Festenstein R, Merienne K. 2012. Transcription elongation and tissue-specific somatic CAG instability. *PLoS genetics* 8: e1003051

Graham RK, Deng Y, Slow EJ, Haigh B, Bissada N, et al. 2006. Cleavage at the caspase-6 site is required for neuronal dysfunction and degeneration due to mutant huntingtin. *Cell* 125: 1179-91

Gray SG. 2010. Targeting histone deacetylases for the treatment of Huntington's disease. *CNS neuroscience & therapeutics* 16: 348-61

Grondin R, Kaytor MD, Ai Y, Nelson PT, Thakker DR, et al. 2012. Six-month partial suppression of Huntingtin is well tolerated in the adult rhesus striatum. *Brain : a journal of neurology* 135: 1197-209

Gu M, Gash MT, Mann VM, Javoy-Agid F, Cooper JM, Schapira AH. 1996. Mitochondrial defect in Huntington's disease caudate nucleus. *Annals of neurology* 39: 385-9

Gusella JF, MacDonald ME. 1995. Huntington's disease. *Seminars in cell biology* 6: 21-8

Gusella JF, MacDonald ME. 2009. Huntington's disease: the case for genetic modifiers. *Genome medicine* 1: 80

Gusella JF, MacDonald ME, Lee JM. 2014. Genetic modifiers of Huntington's disease. *Movement disorders : official journal of the Movement Disorder Society* 29: 1359-65

Gusella JF, Wexler NS, Conneally PM, Naylor SL, Anderson MA, et al. 1983. A polymorphic DNA marker genetically linked to Huntington's disease. *Nature* 306: 234-8

Gutekunst CA, Li SH, Yi H, Mulroy JS, Kuemmerle S, et al. 1999. Nuclear and neuropil aggregates in Huntington's disease: relationship to neuropathology. *The Journal of neuroscience : the official journal of the Society for Neuroscience* 19: 2522-34

Guttman M, Amit I, Garber M, French C, Lin MF, et al. 2009. Chromatin signature reveals over a thousand highly conserved large non-coding RNAs in mammals. *Nature* 458: 223-7

Hallen A, Cooper AJ, Jamie JF, Haynes PA, Willows RD. 2011. Mammalian forebrain ketimine reductase identified as mu-crystallin; potential regulation by thyroid hormones. *Journal of neurochemistry* 118: 379-87

Hallett M. 1993. Physiology of basal ganglia disorders: an overview. *The Canadian journal of neurological sciences. Le journal canadien des sciences neurologiques* 20: 177-83

Hannan AJ. 1996. Trinucleotide-repeat expansions and neurodegenerative disease: a mechanism of pathogenesis. *Clinical and experimental pharmacology & physiology* 23: 1015-20

Hantraye P, Riche D, Maziere M, Isacson O. 1990. A primate model of Huntington's disease: behavioral and anatomical studies of unilateral excitotoxic lesions of the caudate-putamen in the baboon. *Experimental neurology* 108: 91-104

Hantraye P, Riche D, Maziere M, Isacson O. 1992. Intrastriatal transplantation of cross-species fetal striatal cells reduces abnormal movements in a primate model of Huntington disease. *Proceedings of the National Academy of Sciences of the United States of America* 89: 4187-91

Harjes P, Wanker EE. 2003. The hunt for huntingtin function: interaction partners tell many different stories. *Trends Biochem Sci* 28: 425-33

Hawley SA, Fullerton MD, Ross FA, Schertzer JD, Chevtzoff C, et al. 2012. The ancient drug salicylate directly activates AMP-activated protein kinase. *Science* 336: 918-22

HDCRG. 1993. A novel gene containing a trinucleotide repeat that is expanded and unstable on Huntington's disease chromosomes. The Huntington's Disease Collaborative Research Group. *Cell* 72: 971-83

HDSG. 1996. Unified Huntington's Disease Rating Scale: reliability and consistency. Huntington Study Group. *Movement disorders : official journal of the Movement Disorder Society* 11: 136-42

Heikkinen T, Lehtimaki K, Vartiainen N, Puolivali J, Hendricks SJ, et al. 2012. Characterization of neurophysiological and behavioral changes, MRI brain volumetry

and 1H MRS in zQ175 knock-in mouse model of Huntington's disease. *PloS one* 7: e50717

Helmlinger D, Tora L, Devys D. 2006. Transcriptional alterations and chromatin remodeling in polyglutamine diseases. *Trends in genetics : TIG* 22: 562-70

Herdegen T, Waetzig V. 2001. AP-1 proteins in the adult brain: facts and fiction about effectors of neuroprotection and neurodegeneration. *Oncogene* 20: 2424-37

Hickey MA, Zhu C, Medvedeva V, Lerner RP, Patassini S, et al. 2012. Improvement of neuropathology and transcriptional deficits in CAG 140 knock-in mice supports a beneficial effect of dietary curcumin in Huntington's disease. *Molecular neurodegeneration* 7: 12

Hindie V, Stroba A, Zhang H, Lopez-Garcia LA, Idrissova L, et al. 2009. Structure and allosteric effects of low-molecular-weight activators on the protein kinase PDK1. *Nature chemical biology* 5: 758-64

Ho AK, Sahakian BJ, Brown RG, Barker RA, Hodges JR, et al. 2003. Profile of cognitive progression in early Huntington's disease. *Neurology* 61: 1702-6

Hobbs NZ, Barnes J, Frost C, Henley SM, Wild EJ, et al. 2010. Onset and progression of pathologic atrophy in Huntington disease: a longitudinal MR imaging study. *AJNR. American journal of neuroradiology* 31: 1036-41

Hockly E, Richon VM, Woodman B, Smith DL, Zhou X, et al. 2003. Suberoylanilide hydroxamic acid, a histone deacetylase inhibitor, ameliorates motor deficits in a mouse model of Huntington's disease. *Proceedings of the National Academy of Sciences of the United States of America* 100: 2041-6

Hodges A, Strand AD, Aragaki AK, Kuhn A, Sengstag T, et al. 2006. Regional and cellular gene expression changes in human Huntington's disease brain. *Human molecular genetics* 15: 965-77

Hu J, Matsui M, Gagnon KT, Schwartz JC, Gabillet S, et al. 2009. Allele-specific silencing of mutant huntingtin and ataxin-3 genes by targeting expanded CAG repeats in mRNAs. *Nature biotechnology* 27: 478-84

Humbert S, Bryson EA, Cordelieres FP, Connors NC, Datta SR, et al. 2002. The IGF-1/Akt pathway is neuroprotective in Huntington's disease and involves Huntingtin phosphorylation by Akt. *Dev Cell* 2: 831-7

Im W, Kim M. 2014. Cell Therapy Strategies vs. Paracrine Effect in Huntington's Disease. *Journal of movement disorders* 7: 1-6

Jeon I, Lee N, Li JY, Park IH, Park KS, et al. 2012. Neuronal properties, in vivo effects, and pathology of a Huntington's disease patient-derived induced pluripotent stem cells. *Stem cells* 30: 2054-62

Jeong H, Then F, Melia TJ, Jr., Mazzulli JR, Cui L, et al. 2009. Acetylation targets mutant huntingtin to autophagosomes for degradation. *Cell* 137: 60-72

Jia H, Kast RJ, Steffan JS, Thomas EA. 2012. Selective histone deacetylase (HDAC) inhibition imparts beneficial effects in Huntington's disease mice: implications for the ubiquitin-proteasomal and autophagy systems. *Human molecular genetics* 21: 5280-93

Jiang H, Poirier MA, Liang Y, Pei Z, Weiskittel CE, et al. 2006. Depletion of CBP is directly linked with cellular toxicity caused by mutant huntingtin. *Neurobiology of disease* 23: 543-51

Johann V, Schiefer J, Sass C, Mey J, Brook G, et al. 2007. Time of transplantation and cell preparation determine neural stem cell survival in a mouse model of Huntington's disease. *Experimental brain research* 177: 458-70

Johnson R, Buckley NJ. 2009. Gene dysregulation in Huntington's disease: REST, microRNAs and beyond. *Neuromolecular medicine* 11: 183-99

Johnson R, Noble W, Tartaglia GG, Buckley NJ. 2012. Neurodegeneration as an RNA disorder. *Progress in neurobiology* 99: 293-315

Johnson R, Zuccato C, Belyaev ND, Guest DJ, Cattaneo E, Buckley NJ. 2008. A microRNA-based gene dysregulation pathway in Huntington's disease. *Neurobiology of disease* 29: 438-45

Johnson SA, Stout JC, Solomon AC, Langbehn DR, Aylward EH, et al. 2007. Beyond disgust: impaired recognition of negative emotions prior to diagnosis in Huntington's disease. *Brain : a journal of neurology* 130: 1732-44

Julien CL, Thompson JC, Wild S, Yardumian P, Snowden JS, et al. 2007. Psychiatric disorders in preclinical Huntington's disease. *Journal of neurology, neurosurgery, and psychiatry* 78: 939-43

Kalathur RK, Hernandez-Prieto MA, Futschik ME. 2012. Huntington's disease and its therapeutic target genes: a global functional profile based on the HD Research Crossroads database. *BMC neurology* 12: 47

Karpuj MV, Becher MW, Springer JE, Chabas D, Youssef S, et al. 2002. Prolonged survival and decreased abnormal movements in transgenic model of Huntington disease, with administration of the transglutaminase inhibitor cystamine. *Nature medicine* 8: 143-9

Kawaguchi Y, Wilson CJ, Augood SJ, Emson PC. 1995. Striatal interneurones: chemical, physiological and morphological characterization. *Trends in neurosciences* 18: 527-35

Kazantsev A, Preisinger E, Dranovsky A, Goldgaber D, Housman D. 1999. Insoluble detergent-resistant aggregates form between pathological and nonpathological lengths of polyglutamine in mammalian cells. *Proceedings of the National Academy of Sciences of the United States of America* 96: 11404-9

Kegel KB, Kim M, Sapp E, McIntyre C, Castano JG, et al. 2000. Huntingtin expression stimulates endosomal-lysosomal activity, endosome tubulation, and autophagy. *The Journal of neuroscience : the official journal of the Society for Neuroscience* 20: 7268-78

Kegel KB, Meloni AR, Yi Y, Kim YJ, Doyle E, et al. 2002. Huntingtin is present in the nucleus, interacts with the transcriptional corepressor C-terminal binding protein, and represses transcription. *The Journal of biological chemistry* 277: 7466-76

Kegel KB, Sapp E, Alexander J, Valencia A, Reeves P, et al. 2009. Polyglutamine expansion in huntingtin alters its interaction with phospholipids. *Journal of neurochemistry* 110: 1585-97

Khalil AM, Guttman M, Huarte M, Garber M, Raj A, et al. 2009. Many human large intergenic noncoding RNAs associate with chromatin-modifying complexes and affect gene expression. *Proceedings of the National Academy of Sciences of the United States of America* 106: 11667-72

Kiechle T, Dedeoglu A, Kubilus J, Kowall NW, Beal MF, et al. 2002. Cytochrome C and caspase-9 expression in Huntington's disease. *Neuromolecular medicine* 1: 183-95

Kim RY, Gasser R, Wistow GJ. 1992. mu-crystallin is a mammalian homologue of Agrobacterium ornithine cyclodeaminase and is expressed in human retina. *Proceedings of the National Academy of Sciences of the United States of America* 89: 9292-6

Kirik D, Bjorklund A. 2003. Modeling CNS neurodegeneration by overexpression of disease-causing proteins using viral vectors. *Trends in neurosciences* 26: 386-92

Kloppel S. 2009. Brain morphometry and functional imaging techniques in dementia: methods, findings and relevance in forensic neurology. *Current opinion in neurology* 22: 612-6

Kloppel S, Draganski B, Golding CV, Chu C, Nagy Z, et al. 2008. White matter connections reflect changes in voluntary-guided saccades in pre-symptomatic Huntington's disease. *Brain : a journal of neurology* 131: 196-204

Kordasiewicz HB, Stanek LM, Wancewicz EV, Mazur C, McAlonis MM, et al. 2012. Sustained therapeutic reversal of Huntington's disease by transient repression of huntingtin synthesis. *Neuron* 74: 1031-44

Kremer HP, Roos RA, Dingjan G, Marani E, Bots GT. 1990. Atrophy of the hypothalamic lateral tuberal nucleus in Huntington's disease. *Journal of neuropathology and experimental neurology* 49: 371-82

Kung JT, Colognori D, Lee JT. 2013. Long noncoding RNAs: past, present, and future. *Genetics* 193: 651-69

Labbadia J, Novoselov SS, Bett JS, Weiss A, Paganetti P, et al. 2012. Suppression of protein aggregation by chaperone modification of high molecular weight complexes. *Brain : a journal of neurology* 135: 1180-96

Lasker AG, Zee DS. 1997. Ocular motor abnormalities in Huntington's disease. *Vision research* 37: 3639-45

Lausted C, Lee I, Zhou Y, Qin S, Sung J, et al. 2014. Systems approach to neurodegenerative disease biomarker discovery. *Annual review of pharmacology and toxicology* 54: 457-81

Lazzeroni G, Benicchi T, Heitz F, Magnoni L, Diamanti D, et al. 2013. A phenotypic screening assay for modulators of huntingtin-induced transcriptional dysregulation. *Journal of biomolecular screening* 18: 984-96

Leavitt BR, van Raamsdonk JM, Shehadeh J, Fernandes H, Murphy Z, et al. 2006. Wild-type huntingtin protects neurons from excitotoxicity. *Journal of neurochemistry* 96: 1121-9

Lee JM, Ramos EM, Lee JH, Gillis T, Mysore JS, et al. 2012. CAG repeat expansion in Huntington disease determines age at onset in a fully dominant fashion. *Neurology* 78: 690-5

Lee ST, Chu K, Im WS, Yoon HJ, Im JY, et al. 2011. Altered microRNA regulation in Huntington's disease models. *Experimental neurology* 227: 172-9

Li JL, Hayden MR, Almqvist EW, Brinkman RR, Durr A, et al. 2003. A genome scan for modifiers of age at onset in Huntington disease: The HD MAPS study. *American journal of human genetics* 73: 682-7

Li M, Pevny L, Lovell-Badge R, Smith A. 1998. Generation of purified neural precursors from embryonic stem cells by lineage selection. *Current biology : CB* 8: 971-4

Li SH, Cheng AL, Zhou H, Lam S, Rao M, et al. 2002. Interaction of Huntington disease protein with transcriptional activator Sp1. *Mol Cell Biol* 22: 1277-87

Li X, DiFiglia M. 2012. The recycling endosome and its role in neurological disorders. *Progress in neurobiology* 97: 127-41

Lin CH, Tallaksen-Greene S, Chien WM, Cearley JA, Jackson WS, et al. 2001. Neurological abnormalities in a knock-in mouse model of Huntington's disease. *Human molecular genetics* 10: 137-44

Lin X, Yang M, Xia T, Guo J. 2014. Increased expression of long noncoding RNA ABHD11-AS1 in gastric cancer and its clinical significance. *Medical oncology* 31: 42

Liu YF, Dorow D, Marshall J. 2000. Activation of MLK2-mediated signaling cascades by polyglutamine-expanded huntingtin. *The Journal of biological chemistry* 275: 19035-40

Lombardi MS, Jaspers L, Spronkmans C, Gellera C, Taroni F, et al. 2009. A majority of Huntington's disease patients may be treatable by individualized allele-specific RNA interference. *Experimental neurology* 217: 312-9

Long YC, Tan TM, Takao I, Tang BL. 2014. The biochemistry and cell biology of aging: metabolic regulation through mitochondrial signaling. *American journal of physiology. Endocrinology and metabolism* 306: E581-91

Lu B, Al-Ramahi I, Valencia A, Wang Q, Berenshteyn F, et al. 2013. Identification of NUB1 as a suppressor of mutant Huntington toxicity via enhanced protein clearance. *Nature neuroscience* 16: 562-70

Ludolph AC, He F, Spencer PS, Hammerstad J, Sabri M. 1991. 3-Nitropropionic acid-exogenous animal neurotoxin and possible human striatal toxin. *The Canadian journal of neurological sciences. Le journal canadien des sciences neurologiques* 18: 492-8

Lunkes A, Lindenberg KS, Ben-Haiem L, Weber C, Devys D, et al. 2002. Proteases acting on mutant huntingtin generate cleaved products that differentially build up cytoplasmic and nuclear inclusions. *Molecular cell* 10: 259-69

Luthi-Carter R, Hanson SA, Strand AD, Bergstrom DA, Chun W, et al. 2002. Dysregulation of gene expression in the R6/2 model of polyglutamine disease: parallel changes in muscle and brain. *Human molecular genetics* 11: 1911-26

Luthi-Carter R, Strand A, Peters NL, Solano SM, Hollingsworth ZR, et al. 2000. Decreased expression of striatal signaling genes in a mouse model of Huntington's disease. *Human molecular genetics* 9: 1259-71

Magen I, Hornstein E. 2014. Oligonucleotide-based therapy for neurodegenerative diseases. *Brain research*

Malinowska K, Cavarretta IT, Susani M, Wrulich OA, Uberall F, et al. 2009. Identification of mu-crystallin as an androgen-regulated gene in human prostate cancer. *Prostate* 69: 1109-18

Mandel RJ, Manfredsson FP, Foust KD, Rising A, Reimsnider S, et al. 2006. Recombinant adeno-associated viral vectors as therapeutic agents to treat neurological disorders. *Molecular therapy : the journal of the American Society of Gene Therapy* 13: 463-83

Mangiarini L, Sathasivam K, Seller M, Cozens B, Harper A, et al. 1996. Exon 1 of the HD gene with an expanded CAG repeat is sufficient to cause a progressive neurological phenotype in transgenic mice. *Cell* 87: 493-506

Marcellin D, Abramowski D, Young D, Richter J, Weiss A, et al. 2012. Fragments of HdhQ150 mutant huntingtin form a soluble oligomer pool that declines with aggregate deposition upon aging. *PloS one* 7: e44457

Margulis J, Finkbeiner S. 2014. Proteostasis in striatal cells and selective neurodegeneration in Huntington's disease. *Frontiers in cellular neuroscience* 8: 218

Mariner PD, Walters RD, Espinoza CA, Drullinger LF, Wagner SD, et al. 2008. Human Alu RNA is a modular transacting repressor of mRNA transcription during heat shock. *Molecular cell* 29: 499-509

Marti E, Pantano L, Banez-Coronel M, Llorens F, Minones-Moyano E, et al. 2010. A myriad of miRNA variants in control and Huntington's disease brain regions detected by massively parallel sequencing. *Nucleic acids research* 38: 7219-35

Martindale D, Hackam A, Wieczorek A, Ellerby L, Wellington C, et al. 1998. Length of huntingtin and its polyglutamine tract influences localization and frequency of intracellular aggregates. *Nature genetics* 18: 150-4

Martinez-Vicente M, Talloczy Z, Wong E, Tang G, Koga H, et al. 2010. Cargo recognition failure is responsible for inefficient autophagy in Huntington's disease. *Nature neuroscience* 13: 567-76

Martinez T, Wright N, Lopez-Fraga M, Jimenez AI, Paneda C. 2013. Silencing human genetic diseases with oligonucleotide-based therapies. *Human genetics* 132: 481-93

Mascalchi M, Lolli F, Della Nave R, Tessa C, Petralli R, et al. 2004. Huntington disease: volumetric, diffusion-weighted, and magnetization transfer MR imaging of brain. *Radiology* 232: 867-73

Mazarei G, Neal SJ, Becanovic K, Luthi-Carter R, Simpson EM, Leavitt BR. 2009. Expression analysis of novel striatal-enriched genes in Huntington disease. *Human molecular genetics* 19: 609-22

McBride JL, Behrstock SP, Chen EY, Jakel RJ, Siegel I, et al. 2004. Human neural stem cell transplants improve motor function in a rat model of Huntington's disease. *The Journal of comparative neurology* 475: 211-9

McBride JL, Pitzer MR, Boudreau RL, Dufour B, Hobbs T, et al. 2011. Preclinical safety of RNAi-mediated HTT suppression in the rhesus macaque as a potential therapy for Huntington's disease. *Molecular therapy : the journal of the American Society of Gene Therapy* 19: 2152-62

McMahon MT, Gilad AA, Zhou J, Sun PZ, Bulte JW, van Zijl PC. 2006. Quantifying exchange rates in chemical exchange saturation transfer agents using the saturation time and saturation power dependencies of the magnetization transfer effect on the magnetic resonance imaging signal (QUEST and QUESP): Ph calibration for poly-L-lysine and a starburst dendrimer. *Magnetic resonance in medicine : official journal of the Society of Magnetic Resonance in Medicine / Society of Magnetic Resonance in Medicine* 55: 836-47

Menalled LB, Kudwa AE, Miller S, Fitzpatrick J, Watson-Johnson J, et al. 2012. Comprehensive behavioral and molecular characterization of a new knock-in mouse model of Huntington's disease: zQ175. *PloS one* 7: e49838

Menalled LB, Sison JD, Dragatsis I, Zeitlin S, Chesselet MF. 2003. Time course of early motor and neuropathological anomalies in a knock-in mouse model of Huntington's disease with 140 CAG repeats. *The Journal of comparative neurology* 465: 11-26

Merienne K, Helmlinger D, Perkin GR, Devys D, Trottier Y. 2003. Polyglutamine expansion induces a protein-damaging stress connecting heat shock protein 70 to the JNK pathway. *The Journal of biological chemistry* 278: 16957-67

Micale L, Fusco C, Augello B, Napolitano LM, Dermitzakis ET, et al. 2008. Williams-Beuren syndrome TRIM50 encodes an E3 ubiquitin ligase. *Eur J Hum Genet* 16: 1038-49

Mielcarek M, Benn CL, Franklin SA, Smith DL, Woodman B, et al. 2011. SAHA decreases HDAC 2 and 4 levels in vivo and improves molecular phenotypes in the R6/2 mouse model of Huntington's disease. *PloS one* 6: e27746

Mochel F, Haller RG. 2011. Energy deficit in Huntington disease: why it matters. *The Journal of clinical investigation* 121: 493-9

Moffitt H, McPhail GD, Woodman B, Hobbs C, Bates GP. 2009. Formation of polyglutamine inclusions in a wide range of non-CNS tissues in the HdhQ150 knock-in mouse model of Huntington's disease. *PloS one* 4: e8025

Monroy A, Lithgow GJ, Alavez S. 2013. Curcumin and neurodegenerative diseases. *BioFactors* 39: 122-32

Montoya A, Pelletier M, Menear M, Duplessis E, Richer F, Lepage M. 2006a. Episodic memory impairment in Huntington's disease: a meta-analysis. *Neuropsychologia* 44: 1984-94

Montoya A, Price BH, Menear M, Lepage M. 2006b. Brain imaging and cognitive dysfunctions in Huntington's disease. *Journal of psychiatry & neuroscience : JPN* 31: 21-9

Muhlau M, Winkelmann J, Rujescu D, Giegling I, Koutsouleris N, et al. 2012. Variation within the Huntington's disease gene influences normal brain structure. *PloS one* 7: e29809

Muhr J, Andersson E, Persson M, Jessell TM, Ericson J. 2001. Groucho-mediated transcriptional repression establishes progenitor cell pattern and neuronal fate in the ventral neural tube. *Cell* 104: 861-73

Nagai Y, Fujikake N, Ohno K, Higashiyama H, Popiel HA, et al. 2003. Prevention of polyglutamine oligomerization and neurodegeneration by the peptide inhibitor QBP1 in Drosophila. *Human molecular genetics* 12: 1253-9

Nakao N, Grasbon-Frodl EM, Widner H, Brundin P. 1996. DARPP-32-rich zones in grafts of lateral ganglionic eminence govern the extent of functional recovery in skilled paw reaching in an animal model of Huntington's disease. *Neuroscience* 74: 959-70

Noack H, Kube U, Augustin W. 1994. Relations between tocopherol depletion and coenzyme Q during lipid peroxidation in rat liver mitochondria. *Free radical research* 20: 375-86

Novak MJ, Seunarine KK, Gibbard CR, Hobbs NZ, Scahill RI, et al. 2014. White matter integrity in premanifest and early Huntington's disease is related to caudate loss and disease progression. *Cortex; a journal devoted to the study of the nervous system and behavior* 52: 98-112

Nucifora FC, Jr., Sasaki M, Peters MF, Huang H, Cooper JK, et al. 2001. Interference by huntingtin and atrophin-1 with cbp-mediated transcription leading to cellular toxicity. *Science* 291: 2423-8

Obeso JA, Rodriguez-Oroz MC, Stamelou M, Bhatia KP, Burn DJ. 2014. The expanding universe of disorders of the basal ganglia. *Lancet* 384: 523-31

Ohmae S, Takemoto-Kimura S, Okamura M, Adachi-Morishima A, Nonaka M, et al. 2006. Molecular identification and characterization of a family of kinases with homology to Ca2+/calmodulin-dependent protein kinases I/IV. *The Journal of biological chemistry* 281: 20427-39

Okamoto Y, Nagai Y, Fujikake N, Akiko Popiel H, Yoshioka T, et al. 2009. Surface plasmon resonance characterization of specific binding of polyglutamine aggregation inhibitors to the expanded polyglutamine stretch. *Biochemical and biophysical research communications* 378: 634-9

Oshima A, Suzuki S, Takumi Y, Hashizume K, Abe S, Usami S. 2006. CRYM mutations cause deafness through thyroid hormone binding properties in the fibrocytes of the cochlea. *Journal of medical genetics* 43: e25

Palfi S, Brouillet E, Jarraya B, Bloch J, Jan C, et al. 2007. Expression of mutated huntingtin fragment in the putamen is sufficient to produce abnormal movement in non-human primates. *Molecular therapy : the journal of the American Society of Gene Therapy* 15: 1444-51

Palfi S, Conde F, Riche D, Brouillet E, Dautry C, et al. 1998. Fetal striatal allografts reverse cognitive deficits in a primate model of Huntington disease. *Nature medicine* 4: 963-6

Pandey RR, Mondal T, Mohammad F, Enroth S, Redrup L, et al. 2008. Kcnq1ot1 antisense noncoding RNA mediates lineage-specific transcriptional silencing through chromatin-level regulation. *Molecular cell* 32: 232-46

Panov AV, Gutekunst CA, Leavitt BR, Hayden MR, Burke JR, et al. 2002. Early mitochondrial calcium defects in Huntington's disease are a direct effect of polyglutamines. *Nature neuroscience* 5: 731-6

Paoletti P, Vila I, Rife M, Lizcano JM, Alberch J, Gines S. 2008. Dopaminergic and glutamatergic signaling crosstalk in Huntington's disease neurodegeneration: the role of p25/cyclin-dependent kinase 5. *The Journal of neuroscience : the official journal of the Society for Neuroscience* 28: 10090-101

Pattison LR, Kotter MR, Fraga D, Bonelli RM. 2006. Apoptotic cascades as possible targets for inhibiting cell death in Huntington's disease. *Journal of neurology* 253: 1137-42

Perrin S. 2014. Preclinical research: Make mouse studies work. *Nature* 507: 423-5
Perrin V, Dufour N, Raoul C, Hassig R, Brouillet E, et al. 2009. Implication of the JNK pathway in a rat model of Huntington's disease. *Experimental neurology* 215: 191-200
Perrin V, Regulier E, Abbas-Terki T, Hassig R, Brouillet E, et al. 2007. Neuroprotection by Hsp104 and Hsp27 in lentiviral-based rat models of Huntington's disease. *Molecular therapy : the journal of the American Society of Gene Therapy* 15: 903-11
Perutz MF. 1995. Polar zippers: their role in human disease. *Pharm Acta Helv* 69: 213-24
Politis M, Pavese N, Tai YF, Tabrizi SJ, Barker RA, Piccini P. 2008. Hypothalamic involvement in Huntington's disease: an in vivo PET study. *Brain : a journal of neurology* 131: 2860-9
Ponting CP, Oliver PL, Reik W. 2009. Evolution and functions of long noncoding RNAs. *Cell* 136: 629-41
Poudel GR, Stout JC, Dominguez DJ, Salmon L, Churchyard A, et al. 2014. White matter connectivity reflects clinical and cognitive status in Huntington's disease. *Neurobiology of disease* 65: 180-7
Pouladi MA, Morton AJ, Hayden MR. 2013. Choosing an animal model for the study of Huntington's disease. *Nature reviews. Neuroscience* 14: 708-21
Qin ZH, Gu ZL. 2004. Huntingtin processing in pathogenesis of Huntington disease. *Acta pharmacologica Sinica* 25: 1243-9
Qin ZH, Wang Y, Kegel KB, Kazantsev A, Apostol BL, et al. 2003. Autophagy regulates the processing of amino terminal huntingtin fragments. *Human molecular genetics* 12: 3231-44
Ramachandran PS, Keiser MS, Davidson BL. 2013. Recent advances in RNA interference therapeutics for CNS diseases. *Neurotherapeutics : the journal of the American Society for Experimental NeuroTherapeutics* 10: 473-85
Ramaswamy S, McBride JL, Kordower JH. 2007. Animal models of Huntington's disease. *ILAR journal / National Research Council, Institute of Laboratory Animal Resources* 48: 356-73
Ratovitski T, Nakamura M, D'Ambola J, Chighladze E, Liang Y, et al. 2007. N-terminal proteolysis of full-length mutant huntingtin in an inducible PC12 cell model of Huntington's disease. *Cell cycle* 6: 2970-81
Ravikumar B, Vacher C, Berger Z, Davies JE, Luo S, et al. 2004. Inhibition of mTOR induces autophagy and reduces toxicity of polyglutamine expansions in fly and mouse models of Huntington disease. *Nature genetics* 36: 585-95
Raymond LA, Andre VM, Cepeda C, Gladding CM, Milnerwood AJ, Levine MS. 2011. Pathophysiology of Huntington's disease: time-dependent alterations in synaptic and receptor function. *Neuroscience* 198: 252-73
Reading SA, Yassa MA, Bakker A, Dziorny AC, Gourley LM, et al. 2005. Regional white matter change in pre-symptomatic Huntington's disease: a diffusion tensor imaging study. *Psychiatry research* 140: 55-62
Reed PW, Corse AM, Porter NC, Flanigan KM, Bloch RJ. 2007. Abnormal expression of mu-crystallin in facioscapulohumeral muscular dystrophy. *Experimental neurology* 205: 583-6
Reiner A, Albin RL, Anderson KD, D'Amato CJ, Penney JB, Young AB. 1988. Differential loss of striatal projection neurons in Huntington disease. *Proceedings of the National Academy of Sciences of the United States of America* 85: 5733-7
Reiner O, Coquelle FM, Peter B, Levy T, Kaplan A, et al. 2006. The evolving doublecortin (DCX) superfamily. *BMC genomics* 7: 188
Remaud S, Gothie JD, Morvan-Dubois G, Demeneix BA. 2014. Thyroid hormone signaling and adult neurogenesis in mammals. *Frontiers in endocrinology* 5: 62

Rigamonti D, Bauer JH, De-Fraja C, Conti L, Sipione S, et al. 2000. Wild-type huntingtin protects from apoptosis upstream of caspase-3. *The Journal of neuroscience : the official journal of the Society for Neuroscience* 20: 3705-13

Rigamonti D, Sipione S, Goffredo D, Zuccato C, Fossale E, Cattaneo E. 2001. Huntingtin's neuroprotective activity occurs via inhibition of procaspase-9 processing. *The Journal of biological chemistry* 276: 14545-8

Rindt H, Yen PF, Thebeau CN, Peterson TS, Weisman GA, Lorson CL. 2012. Replacement of huntingtin exon 1 by trans-splicing. *Cellular and molecular life sciences : CMLS* 69: 4191-204

Rising AC, Xu J, Carlson A, Napoli VV, Denovan-Wright EM, Mandel RJ. 2011. Longitudinal behavioral, cross-sectional transcriptional and histopathological characterization of a knock-in mouse model of Huntington's disease with 140 CAG repeats. *Experimental neurology* 228: 173-82

Rockabrand E, Slepko N, Pantalone A, Nukala VN, Kazantsev A, et al. 2007. The first 17 amino acids of Huntingtin modulate its sub-cellular localization, aggregation and effects on calcium homeostasis. *Human molecular genetics* 16: 61-77

Roos RA. 2010. Huntington's disease: a clinical review. *Orphanet journal of rare diseases* 5: 40

Rosas HD, Goodman J, Chen YI, Jenkins BG, Kennedy DN, et al. 2001. Striatal volume loss in HD as measured by MRI and the influence of CAG repeat. *Neurology* 57: 1025-8

Rosas HD, Reuter M, Doros G, Lee SY, Triggs T, et al. 2011. A tale of two factors: what determines the rate of progression in Huntington's disease? A longitudinal MRI study. *Movement disorders : official journal of the Movement Disorder Society* 26: 1691-7

Rosas HD, Tuch DS, Hevelone ND, Zaleta AK, Vangel M, et al. 2006. Diffusion tensor imaging in presymptomatic and early Huntington's disease: Selective white matter pathology and its relationship to clinical measures. *Movement disorders : official journal of the Movement Disorder Society* 21: 1317-25

Ross CA, Aylward EH, Wild EJ, Langbehn DR, Long JD, et al. 2014. Huntington disease: natural history, biomarkers and prospects for therapeutics. *Nature reviews. Neurology* 10: 204-16

Ross CA, Tabrizi SJ. 2011. Huntington's disease: from molecular pathogenesis to clinical treatment. *The Lancet. Neurology* 10: 83-98

Rovet JF. 2014. The role of thyroid hormones for brain development and cognitive function. *Endocrine development* 26: 26-43

Ruiz M, Deglon N. 2012. Viral-mediated overexpression of mutant huntingtin to model HD in various species. *Neurobiology of disease* 48: 202-11

Runne H, Regulier E, Kuhn A, Zala D, Gokce O, et al. 2008. Dysregulation of gene expression in primary neuron models of Huntington's disease shows that polyglutamine-related effects on the striatal transcriptome may not be dependent on brain circuitry. *The Journal of neuroscience : the official journal of the Society for Neuroscience* 28: 9723-31

Saleh N, Moutereau S, Durr A, Krystkowiak P, Azulay JP, et al. 2009. Neuroendocrine disturbances in Huntington's disease. *PloS one* 4: e4962

Salta E, De Strooper B. 2012. Non-coding RNAs with essential roles in neurodegenerative disorders. *The Lancet. Neurology* 11: 189-200

San Sebastian W, Samaranch L, Kells AP, Forsayeth J, Bankiewicz KS. 2013. Gene therapy for misfolding protein diseases of the central nervous system. *Neurotherapeutics : the journal of the American Society for Experimental NeuroTherapeutics* 10: 498-510

Sandhir R, Yadav A, Mehrotra A, Sunkaria A, Singh A, Sharma S. 2014. Curcumin nanoparticles attenuate neurochemical and neurobehavioral deficits in experimental model of Huntington's disease. *Neuromolecular medicine* 16: 106-18

Sapp E, Schwarz C, Chase K, Bhide PG, Young AB, et al. 1997. Huntingtin localization in brains of normal and Huntington's disease patients. *Annals of neurology* 42: 604-12

Saudou F, Humbert S. 2006. [Cysteamine restores intracellular dynamics and BDNF secretion in Huntington's disease]. *Medecine sciences : M/S* 22: 906-8

Schaefer MH, Wanker EE, Andrade-Navarro MA. 2012. Evolution and function of CAG/polyglutamine repeats in protein-protein interaction networks. *Nucleic acids research* 40: 4273-87

Schapira AH, Olanow CW, Greenamyre JT, Bezard E. 2014. Slowing of neurodegeneration in Parkinson's disease and Huntington's disease: future therapeutic perspectives. *Lancet* 384: 545-55

Scherzinger E, Lurz R, Turmaine M, Mangiarini L, Hollenbach B, et al. 1997. Huntingtin-encoded polyglutamine expansions form amyloid-like protein aggregates in vitro and in vivo. *Cell* 90: 549-58

Schilling G, Becher MW, Sharp AH, Jinnah HA, Duan K, et al. 1999. Intranuclear inclusions and neuritic aggregates in transgenic mice expressing a mutant N-terminal fragment of huntingtin. *Human molecular genetics* 8: 397-407

Schilling G, Savonenko AV, Klevytska A, Morton JL, Tucker SM, et al. 2004. Nuclear-targeting of mutant huntingtin fragments produces Huntington's disease-like phenotypes in transgenic mice. *Human molecular genetics* 13: 1599-610

Schoenherr CJ, Paquette AJ, Anderson DJ. 1996. Identification of potential target genes for the neuron-restrictive silencer factor. *Proceedings of the National Academy of Sciences of the United States of America* 93: 9881-6

Schroeder AC, Privalsky ML. 2014. Thyroid hormones, t3 and t4, in the brain. *Frontiers in endocrinology* 5: 40

Schulte J, Littleton JT. 2011. The biological function of the Huntingtin protein and its relevance to Huntington's Disease pathology. *Current trends in neurology* 5: 65-78

Senut MC, Suhr ST, Kaspar B, Gage FH. 2000. Intraneuronal aggregate formation and cell death after viral expression of expanded polyglutamine tracts in the adult rat brain. *The Journal of neuroscience : the official journal of the Society for Neuroscience* 20: 219-29

Sepers MD, Raymond LA. 2014. Mechanisms of synaptic dysfunction and excitotoxicity in Huntington's disease. *Drug discovery today* 19: 990-6

Sherry AD, Woods M. 2008. Chemical exchange saturation transfer contrast agents for magnetic resonance imaging. *Annual review of biomedical engineering* 10: 391-411

Shoulson I, Chase TN. 1975. Huntington's disease. *Annual review of medicine* 26: 419-36

Siemers E, Foroud T, Bill DJ, Sorbel J, Norton JA, Jr., et al. 1996. Motor changes in presymptomatic Huntington disease gene carriers. *Archives of neurology* 53: 487-92

Simmons DA, Belichenko NP, Yang T, Condon C, Monbureau M, et al. 2013. A small molecule TrkB ligand reduces motor impairment and neuropathology in R6/2 and BACHD mouse models of Huntington's disease. *The Journal of neuroscience : the official journal of the Society for Neuroscience* 33: 18712-27

Simon MD, Wang CI, Kharchenko PV, West JA, Chapman BA, et al. 2011. The genomic binding sites of a noncoding RNA. *Proceedings of the National Academy of Sciences of the United States of America* 108: 20497-502

Sitek EJ, Thompson JC, Craufurd D, Snowden JS. 2014. Unawareness of Deficits in Huntington's Disease. *Journal of Huntington's disease* 3: 125-35

Slow EJ, van Raamsdonk J, Rogers D, Coleman SH, Graham RK, et al. 2003. Selective striatal neuronal loss in a YAC128 mouse model of Huntington disease. *Human molecular genetics* 12: 1555-67

Snowden JS, Craufurd D, Griffiths HL, Neary D. 1998. Awareness of involuntary movements in Huntington disease. *Archives of neurology* 55: 801-5

Soldati C, Bithell A, Johnston C, Wong KY, Stanton LW, Buckley NJ. 2013. Dysregulation of REST-regulated coding and non-coding RNAs in a cellular model of Huntington's disease. *Journal of neurochemistry* 124: 418-30

Sondhi D, Hackett NR, Peterson DA, Stratton J, Baad M, et al. 2007. Enhanced survival of the LINCL mouse following CLN2 gene transfer using the rh.10 rhesus macaque-derived adeno-associated virus vector. *Molecular therapy : the journal of the American Society of Gene Therapy* 15: 481-91

Song C, Zhang Y, Parsons CG, Liu YF. 2003. Expression of polyglutamine-expanded huntingtin induces tyrosine phosphorylation of N-methyl-D-aspartate receptors. *The Journal of biological chemistry* 278: 33364-9

Song J, Lee ST, Kang W, Park JE, Chu K, et al. 2007. Human embryonic stem cell-derived neural precursor transplants attenuate apomorphine-induced rotational behavior in rats with unilateral quinolinic acid lesions. *Neuroscience letters* 423: 58-61

Steffan JS, Bodai L, Pallos J, Poelman M, McCampbell A, et al. 2001. Histone deacetylase inhibitors arrest polyglutamine-dependent neurodegeneration in Drosophila. *Nature* 413: 739-43

Steffan JS, Kazantsev A, Spasic-Boskovic O, Greenwald M, Zhu YZ, et al. 2000. The Huntington's disease protein interacts with p53 and CREB-binding protein and represses transcription. *Proceedings of the National Academy of Sciences of the United States of America* 97: 6763-8

Su SC, Tsai LH. 2011. Cyclin-dependent kinases in brain development and disease. *Annual review of cell and developmental biology* 27: 465-91

Sun Y, Savanenin A, Reddy PH, Liu YF. 2001. Polyglutamine-expanded huntingtin promotes sensitization of N-methyl-D-aspartate receptors via post-synaptic density 95. *The Journal of biological chemistry* 276: 24713-8

Suzuki S, Mori J, Hashizume K. 2007a. mu-crystallin, a NADPH-dependent T(3)-binding protein in cytosol. *Trends in endocrinology and metabolism: TEM* 18: 286-9

Suzuki S, Suzuki N, Mori J, Oshima A, Usami S, Hashizume K. 2007b. micro-Crystallin as an intracellular 3,5,3'-triiodothyronine holder in vivo. *Mol Endocrinol* 21: 885-94

Tabrizi SJ, Cleeter MW, Xuereb J, Taanman JW, Cooper JM, Schapira AH. 1999. Biochemical abnormalities and excitotoxicity in Huntington's disease brain. *Annals of neurology* 45: 25-32

Tabrizi SJ, Langbehn DR, Leavitt BR, Roos RA, Durr A, et al. 2009. Biological and clinical manifestations of Huntington's disease in the longitudinal TRACK-HD study: cross-sectional analysis of baseline data. *The Lancet. Neurology* 8: 791-801

Takahashi K, Yamanaka S. 2006. Induction of pluripotent stem cells from mouse embryonic and adult fibroblast cultures by defined factors. *Cell* 126: 663-76

Tam S, Geller R, Spiess C, Frydman J. 2006. The chaperonin TRiC controls polyglutamine aggregation and toxicity through subunit-specific interactions. *Nature cell biology* 8: 1155-62

Tang TS, Tu H, Chan EY, Maximov A, Wang Z, et al. 2003. Huntingtin and huntingtin-associated protein 1 influence neuronal calcium signaling mediated by inositol-(1,4,5) triphosphate receptor type 1. *Neuron* 39: 227-39

Taylor-Robinson SD, Weeks RA, Sargentoni J, Marcus CD, Bryant DJ, et al. 1994. Evidence for glutamate excitotoxicity in Huntington's disease with proton magnetic resonance spectroscopy. *Lancet* 343: 1170

Tepper JM, Wilson CJ, Koos T. 2008. Feedforward and feedback inhibition in neostriatal GABAergic spiny neurons. *Brain research reviews* 58: 272-81

Thevandavakkam MA, Schwarcz R, Muchowski PJ, Giorgini F. 2010. Targeting kynurenine 3-monooxygenase (KMO): implications for therapy in Huntington's disease. *CNS & neurological disorders drug targets* 9: 791-800

Tian J, Yan YP, Zhou R, Lou HF, Rong Y, Zhang BR. 2014. Soluble N-terminal fragment of mutant Huntingtin protein impairs mitochondrial axonal transport in cultured hippocampal neurons. *Neuroscience bulletin* 30: 74-80

Todd D, Gowers I, Dowler SJ, Wall MD, McAllister G, et al. 2014. A monoclonal antibody TrkB receptor agonist as a potential therapeutic for Huntington's disease. *PloS one* 9: e87923

Trottier Y, Biancalana V, Mandel JL. 1994. Instability of CAG repeats in Huntington's disease: relation to parental transmission and age of onset. *Journal of medical genetics* 31: 377-82

Trushina E, Dyer RB, Badger JD, 2nd, Ure D, Eide L, et al. 2004. Mutant huntingtin impairs axonal trafficking in mammalian neurons in vivo and in vitro. *Mol Cell Biol* 24: 8195-209

Tsai MC, Spitale RC, Chang HY. 2011. Long intergenic noncoding RNAs: new links in cancer progression. *Cancer research* 71: 3-7

Tsunemi T, Ashe TD, Morrison BE, Soriano KR, Au J, et al. 2012. PGC-1alpha rescues Huntington's disease proteotoxicity by preventing oxidative stress and promoting TFEB function. *Science translational medicine* 4: 142ra97

Tuy FP, Saillour Y, Kappeler C, Chelly J, Francis F. 2008. Alternative transcripts of Dclk1 and Dclk2 and their expression in doublecortin knockout mice. *Developmental neuroscience* 30: 171-86

Ulitsky I, Bartel DP. 2013. lincRNAs: genomics, evolution, and mechanisms. *Cell* 154: 26-46

Valor LM. 2014. Transcription, Epigenetics and Ameliorative Strategies in Huntington's Disease: a Genome-Wide Perspective. *Molecular neurobiology*

Varjosalo M, Keskitalo S, Van Drogen A, Nurkkala H, Vichalkovski A, et al. 2013. The protein interaction landscape of the human CMGC kinase group. *Cell reports* 3: 1306-20

Vecsei L, Beal MF. 1991. Comparative behavioral and neurochemical studies with striatal kainic acid- or quinolinic acid-lesioned rats. *Pharmacology, biochemistry, and behavior* 39: 473-8

Venkatraman P, Wetzel R, Tanaka M, Nukina N, Goldberg AL. 2004. Eukaryotic proteasomes cannot digest polyglutamine sequences and release them during degradation of polyglutamine-containing proteins. *Molecular cell* 14: 95-104

Verissimo CS, Molenaar JJ, Fitzsimons CP, Vreugdenhil E. 2011. Neuroblastoma therapy: what is in the pipeline? *Endocrine-related cancer* 18: R213-31

Visnyei K, Tatsukawa KJ, Erickson RI, Simonian S, Oknaian N, et al. 2006. Neural progenitor implantation restores metabolic deficits in the brain following striatal quinolinic acid lesion. *Experimental neurology* 197: 465-74

Visser WE, Wong WS, van Mullem AA, Friesema EC, Geyer J, Visser TJ. 2010. Study of the transport of thyroid hormone by transporters of the SLC10 family. *Molecular and cellular endocrinology* 315: 138-45

Vonsattel JP, DiFiglia M. 1998. Huntington disease. *Journal of neuropathology and experimental neurology* 57: 369-84

Wada T, Honda M, Minami I, Tooi N, Amagai Y, et al. 2009. Highly efficient differentiation and enrichment of spinal motor neurons derived from human and monkey embryonic stem cells. *PloS one* 4: e6722

Walker FO. 2007. Huntington's disease. *Lancet* 369: 218-28

Wang N, Gray M, Lu XH, Cantle JP, Holley SM, et al. 2014. Neuronal targets for reducing mutant huntingtin expression to ameliorate disease in a mouse model of Huntington's disease. *Nature medicine* 20: 536-41

Ward KM, Aletras AH, Balaban RS. 2000. A new class of contrast agents for MRI based on proton chemical exchange dependent saturation transfer (CEST). *Journal of magnetic resonance* 143: 79-87

Weimer JM, Anton ES. 2006. Doubling up on microtubule stabilizers: synergistic functions of doublecortin-like kinase and doublecortin in the developing cerebral cortex. *Neuron* 49: 3-4

Weitzel JM, Iwen KA. 2011. Coordination of mitochondrial biogenesis by thyroid hormone. *Molecular and cellular endocrinology* 342: 1-7

Wexler NS, Lorimer J, Porter J, Gomez F, Moskowitz C, et al. 2004. Venezuelan kindreds reveal that genetic and environmental factors modulate Huntington's disease age of onset. *Proceedings of the National Academy of Sciences of the United States of America* 101: 3498-503

Wheeler VC, Gutekunst CA, Vrbanac V, Lebel LA, Schilling G, et al. 2002. Early phenotypes that presage late-onset neurodegenerative disease allow testing of modifiers in Hdh CAG knock-in mice. *Human molecular genetics* 11: 633-40

Wheeler VC, White JK, Gutekunst CA, Vrbanac V, Weaver M, et al. 2000. Long glutamine tracts cause nuclear localization of a novel form of huntingtin in medium spiny striatal neurons in HdhQ92 and HdhQ111 knock-in mice. *Human molecular genetics* 9: 503-13

Wichmann T, Delong MR. 2007. Anatomy and physiology of the basal ganglia: relevance to Parkinson's disease and related disorders. *Handbook of clinical neurology* 83: 1-18

Wierinckx A, Auger C, Devauchelle P, Reynaud A, Chevallier P, et al. 2007. A diagnostic marker set for invasion, proliferation, and aggressiveness of prolactin pituitary tumors. *Endocrine-related cancer* 14: 887-900

Wild EJ, Tabrizi SJ. 2014. Targets for future clinical trials in Huntington's disease: What's in the pipeline? *Movement disorders : official journal of the Movement Disorder Society*

Xia J, Lee DH, Taylor J, Vandelft M, Truant R. 2003. Huntingtin contains a highly conserved nuclear export signal. *Human molecular genetics* 12: 1393-403

Xiao B, Sanders MJ, Carmena D, Bright NJ, Haire LF, et al. 2013. Structural basis of AMPK regulation by small molecule activators. *Nature communications* 4: 3017

Yamamoto A, Lucas JJ, Hen R. 2000. Reversal of neuropathology and motor dysfunction in a conditional model of Huntington's disease. *Cell* 101: 57-66

Yang B, Treweek JB, Kulkarni RP, Deverman BE, Chen CK, et al. 2014. Single-Cell Phenotyping within Transparent Intact Tissue through Whole-Body Clearing. *Cell* 158: 945-58

Yang L, Calingasan NY, Wille EJ, Cormier K, Smith K, et al. 2009. Combination therapy with coenzyme Q10 and creatine produces additive neuroprotective effects in models of Parkinson's and Huntington's diseases. *Journal of neurochemistry* 109: 1427-39

Yu S, Liang Y, Palacino J, Difiglia M, Lu B. 2014. Drugging unconventional targets: insights from Huntington's disease. *Trends in pharmacological sciences* 35: 53-62

Zala D, Colin E, Rangone H, Liot G, Humbert S, Saudou F. 2008. Phosphorylation of mutant huntingtin at S421 restores anterograde and retrograde transport in neurons. *Human molecular genetics* 17: 3837-46

Zavan B, Vindigni V, Gardin C, D'Avella D, Della Puppa A, et al. 2010. Neural potential of adipose stem cells. *Discovery medicine* 10: 37-43

Zeron MM, Chen N, Moshaver A, Lee AT, Wellington CL, et al. 2001. Mutant huntingtin enhances excitotoxic cell death. *Mol Cell Neurosci* 17: 41-53

Zhang H, Li Q, Graham RK, Slow E, Hayden MR, Bezprozvanny I. 2008. Full length mutant huntingtin is required for altered Ca2+ signaling and apoptosis of striatal neurons in the YAC mouse model of Huntington's disease. *Neurobiology of disease* 31: 80-8

Zuccato C, Cattaneo E. 2007. Role of brain-derived neurotrophic factor in Huntington's disease. *Progress in neurobiology* 81: 294-330

Zuccato C, Ciammola A, Rigamonti D, Leavitt BR, Goffredo D, et al. 2001. Loss of huntingtin-mediated BDNF gene transcription in Huntington's disease. *Science* 293: 493-8

Zuccato C, Tartari M, Crotti A, Goffredo D, Valenza M, et al. 2003. Huntingtin interacts with REST/NRSF to modulate the transcription of NRSE-controlled neuronal genes. *Nature genetics* 35: 76-83

Harper P (2002). "The epidemiology of Huntington's disease". In Bates G, Harper P, and Jones L. Huntington's Disease – Third Edition. Oxford: Oxford University Press. pp. 159–189

RESUME

Etude de marqueurs du striatum comme modificateurs d'atteinte pathologique dans la maladie de Huntington

La maladie de Huntington (MH) est une affection neurodégénérative héréditaire dont la mutation conduit à une expansion anormale d'un segment polyglutamine dans la protéine Huntingtine (Htt). La Htt mutée, bien qu'ubiquitaire dans le cerveau, conduit à une neurodégénérescence préférentielle du striatum. Cette atteinte pourrait en partie s'expliquer par la présence de produits de gènes sélectivement exprimés dans le striatum. Le laboratoire étudie depuis plusieurs années l'implication potentielle de marqueurs moléculaires du striatum dans la vulnérabilité des neurones de cette structure cérébrale vis-à-vis de la Htt mutée. Durant ma thèse, j'ai étudié plus spécifiquement trois de ces marqueurs du striatum: l'ARN long intergénique non-codant Abhd11os et les protéines µ-crystalline (CRYM) et Doublecortin-like kinase 3 (DCLK3). Une étude préliminaire avait montré l'effet neuroprotecteur de Abhd11os et DCLK3 contre la toxicité induite par un fragment court de la Htt mutée dans un modèle murin aigu de la MH. J'ai donc étudié plus en détails les caractéristiques de ces "modificateurs" de la MH, ainsi que les mécanismes moléculaires potentiels permettant d'expliquer leur effet neuroprotecteur dans un contexte de la MH. J'ai également mené une expérience de thérapie génique en surexprimant le marqueur striatal DCLK3 dans deux modèles transgéniques de la MH. Cette étude nous a permis de valider le haut potentiel thérapeutique de cette protéine.

L'élucidation précise des mécanismes d'action de ces modificateurs de la MH reste encore à résoudre, mais plusieurs pistes sont maintenant possiblement envisagées par rapport à leurs caractéristiques moléculaires.

Outre la découverte de nouveaux marqueurs striataux neuroprotecteurs qui pourrait permettre de développer de nouvelles cibles thérapeutiques, cette étude a permis d'envisager de nouvelles hypothèses permettant de mieux comprendre la vulnérabilité striatale dans la MH et de donner une vue d'ensemble des voies sur lesquelles il serait possible d'agir pour induire des effets neuroprotecteurs dans ce contexte.

Mots-clés : maladie de Huntington, marqueurs du striatum, neuroprotection, modificateurs de la MH.

ABSTRACT

A study of striatal markers as disease modifiers in Huntington's Disease

Huntington's disease (HD) is a autosomal dominant neurodegenerative disorder caused by CAG repeat expansion in the huntingtin gene (HTT), which leads to an abnormal polyglutamine stretch within the Huntingtin protein (Htt).
Whereas mutant Htt (mHtt) is ubiquitously expressed in the brain and peripheral system, it preferentially affects the striatum. Our hypothesis is that genes products selectively expressed in the striatum could be involved in the high vulnerability of the striatum.

From this hypothesis, numerous teams studied "markers of the striatum", that are genes products enriched in the striatum whose expression are up- or down-regulated in HD compared to healthy condition.

During my thesis, I studied three of these striatal markers: the long intergenic non-coding RNA Abhd11os, and the two proteins µ-crystallin (CRYM) and Doublecortin-like kinase 3 (DCLK3). A preliminary study from the laboratory has shown that these three markers have neuroprotective effects against a toxic fragment of mHtt *in vivo*.
The aims of my thesis were to further characterize these three ill-defined disease modifiers and to better understand the putative molecular mechanisms underlying their neuroprotective effects against mHtt.

I also conducted a translational study on DCLK3, whose results validate the high therapeutic potential of this protein.

The elucidation of the mechanisms underlying the neuroprotective effects of these disease modifiers against mHtt toxicity will require further studies, but new trails can be envisioned, according to their characteristics.

My study has enlightened new therapeutic targets and more globally gives an overview of molecular mechanisms to modulate and induce neuroprotective effects in this context, leading to new hypotheses explaining striatal vulnerability in HD.

Key words: Huntington's disease, striatal markers, neuroprotection, disease modifiers.